Electronic Thesis and Dissertation Repository

4-18-2017 12:00 AM

Investigating E2F independent cell cycle control and tumor suppression by pRB

Michael J. Thwaites, *The University of Western Ontario*

Supervisor: Dr. Fred Dick, *The University of Western Ontario*
A thesis submitted in partial fulfillment of the requirements for the Doctor of Philosophy degree in Biochemistry
© Michael J. Thwaites 2017

Follow this and additional works at: https://ir.lib.uwo.ca/etd

Part of the Biochemistry Commons, Molecular Biology Commons, Neoplasms Commons, and the Systems Biology Commons

Abstract

Cellular division is primarily controlled at the G1 to S-phase transition of the cell cycle by the retinoblastoma tumor-suppressor protein (pRB). The ability of pRB to restrict S-phase entry is primarily attributed to the repression of E2F transcription factors required to upregulate cell cycle target genes necessary for cellular division. Interestingly, while pRB is disrupted in the vast majority of human cancers, mutations typically target upstream regulators of pRB leading to inactivation through hyperphosphorylation. The rarity of direct pRB mutations suggests that the regulation of the cell cycle by pRB may involve additional mechanisms outside of E2F repression, as this could to be eliminated via point mutations. Indeed, the $Rb1^{G/G}$ mouse model developed by Cecchini *et al.,* which lacks the ability to form pRB-E2F complexes, showed minimal phenotypic alterations. As described in chapter 2, pRB can stabilize p27 in the absence of pRB-E2F interaction, maintaining cell cycle control. Importantly, the loss of pRB-E2F interactions in addition to the loss of p27 leads to a defective DNA damage response, and ultimately pituitary tumor development. The minimal region of pRB necessary to elicit a cell cycle arrest is the pRB large pocket which contains 3 distinct binding surfaces. Using synthetic mutants of pRB we show that all three of these sites play a role in regulating the cell cycle both *in vitro* and *in vivo*. Finally, to understand E2F independent pRB-mediated tumor-suppression, $Rb1^{G/G}$ mice were intercrossed with mice harboring oncogenic $Kras^{G12D}$, or deletions of p21 or p53. While $Kras^{G12D}$ expression-induced tumorigenesis was not further affected by the $Rb1^{G}$ mutation, the phenotype of p53 null animals was exacerbated by the $Rb1^{G}$ mutation. Interestingly, the loss of p21 in $Rb1^{G/G}$ mice showed no tumor development despite the overlapping function with p27. While it is unclear why there is a discrepancy in phenotype between $Rb1^{G/G}$ mice lacking p21 and those lacking p27, p27 has non-canonical functions which may be contributing to tumor development. Taken together this work describes E2F independent functions of pRB in cell cycle control and tumor suppression and provides a rationale for the unusual disruption of pRB in human cancers by hyperphosphorylation.

Keywords

Co-Authorship Statement

All chapters were written by Michael Thwaites and edited by Dr. Fred Dick.

All experiments in Chapter 2 were performed by Michael Thwaites with the exception of Figure 2.2 which was performed by Matthew Cecchini and Daniel Passos.

All experiments in Chapter 3 were performed by Michael Thwaites with the exception of Figure 3.2C-F which was performed by Matthew Cecchini and Figure 3.4 which was performed by Matthew Cecchini, Srikanth Talluri, Daniel Passos, and Jasmyne Carnevale.

All experiments in Chapter 4 were performed by Michael Thwaites

Dedication

For my son Noah, may all your hopes and dreams come true.

And for his mother Catherine my partner on this adventure

Acknowledgments

First and foremost, I would like to thank my family, Catherine and Noah for all your support and giving me the motivation to complete my Ph.D. Thank you for being there when I needed you the most, I would not have made it this far without you guys by my side. Thank you as well to my parents for giving me everything I need to succeed and the support to do so, and my sister for providing some friendly competition.

To my supervisor, Dr. Fred Dick, I would like to thank you for pushing me to be the best scientist I can be. You let me find my own way but at the same time provided guidance when it was needed. Under your leadership, I believe I have become a more thoughtful and inquisitive scientist and a better communicator. Lastly, thank you for being an excellent mentor driving me to do better, and being supportive when called upon. Thank you to Dr. Joe Mymryk, and Dr. Gabe Dimattia, my advisory committee for providing thoughtful advice, suggestions, and conversations over the years.

To my fellow lab mates, I want to thank you all for your help and comradery in this pursuit. Charles, our frequent scientific discussions and your friendship has led to a productive and supportive relationship over the years, for which I am grateful. Courtney, your support both in and outside of the lab was more than I could ask for, and is greatly appreciated. Finally, thanks to all my friends over the years who have had to listen to me talk about science, and giving me much needed distractions.

Abbreviations

°C: Degrees Celsius

β-Gal: Beta-galactosidase

μCi: Microcurie

μg: Microgram

μl: Microliter

μm: Micrometer

μM: Micromolar

129/B6: mouse with a mixed genetic background of 129 and C57BL/6

3T3: 3-day transfer protocol to immortalize cells

^{32}P: Radiolabelled Phosphorus 32

Adenovirus E1A: adenovirus early region 1

ANOVA: Analysis of variance

APC: Anaphase promoting complex

AS: Asynchronously cycling cells

ATM: Ataxia-telangiectasia mutated

ATP: Adenosine triphosphate

ATR: Ataxia telangiectasia and Rad3 related

Atypical E2Fs: E2F6-8

BrdU: Bromodeoxyuridine

C33A: Human cervical carcinoma cell line

CD20: B-lymphocyte antigen CD20

CDH1: Adaptor protein of the anaphase promoting complex

CDK: Cyclin dependent kinase

CKI: Cyclin dependent kinase inhibitor

CMV: Cytomegalovirus

CR1: Conserved region 1

CR2: Conserved region 2

CRF: Chromatin regulatory factors

CSC: Cancer stem cells

C-terminal domain: Region of the retinoblastoma protein ranging from amino acid 787 to 928

Cyclin: Activator subunits of cyclin dependent kinases

DAPI: 4,6-diamidino-2-phenylindole

DBD: DNA binding domain

DP1: Differentiation related transcription factor-1 polypeptide-1

DNA: Deoxyribonucleic acid

DMEM: Dulbecco's modified Eagle's medium

DMZ: Dimerization domain

DTT: Dithiothreitol

E: Embryonic day

E: Glutamic acid

E3: Ubiquitin protein ligase

E2F: E2 promoter binding factor

E2F1 specific binding site: Region in the C-terminus of the retinoblastoma protein responsible for binding E2F1 in a unique conformation

E2F transcriptional activators: E2F1-3

E2F transcriptional repressors: E2F4-5

EDTA: Ethylenediaminetetraacetic acid

EGF: Epidermal growth factor

ERK1/2: Extracellular signal-regulated kinase

ERT: Estrogen receptor which binds tamoxifen

FBS: fetal bovine serum

Fwd: Forward PCR primer

G0: quiescence

G1: Gap 1 phase of the cell division cycle

G1: Gap 2 phase of the cell division cycle

GAPDH: Glyceraldehyde 3-phosphate dehydrogenase

General binding site: Region of the retinoblastoma protein responsible for binding E2F1-4

GRB2: Growth factor receptor-bound protein 2

GSE: Gel shift extract buffer

GST: Glutathione S-transferase

Gy: Gray, unit referring to ionizing radiation

h: Hours

H&E: Hematoxylin and Eosin staining

H_2O_2: Hydrogen peroxide

HA-Tag: Human influenza hemagglutinin tag derived from amino acid 98-106

HCL: Hydrochloric acid

HDAC: Histone deacetylase

HPV-E7: Human papilloma virus early gene 7

IgG: Immunoglobulin G

INK4: inhibitors of CDK4

IP: Immunoprecipitation

IR: Ionizing radiation

K: Lysine

KCl: Potassium Chloride

kg: kilogram

Large pocket: Region of the retinoblastoma protein ranging from amino acid 379 to 928

LOH: Loss of heterozygosity

LSL: Lox-Stop-Lox

LxCxE: leucine-any amino acid-cysteine-any amino acid-glutamate

M: Mitosis phase of the cell division cycle

mg: Milligram

MapK: Mitogen associated protein kinase

Max: Myc associated factor x

MB: Marked box domain

Mcm: Minichromosome maintenance

MEF: Mouse embryonic fibroblast

MEK1/2: Mitogen-activated protein kinase

mins: Minutes

MgCl$_2$: Magnesium chloride

mM: Millimolar

mRNA: Messenger ribonucleic acid

N: haploid ploidy

Na$_2$B$_4$O$_7$: Sodium Tetraborate

NaCl: Sodium Chloride

NaF: Sodium Floride

Na$_3$VO$_4$: Sodium orthovanadate

NP-40: Nonyl phenoxypolyethoxylethanol

P: Phosphorylation

p14^{ARF}: Alternative reading frame protein product of INK4a

p15^{INK4}: Cyclin dependent kinase 4 inhibitor B

p16^{INK4}: Cyclin dependent kinase inhibitor 2A

p18^{INK4}: Cyclin dependent kinase 4 inhibitor C

p21^{Cip}: Cyclin dependent kinase inhibitor 1

p27^{Kip1}: Cyclin dependent kinase inhibitor 1B

p53: Tumor suppressor p53

p57^{Kip2}: Cyclin dependent kinase inhibitor 1C

p107: Protein encoded by *RBL1*

p130: Protein encoded by *RBL2*

PBS: Phosphate buffered saline

PCNA: proliferating nuclear cell antigen

PCR: Polymerase chain reaction

PFA: Paraformaldehyde

pH: Potential of Hydrogen

PI: Propidium Iodide

PMSF: Phenylmethylsulfonyl fluoride

pRB: Human retinoblastoma tumor suppressor protein

pRb: Mouse retinoblastoma tumor suppressor protein

qRT-PCR: Quantitative real-time polymerase chain reaction

R: Arginine

***RB1*:** Human retinoblastoma tumor suppressor gene

***Rb1*:** Mouse retinoblastoma tumor suppressor gene

***RB1^C*:** Human retinoblastoma tumor suppressor gene containing the LxCxE binding cleft mutations (Y756W)

***RB1^G*:** Human retinoblastoma tumor suppressor gene containing the general binding mutations (K467E and R548E)

***Rb1^G*:** Mouse retinoblastoma tumor suppressor gene containing the general binding mutations (K461E and R542E)

***RB1^L*:** Human retinoblastoma tumor suppressor gene containing the LxCxE binding cleft mutations (I753A, N757A, M761A)

***Rb1^L*:** Mouse retinoblastoma tumor suppressor gene containing the LxCxE binding cleft mutations (I746A, N750A, M754A)

***RB1^S*:** Human retinoblastoma tumor suppressor gene containing the pRB-E2F1

specific binding site mutations (M851A, V852A)

$Rb1^S$: Mouse retinoblastoma tumor suppressor gene containing the pRB-E2F1 specific binding site mutation (F832A)

RBLP: Large pocket of the retinoblastoma protein

Rev: Reverse PCR primer

RNA: Ribonucleic acid

RTK: Receptor tyrosine kinase

S: Synthesis phase of the cell division cycle

Saos-2: Cell line derived from a primary osteosarcoma

SCF: Skp, Cullin, F-box containing complex

SCLC: Small cell lung cancer

SDS-PAGE: sodium dodecyl sulfate polyacrylamide gel electrophoresis

SKP2: S-phase kinase associated protein 2

Small pocket: Region of the retinoblastoma protein ranging from amino acid 379 to 787

SOS: Son of sevenless

SRR2: Sox2 regulatory region 2

SS: serum starved cells

SV-40 Large T antigen: Simian Vacuolating Virus 40 Tag

TA: Transactivation domain

TGF-β: Transforming growth factor beta

TUNEL: Terminal deoxynucleotidyl transferase dUTP nick end labeling

Tyms: Thymidylate synthase

Ub: Ubiquitination

Table of Contents

List of Tables

List of Figures

List of Appendices

Chapter 1

1 Introduction

1.1 Overview

Cancer can be characterized as an overall loss of homeostasis in a multicellular organism resulting in aberrant growth and the development of a tumor[1]. Over the years, several pathways have been described as playing critical roles in carcinogenesis[1]. Several factors work together to bring about this phenotype, ranging from the ability to proliferate independent of growth signals, to bypassing fail-safe mechanisms designed to inhibit cell growth or initiate programmed cell death in response to aberrant cell growth[1]. Therefore, the mechanisms that are involved in regulating cell cycle control are often targets of cancer causing mutations[1]. Once mutations arise in these critical pathways the affected cell is then capable of bypassing the various tumor suppressive functions and divide uncontrollably resulting in tumor formation. As such, cellular proliferation is a key component of cancer development and progression. Understanding the mechanisms that control proliferation is critical to the development of novel targeted therapies that aim to re-establish proliferative control in cancer cells.

1.2 Cellular division

The process through which cells proliferate is known as the cell division cycle[2]. The cycle is split into 4 main phases separated by 3 checkpoints to regulate the transitions between them (**Figure 1.1**)[3,4]. Cellular division is tightly regulated in the body to ensure that various tissues are sustained at appropriate sizes, and vital structures are maintained[5].
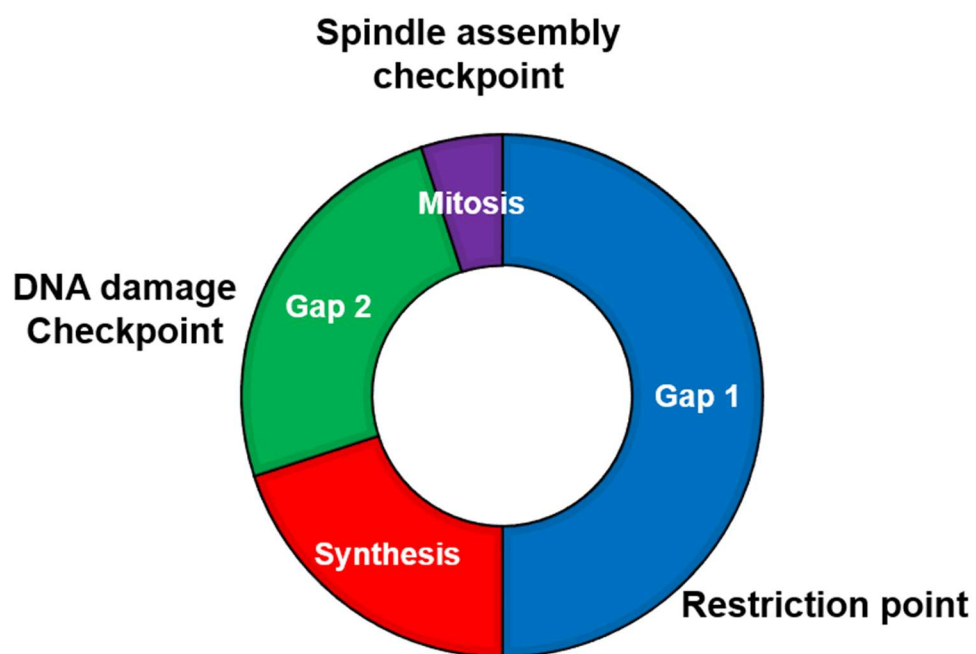
Figure 1.1: Depiction of the mammalian cell cycle.

The 4 phases of the cell cycle are indicated: Gap 1 (G1), Synthesis (S), Gap 2 (G2), and Mitosis (M). Also indicated are the 3 main checkpoints that regulate cell cycle progression at various stages. The restriction point controls the transition between G1 and S-phase ensuring appropriate proliferation. The DNA damage checkpoint occurs in G2 and ensures the DNA is intact prior to Mitosis. Finally, the spindle assemble checkpoint confirms that each chromosome pair is attached to both spindle poles prior to cytokinesis.

As such, several pathways including but not limited to, growth factors, cell to cell contacts and mitogen availability are all important to controlling cellular division[6-8]. Due to the critical involvement of cellular proliferation in carcinogenesis all cancer cells must bypass these growth regulatory pathways[1,6,8]. While normal cells without appropriate signals will not enter the cell cycle, the acquisition of mutations in critical tumor-suppressive or oncogenic pathways can lead to the re-entry of these cells into the cell cycle and potentially lead to tumor development[1,9].

Given the possibility of cancer developing due to a defective cell division cycle, cellular proliferation is tightly controlled to ensure that 2 daughter cells are faithfully produced and only when it is appropriate to do so. For actively cycling normal cells, the first phase of the cell cycle known as Gap 1 phase (G1) in which the cell, through a series of growth signalling pathways, determines if conditions are appropriate to initiate cell cycle progression[10,11]. Additionally, in this phase the cell physically grows and produces a variety of proteins that are needed for DNA replication[12]. Once appropriate conditions are met for cell cycle entry, the cell then transitions into the synthesis-phase also known as S-phase in which DNA is replicated[13]. To ensure that the DNA is only replicated once per division it is critical that once a cell has begun to replicate its DNA that the cell cycle is completed and cells do not revert to an earlier phase[14-16]. Therefore, given the importance of the G1-S transition phase boundary, it is understandable that this transition is tightly regulated and known as the restriction point and the first major checkpoint in the eukaryotic cell cycle (**Figure 1.1**)[15,16].

In late G1 phase, a variety of proteins which are needed for DNA replication are transcribed and translated[17]. These include a number of kinases, transcription factors, as

well as replication fork components[17]. The prereplication complexes are then loaded on the chromatin at origins of replications[18]. Following activation by S-phase kinases these proteins can then unwind the DNA and begin the process of replicating the genome[18]. Since prereplication complexes can only be loaded in G1 this ensures that DNA is only copied once per cell cycle[18]. Once the genome is fully replicated, the cell is then said to be in the Gap 2 phase of the cell cycle or G2. Again, in this phase more proteins and lipids are made in preparation for mitosis. In addition, the G2 phase of the cell cycle also contains a DNA damage checkpoint in which the cell ensures that the genome is intact and fully replicated prior to entry into mitosis (**Figure 1.1**)[19].

During the fourth phase of cell division, mitosis (M-phase), the genome condenses greatly, the nuclear envelop disintegrates, and the duplicated sister chromatids are aligned in the center of the cell at the metaphase plate[20]. The final checkpoint of the cell cycle then ensures that each pair of sister chromatids are bound by a spindle emanating from the centrioles on either side of the cell[21]. Once this is confirmed the sister chromatids are separated and one set is pulled towards each pole located at the periphery of the cell[21]. The cell then pinches in the middle leading to cleavage and the creation of two daughter cells in the G1 phase of the cell cycle through a process known as cytokinesis[22]. While there are 3 main checkpoints in the cell cycle, the G1 restriction point is unique in the ability to determine whether the cell divides or not[12,14,19,21]. The remaining two checkpoints, the G2 DNA damage checkpoint and the spindle assembly checkpoint, are only able to stall the cell cycle and once the problems are corrected the cell then resumes the cell division cycle (**Figure 1.1**)[19,21].

As the G1 to S-phase transition is unique in its ability to determine if the cell will divide or remain quiescent, the pathways involved in this transition are highly regulated[8,14]. Moreover, with the importance of this restriction point in regulating the proliferation of cells it is often targeted by mutation in human cancers[1]. There are several proteins which help to regulate this critical restriction point of the cell cycle[8,10]. These proteins translate intra- and intercellular signals that ultimately influence the activity of two protein families which work in opposition to one another[23]. The branch which promotes cell cycle entry is a group of kinases known as Cyclin dependent kinases (CDKs)[23]. In contrast, a second group known as Cyclin dependent kinase inhibitors (CKIs) works to prevent cell cycle advancement through direct interaction with CDKs, inhibiting their activity[23]. Ultimately, these two sets of proteins determine the activity of one of the key regulators of the G1-S transition, the retinoblastoma tumor suppressor protein (pRB)[24]. The interactions between CDKs, CKIs, and pRB and how they influence one another in the context of cell cycle control is the focus of this thesis.

1.3   Identification of the retinoblastoma susceptibility gene

The retinoblastoma tumor suppressor gene was first predicted through the study of the childhood eye cancer, retinoblastoma[25]. Retinoblastoma presents in two different forms, either unilateral, occurring in one eye, or bilateral, occurring in both eyes[25]. In 1971, Alfred Knudsen discovered that those children developing bilateral retinoblastoma typically had a family history of the disease[25]. These children also developed cancer far earlier than those developing unilateral cancer, which occurred later and typically had no family history of retinoblastoma[25]. From this study Knudsen suggested his 2 hit

hypothesis, which states that the development of retinoblastoma requires the loss or mutation of both copies of a retinoblastoma susceptibility gene[25]. This description of the retinoblastoma susceptibility gene is the first example of a tumor suppressor protein, which has since gone on to describe several proteins involved in the maintenance of cellular homeostasis and the prevention of tumorigenesis.

1.4   Cloning of the RB1 gene.

The susceptibility factor associated with retinoblastoma development predicted by Knudsen in 1971 was eventually found to be contained within a region on the q arm of chromosome 13[26]. In 1986 two independent groups cloned this retinoblastoma susceptibility gene referred to as the retinoblastoma gene (*RB1*)[27,28]. Consistent with Knudsen's hypothesis, patients with heritable forms of retinoblastoma were found to have mutations in one copy of this gene throughout their body[29]. A second genetic event then occurs somatically in the retina leading to the development of retinoblastoma in children. This confirmed Knudsen's two hit hypothesis and identified the first tumor suppressor gene.

This disruption of the *RB1* gene while critical for the development of retinoblastoma started to be seen in other cancers[26,30,31]. First, those patients who survive retinoblastoma as children have a likelihood of developing osteosarcoma far greater than that of the general population[26]. Furthermore, these cancers also displayed the loss of heterozygosity (LOH) or loss of the wild-type allele of the *RB1* gene similar to the development of retinoblastoma[26]. Additionally, direct *RB1* mutation has also been identified in a large majority of small cell lung cancers (SCLC) and a sizable proportion of breast cancers[30,31]. However, typically mutations in the pRB pathway occur upstream of pRB resulting in the

hyperphosphorylation of pRB leading to its functional inactivation[30]. Two of the most common pathway mutations are deletion of p16 or amplification of Cyclin D both of which lead to constitutive pRB hyperphosphorylation, inhibiting its various functions[30] The repercussions of functional disruption of pRB will be discussed later on. The prevalence of pRB pathway disruption through direct or indirect mutation in cancers from various disease sites suggests that the retinoblastoma gene product (pRB) encoded by the *RB1* gene is important in some vital cellular process which cells must bypass to become tumorigenic.

1.5   pRB and viral oncoproteins

Shortly after cloning the *RB1* gene, pRB was shown to directly interact with a variety of viral oncoproteins including HPV-E7, SV-40 Large T antigen and Adenovirus E1A[32-34]. As their name suggests, these viral oncoproteins can transform cells leading to tumorigenesis[35]. Unsurprisingly then, when expressed these viral oncoproteins cause cells to re-enter the cell cycle regardless of the presence or absence of growth factors[35]. Importantly, the association between pRB and viral oncoproteins leads to a disruption of pRB function either through the degradation or sequestration of pRB molecules[36]. Given the importance of pRB in tumor suppression both in retinoblastoma as well as a large variety of other cancers, and the fact that disruption of pRB function by viral oncoproteins is coincident with cellular proliferation, it was suggested that pRB had a role in the regulation of cell cycle progression[32-35] Finally, this role is likely ubiquitous as the regulation of the cell cycle is important in all cells and not just the tumor cells in which they are mutated.

1.6   pRB-family proteins

The pRB family of proteins which consists of pRB, p107, and p130, are collectively known as the pocket proteins as they all contain the characteristic pocket domain[37-39]. Furthermore, these were all identified through their ability to interact with the viral oncoproteins E1A, E7 and SV-40 T antegin[39-41]. The characteristic pocket domain is formed from two cyclin folds in the A and B domains of these proteins and facilitates the association between the pocket protein and the E2 promoter binding factor (E2F) transcription factors (**Figure 1.2**)[42]. While all three proteins contain this structure, p107 and p130 are more similar to each other in terms of sequence and have slightly different pocket domains compared to pRB[37]. In particular, p107 and p130 contain an insertion into the B domain of the pocket which may have implications in regulating their specific binding partners (**Figure 1.2**)[37]. Pocket proteins lack DNA binding ability and therefore must be recruited onto DNA by the various E2Fs with which they associate[43]. This means that chromatin localization relies not on the pocket protein itself but rather the consensus sequence of the E2F transcription factors. Furthermore, in addition to binding to E2F transcription factors, pocket proteins can also act as a scaffold to bring much larger complexes to specific locations on the DNA which can further repress transcription[44].

1.7   Regulation of pocket proteins

The ability of the pocket proteins to influence E2F transcription factors is regulated by two independent factors, expression and phosphorylation status. In general, the expression of p107 and p130 fluctuate throughout the cell cycle with p130 being expressed at high levels in quiescence, or G0 of the cell cycle and diminishing as the cell progresses through G1 and S[37]. p107 by contrast, is most highly expressed in S-phase as
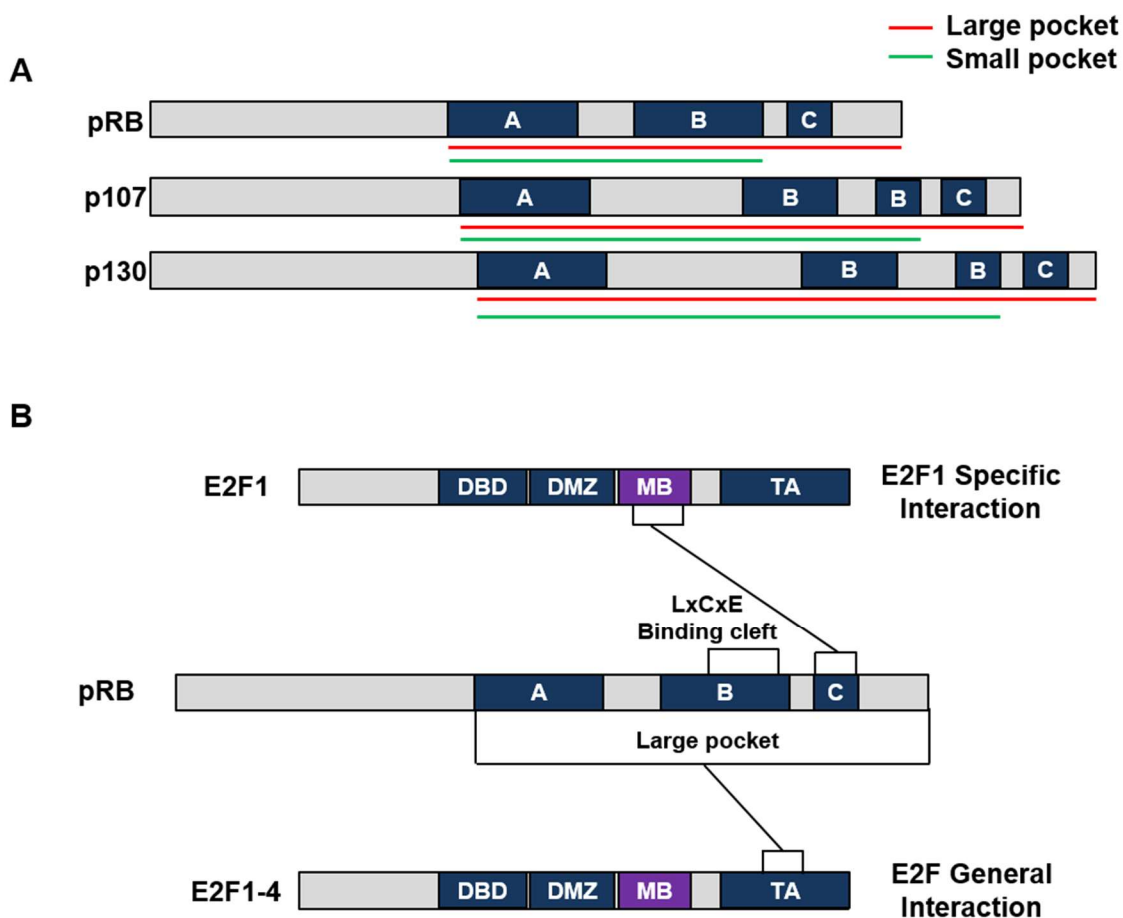
Figure 1.2: Domain structure and interaction surfaces of pocket proteins.

(A) The A, B, and the C-terminal domains are shown for all 3 pocket proteins. The large pocket is denoted by the red line and the small pocket is identified by the green line. **(B)** The three large pocket interaction sites in pRB are shown. These are the E2F general interaction facilitated by the entire large pocket, the LxCxE binding cleft located in the B region of the pocket and the E2F1 specific interaction site which associates with pRB through an interaction site in the C-terminus.

it is a target of E2F dependent transcription[37]. pRB, on the other hand remains relatively stable throughout the cell cycle with a slight increase in expression in S-phase due to E2F dependent transcription[37]. The relative stability of pRB expression throughout the cell cycle indicates that control of its function is largely independent of transcription and is controlled instead by post-translational modifications, in particular phosphorylation[45]. Phosphorylation of pRB as well as the other pocket proteins is largely carried out by Cyclin/CDK complexes[45,46]. Once a cell is stimulated to divide there is an increase in the activity of Cyclin/CDK complexes leading to the phosphorylation of pRB disrupting various interactions due to conformational changes[45,46].

1.8   Structure of pRB

The retinoblastoma gene product (pRB) is a globular protein which contains several interacting domains which together regulate numerous cellular proteins influencing the cell cycle[45,47]. The majority of these characterized domains are located in the C-terminal two thirds of the protein which is referred to as the large pocket (**Figure 1.2A**)[47]. The large pocket itself is made up of 3 main structures, the A and B domains each comprise of cyclin folds which are joined together with a spacer creating the small pocket (**Figure 1.2A**)[42]. The large pocket is made up of this small pocket and the unstructured C-terminal domain[47]. This thesis focuses on three independent binding interactions located in the large pocket of pRB. These interactions are known as the general E2F binding site, the LxCxE binding cleft and the E2F1 specific binding site (**Figure 1.2B**)[42,45,48].

1.9 pRB-E2F interactions

First, and most well known of the various pRB interactors are the E2F transcription factors[43]. This interaction is facilitated through the pocket domain of pRB and is involved in pRB-mediated regulation of the cell cycle[43]. The importance of pRB-E2F regulation in the cell cycle was initially identified through the use of Saos-2 arrest assays[49,50]. In these early experiments, it was shown that the minimal interacting domain necessary for pRB-E2F association was also able to initiate a cell cycle arrest when expressed in Saos-2 cells[49,50]. Given this correlation, it is logical to assume that pRB-E2F interaction is critical to regulation of the restriction point[49,50]. However, as shown in **Figure 1.2**, the minimal domain required for pRB-E2F interaction, the large pocket, also contains a least two other binding surfaces, the LxCxE binding cleft and the C-terminal E2F1 specific interaction site (**Figure 1.2B**)[42,50,51]. This suggests that the ability of pRB to regulate the cell cycle may be dependent on several interactions not just pRB binding to E2Fs.

1.10 Disruption of pRB by viral oncoproteins

Of particular note both viral oncoproteins, HPV-E7 and Adenovirus E1A have multiple domains that are required for the effective association and inactivation of pRB as well as their ability to transform cells[52,53]. HPV-E7 eliminates pRB function by targeting the protein for degradation[53]. As such, HPV-E7 requires both the CR2 domain which contains the LxCxE motif to associate with pRB, as well as the CR1 domain which recruits additional factors targeting the protein for degradation[35,53]. Additionally, the C-terminus of HPV-E7 contains a low affinity pRB binding domain which is thought to interact with the pRB-E2F binding pocket preventing E2F binding[35]. By contrast, E1A eliminates pRB function through sequestration of pRB preventing it from functioning

properly[53]. E1A contains two binding domains that are essential to oncogenic

transformation[52]. The CR1 domain mimics the transactivation domain of E2F and binds

in the pocket of pRB, this however is not sufficient to transform cells[52]. The CR2 domain

of E1A contains the LxCxE domain which also allows for association between pRB and

E1A, however, once again this is not sufficient to allow for oncogenic transformation[52].

The requirement for disruption of both the pocket domain and the LxCxE binding domain

to successfully sequester pRB was some of the first evidence that pRB-E2F interactions

are not solely responsible for the tumor suppressive abilities of pRB. Presented in this

thesis are experiments which attempt to further explore the various functions of pRB

outside of the dogma of pRB repressing E2F dependent transcription.

1.11   E2F transcription factors as regulators of the cell cycle

The E2F proteins are a family of transcription factors which bind to a variety of target

gene promoters to influence transcription necessary for regulating cell cycle entry[54]. This

family can be further divided into transcriptional activators (E2F1-3) and transcriptional

repressors (E2F4-5)[54]. Finally, there are three atypical E2Fs, (E2F6-8) whose function is

currently being explored, but are generally thought to be repressive and function

independently of pocket proteins[55]. Together with their dimerization partner,

Differentiation related transcription factor-1 polypeptide-1 (DP1) the activator E2Fs form

a heterodimer which binds to promoters of genes involved in DNA synthesis and cell

cycle progression[54]. Critically, activator E2Fs (E2F1-3) have been shown to be necessary

to allow for cellular division[56]. This function of E2F transcription factors is facilitated

through the transactivation domain located in the C-terminus of the activator E2Fs[54]. This

domain is responsible for recruiting transcriptional co-activators such as p300 leading to the upregulation of genes important for S-phase progression[43]. Importantly, in cells stimulated to enter the cell cycle, E2F target genes are greatly upregulated coincident with S-phase entry and DNA synthesis[43]. To prevent aberrant cell cycle entry, pRB regulates E2F-mediated transcription through the pRB pocket domain[45]. pRB is unique among pocket proteins for its ability to bind to activator E2Fs (E2F1-3), in addition to the repressor E2F4[43,57]. By contrast p107 and p130 both only associate with the repressive E2Fs (E2F4-5)[43]. This pocket formed between the A and B domains in pRB creates a docking site which binds to the transactivation domain of E2F1-4[45]. This interaction precludes any recruitment of co-activators by E2Fs preventing the upregulation of genes that are necessary to drive the cell into S-phase (**Figure 1.3**)[58]. Finally, by high jacking E2F DNA binding ability, pRB can act as a scaffold recruiting a variety of chromatin remodeling factors which can further condense chromatin and prevent the transcription of E2F targets (**Figure 1.3**)[46,59,60].

1.12   Additional RB binding sites

The characteristic pocket domain of pRB is created through the folding together of the two cyclin folds in the small pocket of pRB known as the A and B domain (**Figure 1.2**)[45]. In addition to contributing to the small pocket binding domain, the B-domain of pRB also contains a protein interacting region known as the LxCxE binding cleft[47]. This surface is so named as viral oncoprotein binding to pRB is mediated through the LxCxE peptide sequence present on these viral oncoproteins[61]. In addition to being a binding site for viral oncoproteins that inactivate pRB, several cellular proteins have now been
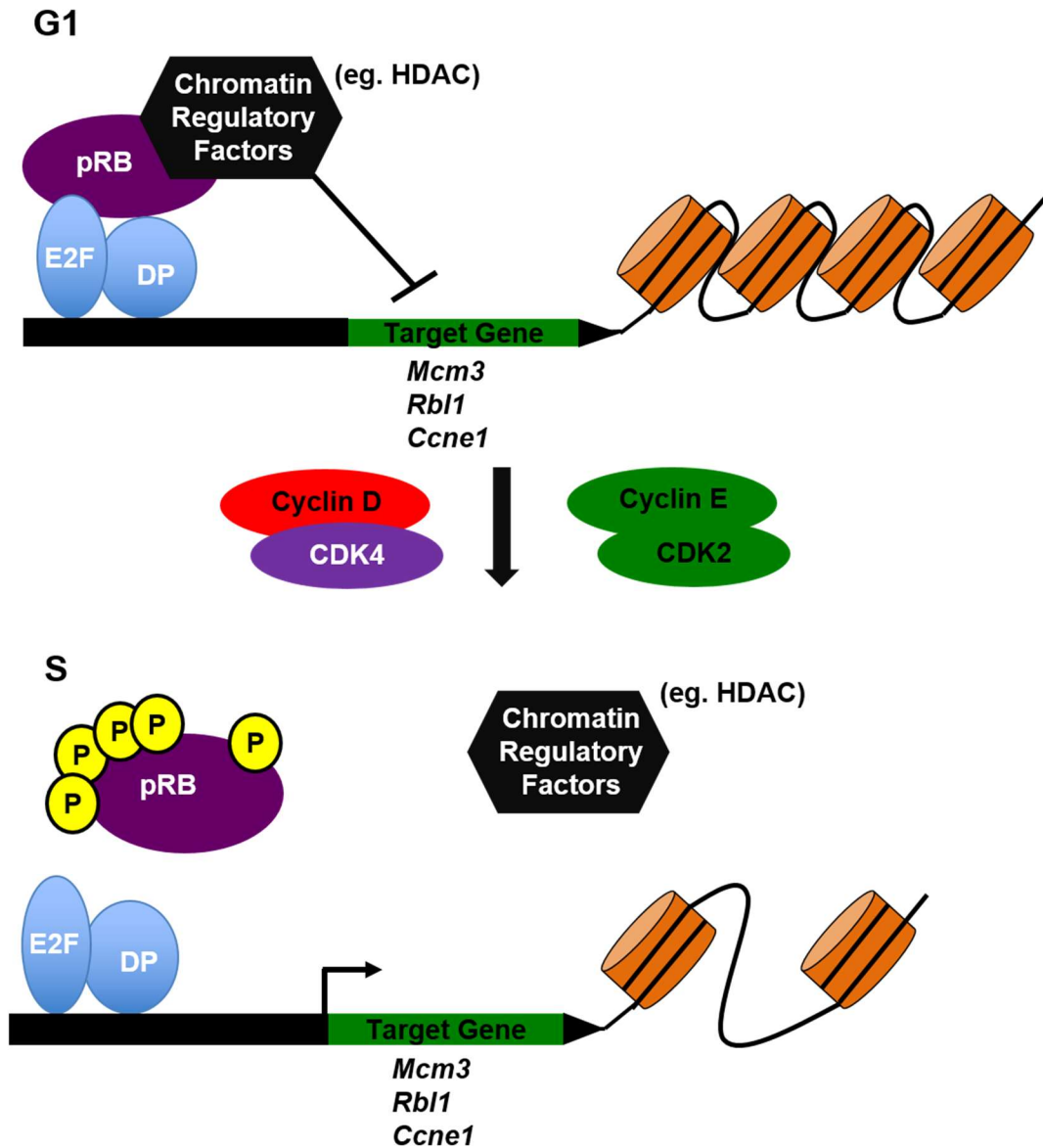
Figure 1.3: Regulation of the G1 to S-phase transition by pRB.

In G1 hypophosphorylated pRB binds to E2F/DP heterodimers masking their ability to stimulate the transcription of genes including but not limited to *Mcm3, Rbl1,* and, *Ccne1*, which are required for cell cycle entry. Additionally, pRB can recruit chromatin regulatory factors (CRFs) through its LxCxE binding cleft, which compact the DNA at these genes further repressing transcription. Once the cell is stimulated to divide an increase in Cyclin/CDK activity, particularly Cyclin E/CDK2 and Cyclin D/CDK4/6, results in the hyperphosphorylation of pRB. These phosphorylation events lead to large scale conformational changes to the pRB protein resulting in the disruption of both E2F/DP interactions and interactions with LxCxE interactors including Chromatin regulatory factors. E2F/DP heterodimers are then capable of stimulating S-phase required genes promoting cell cycle entry.

suggested to interact with pRB through the LxCxE binding cleft[47,62]. Some of these proteins include a variety of chromatin remodelers such as HDACs, and Condensin II, which influence the accessibility of chromatin to transcriptional machinery[44,60,61,63]. Interestingly, as pRB contains no known DNA binding activity, pRB is carried to E2F target genes essentially changing the E2F-DP transcription factor from a transcriptional activator into a repressive complex[43]. This is accomplished both by the masking of the transactivation domain on E2F as well as the recruitment of chromatin remodelers which further compact chromatin preventing transcription specifically at genes regulated by E2Fs. Finally, a third binding site exists in the C-terminus of pRB which has been less well characterized as the other two, through which E2F1 can bind to pRB in a unique conformation[51]. This interaction has recently been established as a method through which pRB can inhibit the expression of repeat elements in the genome, such as endogenous retroviruses[60].

The combined action of pRB direct inhibition of the transactivation domain of E2Fs and the recruitment of chromatin remodelers together comprise a model of cell cycle restriction and tumor suppression through the which pRB inhibits the expression of genes required for S-phase progression (**Figure 1.3**). However recent findings have presented doubt on this dogma. As an example, the development of mutations which target pRB transcriptional regulation have relatively minimal effects on the cell cycle regulatory functions of pRB[48,64,65]. In this thesis, I explore the importance of the transcriptional independent functions of pRB and present evidence which disputes this linear view of pRB function at the G1 to S transition (**Figure 1.3**).

1.13　Regulation of pRB activity by CDK phosphorylation

Expression of pRB is relatively stable throughout the cell cycle and in fact increases as the cell progresses through S-phase[37]. This increase is a result of an increase in E2F activity as the *RB1* gene is upregulated by E2F transcription factors[66]. Given that pRB is an inhibitor of S-phase entry, increasing expression of *RB1* during this transition implies that the regulation of the RB protein is controlled not through transcription. In addition to the increased protein levels as the cell progresses through G1 and into S-phase, pRB becomes hyperphosphorylated (**Figure 1.3**)[67]. pRB contains no less than 13 CDK phosphorylation sites which are located throughout the protein, primarily in intrinsically disordered regions[45]. These sites are targeted by Cyclin D/CDK4/6 complexes as well as Cyclin A/E /CDK2 complexes[67]. Importantly, Cyclin/CDK complexes are the main proteins responsible for driving the cell cycle, further supporting the role of pRB as a repressor of cell cycle progression[68].

Once activated, the Cyclin/CDK phosphorylation of pRB results in the compaction of the pRB protein in such a way that it no longer has open binding surfaces in the large pocket (**Figure 1.4**)[45]. The pRB N-terminus and the pocket domain fold together due to phosphorylation at T373 (**Figure 1.4**)[45]. The linker present in the B-Box becomes phosphorylated at S608 and S612, and sits in the E2F binding site, and the pRB C-terminus is phosphorylated at residues T821 and T826 causing folding into the LxCxE binding cleft (**Figure 1.4**)[45]. The result of these phosphorylation events is the disruption of both the pRB-E2F general interaction and the LxCxE binding cleft (**Figure 1.4**)[45].
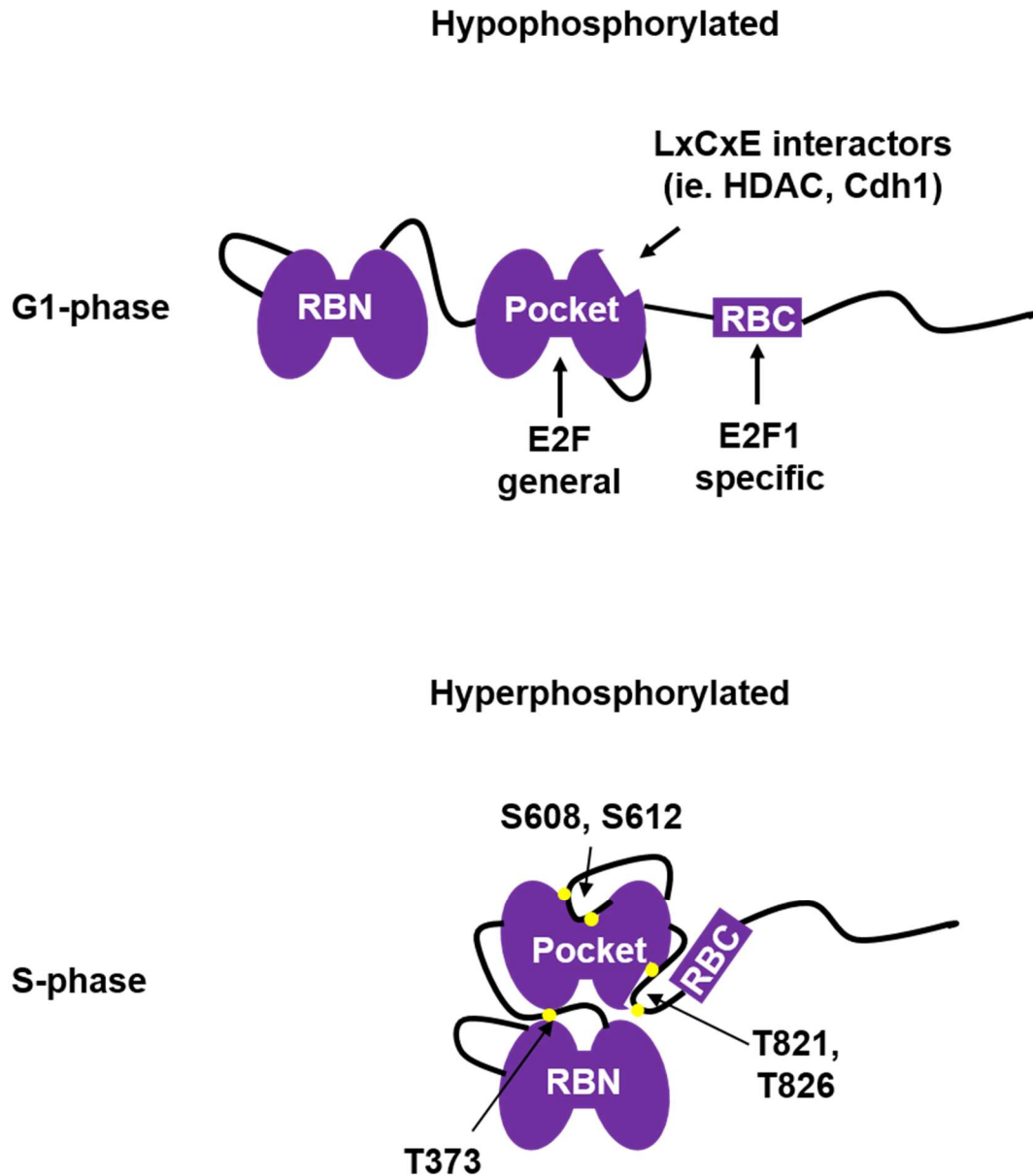
Figure 1.4: Compaction of pRB following phosphorylation.

When pRB is hypophosphorylated in the G1 phase of the cell cycle all three of the interaction surfaces in the pRB large pocket, the E2F general site, LxCxE binding cleft and the E2F1 specific site are free to bind their ligands. In S-phase, pRB is hyperphosphorylated leading to compaction of the pRB molecule through the interaction of the pRB N-terminal domain (RBN) binding to the Pocket domain controlled by phosphorylation at T373. Furthermore, E2F general interactions and the LxCxE interactions are disrupted through phosphorylation and docking of the pocket loop (S608, S612) and pRB C-terminal domain (RBC) (T821, T826) respectively. Yellow circles denote phosphorylation events.

Importantly, this compaction of the pRB protein suggests that both the LxCxE binding

cleft and pocket domain are important for cell cycle control. However, classical models

of pRB cell cycle restriction suggest that the LxCxE binding cleft is responsible for

compacting chromatin around E2F target genes preventing their transcription (**Figure

1.3**)[45]. If this is in fact the case, disruption of the LxCxE binding cleft would be

unnecessary as loss of E2F interaction with pRB would prevent LxCxE interactors from

associating with E2F target genes. This begs the question, why are LxCxE interactors

also perturbed by pRB phosphorylation? The disruption of the LxCxE binding cleft by

pRB compaction following phosphorylation suggests that the LxCxE binding cleft can

facilitate interactions when not bound to DNA that are important to the tumor-

suppressive function of pRB.

1.14   Cell cycle entry as controlled by pRB

Once a cell is stimulated to divide, a variety of signal transduction pathways are

activated leading to cellular division. One critical pathway involved in transducing

extracellular signals to trigger cellular division is the Ras/MAPK pathway[2]. Following

stimulation by growth factors, membrane spanning cell surface receptor tyrosine kinases

(RTKs) lead to the activation of Ras, triggering a signaling cascade which ultimately

results Myc activation[2]. Myc then initiates a transcriptional program that promotes cell

cycle progression[69]. This includes the upregulation of Cyclins, E2Fs, as well as the

repression of CKIs[69]. The increased CDK4/6 activity through the increased expression of

Cyclin D promoted by Myc activity results in the phosphorylation of pRB at several CDK

sites located in unstructured regions of the protein[70,71]. These phosphorylation events

trigger the conformational shift in pRB described above resulting in the disruption of

pRB function[45]. This structural change prevents both the pocket of pRB from associating with E2Fs as well as the large variety of LxCxE interactors from binding the LxCxE binding cleft[45]. Activator E2Fs are then free to recruit transcriptional co-factors enhancing the transcription of S-phase genes including Cyclins, replication complex members, and many other genes required for cellular division[54]. Critically, one such E2F target gene is *CCNE1* which encodes for Cyclin E which together with CDK2 forces the G1 to S-phase transition committing the cell to the cell cycle (**Figure 1.5**)[67,72]. This feed forward loop ensures that the cell proceeds through the entire cell cycle regardless of continual stimulation[73]. This allows pRB to translate the various growth stimulating signals into an all or nothing E2F response, which, once activated, will complete the cell cycle independent of stimulation by serum or other growth factors[73]. Taken together this suggests that pRB is a critical gate-keeper of the G1 to S-phase transition, and ultimately the cell division cycle.

The study of pRB-E2F interactions has largely focused on the transition from the G1 to S-phase of the cell cycle. As such the majority of experiments have been performed in quiescent cells that are stimulated to divide[43]. Coincident with cell cycle entry, pRB becomes hyperphosphorylated and E2F target gene expression levels increase[74,75]. Importantly, activator E2Fs (E2F1-3) have been shown to be required to allow for cell cycle entry[56,74,75]. Finally, the overexpression of E2F1 in quiescent cells was sufficient to drive the cell into S-phase as denoted by BrdU incorporation[76]. While this model has been well established for cell cycle entry far fewer studies have looked at cell cycle exit, an oversight pointed out in 1998 by Dyson in his seminal review[43].
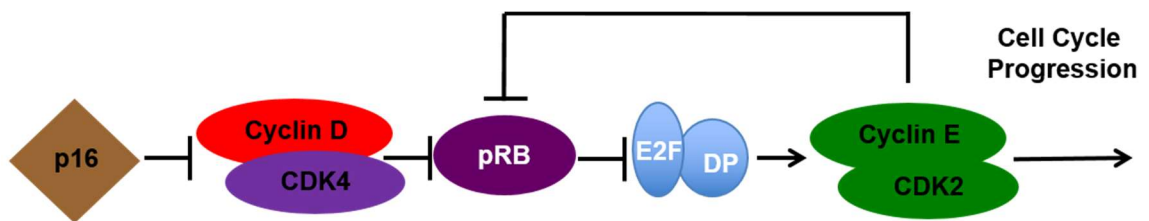
Figure 1.5: Schematic representation of the pRB pathway.

The activity of pRB is controlled largely by phosphorylation. When there is increased Cyclin D/CDK4 activity due to increased expression or loss of p16 inhibition, pRB becomes hyperphosphorylation. This allows for the release of E2F transcription factors and the upregulation of S-phase genes including Cyclin E. Cyclin E/CDK2 complexes are responsible for further inactivating pRB through hyperphosphorylation as well as driving the cell into S-phase.

1.15   Consequences of pRB loss *in vivo*

In 1992, to better understand the role of the *Rb1* gene, three knockout mouse models

of pRb loss were created resulting in animals which do not express pRb[77-79]. Loss of pRb

is relatively well tolerated in early embryogenesis and *Rb1*^{-/-} knockout embryos are

indistinguishable from littermates[77]. However, loss of pRb results in embryonic lethality

between E14 and E15 days of gestation[77]. This is largely attributed to hyperplasia

occurring in the trophoblasts of the placenta[80]. This overgrowth leads to decreased space

between the mother and fetal blood supply and subsequent reduction of nutrient flow to

the developing embryo[80]. Interestingly if the *Rb1*^{-/-} embryo is supplemented with a

normal placenta the embryos can develop normally until birth[80,81]. These animals die

shortly after birth due to inadequate skeletal muscle development in the diaphragm

preventing the newborn lungs from inflating properly[81]. Additionally, fibroblasts isolated

from *Rb1*^{-/-} embryos have demonstrated that pRB plays key roles in the ability of cells to

respond appropriately to a variety of cellular stressors including DNA damage, serum

starvation, TGF-β treatment, expression of p16 as well as others[64,82-84]. Consistent with

the established paradigm of pRB-mediated regulation of cell cycle control through the

disruption of E2F driven transcription, codeletion of *E2f1* or *E2f3* with *Rb1* loss, partially

rescued pRb deletion resulting in prolonged viability of embryos extending life from E14

to E17.5 days[54,85,86].

While complete *Rb1* knockout is embryonic lethal, mice which are heterozygous

for the *Rb1* gene (*Rb1*^{+/-}) do develop normally into adulthood[77,87,88]. Beginning around

300 days of age *Rb1*^{+/-} mice develop pituitary adenocarcinomas arising from the

intermediate lobe of the pituitary[64,87-89]. Importantly, this occurs following loss of

heterozygosity of the wild-type allele of *Rb1*[90]. This genetic alteration results in an *Rb1*

null cell which has already bypassed all the developmental problems associated with *Rb1*

homozygous deletion[77]. These cells then have perturbed cell cycle control, and following

additional mutations in critical pathways can develop into pituitary tumors[64,87,88].

Furthermore, several groups have created conditional knockout models of pRB[91-94].

While it is beyond the scope of this thesis to discuss all the various conditional knockouts

of pRb, some studies have demonstrated a loss of cell cycle control and hyperplasia in

conjugation with deregulation of E2F transcription factor activity however, this is far

from consistent and E2F target gene expression changes are not always the most dramatic

shifts in the transcriptome[91-94].

Lastly, 2 groups in 1994 independently developed chimeric mouse models of pRb

loss[95,96]. These animals contained cells harboring homozygous deletion of the *Rb1* gene

as well as heterozygous *Rb1*^{+/-} cells[95,96]. Surprisingly, the contribution of some

heterozygous *Rb1*^{+/-} cells is sufficient to allow for proper development, despite the a

large proportion of *Rb1*^{-/-} cells in these mice making up 40% to 80% of a given tissue[96].

Similar to *Rb1*^{+/-} mice these chimeric animals develop pituitary adenocarcinomas at an

accelerated rate[96]. These studies demonstrate that even in the case of a complete loss of

pRb, cells they can still differentiate and contribute to tissues in an adult animal.

Overall, mouse models lacking pRb have played a significant role in determining the

effect of pRB on development as well as tumorigenesis. Homozygous deletion of *Rb1* is

embryonic lethal in mice due to hyperplasia of the placenta and subsequent starvation of

the embryo[77,80]. Interestingly, *Rb1*^{+/-} animals bypasses the embryonic lethality, however

eventually loss of the wild-type allele of *Rb1* allows for the development of a tumor

phenotype later in life (~300 days)[64,87-89]. This type of genetic background is more

representative of children with retinoblastoma. Most often, these children inherent one

copy of the *RB1* gene which is mutated and develop the second mutation somatically[25].

This eventually leads to the formation of the retinoblastoma. This finding that both alleles

of the *Rb1* gene must be deleted to form tumors in mice supports Knudsen's two hit

hypothesis[25,90].

1.16 Regulation of pRB through CDK phosphorylation

pRB is typically regulated through phosphorylation[67]. This phosphorylation leads to

the compaction of the pRB protein blocking the various binding surfaces in the large

pocket, releasing E2Fs, and allowing the cell to move into S-phase (**Figure 1.4**)[45]. These

phosphorylation marks are added by a family of proteins known as the Cyclin dependent

kinases (CDKs)[68]. These complexes are made up of two individual proteins, the catalytic

CDK protein and a regulatory Cyclin component[68]. In general, CDK levels are relatively

stable throughout the cell cycle however the specific Cyclins associated with them

fluctuate greatly depending on the phase of the cell cycle (**Figure 1.6**)[4]. This ensures that

the correct CDK is activated during the right phase of the cell cycle, resulting in one

complete round of DNA synthesis and division only when instructed to do so by various

signals.

1.17 CDK activity throughout the cell cycle

There are 4 main Cyclin/CDK pairs that regulate the mammalian cell cycle[68].

Beginning in G1, a variety of growth factors such as EGF bind to receptors on the surface

of cells[2]. This signal is then propagated through a number of signalling kinases, in the
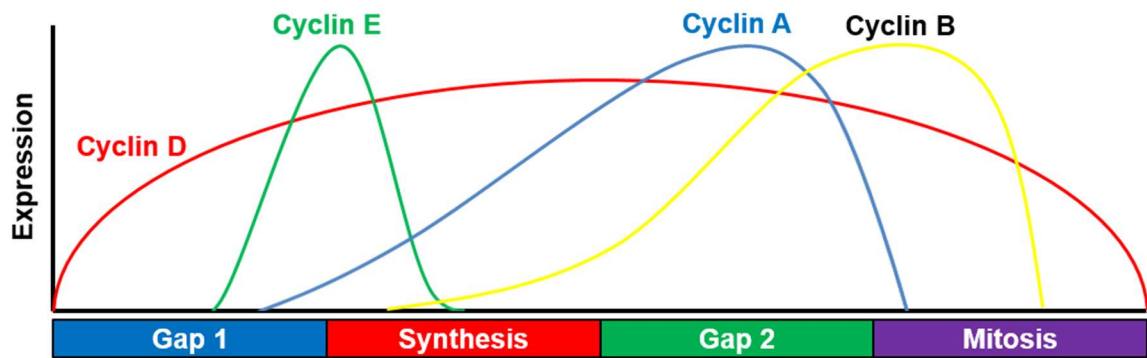
Figure 1.6: Expression patterns of various Cyclins control cell cycle progression.

Idealized expression patterns of 4 key Cyclins over the course of the cell cycle. Once expressed each Cyclin can associate with its catalytic partner CDKs facilitating the phosphorylation of substrates necessary for that particular section of the cell cycle. In general, Cyclin D is expressed beginning in G1 and persists through mitosis. By comparison Cyclin E, Cyclin A, and Cyclin B all peak at more defined times, G1-S, G2, and mitosis respectively.

case of EGF, the Ras, Raf, MAPK pathway[97]. The expression of Cyclin D is then upregulated, which can bind to its catalytic subunits, CDK4 or CDK6[97]. This complex is then able to bind to and phosphorylate pRB[98]. E2F-DP transcription factors are then free to activate transcription of S-phase required genes[98]. One critical gene activated by E2F transcription factors is *CCNE1* which encodes for the Cyclin E protein[72]. Once in complex with CDK2, Cyclin E/CDK2 phosphorylates a variety of targets that are necessary for DNA synthesis including the firing of pre-replication complexes[68,99]. Importantly, Cyclin E/CDK2 complexes also phosphorylate pRB ensuring that the cell continues through S-phase and completes cellular division before returning to a G1 state[100]. As the cell progresses through DNA synthesis phase, Cyclin A, another E2F target gene, replaces Cyclin E as the regulator subunit of CDK2[68,101]. Finally, after the cell has completed DNA synthesis and traversed the G2 phase, the final of the 4 main Cyclin/CDK complexes Cyclin B and its binding partner CDK1 drive the cell through mitosis[68]. These 4 complexes together control the cell cycle[68]. Importantly, cell cycle regulation by Cyclin A/CDK2 and Cyclin B/CDK1 complexes can only be temporarily stalled via the DNA damage and spindle assembly checkpoints[19,21]. This leaves regulation at the G1 to S-phase boundary the critical road block in the prevention of aberrant cell growth[24]. As such this transition is highly regulated through both Cyclin/CDK activity as well as by pRB, and pathways influencing these genes are often targets of cancer causing mutations[30,102]. These two pathways form a critical hub through which a variety of signals are funneled determining if the cell will divide or not.

1.18 Cyclin dependent kinase inhibitors and their role in regulating the cell cycle.

Transcriptional control of Cyclins ensures that the appropriate CDK is activated during the proper phase of the cycle[103]. In addition to this regulation, Cyclin/CDK complexes are further controlled by 2 families of CKIs which further influence the cell cycle[104,105]. The two families are divided up based on the CDK complexes which they can inhibit[104,106]. First, the INK4 family consists of 4 members p14, p15, p16, and p18, all of which are specific inhibitors of Cyclin D/CDK4/6 complexes and are involved in cellular senescence, apoptosis and DNA repair (**Figure 1.7**)[105,106]. As these proteins specifically influence Cyclin D/CDK4/6 activity, their role is primarily contained to the G1 phase of the cell cycle[105,106]. The second family of CKIs is the CIP/KIP family which is made up of p21, p27 and p57 (**Figure 1.7**)[104]. These proteins more broadly influence the activity of CDKs as there can inhibit all 4 major Cyclin/CDK complexes which drive the mammalian cell cycle[68,104]. Similarly, CIP/KIP family proteins are responsible for arresting the cell in response to a variety stimuli such as genetic insults or loss of mitogen signalling[107]. This family is more universal than the INK4 family as they can inhibit many CDKs and as such can elicit a cell cycle arrest in multiple phases of the cell cycle[108].

While the three members of the CIP/KIP family of proteins are capable of interacting with the same Cyclin/CDK complexes, each member is expressed in different circumstances[104]. In particular, p21 is critical to the DNA damage response and its expression is directly regulated in response to p53 activation[109]. By contrast, p27 is more typically associated with the G1 phase of the cell cycle and is involved in cell cycle arrest
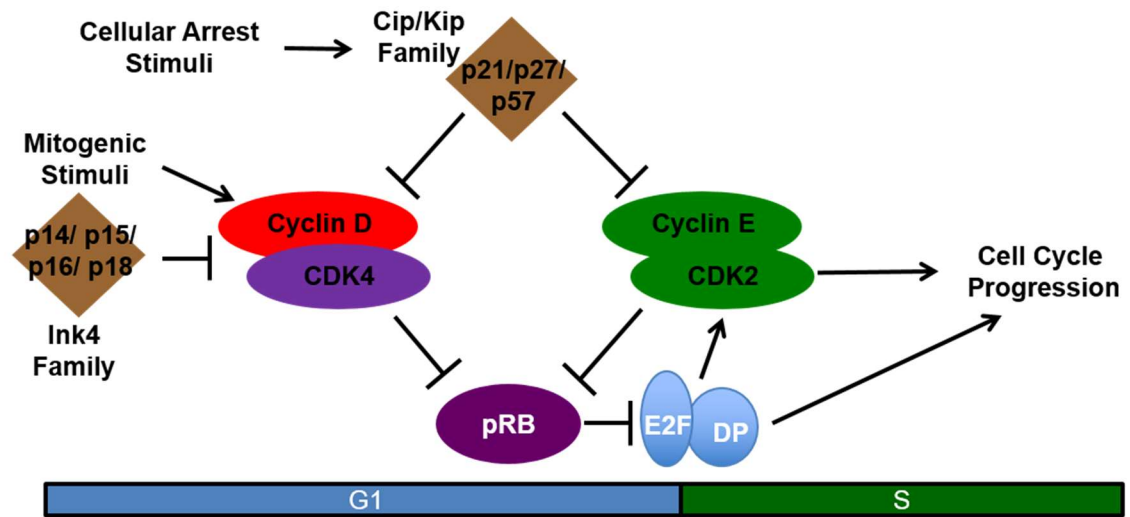
Figure 1.7: Schematic representation of the G1-S-phase transition of the cell cycle.

Following mitogenic stimulation in the G1 phase of the cell cycle an increase in Cyclin D/ CDK4/6 activity hyperphosphorylates pRB, releasing the E2F/DP transcription factor. Once free, E2F upregulates several genes including *CCNE1,* encoding for Cyclin E, which together with CDK2 can also phosphorylate pRB. This creates a feed forward loop ensuring that once started the cell cycle is completed. In addition, two families of Cyclin dependent kinase inhibitor CKIs restrict the activity of Cyclin/CDKs. The Ink4 family consists of p14, p15, p16, and p18, and inhibits Cyclin D/ CDK4/6 complexes. The CIP/KIP family consists of p21, p27, and p57 which can broadly inhibit Cyclin/ CDK complexes. The activity of these CKIs are influences by both extracellular cues such at mitogen deprivation as well as intracellular cues such as DNA damage. The overall balance of Cyclin/CDKs and CKIs determine whether the cell will enter the cell cycle.

following growth factor deprivation, TGF-β treatment, as well as contact inhibition[104]. Finally, p57 appears to be involved primarily in development as p57 knockout animals die immediately following birth due to several developmental defects including cleft plate, abdominal muscle defect as well as skeletal defects[104]. The balance of Cyclin/CDKs and CKI expression together determine the overall activity of the various Cyclin/CDK complexes and ultimately whether the cell will undergo division[104,105,108]. Additionally, this interplay also underpins the cellular arrest in response to various stimuli such as DNA damage, quiescence induction and differentiation[104].

The precise balance of Cyclin/CDK complexes to CKIs is critical to determine whether a cell will traverse the G1 to S phase checkpoint. Once kinase activity, in particular Cyclin E/CDK2, reaches a certain threshold the cell activates a feed forward cascade which commits the cell to division[110]. This feed forward loop is initiated by Cyclin E/CDK2-mediated phosphorylation of pRB[110]. As discussed above these phosphorylation events result in a conformational change in the pRB molecule, releasing E2Fs causing the expression of *CCNE1* and *CCNA2,* both of which complex with CDK2 further phosphorylating pRB molecules[45,72,101]. This loop ensures that pRB is maintained in a hyperphosphorylated state throughout S-phase and G2 allowing for the expression of E2F target genes which are needed to complete DNA replication and the cell cycle[67]. In addition to phosphorylating pRB, Cyclin/CDKs also target a variety of cellular proteins, including transcription factors and most importantly activate a cascade leading to the firing of replication origins, beginning the process of DNA replication[68,111]. Importantly, while pRB can influence cell cycle progression at the G1 to S-phase boundary, ultimately S-phase entry is determined by the overall level of CDK activity and in particular Cyclin

E/CDK2 activity (**Figure 1.7**)[68,111]. Therefore, the combined inputs of pRB-mediated repression of *CCNE1* and the expression of CKIs control CDK activity and cell cycle progression. Both the pRB and CKI pathways play integral roles in regulating CDKs and the cell cycle and the interconnectedness of these two pathways, suggests that there could be some level of redundancy involved between them (**Figure 1.7**).

1.19   Disruption of the pRB pathway in cancer

Given that pRB acts as a critical gate-keeper to cellular division it is perhaps unsurprising that the pRB pathway is perturbed in a large majority of human cancers[30]. Interestingly however, mutations in pRB itself is relatively rare outside of small cell lung cancer, retinoblastoma and osteosarcoma[30]. Instead upstream disruption of the kinases involved in phosphorylating pRB are targeted for mutation resulting in constitutive pRB hyperphosphorylation, inhibiting its various functions[30]. The complete disruption of the pRB protein by phosphorylation in the majority of cancers suggests pRB performs multiple critical functions to maintain cell cycle control and is not limited solely to the repression of E2Fs[30].

Early Saos-2 cell cycle arrest assays demonstrated that the minimal region of pRB capable of arresting the cell cycle was also capable of binding E2Fs[49,50]. Importantly, this fragment also contains the LxCxE binding cleft which binds several cellular proteins (**Figure 1.2B**)[47,49,50]. More recently, Soas-2 arrest assays were performed using the partial penetrant familial retinoblastoma mutant *RB1^{R661W}* [112]. This mutant has defective binding to E2F-DP heterodimers and gives rise to benign retinomas and rare retinoblastoma in children[112,113]. Surprisingly however, this mutant version of pRB is still capable of restricting the cell cycle when expressed in Saos-2 cells despite the apparent lack of E2F

repression[112]. It is important to note, however, that the $RB1^{R661W}$ mutant does have partial

disruption of LxCxE interactions and the G1 cell cycle arrest conveyed in Saos-2 cells is

unstable[112]. These results provided an important basis for the study of pRB-mediated cell

cycle control independent of E2F, however given the caveats associated with the

$RB1^{R661W}$ mutation a new model was needed.

1.20   Development of the $Rb1^{G/G}$ mouse model

Building on the results from Sellers *et al.* demonstrating that the E2F-binding

deficient mutant $RB1^{R661W}$ could induce a G1 cell cycle arrest in Saos-2 cells, Cecchini *et*

al. developed a targeted mutation in the pRB pocket which successfully disrupted the

ability of pRB from associating with E2Fs through the pocket domain (**See appendix**

A)[64,65]. This mutation referred to as the $RB1^G$ mutation contains two amino acid

substitutions (K467E and R548E) which change key pocket residues from a basic charge

to an acidic one[64]. This therefore prevents the pocket from binding to the acidic regions in

the transactivation domain of E2F leading to charge repulsion and an inability to bind

pRB[65]. As expected, cells homozygous for the $Rb1^G$ mutation do show a loss of pRb

binding to E2F target gene promoters as pRb can no longer be carried to promoters via

E2Fs[64]. Consistent with this finding, the depletion of pRb from the DNA results in an

increase in the expression of E2F target genes[64]. Surprisingly, despite the loss of E2F

repression caused by the $Rb1^G$ mutation, these cells eventually give rise to viable animals,

which display no overt phenotype[64]. These mice developed normally, are fertile and show

no tumor phenotype or lifespan changes[64]. This is in direct contrast to complete knockout

of the *Rb1* gene, which, as previously mentioned is embryonic lethal between E14 and

E15[77]. Taken together, this suggests that E2F regulation by pRB is dispensable for pRB-mediated development and tumor-suppression.

The role for pRB in cell cycle control has been well established as cells lacking pRB are not capable of appropriately restricting cell cycle entry following treatment with a variety of conditions[82-84]. Interestingly, when $Rb1^{G/G}$ cells were deprived of serum or treated with ionizing radiation, a successful G1 cell cycle arrest occurred as efficiently as wildtype cells[64]. Furthermore, even in this context, $Rb1^{G/G}$ cells still maintain elevated levels of E2F target gene expression, equivalent to $Rb1^{-/-}$ cells which failed to arrest[64]. These experiments indicated that E2F regulation by pRB is dispensable to enact a G1 cell cycle arrest in response to cellular stressors. While this finding was surprising, it is important to note that the majority of studies highlighting the importance E2F in cell cycle focus on its ability to stimulate the entry into S-phase of the cell cycle[43]. However, consistent with the importance of E2F target gene induction in cell cycle entry, $Rb1^{G/G}$ cells stimulated to divide from a quiescent state entered the cell cycle far earlier than wildtype cells and at a similar rate to $Rb1^{-/-}$ cells[64].

This study identified that the linear model of pRB regulation of the cell cycle through the repression of E2Fs is incomplete, at least for cell cycle exit[64]. Therefore, additional pathways must be active to arrest the cell following treatment with these agents. As discussed above, Cyclin/CDK complexes are crucial to cell cycle progression[68]. When a cell must arrest the cell cycle due to DNA damage or serum deprivation CKIs become active, inhibiting the activity of Cyclin/CDK complexes[104,105]. This then leads to the hypophoshorylation of pRB preventing the activity of E2F transcription factors. Additionally, the inhibition of Cyclin E/CDK2 by CKIs prevent the firing of replication

origins which is the definitive transition from G1-S phase[111]. Furthermore, as Cyclin E expression is regulated by E2F activity, Cyclin E/CDK2 therefore is upstream and downstream of pRB regulation[72]. Therefore, in the context of $Rb1^{G/G}$ cells, perhaps the arrest is achieved through the direct inhibition of Cyclin E/CDK2, independent of E2F repression. Lastly, this function must be pRB dependent as $Rb1^{-/-}$ cells are incapable of initiating an arrest under the same conditions that lead to an arrest in $Rb1^{G/G}$ cells[64].

1.21   E2F independent regulation of the cell cycle by pRB

One possible explanation for the G1 cell cycle arrest in $Rb1^{G/G}$ cells which is independent of E2F regulation is through the CKI p27[64]. Previous work has identified that $RB1^{R661W}$ can initiate a G1 cell cycle arrest in Soas-2 cells despite lacking the ability to associate with E2Fs[112]. Ji *et al.* confirmed this finding and showed that both wild-type $RB1$ and the mutant $RB1^{R661W}$ increased the protein level of p27 coincident with cell cycle arrest in Saos-2 cells[114]. Higher expression of p27 in turn can inhibit the activity of Cyclin E/CDK2 and prevent cell cycle progression[68]. Importantly, p27 has also been implicated in regulating a variety of oncogenic and tumor-suppressive functions in addition to CDK inhibition[115]. These non-canonical functions of p27 will be discussed in greater detail at the end of this thesis as they will be more relevant in the context of some experiments performed. Finally, given the inability of $RB1^{R661W}$ to associate with E2Fs, any regulation must exist independent of transcriptional control[113].

1.22   Modulation of p27 activity through the cell cycle.

The level of p27 is generally controlled by the rate at which it is degraded (**Figure 1.8**)[99]. During cell cycle initiation, p27 is degraded through the combined activity of
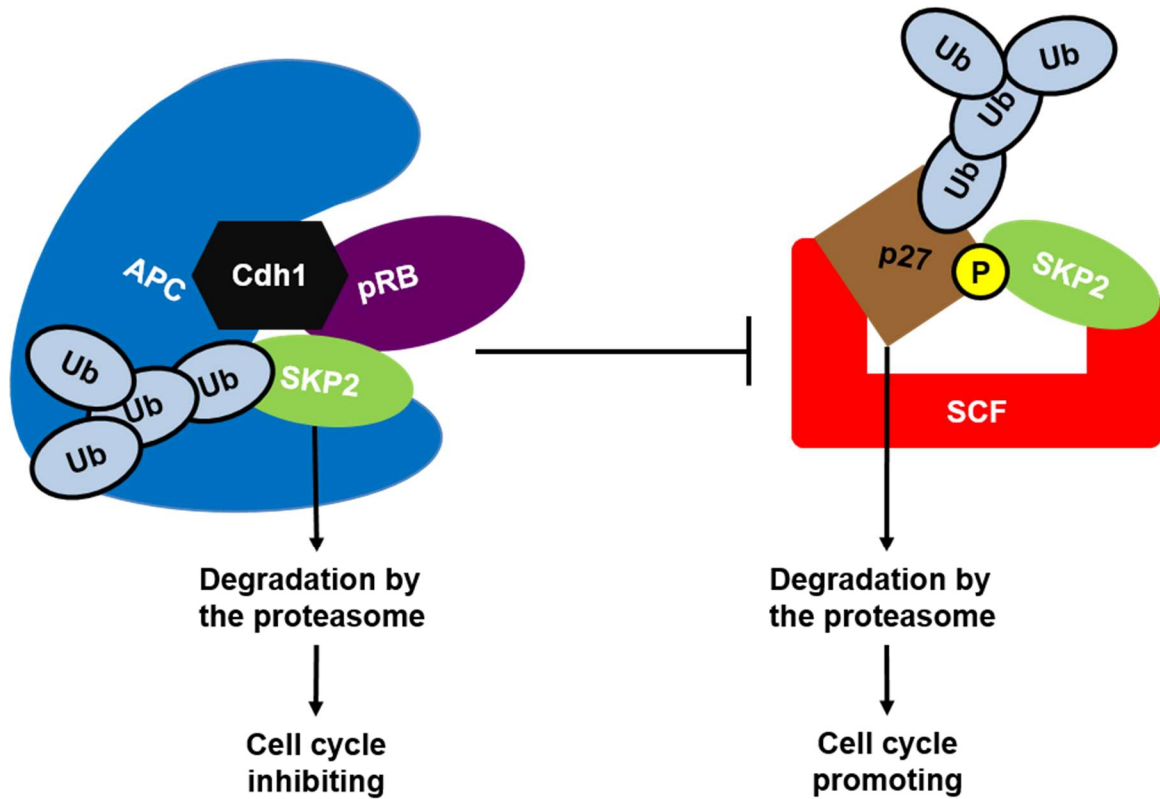
Figure 1.8: Schematic representation of E2F-independent pRB-mediated cell cycle regulation through the pRB-SKP2-p27 axis.

pRB associates with both the anaphase promoting complex containing Cdh1 (APC^{Cdh1}) and SKP2. By serving as a scaffold, pRB facilitates poly-ubiquitination (Ub) of SKP2 by the APC^{Cdh1}. The degradation of SKP2 prevents p27 polyubiquitination by the SCF complex as SKP2 is required for p27 targeting. The pRB-mediated ubiquitination and subsequent degradation of SKP2 by the APC^{Cdh1} and the proteasome results in the stabilization of p27 and inhibition of the cell cycle.

CDK phosphorylation and degradation by the proteasome allowing for the cell to progress into S-phase[99]. This degradation is primarily controlled by the SCF complex containing the targeting E3 ligase SKP2[116]. Following CDK phosphorylation of p27, SKP2 can associate with p27 resulting in the poly-ubiquitination of p27 targeting it to the proteasome for degradation[116]. As SKP2 is the protein involved in targeting p27 for poly-ubiquitination, this reaction is controlled by the level of available SKP2 to associate with the SCF complex[116].

The involvement of pRB in regulating p27 in this manner has been analyzed in two landmark studies[114,117]. Collectively, these reports demonstrate that pRB is capable of binding to both SKP2 as well as the Cdh1 containing APC complex (APC^{Cdh1}) (**Figure 1.8**)[114,117]. Importantly, APC^{Cdh1} has ubiquitin ligase activity and is active in G1 to poly-ubiquitinate a large variety of proteins, including those involved in mitosis leading to their degradation[118]. This ensures that the cell is returned to a G1 state prior to re-entering the cell cycle[118]. One such target of the APC^{Cdh1} is SKP2, which when degraded, effectively stabilizes p27 (**Figure 1.8**)[116,119]. The finding that pRB can bind to both APC^{Cdh1} and SKP2 suggest that pRB may be acting as a scaffold to facilitate the degradation of SKP2[114,117]. Furthermore, the ability of pRB to interact with SKP2 and stabilize p27 is maintained when the *RB1^{R661W}* is expressed in Soas-2 cells indicating that E2F binding is not required for this process[114].

This second axis of pRB-mediated cell cycle control is particularly intriguing as it appears to be E2F independent and functional in cells containing *RB1^{R661W}*[114]. Previous work has created a mouse model harboring the equivalent mutation to R661W in mice (*Rb1^{R654W}*) which displayed a similar phenotype to *Rb1$^{-/-}$* animals dying embryonically

due to placental defects[120]. This effect is less severe however as *Rb1^R654W* animals survive slightly longer dying around E15 to E17[120]. Importantly, in addition to disrupting pRB-E2F interactions, this mutation also partially disrupts LxCxE interactors which may also have roles in regulating the cell cycle[121]. By contrast, the *Rb1^G/G* mutant mice developed by Cecchini *et al.* contain a much more targeted mutation which specifically eliminated pRB-E2F interactions through the general site while maintaining LxCxE interaction and the pRB-E2F1 specific interaction[64]. Moreover, *Rb1^G/G* mutant animals are viable and show no long-term consequences of E2F deregulation[64]. This implies that pRB must be playing additional roles to regulate the cell cycle independent of E2F repression. The pRB-SKP2-p27 axis of regulation discussed above is an intriguing possibility to account for the dispensability of pRB-E2F interactions (**Figure 1.8**). The *Rb1^G/G* model allows for the unique opportunity to study E2F independent regulation of cell cycle control and tumor suppression by pRB, including the pRB-SKP2-p27 axis, in an *in vivo* context.

1.23   Objectives

One of the main functions of pRB-mediated cell cycle control is the repression of E2F transcription factors preventing the upregulation of genes required for S-phase progression[10]. However, considering recent evidence discussed in the introductory chapter it is now clear that explanation is not complete[64,112,114]. Instead, it suggests that pRB can regulate the cell cycle though multiple pathways influencing the G1 to S-phase transition. The *Rb1^G/G* mouse model developed in our lab provides an excellent tool to study these alternative functions of pRB[64]. Given the normal development and lifespan of the *Rb1^G/G* mice we can combine these mice with other mutant mouse strains to attempt

to recapitulate the phenotype of $Rb1^{-/-}$ mice thereby accounting for all the functions of RB-mediated cell cycle control and tumor suppression[64,77].

In the first chapter I characterized the pRB-p27 axis of pRB-mediated cell cycle control. I hypothesized that the maintenance of cell cycle control in $Rb1^{G/G}$ cells is due to the stabilization of p27 mediated by the LxCxE binding cleft on pRB[114,117]. By combining our $Rb1^{G/G}$ mutant mice with those harboring a null allele for p27 ($Cdkn1b^{-/-}$), we could address the importance of the pRB-p27 axis of pRB tumor suppression both in cell culture and *in vivo*[122]. Using double mutant $Rb1^{G/G}$; $Cdkn1b^{-/-}$ cells as well as single mutant controls I analyzed the ability of cells to arrest the cell cycle under different treatment conditions. Furthermore, we were then able to confirm these results in the double mutant $Rb1^{G/G}$; $Cdkn1b^{-/-}$ mice. These results will be discussed in detail in chapter 2 of this thesis.

In addition to the pRB-mediated regulation of E2F and p27, several other proteins interact with pRB and as such may influence the cell cycle or tumor-suppressive properties of pRB[47,51,62]. As such we hypothesized that the three distinct binding surfaces in the pRB large pocket discussed above play a role in regulating the function of pRB. Using mutations developed in our lab we could individually and simultaneously disrupt the general pRB-E2F pocket, the LxCxE binding cleft, and the pRB-E2F1 specific interaction[62,65,123]. Following expression of these mutant versions of $RB1$ in Saos-2 cells we can directly measure the contribution that each individual binding surface makes towards pRB-mediated G1 arrest. Further, by intercrossing our $Rb1^{G/G}$; $Cdkn1b^{-/-}$ mice generated in chapter two into the E2f1 null background we could create an *in vivo* model of disruption of all three binding surfaces. Analysis of livers was carried out to determine

if we had in fact recapitulated *Rb1* loss in adult tissues. A detailed description of the results of these experiments can be found in chapter 3 of this thesis.

pRB pathway mutations have been well documented in a variety of human cancers[30]. As discussed in the introduction, the majority of these mutations occur upstream of pRB leading to hyperphosphorylation and inactivation of the pRB protein[30]. This finding suggests that single point mutations which target a specific domain such as the E2F binding pocket on pRB would be ineffective in eliminating pRB functionality. This hypothesis is further collaborated by the lack of effect on tumor suppression displayed by the *Rb1*[G] mutation[64]. However, the disruption of pRB-E2F interactions would reduce the pathways through which pRB can regulate the cell cycle and thus we hypothesized that *Rb1*[G/G] would display increased sensitivity to tumorigenesis when combined with activated oncogenes or loss of tumor-suppressors. In chapter 4 I tested this hypothesis by combining our *Rb1*[G/G] mutant animals with three different genetic backgrounds. The *Rb1*[G/G] mutation was introduced into mouse lines containing oncogenic *Kras*[G12D], or deletions of p53 or p21 tumor suppressors[64,124-127]. Detailed explanations of the results of these experiments are presented in chapter 4.

1.24   References

1   Hanahan, D. & Weinberg, R. A. Hallmarks of cancer: the next generation. *Cell* **144**, 646-674, doi:10.1016/j.cell.2011.02.013 (2011).

2   Coleman, M. L., Marshall, C. J. & Olson, M. F. RAS and RHO GTPases in G1-phase cell-cycle regulation. *Nat Rev Mol Cell Biol* **5**, 355-366, doi:10.1038/nrm1365 (2004).

3   Kastan, M. B. & Bartek, J. Cell-cycle checkpoints and cancer. *Nature* **432**, 316-323, doi:10.1038/nature03097 (2004).

4   Malumbres, M. & Barbacid, M. Cell cycle, CDKs and cancer: a changing paradigm. *Nat Rev Cancer* **9**, 153-166, doi:10.1038/nrc2602 (2009).

5   Hafen, E. & Stocker, H. How are the sizes of cells, organs, and bodies controlled? *PLoS Biol* **1**, E86, doi:10.1371/journal.pbio.0000086 (2003).

6   Pruitt, K. & Der, C. J. Ras and Rho regulation of the cell cycle and oncogenesis. *Cancer Lett* **171**, 1-10 (2001).

7   Gumbiner, B. M. Cell adhesion: the molecular basis of tissue architecture and morphogenesis. *Cell* **84**, 345-357 (1996).

8   Massague, J. G1 cell-cycle control and cancer. *Nature* **432**, 298-306 (2004).

9   Sherr, C. J. & McCormick, F. The RB and p53 pathways in cancer. *Cancer Cell* **2**, 103-112 (2002).

10   Sherr, C. J. G1 phase progression: cycling on cue. *Cell* **79**, 551-556 (1994).

11   Vermeulen, K., Van Bockstaele, D. R. & Berneman, Z. N. The cell cycle: a review of regulation, deregulation and therapeutic targets in cancer. *Cell Prolif* **36**, 131-149 (2003).

12   Pardee, A. B. G1 events and regulation of cell proliferation. *Science* **246**, 603-608 (1989).

13   Bartek, J. & Lukas, J. Pathways governing G1/S transition and their response to DNA damage. *FEBS Lett.* **490**, 117-122 (2001).

14   Zetterberg, A., Larsson, O. & Wiman, K. G. What is the restriction point? *Current opinion in Cell Biology* **7**, 835-842 (1995).

15   Blagosklonny, M. V. & Pardee, A. B. The restriction point of the cell cycle. *Cell Cycle* **1**, 103-110 (2002).

16   Planas-Silva, M. D. & Weinberg, R. A. The restriction point and control of cell proliferation. *Curr Opin Cell Biol* **9**, 768-772 (1997).

17   Bell, S. P. & Dutta, A. DNA replication in eukaryotic cells. *Annual review of biochemistry* **71**, 333-374, doi:10.1146/annurev.biochem.71.110601.135425 (2002).

18   Cimbora, D. M. & Groudine, M. The control of mammalian DNA replication: a brief history of space and timing. *Cell* **104**, 643-646 (2001).

19   O'Connell, M. J., Walworth, N. C. & Carr, A. M. The G2-phase DNA-damage checkpoint. *Trends in cell biology* **10**, 296-303 (2000).

20   Nigg, E. A. Mitotic kinases as regulators of cell division and its checkpoints. *Nat Rev Mol Cell Biol* **2**, 21-32, doi:10.1038/35048096 (2001).

21   Musacchio, A. & Hardwick, K. G. The spindle checkpoint: structural insights into dynamic signalling. *Nat Rev Mol Cell Biol* **3**, 731-741, doi:10.1038/nrm929 (2002).

22   Glotzer, M. Animal cell cytokinesis. *Annu Rev Cell Dev Biol* **17**, 351-386, doi:10.1146/annurev.cellbio.17.1.351 (2001).

23   Lim, S. & Kaldis, P. Cdks, cyclins and CKIs: roles beyond cell cycle regulation. *Development* **140**, 3079-3093, doi:10.1242/dev.091744 (2013).

24   Weinberg, R. A. The retinoblastoma protein and cell cycle control. *Cell* **81**, 323-330, doi:0092-8674(95)90385-2 [pii] (1995).

25   Knudson, A. G., Jr. Mutation and cancer: statistical study of retinoblastoma. *Proc Natl Acad Sci U S A* **68**, 820-823 (1971).

26   Dryja, T. P. *et al.* Chromosome 13 homozygosity in osteogenic sarcoma without retinoblastoma. *Am. J. Hum. Genet.* **38**, 59-66 (1986).

27   Friend, S. H. *et al.* A human DNA segment with properties of the gene that predisposes to retinoblastoma and osteosarcoma. *Nature* **323**, 643-646 (1986).

28   Lee, W. H. *et al.* Human retinoblastoma susceptibility gene: Cloning, identification, and sequence. *Science* **235**, 1394-1399 (1987).

29   Dryja, T. P. *et al.* Homozygosity of chromosome 13 in retinoblastoma. *N Engl J Med* **310**, 550-553 (1984).

30   Burkhart, D. L. & Sage, J. Cellular mechanisms of tumour suppression by the retinoblastoma gene. *Nat Rev Cancer* **8**, 671-682, doi:nrc2399 [pii]10.1038/nrc2399 (2008).

31   Bosco, E. E. & Knudsen, E. S. RB in breast cancer: at the crossroads of tumorigenesis and treatment. *Cell Cycle* **6**, 667-671, doi:10.4161/cc.6.6.3988 (2007).

32   Dyson, N., Buchkovich, K., Whyte, P. & Harlow, E. The cellular 107K protein that binds to adenovirus E1A also associates with the large T antigens of SV40 and JC virus. *Cell* **58**, 249-255 (1989).

33   DeCaprio, J. A. *et al.* SV40 large tumor antigen forms a specific complex with the product of the retinoblastoma susceptibility gene. *Cell* **54**, 275-283 (1988).

34   Whyte, P. *et al.* Association between an oncogene and an anti-oncogene: the adenovirus E1A proteins bind to the retinoblastoma gene product. *Nature* **334**, 124-129 (1988).

35   Helt, A. M. & Galloway, D. A. Mechanisms by which DNA tumor virus oncoproteins target the Rb family of pocket proteins. *Carcinogenesis* **24**, 159-169 (2003).

36   Vousden, K. H. Regulation of the cell cycle by viral oncoproteins. *Semin Cancer Biol* **6**, 109-116, doi:10.1006/scbi.1995.0014 (1995).

37   Classon, M. & Dyson, N. p107 and p130: versatile proteins with interesting pockets. *Exp Cell Res* **264**, 135-147, doi:10.1006/excr.2000.5135S0014-4827(00)95135-8 [pii] (2001).

38   Zhu, L. *et al.* Inhibition of cell proliferation by p107, a relative of the retinoblastoma protein. *Genes Dev* **7**, 1111-1125 (1993).

39   Li, Y., Graham, C., Lacy, S., Duncan, A. M. & Whyte, P. The adenovirus E1A-associated 130-kD protein is encoded by a member of the retinoblastoma gene family and physically interacts with cyclins A and E. *Genes Dev* **7**, 2366-2377 (1993).

40   Cobrinik, D., Whyte, P., Peeper, D. S., Jacks, T. & Weinberg, R. A. Cell cycle-specific association of E2F with the p130 E1A-binding domain. *Genes and Development* **7**, 2392-2404 (1993).

41   Mayol, X. *et al.* Cloning of a new member of the retinoblastoma gene family (pRb2) which binds to the E1A transforming domain. *Oncogene* **8**, 2561-2566 (1993).

42   Lee, J.-O., Russo, A. A. & Pavletich, N. P. Structure of the retinoblastoma tumour-suppressor pocket domain bound to a peptide from HPV E7. *Nature* **391**, 859-865 (1998).

43   Dyson, N. The regulation of E2F by pRB-family proteins. *Genes Dev* **12**, 2245-2262 (1998).

44   Talluri, S. & Dick, F. A. Regulation of transcription and chromatin structure by pRB: here, there and everywhere. *Cell Cycle* **11**, 3189-3198, doi:10.4161/cc.21263 (2012).

45   Dick, F. A. & Rubin, S. M. Molecular mechanisms underlying RB protein function. *Nat Rev Mol Cell Biol* **14**, 297-306, doi:10.1038/nrm3567 (2013).

46   Giacinti, C. & Giordano, A. RB and cell cycle progression. *Oncogene* **25**, 5220-5227 (2006).

47   Dick, F. A. Structure-function analysis of the retinoblastoma tumor suppressor protein - is the whole a sum of its parts? *Cell Div* **2**, 26 (2007).

48   Dick, F. A. & Dyson, N. pRB contains an E2F1-specific binding domain that allows E2F1-induced apoptosis to be regulated separately from other E2F activities. *Mol Cell* **12**, 639-649 (2003).

49   Hiebert, S. W. - Regions of the retinoblastoma gene product required for its interaction with the E2F transcription factor are necessary for E2 promoter repression and pRb-mediated growth suppression. - *Mol Cell Biol* **- 13**, - 3384-3391 (1993).

50   Qin, X. Q., Chittenden, T., Livingston, D. M. & Kaelin, W. G., Jr. Identification of a growth suppression domain within the retinoblastoma gene product. *Genes Dev* **6**, 953-964 (1992).

51   Dick, F. A. & Dyson, N. pRB Contains an E2F1 Specific Binding Domain that Allows E2F1 Induced Apoptosis to be Regulated Separately from other E2F Activities. *Mol Cell* **12**, 639-649 (2003).

52   Pelka, P., Ablack, J. N., Fonseca, G. J., Yousef, A. F. & Mymryk, J. S. Intrinsic structural disorder in adenovirus E1A: a viral molecular hub linking multiple diverse processes. *J Virol* **82**, 7252-7263, doi:10.1128/JVI.00104-08 (2008).

53   McLaughlin-Drubin, M. E. & Munger, K. The human papillomavirus E7 oncoprotein. *Virology* **384**, 335-344, doi:10.1016/j.virol.2008.10.006 (2009).

54   Chen, H. Z., Tsai, S. Y. & Leone, G. Emerging roles of E2Fs in cancer: an exit from cell cycle control. *Nat Rev Cancer* **9**, 785-797, doi:nrc2696 [pii]10.1038/nrc2696 (2009).

55   Lammens, T., Li, J., Leone, G. & De Veylder, L. Atypical E2Fs: new players in the E2F transcription factor family. *Trends in cell biology* **19**, 111-118, doi:10.1016/j.tcb.2009.01.002 (2009).

56   Wu, L. *et al.* The E2F1-3 transcription factors are essential for cellular proliferation. *Nature* **414**, 457-462 (2001).

57   Bertoli, C., Skotheim, J. M. & de Bruin, R. A. Control of cell cycle transcription during G1 and S phases. *Nat Rev Mol Cell Biol* **14**, 518-528, doi:10.1038/nrm3629 (2013).

58   Harbour, J. W. & Dean, D. C. Rb function in cell-cycle regulation and apoptosis. *Nat Cell Biol* **2**, E65-67, doi:10.1038/35008695 (2000).

59   Coschi, C. H. *et al.* Haploinsufficiency of an RB-E2F1-Condensin II complex leads to aberrant replication and aneuploidy. *Cancer discovery* **4**, 840-853, doi:10.1158/2159-8290.CD-14-0215 (2014).

60   Ishak, C., Marshall, AE., Passos, DT., White, CR., Kim, SJ., Cecchini, MJ., Ferwati, S., MacDonald, WA., Howlett, CJ., Welch, ID., Rubin, SM., Mann, MRW., and Dick, FA. An RB-EZH2 Complex Mediates Silencing of Repetitive DNA Sequences. *Molecular Cell*, doi:http://dx.doi.org/10.1016/j.molcel.2016.10.021 (2016).

61   Brehm, A. *et al.* Retinoblastoma protein recruits histone deacetylase to repress transcription. *Nature* **391**, 597-601, doi:10.1038/35404 (1998).

62   Dick, F. A., Sailhamer, E. & Dyson, N. J. Mutagenesis of the pRB pocket reveals that cell cycle arrest functions are separable from binding to viral oncoproteins. *Mol Cell Biol* **20**, 3715-3727 (2000).

63   Coschi, C. H. *et al.* Mitotic chromosome condensation mediated by the retinoblastoma protein is tumor-suppressive. *Genes Dev* **24**, 1351-1363, doi:10.1101/gad.1917610 (2010).

64   Cecchini, M. J. *et al.* A retinoblastoma allele that is mutated at its common E2F interaction site inhibits cell proliferation in gene-targeted mice. *Mol Cell Biol* **34**, 2029-2045, doi:10.1128/MCB.01589-13 (2014).

65   Cecchini, M. J. & Dick, F. A. The biochemical basis of CDK phosphorylation-independent regulation of E2F1 by the retinoblastoma protein. *Biochem J* **434**, 297-308, doi:10.1042/BJ20101210 (2011).

66   Hamel, P. A., Gill, R. M., Phillips, R. A. & Gallie, B. L. Transcriptional repression of the E2-containing promoters EIIaE, c-myc, and RB1 by the product of the RB1 gene. *Mol. Cell. Biol.* **12**, 3431-3438 (1992).

67   Mittnacht, S. Control of pRB phosphorylation. *Current Opinion in Genetics and Development* **8**, 21-27 (1998).

68   Hydbring, P., Malumbres, M. & Sicinski, P. Non-canonical functions of cell cycle cyclins and cyclin-dependent kinases. *Nat Rev Mol Cell Biol* **17**, 280-292, doi:10.1038/nrm.2016.27 (2016).

69   Bretones, G., Delgado, M. D. & Leon, J. Myc and cell cycle control. *Biochimica et biophysica acta* **1849**, 506-516, doi:10.1016/j.bbagrm.2014.03.013 (2015).

70   Mateyak, M. K., Obaya, A. J. & Sedivy, J. M. c-Myc regulates cyclin D-Cdk4 and -Cdk6 activity but affects cell cycle progression at multiple independent points. *Mol Cell Biol* **19**, 4672-4683 (1999).

71   Connell-Crowley, L., Harper, J. W. & Goodrich, D. W. Cyclin D1/Cdk4 regulates retinoblastoma protein-mediated cell cycle arrest by site-specific phosphorylation. *Mol. Biol. Cell.* **8**, 287-301 (1997).

72   Ohtani, K., DeGregori, J. & Nevins, J. R. Regulation of the cyclin E gene by transcription factor E2F1. *Proc Natl Acad Sci U S A* **92**, 12146-12150 (1995).

73   Yao, G., Lee, T. J., Mori, S., Nevins, J. R. & You, L. A bistable Rb-E2F switch underlies the restriction point. *Nat Cell Biol* **10**, 476-482, doi:10.1038/ncb1711 (2008).

74   Mudryj, M. *et al.* Cell cycle regulation of the E2F transcription factor involves an interaction with cyclin A. *Cell* **65**, 1243-1253 (1991).

75   Chittenden, T., Livingston, D. M. & DeCaprio, J. A. Cell cycle analysis of E2F in primary human T cells reveals novel E2F complexes and biochemically distinct forms of free E2F. *Mol Cell Biol* **13**, 3975-3983 (1993).

76   Johnson, D. G., Schwarz, J. K., Cress, W. D. & Nevins, J. R. Expression of transcription factor E2F1 induces quiescent cells to enter S phase. *Nature* **365**, 349-352 (1993).

77   Jacks, T. *et al.* Effects of an Rb mutation in the mouse. *Nature* **359**, 295-300 (1992).

78   Clarke, A. R. *et al.* Requirement for a functional Rb-1 gene in murine development. *Nature* **359**, 328-330 (1992).

79   Lee, E. Y. *et al.* Mice deficient for Rb are nonviable and show defects in neurogenesis and haematopoiesis. *Nature* **359**, 288-294 (1992).

80   Wu, L. *et al.* Extra-embryonic function of Rb is essential for embryonic development and viability. *Nature* **421**, 942-947 (2003).

81   de Bruin, A. *et al.* Rb function in extraembryonic lineages suppresses apoptosis in the CNS of Rb-deficient mice. *Proc Natl Acad Sci U S A* **100**, 6546-6551 (2003).

82   Herrera, R. E., Makela, T. P. & Weinberg, R. A. TGFB-induced growth inhibition in primary fibroblasts requires the retinoblastoma protein. *Molecular Biology of the Cell* **7**, 1335-1342 (1996).

83   Harrington, E. A., Bruce, J. L., Harlow, E. & Dyson, N. pRB plays an essential role in cell cycle arrest induced by DNA damage. *Proc Natl Acad Sci U S A* **95**, 11945-11950 (1998).

84   Medema, R. H., Herrera, R. E., Lam, F. & Weinberg, R. A. Growth suppression by p16ink4 requires functional retinoblastoma protein. *Proc. Natl. Acad. Sci. USA* **92**, 6289-6293 (1995).

85   Tsai, K. Y. *et al.* Mutation of E2f-1 suppresses apoptosis and inappropriate S phase entry and extends survival of Rb-deficient mouse embryos. *Mol Cell* **2**, 293-304 (1998).

86   Chong, J. L. *et al.* E2f3a and E2f3b contribute to the control of cell proliferation and mouse development. *Mol Cell Biol* **29**, 414-424, doi:MCB.01161-08 [pii]10.1128/MCB.01161-08 (2009).

87   Harrison, D. J., Hooper, M. L., Armstrong, J. F. & Clarke, A. R. Effects of heterozygosity for the Rb-1t19neo allele in the mouse. *Oncogene* **10**, 1615-1620 (1995).

88   Hu, N. *et al.* Heterozygous Rb-1 delta 20/+mice are predisposed to tumors of the pituitary gland with a nearly complete penetrance. *Oncogene* **9**, 1021-1027 (1994).

89   Yamasaki, L. *et al.* Loss of E2F-1 reduces tumorigenesis and extends the lifespan of Rb1(+/-)mice. *Nat Genet* **18**, 360-364 (1998).

90   Williams, B. O. *et al.* Cooperative tumorigenic effects of germline mutations in Rb and p53. *Nat Genet* **7**, 480-484 (1994).

91   Kareta, M. S. *et al.* Inhibition of pluripotency networks by the Rb tumor suppressor restricts reprogramming and tumorigenesis. *Cell Stem Cell* **16**, 39-50, doi:10.1016/j.stem.2014.10.019 (2015).

92   Mayhew, C. N. *et al.* Liver-specific pRB loss results in ectopic cell cycle entry and aberrant ploidy. *Cancer Res* **65**, 4568-4577 (2005).

93   Mayhew, C. N. *et al.* RB loss abrogates cell cycle control and genome integrity to promote liver tumorigenesis. *Gastroenterology* **133**, 976-984 (2007).

94   Nicolay, B. N. *et al.* Proteomic analysis of pRb loss highlights a signature of decreased mitochondrial oxidative phosphorylation. *Genes Dev* **29**, 1875-1889, doi:10.1101/gad.264127.115 (2015).

95   Maandag, E. C. R. *et al.* Developmental rescue of an embryonic-lethal mutatuion in the retinoblastoma gene in chimeric mice. *EMBO J.* **13**, 4260-4268 (1994).

96   Williams, B. O. *et al.* Extensive contribution of Rb-deficient cells to adult chimeric mice with limited histopathological consequences. *EMBO J.* **13**, 4251-4259 (1994).

97   Downward, J. Targeting RAS signalling pathways in cancer therapy. *Nat Rev Cancer* **3**, 11-22, doi:10.1038/nrc969 (2003).

98   Kato, J., Matsushime, H., Hiebert, S. W., Ewen, M. E. & Sherr, C. J. Direct binding of cyclin D to the retinoblastoma gene product (pRb) and pRb phosphorylation by the cyclin D-dependent kinase CDK4. *Genes Dev* **7**, 331-342 (1993).

99   Sherr, C. & Roberts, J. CDK inhibitors: positive and negative regulators of G1-phase progression. *Genes and Development* **13**, 1501-1512 (1999).

100   Zarkowska, T. & Mittnacht, S. Differential phosphorylation of the retinoblastoma protein by G1/S cyclin-dependent kinases. *J Biol Chem* **272**, 12738-12746 (1997).

101   Schulze, A. *et al.* Cell cycle regulation of the cyclin A gene promoter is mediated by a variant E2F site. *Proc Natl Acad Sci U S A* **92**, 11264-11268 (1995).

102   Sherr, C. J. & Roberts, J. M. Inhibitors of mammalian G1 cyclin-dependent kinases. *Genes Dev* **9**, 1149-1163 (1995).

103   Hochegger, H., Takeda, S. & Hunt, T. Cyclin-dependent kinases and cell-cycle transitions: does one fit all? *Nat Rev Mol Cell Biol* **9**, 910-916, doi:10.1038/nrm2510 (2008).

104   Nakayama, K. & Nakayama, K. Cip/Kip cyclin-dependent kinase inhibitors: brakes of the cell cycle engine during development. *Bioessays* **20**, 1020-1029, doi:10.1002/(SICI)1521-1878(199812)20:12<1020::AID-BIES8>3.0.CO;2-D (1998).

105   Canepa, E. T. *et al.* INK4 proteins, a family of mammalian CDK inhibitors with novel biological functions. *IUBMB life* **59**, 419-426, doi:10.1080/15216540701488358 (2007).

106   Roussel, M. F. The INK4 family of cell cycle inhibitors in cancer. *Oncogene* **18**, 5311-5317, doi:10.1038/sj.onc.1202998 (1999).

107   Morgan, D. O. Principles of CDK regulation. *Nature*, 131-134 (1995).

108   Besson, A., Dowdy, S. F. & Roberts, J. M. CDK inhibitors: cell cycle regulators and beyond. *Dev Cell* **14**, 159-169 (2008).

109   el-Deiry, W. S. *et al.* WAF1/CIP1 is induced in p53-mediated G1 arrest and apoptosis. *Cancer Res* **54**, 1169-1174 (1994).

110   Sherr, C. J. Cancer cell cycles. *Science* **274**, 1672-1677 (1996).

111   Siddiqui, K., On, K. F. & Diffley, J. F. Regulating DNA replication in eukarya. *Cold Spring Harb Perspect Biol* **5**, doi:10.1101/cshperspect.a012930 (2013).

112   Sellers, W. R. *et al.* Stable binding to E2F is not required for the retinoblastoma protein to activate transcription, promote differentiation, and suppress tumor cell growth. *Genes Dev* **12**, 95-106 (1998).

113   Kratzke, R. *et al.* Partial inactivation of the RB product in a family with incomplete penetrance of familial retinoblastoma and benign retinal tumors. *Oncogene* **9**, 1321-1326 (1994).

114   Ji, P. *et al.* An Rb-Skp2-p27 pathway mediates acute cell cycle inhibition by Rb and is retained in a partial-penetrance Rb mutant. *Mol Cell* **16**, 47-58, doi:S1097276504005726 [pii]10.1016/j.molcel.2004.09.029 (2004).

115   Sharma, S. S. & Pledger, W. J. The non-canonical functions of p27(Kip1) in normal and tumor biology. *Cell Cycle* **15**, 1189-1201, doi:10.1080/15384101.2016.1157238 (2016).

116   Carrano, A. C., Eytan, E., Hershko, A. & Pagano, M. SKP2 is required for ubiquitin-mediated degradation of the CDK inhibitor p27. *Nat Cell Biol* **1**, 193-199 (1999).

117   Binne, U. K. *et al.* Retinoblastoma protein and anaphase-promoting complex physically interact and functionally cooperate during cell-cycle exit. *Nat Cell Biol* **9**, 225-232 (2007).

118   Li, M. & Zhang, P. The function of APC/CCdh1 in cell cycle and beyond. *Cell Div* **4**, 2, doi:10.1186/1747-1028-4-2 (2009).

119   Wei, W. *et al.* Degradation of the SCF component Skp2 in cell-cycle phase G1 by the anaphase-promoting complex. *Nature* **428**, 194-198, doi:10.1038/nature02381 (2004).

120   Sun, H. *et al.* An E2F binding-deficient Rb1 protein partially rescues developmental defects associated with Rb1 nullizygosity. *Mol Cell Biol* **26**, 1527-1537 (2006).

121   Harbour, J. W. Molecular basis of low-penetrance retinoblastoma. *Arch Ophthalmol* **119**, 1699-1704 (2001).

122   Fero, M. L. *et al.* A syndrome of multiorgan hyperplasia with features of gigantism, tumorigenesis, and female sterility in p27(Kip1)-deficient mice. *Cell* **85**, 733-744, doi:S0092-8674(00)81239-8 [pii] (1996).

123   Julian, L. M., Palander, O., Seifried, L. A., Foster, J. E. & Dick, F. A. Characterization of an E2F1-specific binding domain in pRB and its implications for apoptotic regulation. *Oncogene* **27**, 1572-1579 (2008).

124   Deng, C., Zhang, P., Harper, J. W., Elledge, S. J. & Leder, P. Mice lacking p21CIP1/WAF1 undergo normal development, but are defective in G1 checkpoint control. *Cell* **82**, 675-684 (1995).

125   Jacks, T. *et al.* Tumor spectrum analysis in p53-mutant mice. *Curr Biol* **4**, 1-7 (1994).

126   Jackson, E. L. *et al.* Analysis of lung tumor initiation and progression using conditional expression of oncogenic K-ras. *Genes Dev* **15**, 3243-3248, doi:10.1101/gad.943001 (2001).

127   Ventura, A. *et al.* Restoration of p53 function leads to tumour regression in vivo. *Nature* **445**, 661-665, doi:10.1038/nature05541 (2007).

Chapter 2

2 Interchangeable roles for E2F transcriptional repression by the retinoblastoma protein and p27^{KIP1}-CDK regulation in cell cycle control and tumor suppression.

2.1 Abstract

The mammalian G1-S phase transition is controlled by the opposing forces of Cyclin dependent kinases (CDK) and the retinoblastoma protein (pRB). Here we present evidence for systems level control of cell cycle arrest by pRB-E2F and p27-CDK regulation. By introducing a point mutant allele of pRB that is defective for E2F repression (*Rb1^G*) into a p27^{KIP1} null background (*Cdkn1b$^{-/-}$*), both E2F transcriptional repression and CDK regulation are compromised. These double mutant *Rb1$^{G/G}$; Cdkn1b$^{-/-}$* mice are viable and phenocopy *Rb1$^{+/-}$* mice in developing pituitary adenocarcinomas, even though neither single mutant strain is cancer prone. Combined loss of pRB-E2F transcriptional regulation and p27^{KIP1} leads to defective proliferative control in response to various types of DNA damage. In addition, *Rb1$^{G/G}$; Cdkn1b$^{-/-}$* fibroblasts immortalize faster in culture and more frequently than either single mutant genotype. Importantly, the synthetic DNA damage arrest defect caused by *Rb1$^{G/G}$; Cdkn1b$^{-/-}$* mutations is evident in the developing intermediate pituitary lobe where tumors ultimately arise. Our work identifies a unique relationship between pRB-E2F and p27-CDK control and offers *in vivo* evidence that pRB is capable of cell cycle control through E2F independent effects.

2.2 Introduction

Regulation of the cell cycle is critical to maintain cellular homeostasis and to prevent the development of cancer [1]. Mammalian cell division is primarily controlled at

the G1-S phase transition, and the moment of commitment is often described as the restriction point [2]. Commitment to enter the cell cycle is controlled by two opposing forces; the retinoblastoma protein family (including pRB) that blocks entry, and Cyclin Dependent Kinases (CDKs) that drive advancement into S-phase [3]. The RB protein antagonizes S-phase entry by repressing E2F regulated genes necessary for DNA replication [4]. Working in opposition to pRB are CDKs [5], in particular Cyclin D and E associated kinases phosphorylate and inactivate upstream regulators of cell cycle entry including pRB and p27^{KIP1}, as well as stimulate the activation of downstream effectors of DNA replication [6,7]. While this suggests CDKs control pRB, a key target gene that is repressed by pRB-E2F is *CCNE1* that encodes Cyclin E, this creates a regulatory loop whereby Cyclin E/CDK2 becomes maximally active at almost the same time pRB is maximally phosphorylated and finally releases all E2Fs [4]. In addition, CDK2's principal negative regulator p27^{KIP1} is phosphorylated and targeted for degradation at virtually the same time [8]. Due to this interplay between pRB and CDK activity, it has been difficult to place one upstream of the other in a regulatory pathway [4]. Numerous studies suggest that either pRB-E2F or p27^{KIP1}-CDK2 interactions are essential for controlling quiescence or cell cycle entry commitment [9-17]. For this reason, control of the G1-S phase transition remains unclear. Furthermore, since much of the literature investigating G1-S regulation focuses on regulatory events during cell cycle entry [4,18], this leaves the roles for pRB-E2F and p27^{KIP1}-CDK interactions in cell cycle exit much less explored.

Cell cycle arrest by pRB has long been attributed to E2F regulation because the minimal deletion mutant of pRB that is capable of binding E2Fs can block proliferation of Saos-2 cells [19,20]. These studies revealed a close correlation between pRB-E2F

binding, transcriptional repression, and cell cycle arrest [20,21]. However, E2F binding

mutants of pRB have a surprising retention of growth control activity in this assay [22-24],

suggesting that other mechanisms may contribute. Given that cell cycle control

ultimately impinges on CDK regulation, a number of studies have connected pRB growth

arrest activity in Saos-2 cells to CDK regulation through p27^{KIP1} [25-27]. First, E2F binding

deficient mutants of pRB induce p27^{KIP1} expression in Saos-2 cell cycle arrest assays, and

p27 expression is required for these mutants of pRB to induce arrest [27]. Secondly, pRB

stabilizes p27^{KIP1} expression during induction of a G1 arrest quite rapidly, and this

precedes the decline in E2F regulated targets by at least 24 hours, suggesting CDK

regulation occurs first [26]. Moreover, Ji *et al.,* also demonstrated that pRB is capable of

binding and inhibiting the function of Skp2, the E3 ligase targeting subunit responsible

for poly-ubiquitination of p27 [26]. Consistent with this, the increases in p27 levels seen

following pRB expression in Saos-2 cells correlate with a decrease in Skp2 levels [25].

Binne *et al.,* showed that APC complexes containing Cdh1 are capable of using pRB as

an adaptor for Skp2 binding and ubiquitination, thereby stimulating Skp2 degradation and

promoting the stabilization of p27 [25]. Collectively, these studies connect pRB regulation

of the cell cycle to p27. However, the shortcoming of this work is its dependence on

ectopic pRB expression, a physiological context where pRB regulation of p27 genuinely

contributes to proliferative control decisions has yet to emerge. A number of genetic

crosses indicate that Skp2 loss can suppress pituitary tumorigenesis in *Rb1*$^{+/-}$ mice [28],

even in combination with p53 deficiency [29]. However, efforts to find p27 dependent

growth arrest in tissues of these mice have been confounded by other cellular effects such

as apoptosis in the intermediate lobe of the pituitary [28]. This has prevented the

observation of proliferative control decisions in these cells that use a pRB-p27 axis. For this reason, the pRB-p27 connection in proliferative control remains compelling, but its lack of detection in an endogenous scenario is a critical gap in our knowledge.

To study E2F independent functions of pRB at an endogenous level, we developed a mutant mouse model in which pRB binding to E2Fs is disrupted by R461E and K542E mutations (called $Rb1^G$) [30]. Importantly the $Rb1^G$ mutant protein is expressed at wild type levels and makes normal interactions with LXCXE motif containing proteins [30]. Surprisingly, we found that this mutation had little effect on control of cell proliferation, as $Rb1^{G/G}$ fibroblasts are capable of responding to serum starvation, p16 expression, DNA damage, and myogenic differentiation and in all cases show wild type responses [30]. In this study, we find that p27 expression levels are higher in $Rb1^{G/G}$ fibroblasts. In addition, double mutant $Rb1^{G/G}$ and p27 deficient cells are defective for growth arrest in response to DNA damage in a manner that resembles $Rb1^{-/-}$ cells, including misregulation of CDK2 activity. Furthermore, while developmentally unremarkable, $Rb1^{G/G}; Cdkn1b^{-/-}$ mice display a highly penetrant tumor phenotype. Together our study demonstrates systems level redundancy between pRB-E2F regulation and p27-CDK2 control, as the combined loss displays cell cycle defects that are absent from either single mouse mutant. In addition, this work provides proof of principle for transcription independent coordination between the RB and the CDK pathways in endogenous growth control.

2.3   Materials and Methods

2.3.1   Cell culture methods.

Mouse embryonic fibroblasts (MEFs) were derived from E13.5 embryos of the indicated genotypes. Asynchronous cells were cultured using standard methods in Dulbecco's modified Eagle's medium containing 10% fetal bovine serum (FBS), 2mM L-glutamine, 50U/ml penicillin and 50µg/ml streptomycin. Cells subjected to serum deprivation were cultured in the above media however only containing 0.1% FBS.

2.3.2   DNA damage induction.

MEFs subjected to gamma irradiation were plated at low density at passage 4. The next day media was changed prior to exposure to a cobalt 60 source until a dose of 15Gy was received. Media was changed again the next morning and cells were harvested 48 hours after treatment. Cells treated with DNA damaging agents cisplatin and H_2O_2 were plated at low density at passage 4 then the next day switched to media containing the indicated drug at a concentration of 1µM for cisplatin and 250µM for H_2O_2. Cells were incubated in the drug containing media for 48 hours before harvest for downstream applications.

2.3.3   Cell cycle analysis.

Cells were pulsed with BrdU under different growth conditions: asynchronous culture, serum deprived, serum stimulated, or various sources of DNA damage for a duration of 2 hours. Cell cycle analysis was then carried out following previously published protocols [31].

2.3.4   mRNA quantitation.

RNA isolation was carried out using Trizol reagent according to manufacturers instructions and previously published protocols [30]. mRNA levels of p27 were analyzed by qRT-PCR using iQ Sybr-green Super Mix (Bio-Rad) and the following primers against p27 and GAPDH: p27 Fwd (5`AGATACGAGTGGCAGGAGGT 3`), p27 Rev (5` ATGCCGGTCCTCAGAGTTTG 3`), GAPDH Fwd (5` GCACAGTCAAGGCCGAGAAT 3`), GAPDH Fwd. (5` GCCTTCTCCATGGTGGTGAA 3`). Expression levels of common E2F target genes: *Pcna1, Ccne1, Ccna2, Tyms, Rbl1,* and *Mcm3* were determined using the Quantigene Plex 2.0 reagent system from Affymetrix as previously described [32]. Expression levels were normalized to Actin.

2.3.5   3T3 Assay.

Passage 3 MEFs were plated at a density of 1×10^6 cells per 10cm culture dish in Dulbecco's modified Eagle's medium containing 10% Calf serum, 2mM L-glutamine, 50U/ml penicillin and 50µg/ml streptomycin. Three days after plating cells were counted and replated at the same density, 1×10^6 cells per 10cm dish. This procedure was repeated until passage 20. Population increase was calculated according to the following formula: $(\text{Log}_{10}(\text{recovered/seeded})/\text{Log}_{10}2$. Cells were considered successfully immortalized if the population growth was positive at the end of the 20 passages.

2.3.6   Protein interaction analysis and western blotting.

Nuclear extracts were prepared from MEFs and western blotting was carried out using previously described protocols [30]. Antibodies raised against p27 (C-19: sc-528) and Histone H3 (ab70550) were used for western blotting. pRB containing complexes were

immunoprecipitated from whole cell extracts using anti-E2F3 C-18 (Santa Cruz) bound

to G-sepharose beads (GE-healthcare). IPs were rocked for 1h at 4°C then washed twice

with IP wash buffer (10mM Tris pH 7.5, 200mM NaCl, 1.5mM $MgCl_2$, 2mM EDTA,

0.1% NP-40) and boiled in SDS-PAGE sample buffer. Samples were western blotted

using standard techniques. E2F3 was detected by PG37 (Upstate), pRB was detected by

G3-245 (BD Pharmingen), and Actin was detected with monoclonal antibody AC-74

(Sigma).

2.3.7   Phenotypic analysis of animals.

Cdkn1b^{-/-} mice (B6.129S4-Cdkn1b[tm1Mlf]/J) have been described previously and

were obtained from Jackson Laboratory and genotyped as recommended [33]. *Rb1*[G/G] mice

were genotyped as previously described [30]. All animals were housed and handled as

approved by the Canadian Council on Animal Care. Mice were monitored for tumor

development. Mice were sacrificed at natural endpoint. Survival data were subjected to

Kaplan-Meier analysis, and significant differences were compared using a log rank test.

For DNA damage experiments, pregnant mothers at day 13.5 of gestation were subjected

to 10Gy IR followed by a 2h pulse of BrdU 4 hours after IR treatment.

2.3.8   Histology and microscopy.

E13.5 embryos treated with 10Gy of IR were removed from the uterus and fixed

whole in PBS containing 4% PFA for 24h. Next, they were placed in PBS containing

30% sucrose to dehydrate the samples for a minimum of 3 days. Embryos were then dried

and mounted in Cryomatrix (Thermo Scientific 6769006), frozen using liquid nitrogen

and stored at -80°C [34]. Sagittal pituitary sections were cut using a Leica cryostat (CM

3050S) in 8μm sections and mounted on slides which were stored at -80°C. Slides were acclimated to room temperature prior to staining.

For BrdU staining, slides were rehydrated in PBS and inserted into a Shandon Sequenza cassette holder (Thermo Scientific 73310017). 500μL of 2N HCl was added to the slides and incubated for 20 mins at room temperature. Slides were then washed twice with 0.1M $Na_2B_4O_7$ pH 8.5 for 5 mins per wash. Slides were then put into a coplin jar containing 10mM sodium citrate pH 6 and microwaved for 10 mins on low power level, followed by a 20 min incubation at room temperature. Slides were washed again with PBS and reinserted into the Shadon Sequenza holder (Thermo Scientific 73310017). Slides were then washed twice with PBS containing 0.3% Triton-X. Anti-BrdU antibody (BD, 347580) was diluted 1 in 50 in PBS-0.3% Triton-X and incubated on slides overnight. The next day slides were washed three times with PBS-0.3% Triton-X then secondary anti-mouse fluorescein (Vector, FI-2000) was added at a dilution of 1 in 800 in PBS-0.3% Triton-X. Slides were then incubated in secondary for 1h in the dark. Slides were washed 3 times in PBS-0.3% Triton-X then counterstained with DAPI for 5 mins in the dark. Finally, slides were washed twice with PBS-0.3% Triton-X, twice with PBS, mounted with Slowfade (Thermo Scienfic S36937) and sealed.

TUNEL staining was carried out according to manufactures instructions using *In Situ* Cell Death Detection Kit (Roche, 1168479510). Briefly, cells were rehydrated with PBS then permeabilized with PBS-0.3% Triton-X for 2 mins on ice then incubated for 1 hour with TUNEL reagent. After incubation slides were washed 3 times with PBS, counterstained with DAPI for 5 mins followed by 2 washes with PBS-0.3% Triton-X and

2 washes with PBS. Slides were then mounted with Slowfade (Thermo S36937) and

sealed.

Images were acquired using a Zeiss Axioskop 40 microscope and Spot flex

camera, and quantified using velocity image analysis software. (Perkin Elmer)

2.3.9   CDK2 Kinase activity assays.

Nuclear extracts were spun down at 14000 rpm for 30 mins to separate protein from

cellular debris. 250µg of protein from each sample was precleared for 1 hour using

Dynabeads rotating at 4°C. Samples were then split in half and incubated for an hour

with Dynabeads prebound with either IgG or anti-CDK2 (Millipore). Complexes were

then washed twice with IP wash buffer (10mM Tris pH 7.5, 200mM NaCl, 1.5mM

MgCl$_2$, 2mM EDTA, 0.1% NP-40) and twice with kinase buffer (50mM Tris pH 7.5,

10mM MgCl$_2$, 1mM DTT) and resuspended in 49µl of kinase buffer containing 4µg of

recombinant histone H1 (Santa Cruz). 10µCi of ^{32}P radio-labelled ATP was incubated

with immunoprecipitates for 20 mins at 30°C, followed by boiling in SDS-PAGE buffer

to stop the reaction. Samples were then run out on a 15% gel, stained with Coomassie to

check for loading then dried and exposed to a phosphosensitive plate to determine ^{32}P

incorporation.

2.4   Results

2.4.1   Post-translational stabilization of p27 in Rb1$^{G/G}$ fibroblasts during quiescence.

Our previously published analysis of *Rb1$^{G/G}$* primary fibroblasts and mice

indicates that loss of pRB-E2F repression fails to bypass cell cycle exit signals [30]. **Figure**

2.1 shows an example of a serum starvation arrest in which wild type, $Rb1^{G/G}$, and knock out cells were serum starved for 60 hours. Under these culture conditions wild type and $Rb1^{G/G}$ cells reduce BrdU incorporation equivalently, while $Rb1^{-/-}$ cells are defective (**Figure 2.1A**). However, analysis of mRNA levels of common E2F target genes shows that $Rb1^{G/G}$ displays a similar defect in repression as $Rb1^{-/-}$ (**Figure 2.1B**). Importantly, while cell cycle exit is normal in this scenario, pRB's well studied role for restraining E2F activation during cell cycle entry following serum stimulation is compromised in $Rb1^{G/G}$ cells, and they enter the cell cycle with similar kinetics as knock out controls (**Figure 2.1C**). Consistent with these findings, the R461E and K542E mutations encoded by the $Rb1^{G}$ allele prevent stable interactions with E2Fs. We used immunoprecipitation and western blot assays to evaluate pRB-E2F3 interactions in serum starved cells and these reveal a robust defect (**Figure 2.1D**)[30]. Since $Rb1^{G/G}$ cells are functional for cell cycle arrest in assays where $Rb1^{-/-}$ cells are not [30], we searched for parallel growth control mechanisms to pRB-E2F repression that are pRB dependent. Building on previous findings of p27 stabilization in cancer cells and $Rb1^{-/-}$ MEFs, we sought to determine if this same effect was seen in our mutant $Rb1^{G/G}$ cells. Following serum deprivation of asynchronously proliferating cultures, $Rb1^{G/G}$ MEFs demonstrated a modest increase in p27 protein levels coincident with G1 arrest (**Figure 2.1E**). Importantly, p27 mRNA levels quantitated by qRT-PCR remain the same as wild-type cells during serum deprivation, indicating that the change observed is likely due to a post-translational effect (**Figure 2.1F**). This finding is consistent with the post-translational stabilization of p27 observed in Saos2 cells induced to arrest following expression of E2F binding deficient mutants of pRB [27]. The increased p27 in response to loss of E2F regulation may be
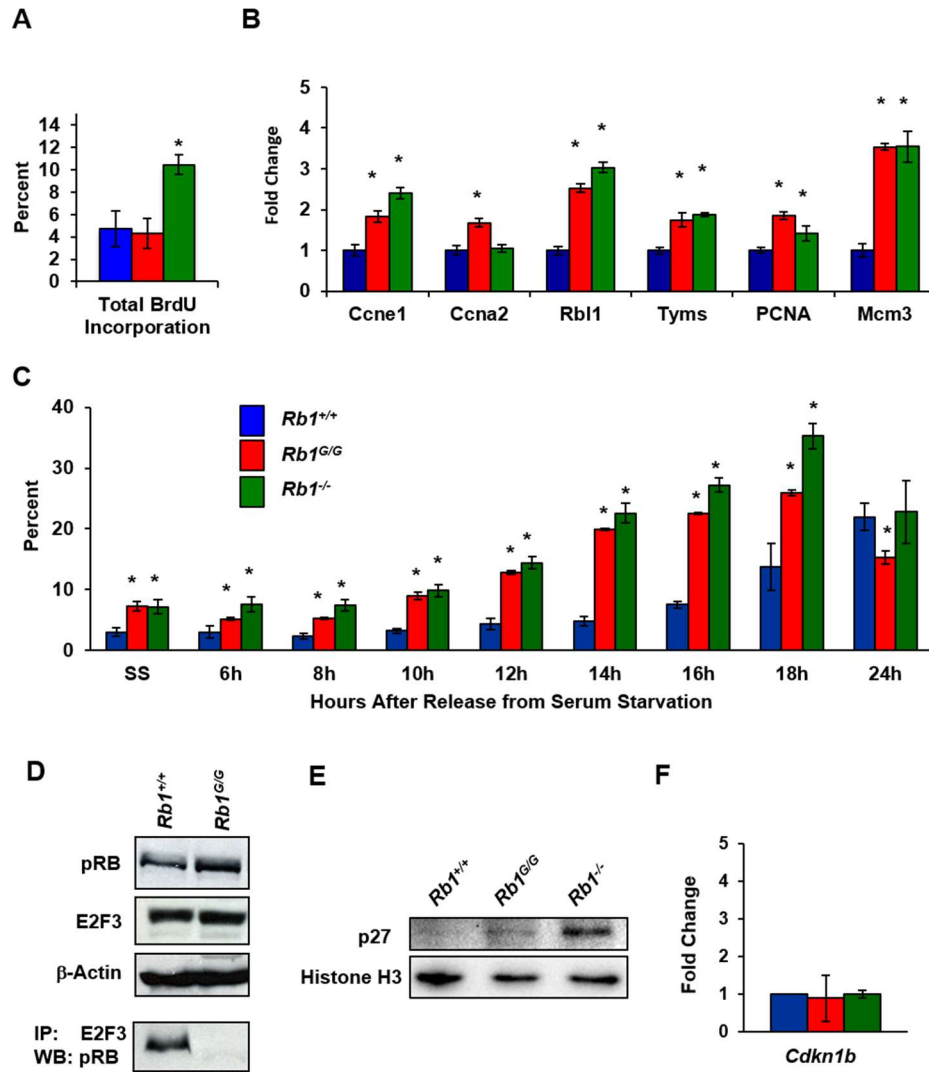
Figure 2.1: Increased expression of p27 in serum starved *Rb1^{G/G}* MEFs.

(A) Fibroblast cells of the indicated genotypes were serum starved for 60 hours, pulse-labelled with BrdU for 2 hours, followed by staining for BrdU incorporation. The proportion of cells incorporating BrdU was determined by flow cytometry. **(B)** Fibroblasts were serum starved as in A and the relative mRNA levels of the indicated genes was determined. **(C)** Following serum starvation for 60 hours, cells were re-stimulated to enter the cell cycle. Cultures were pulse labeled with BrdU and harvested at the indicated time points and analyzed by flow cytometry. **(D)** Whole cell extracts were prepared from serum starved wild type and *Rb1^{G/G}* MEFs. Western blots were performed to assess relative expression of pRB and E2F3. Anti-E2F3 immunoprecipitations were blotted for pRB. **(E)** Immunoblotting of nuclear extracts isolated from serum deprived MEFs using antibodies raised against p27 and Histone H3. **(F)** Real-time quantitative PCR using primers to detect *Cdkn1b*. Values are presented relative to GAPDH. All error bars represent one standard deviation from the mean. * indicates a significant difference from the wild type control using a *t*-test, $p<0.05$.

related to the ability of $Rb1^{G/G}$ MEFs to maintain proliferative control despite defective E2F binding.

2.4.2 $Rb1^{G/G}$; $Cdkn1b^{-/-}$ mice are highly cancer prone.

To determine if p27 expression in $Rb1^{G/G}$ cells is responsible for the maintenance of cell cycle control, we crossed $Rb1^{G/G}$ mice with p27 deficient ($Cdkn1b^{-/-}$) animals. Compound mutant mice display similar viability at weaning as the $Rb1^{G/G}$ genotype alone and without obvious anatomical defects, suggesting the combination of $Rb1^{G/G}$ and $Cdkn1b^{-/-}$ deficiency is no different than either single mutant alone (**Figure 2.2A, Table 2.1**)[30]. While double mutant $Rb1^{G/G}$; $Cdkn1b^{-/-}$ mice show normal development, we aged cohorts of double and single mutant mice and discovered that $Rb1^{G/G}$; $Cdkn1b^{-/-}$ mice succumb to pituitary tumors with an average tumor free survival of 214 days (**Figure 2.2B**). Necropsies of these mice revealed pituitary tumor masses characteristic of $Rb1$ deficient animals (**Figure 2.2C**). By comparison, neither $Rb1^{G/G}$ nor $Cdkn1b^{-/-}$ mice displayed cancer susceptibility (**Figure 2.2BC**), and this is consistent with prior reports of mixed 129/B6 $Cdkn1b^{-/-}$ mice [35]. Interestingly, $Rb1^{G/+}$; $Cdkn1b^{-/-}$ mice also succumb to pituitary tumor formation with a delayed latency compared to double mutants and with approximately 75% penetrance (**Figure 2.2BC**). PCR genotype analysis revealed that loss of the wild type copy of $Rb1$ is ubiquitous in these tumors (**Figure 2.2D**). The $Rb1^{G/+}$; $Cdkn1b^{-/-}$ tumor phenotype is highly reminiscent of $Rb1^{+/-}$; $Cdkn1b^{-/-}$ tumors in terms of latency and the requirement for loss of heterozygosity of $Rb1$ [35]. Based on this observation, the $Rb1^G$ allele appears to be the functional equivalent of an $Rb1$ null allele when combined with p27 deficiency in this context. These genetic data also imply that
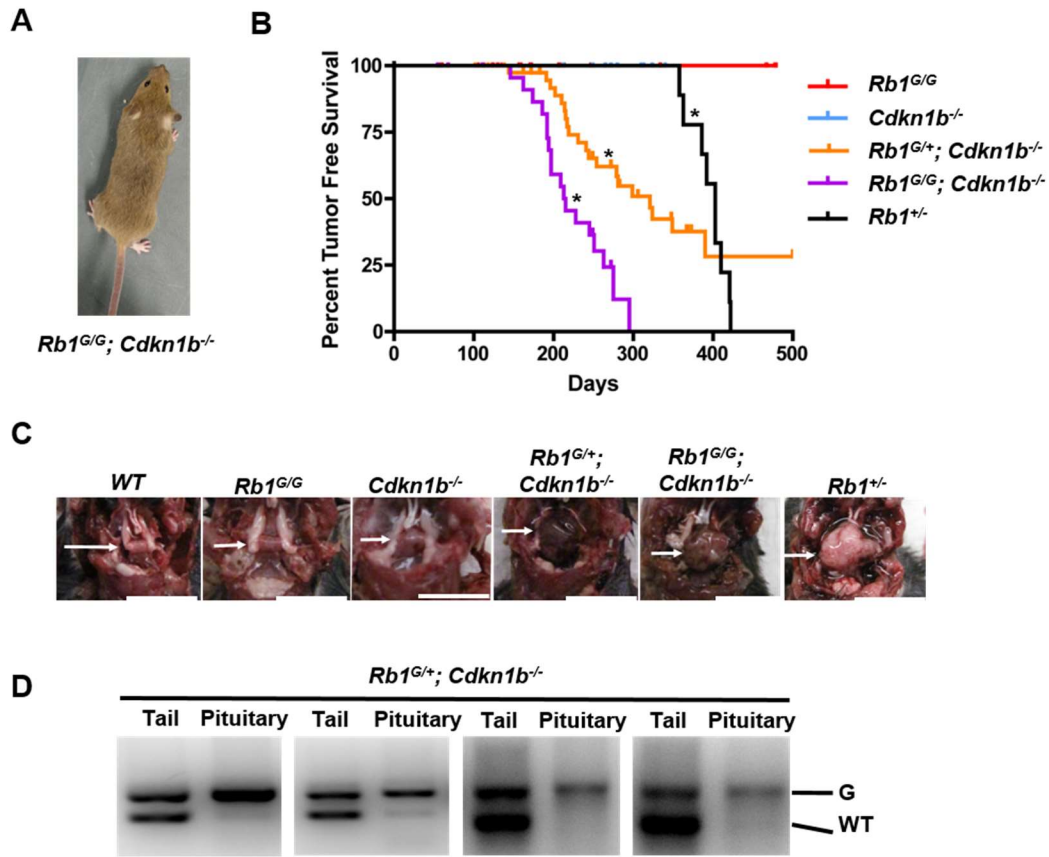
Figure 2.2: Cancer susceptibility in *Rb1$^{G/G}$; Cdkn1b$^{-/-}$* mice.

(A) Picture of young adult double mutant *Rb1$^{G/G}$; Cdkn1b$^{-/-}$* mouse. **(B)** Kaplan-Meyer analysis of tumor-free survival for mice of the indicated genotypes. Mice were monitored until natural endpoint and those having tumors are shown. *Rb1$^{G/G}$; Cdkn1b$^{-/-}$*, *Rb1$^{G/+}$; Cdkn1b$^{-/-}$* and *Rb1$^{+/-}$* are significantly different from one another and from all single mutant controls using Log rank test (*P*<0.05). **(C)** Macroscopic images of pituitaries of mice from the indicated genotypes at necropsy. Scale bars are 1cm. **(D)** Genotyping of tumor and tail DNA isolated from *Rb1$^{G/+}$; Cdkn1b$^{-/-}$* mice demonstrating loss of heterozygosity in the tumor tissue.

p27 function is required for pRB dependent tumor suppression when pRB is defective for E2F binding, and that pRB-E2F control is critical in the absence of p27.

2.4.3 Compound mutant *Rb1*^{G/G}*; Cdkn1b*^{-/-} MEFs enter quiescence following serum deprivation.

The normal development of double mutant animals suggests that pRB-mediated repression of E2Fs, as well as deficiency for p27, are dispensable for a variety of cell cycle exit decisions that occur as part of a normal mammalian developmental program. However, emergence of pituitary adenocarcinomas indicates that this combination is important in some context for the mitigation of tumorigenesis. We therefore sought to understand if specific cell cycle control functions are lost in *Rb1*$^{G/G}$*; Cdkn1b*$^{-/-}$ cells. Since both pRB and p27 are implicated in quiescence, we assessed their separate and combined contributions to serum deprivation-induced arrest [2]. Asynchronously proliferating cultures of primary fibroblasts for each of wild type, *Rb1*$^{G/G}$, *Cdkn1b*$^{-/-}$, double mutant *Rb1*$^{G/G}$*; Cdkn1b*$^{-/-}$, and *Rb1*$^{-/-}$ were analyzed for their proliferative state by BrdU labeling and flow cytometry. **Figure 2.3A** shows baseline levels of BrdU incorporation for each genotype while actively proliferating, and it shows *Rb1*$^{G/G}$*; Cdkn1b*$^{-/-}$, and *Rb1*$^{-/-}$ have statistically elevated BrdU incorporation levels. Cells were subsequently washed and transferred to 0.1% serum to induce arrest for 60 hours before pulse labeling with BrdU. While asynchronously cycling double mutant *Rb1*$^{G/G}$*; Cdkn1b*$^{-/-}$ MEFs exhibit an increase of cells in S-phase while proliferating, these cells could restrict S-phase entry following serum deprivation, to a level equivalent to that of wild type fibroblasts (**Figure 2.3B**). Importantly, the incomplete response in *Rb1*$^{-/-}$ cells indicates that this is a pRB dependent process that *Rb1*$^{G/G}$*; Cdkn1b*$^{-/-}$ cells are capable of
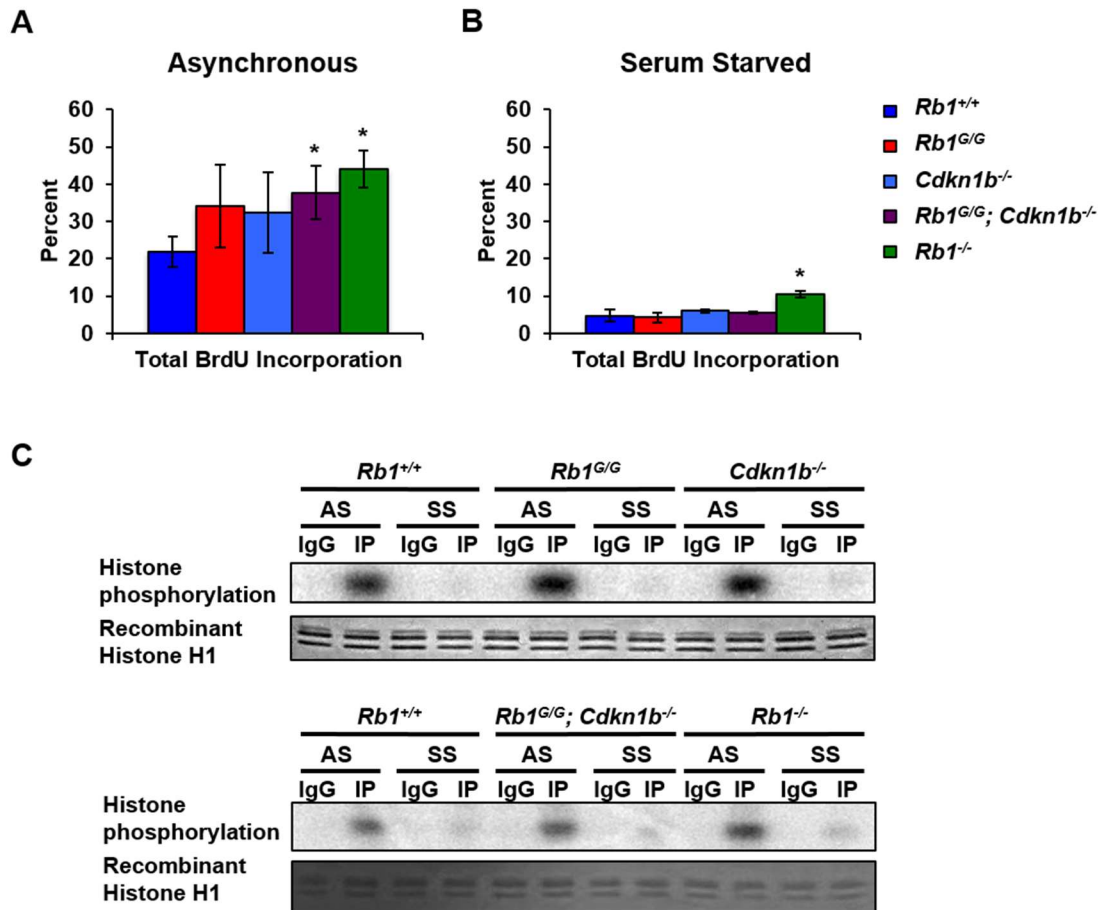
Figure 2.3: Compound mutant *Rb1^{G/G}; Cdkn1b^{-/-}* MEFs enter quiescence.

(A) Asynchronously growing MEFs were pulsed-labelled with BrdU for two hours followed by staining for BrdU incorporation and analysis by flow cytometry. **(B)** Proliferating cells were serum deprived for 60 hours and pulse-labelled with BrdU for two hours followed by staining for BrdU incorporation and flow cytometry. All error bars represent one standard deviation from the mean. * indicates a significant difference from the wild type control using a *t*-test, $p<0.05$. **(C)** CDK2 kinase activity was determined by incubation of immunoprecipitated CDK2 complexes isolated from the indicated genotypes of cells under asynchronous growth conditions (AS), or serum starved conditions (SS). Proteins isolated by immunoprecipitation with anti-CDK2 antibodies (IP) or control (IgG) were mixed with recombinant histone H1 and γ-^{32}P-ATP, incubated, and resolved by gel electrophoresis and exposed to a phosphosensitive plate. Coomassie staining of the recombinant histone H1 serves as a loading control.

executing. Similarly, analysis of CDK2 activity by IP-kinase assays reveals that single

mutant $Rb1^{G/G}$ and $Cdkn1b^{-/-}$ cells were also capable of inhibiting CDK2 kinase activity

(**Figure 2.3C**), as were double mutant $Rb1^{G/G}$; $Cdkn1b^{-/-}$ MEFs. Some residual CDK2

activity was also observed in the $Rb1^{-/-}$ cells following serum deprivation reflecting the

defect in G1 arrest observed in $Rb1^{-/-}$ MEFs (**Figure 2.3C**). Maintenance of quiescence

and CDK2 inhibition in double mutant $Rb1^{G/G}$; $Cdkn1b^{-/-}$ MEFs agrees with the

developmental milestones observed in $Rb1^{G/G}$; $Cdkn1b^{-/-}$ mice, as quiescence induction is

a component of normal development [36].

2.4.4 Compound mutant $Rb1^{G/G}$; $Cdkn1b^{-/-}$ cells display defective cell cycle control in response to DNA damage.

The detection of malignancies later in life in $Rb1^{G/G}$; $Cdkn1b^{-/-}$ mice likely

indicates that additional mutations occur prior to tumorigenesis. Therefore, we next

looked at the ability of single and double mutant $Rb1^{G/G}$; $Cdkn1b^{-/-}$ MEFs to arrest the

cell cycle in response to DNA damage, as a defect in this response could facilitate the

acquisition of new mutations. We subjected asynchronously proliferating cells to three

different DNA damaging agents; gamma irradiation (IR), cisplatin, and hydrogen

peroxide and pulse labelled cells with BrdU 48 hours later. The percentage of BrdU

positive cells was then determined by flow cytometry (**Figure 2.4A**). With each

treatment, double mutant $Rb1^{G/G}$; $Cdkn1b^{-/-}$ and $Rb1^{-/-}$ cells failed to block BrdU

incorporation. Interestingly, some single mutants showed modest defects in their

response to Cisplatin and hydrogen peroxide (**Figure 2.4A**). However, analysis of DNA

content by propidium iodide staining following IR, showed that both double mutant

$Rb1^{G/G}$; $Cdkn1b^{-/-}$ and $Rb1^{-/-}$
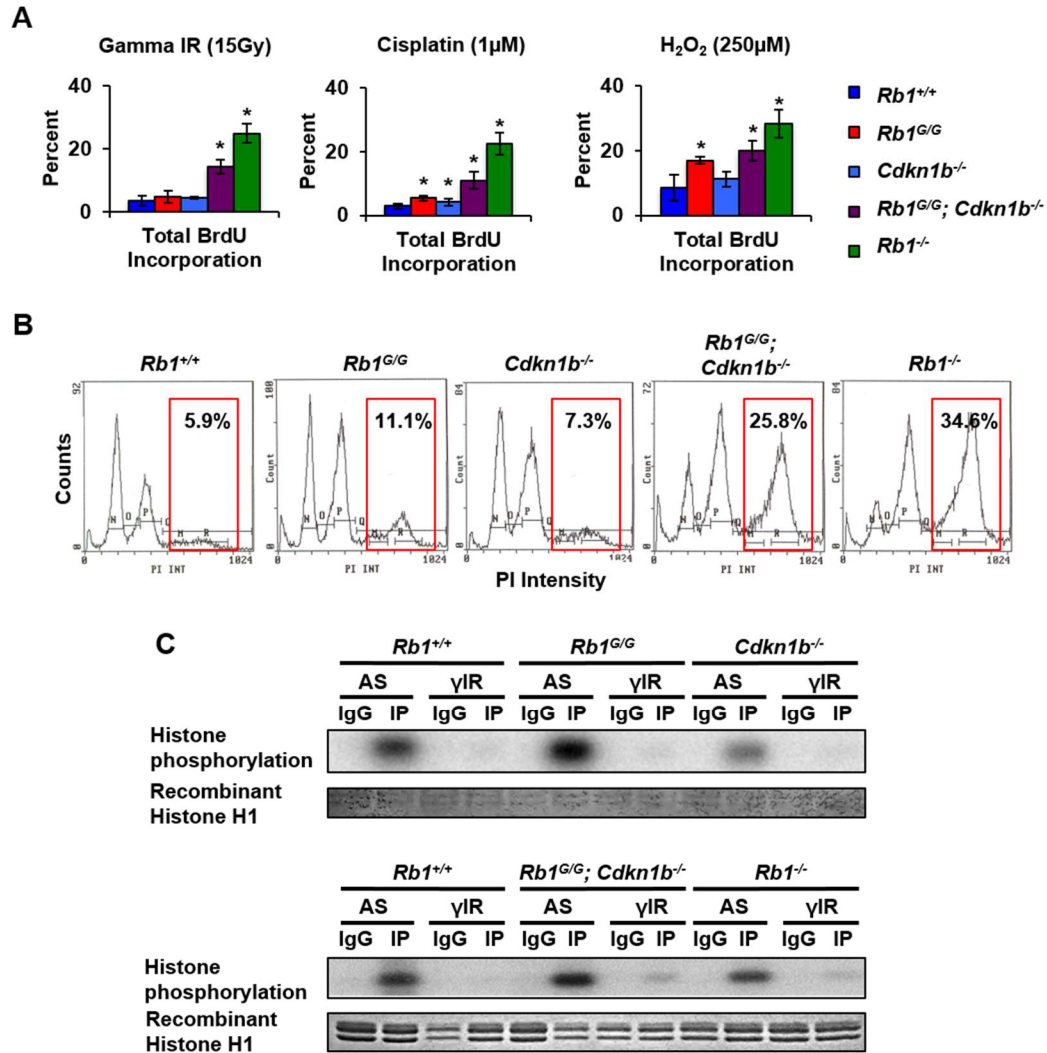
Figure 2.4: Mutant *Rb1^G/G^; Cdkn1b^-/-^* MEFs display defective cell cycle control in response to DNA damage.

(A) MEFs were treated with the indicated dose of DNA damaging agents. 48 hours later cells were pulsed with BrdU, stained and analyzed by flow cytometry. All error bars represent one standard deviation from the mean. * indicates a significant difference from the wild type control using a *t*-test, $P<0.05$. **(B)** Propidium iodide (PI) staining of MEFs treated with 15Gy of ionization radiation showing DNA content of cells. Red boxes outline area of >4N DNA content with the number representing the percentage of cells in that box. **(C)** Kinase assays were performed using CDK2 kinases isolated from asynchronously growing (AS) or following treatment with ionizing radiation (γIR). Kinase activity was determined by incubation of immunoprecipitated CDK2 complexes with recombinant histone H1 with and γ-^{32}P-ATP followed by gel electrophoresis and exposure to a phosphosensitive plate. Coomassie staining of recombinant histone H1 serves as a loading control.

MEFs exhibit a high proportion of cells with 8N DNA content, implying a strong defect

in the regulation of DNA replication following damage (**Figure 2.4B**). This suggests that

loss of both pRB-E2F binding and p27 together results in a defective DNA damage

checkpoint leading to endoreduplication in a manner that is very similar to complete *Rb1*

deficiency. We also tested CDK2 activity from extracts of IR treated cells using an IP-

kinase assay. Once again, *Rb1^{G/G}* and *Cdkn1b^{-/-}* single mutant MEFs could reduce CDK2

kinase activity down to background levels, whereas double mutant *Rb1^{G/G}; Cdkn1b^{-/-}* and

Rb1^{-/-} MEFs were only able to partially restrict CDK2 kinase activity mirroring the result

seen by BrdU incorporation analysis (**Figure 2.4C**). The failure of double mutant

Rb1^{G/G}; Cdkn1b^{-/-} MEFs to arrest in response to DNA damage provides a possible

framework to explain the eventual development of pituitary adenocarcinomas in older

mice. Therefore, in the context of DNA damage, *Rb1^{G/G}; Cdkn1b^{-/-}* animals may be

unable to respond appropriately to the insult, allowing for the development of further

mutations and the clonal expansion tumorigenic cells.

2.4.5   Compound mutant *Rb1^{G/G}; Cdkn1b^{-/-}* fibroblasts undergo rapid immortalization in culture.

We also modeled the acquisition of cancer enabling mutations over time using a

3T3 immortalization assay to assess the different *Rb1* and *Cdkn1b* mutant genotypes. By

passaging primary MEFs in a 3T3 protocol we were able to subject them to long-term

oxidative stress [37], its resultant DNA damage [37], and determine genotype specific

responses. We categorized entry into senescence in this assay as the first passage that

displays a negative population increase. Furthermore, we categorized immortalization as

the first passage where positive population increases resumed and continued

uninterrupted for the remainder of the 20 passage experiment. From this analysis, we note that all attempts to immortalize $Rb1^{G/G}$; $Cdkn1b^{-/-}$ and $Rb1^{-/-}$ MEFs were successful (**Figure 2.5A**), whereas at least half of single mutant or wild type controls entered senescence and never resumed proliferation. All wild type, single mutant, and $Rb1^{G/G}$; $Cdkn1b^{-/-}$ double mutant cells entered senescence as evidenced by negative growth trends (**Figure 2.5B-F**). In this assay, only $Rb1^{-/-}$ cells spontaneously immortalized without entering senescence (**Figure 2.5F**). Notably, double mutant $Rb1^{G/G}$; $Cdkn1b^{-/-}$ cells demonstrated a longer period of positive growth compared to single mutants (**Figure 2.5E**), and they spent fewer passages in senescence before resuming continual expansion. A similar profile of brief arrest before rapid expansion was exhibited by most $Rb1^{-/-}$ cells cultures (**Figure 2.5F**), and this further emphasizes the similarity between the $Rb1^{G/G}$; $Cdkn1b^{-/-}$ and $Rb1^{-/-}$ genotypes in this assay. This result demonstrates that cells containing mutations to abolish pRB-E2F repression and loss of p27, are poised to immortalize and this property is consistent with their inability to arrest the cell cycle following DNA damage.

2.4.6 Compound mutant $Rb1^{G/G}$; $Cdkn1b^{-/-}$ cells in the embryonic intermediate pituitary demonstrate radio resistant DNA synthesis.

Given the propensity of $Rb1^{G/G}$; $Cdkn1b^{-/-}$ mice to develop pituitary tumors as demonstrated in this report, and the long history of $Rb1$ null alleles to predispose mice to this tumor type, we sought to assess cell cycle regulation in this tissue. As the intermediate lobe of the pituitary gland gives rise to the adenocarcinomas previously reported in $Rb1$ mutant mice [38,39], we chose to investigate the DNA damage response
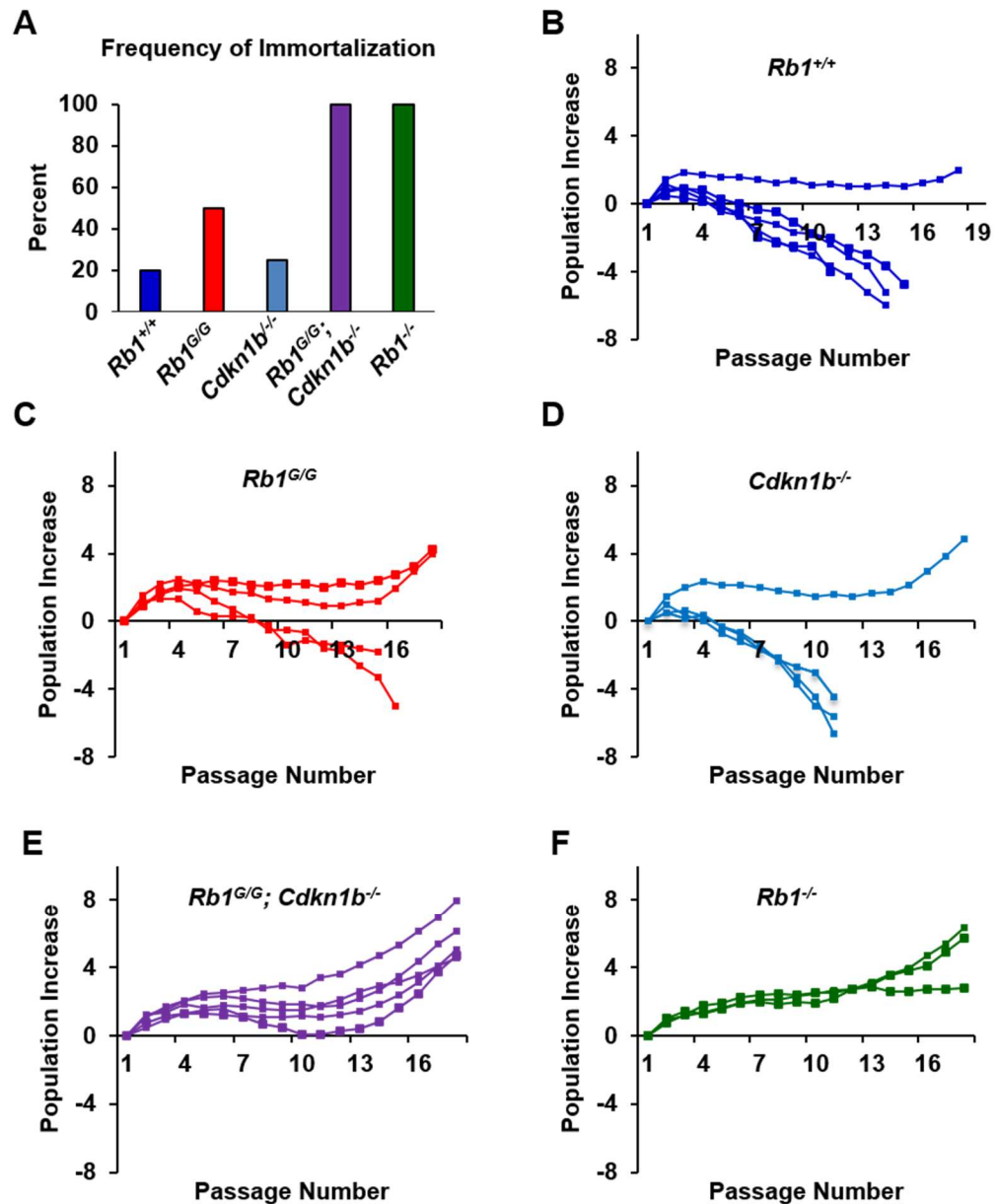
Figure 2.5: *Rb1$^{G/G}$; Cdkn1b$^{-/-}$* **MEFs undergo rapid immortalization in response to oxidative stress.**

(A) Percent of cultures that immortalized within 20 passages of 3T3 culture. Immortalization was defined as continued positive population growth following a decline in cell number at intermediate passages. **(B-F)** Population growth of MEFs of the indicated genotypes was plotted against passage number. Cells were plated at a density of 1×10^6 cells per 10 cm plate, and they were re-seeded at the same density every 3 days. Population increase was calculated according to the formula: (Log_{10}(recovered/seeded))/$Log_{10}2$ and plotted cumulatively over 20 passages, or until no viable cells were left in the culture.

specifically in these cells. To analyze acute response to DNA damage in the pituitary, embryos at 13.5 days of gestation were used as the peak proliferation of the pituitary occurs at this time and postnatal proliferation is largely undetectable [40]. Pregnant mothers were exposed to a dose of 10Gy of ionizing radiation four hours prior to injection with BrdU and sacrificed two hours later. Tissue sections of embryos were cut to expose the developing pituitary and sections were stained to detect BrdU (**Figure 2.6A**). Wild type, as well as single mutant *Rb1^{G/G}* and *Cdkn1b^{-/-}* embryos, displayed a robust reduction in BrdU incorporation following DNA damage, as determined by counting BrdU positive nuclei in the intermediate lobe of the pituitary (**Figure 2.6B**). Similar to our findings in cell culture both *Rb1^{G/G}; Cdkn1b^{-/-}* and *Rb1^{-/-}* embryos did not display a significant reduction of BrdU incorporation following irradiation (**Figure 2.6B**). TUNEL staining of parallel sections was performed to quantitate double stranded DNA breaks and reveals similar levels of damage among all genotypes (**Figure 2.6C**). This outcome indicates that the cell cycle arrest defect following DNA damage in double mutant *Rb1^{G/G}; Cdkn1b^{-/-}* cells is evident in both cell culture and *in vivo* settings, and it occurs in the cell population that eventually gives rise to the tumor phenotype seen in these mice. Thus, the regulation of E2Fs by pRB as well as CDK control via p27 are each individually dispensable for cell cycle control, simultaneous loss of both leads to an insensitivity to DNA damage signalling and a predisposition to cancer.

2.5   Discussion

Our findings support the existence of a link between pRB-mediated growth control and CDK regulation that is independent of pRB-E2F control of transcription. The similar defect in DNA damage induced growth arrest between *Rb1^{G/G}; Cdkn1b^{-/-}* and
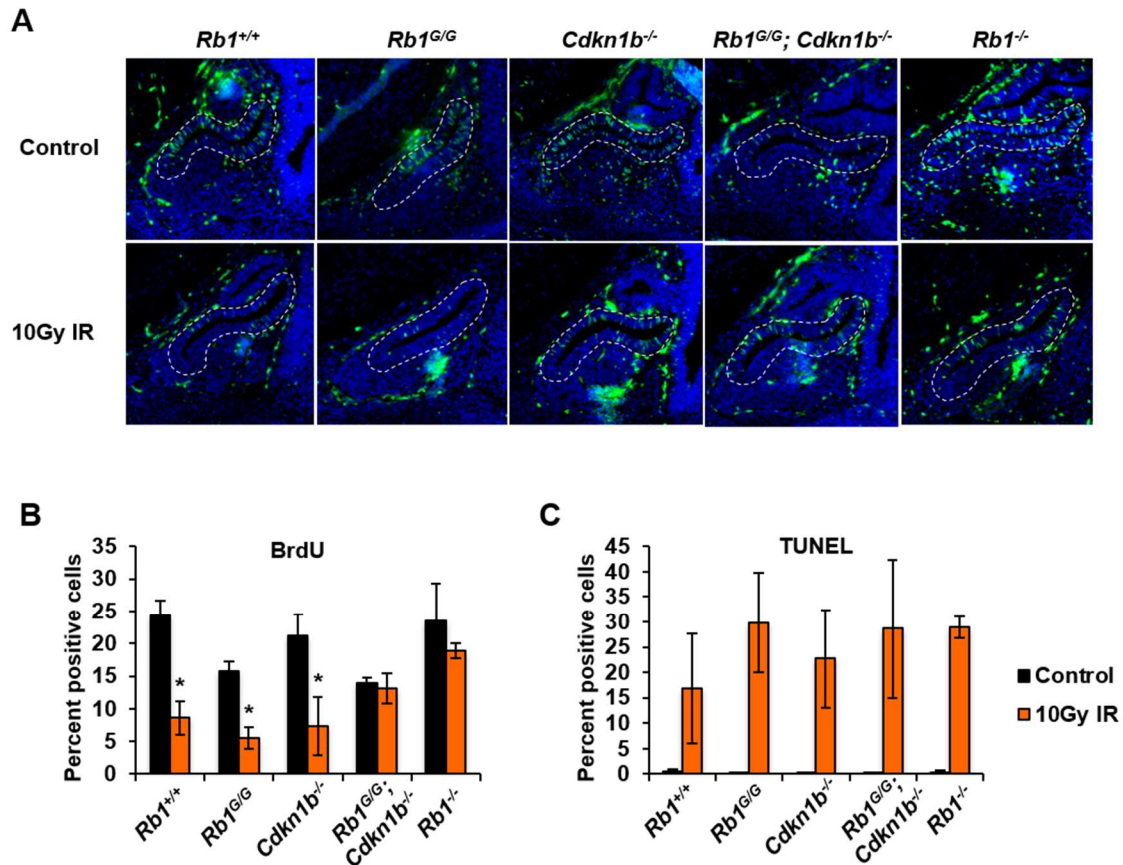
Figure 2.6: Double mutant *Rb1^G/G^ Cdkn1b^-/-^* embryonic pituitaries exhibit radio resistant DNA synthesis.

(A) Representative images of E13.5 pituitaries stained for BrdU from control or irradiated embryos. The intermediate lobe of the pituitary is outlined in dashed white lines. **(B)** The of percentage of BrdU positive cells in the intermediate lobe of the pituitary was determined from the indicated genotypes of mice from control or irradiated groups. All error bars represent one standard deviation from the mean. * indicates a significant difference from the wild type control using a *t*-test, $P<0.05$. **(C)** Tissue sections were stained with TUNEL and positive cells within the intermediate lobe of the pituitary were quantitated for in the indicated genotypes either with or without irradiation. All error bars represent one standard deviation from the mean and there are no significant differences amongst the treated groups.

Rb1$^{-/-}$ implies that E2F independent growth control by pRB is dependent on CDK regulation by p27. In addition, we find that defective E2F binding by pRB, or loss of p27, are individually tolerated in most arrest assays suggesting their functions are somewhat interchangeable. Lastly, cancer incidence and latency is very similar between our *Rb1*$^{G/+}$*; Cdkn1b*$^{-/-}$ mice and previously published *Rb1*$^{+/-}$*; Cdkn1b*$^{-/-}$ mice [35], and this suggests that in the absence of p27, the *Rb1*^{G} allele is approximately equivalent to an *Rb1* null. Collectively, these data point to a strong interdependence of CDK and E2F regulation.

Previous studies of endogenous pRB function in mice have typically relied on knock out alleles. This approach to mechanistic understanding is constrained by several limitations that are overcome in our targeted knock in approach. First, other pRB family members, p107 and p130, increase in expression in pRB's absence [3,41]. Additionally, pRB is reported to interact with over one hundred proteins [42], so complete loss of pRB disrupts all of these binding partners, obscuring the roles of individual interactions. For these reasons, our *Rb1*$^{G/G}$ model specifically mitigates these problems allowing us to demonstrate a role for pRb-E2F interactions *in vivo* in tumor suppression. Surprisingly, these studies and our previous report of these mice, reveal that loss of pRB-E2F transcriptional repression functions in parallel with p27 in growth control and tumor suppression [30].

We have found that disruption of pRB-E2F interactions act synergistically with p27 deletion to bring about a loss of cell cycle control. The degree of disruption is similar to complete pRB knock out and this implies that p27 may lie downstream of pRB in an E2F independent growth arrest pathway. A number of previous reports have

identified a link between pRB and p27 as a means of crosstalk between the RB pathway and the CDK regulatory pathway [25,26]. pRB has been shown to interact with Skp2 as well as the APC[Cdh1] complex[25,26]. These interactions allow pRB to reduce available Skp2 either through facilitation of Skp2 ubiquitination by APC[Cdh1] or through Skp2 sequestration. Ultimately, these interactions stabilize p27 expression and block CDK activity independent of pRB-E2F transcriptional repression. However, each of these reports relies on over expression of pRB as the growth arresting stimulus, leaving in question the physiological circumstance where this mechanism works. We think this report offers proof of principle for a pRB-p27 regulatory axis, in addition to showing that it functions in DNA damage induced arrest, its inactivation renders mice cancer prone. This argues that the pRB-p27 connection is critical to what makes pRB a tumor suppressor.

The interplay between pRB and p27 identified in this study may also provide important insight into the utilization of targeted therapies aiming to restore cell cycle control. A number of CDK4/6 inhibitors have been developed in attempts to re-establish the G1 checkpoint in cancer cells[43-45]. Since CDK4/6 inhibition is known to arrest proliferation only when pRB is functional, these inhibitors are generally given to patients with pRB positive cancers. However, pRB status alone does not indicate the effectiveness of these treatments [46]. Our analysis of G1 checkpoint control may provide some insight into ways to maximize the effectiveness of these treatments. We suggest that reactivation of the pRB pathway by CDK4/6 inhibitors may be more effective in cancers with inherently high p27 expression, or whose p27 stabilization pathways remain active.

Overall, our findings reveal a role for pRB in DNA damage induced cell cycle arrest, beyond repression of E2F transcriptional activity that utilizes p27 and CDK inhibition. Furthermore, our work suggests a functional context for the regulation of p27 by pRB that has been elusive.

2.6   References

1   Hanahan, D. & Weinberg, R. A. Hallmarks of cancer: the next generation. *Cell* **144**, 646-674, doi:10.1016/j.cell.2011.02.013 (2011).

2   Coller, H. A. What's taking so long? S-phase entry from quiescence versus proliferation. *Nat Rev Mol Cell Biol* **8**, 667-670, doi:10.1038/nrm2223 (2007).

3   Dick, F. A. & Rubin, S. M. Molecular mechanisms underlying RB protein function. *Nat Rev Mol Cell Biol* **14**, 297-306, doi:10.1038/nrm3567 (2013).

4   Bertoli, C., Skotheim, J. M. & de Bruin, R. A. Control of cell cycle transcription during G1 and S phases. *Nat Rev Mol Cell Biol* **14**, 518-528, doi:10.1038/nrm3629 (2013).

5   Deshpande, A., Sicinski, P. & Hinds, P. W. Cyclins and cdks in development and cancer: a perspective. *Oncogene* **24**, 2909-2915, doi:10.1038/sj.onc.1208618 (2005).

6   Hydbring, P., Malumbres, M. & Sicinski, P. Non-canonical functions of cell cycle cyclins and cyclin-dependent kinases. *Nat Rev Mol Cell Biol* **17**, 280-292, doi:10.1038/nrm.2016.27 (2016).

7   Sherr, C. J. & McCormick, F. The RB and p53 pathways in cancer. *Cancer Cell* **2**, 103-112 (2002).

8   Vervoorts, J. & Luscher, B. Post-translational regulation of the tumor suppressor p27(KIP1). *Cell Mol Life Sci* **65**, 3255-3264, doi:10.1007/s00018-008-8296-7 (2008).

9   Besson, A. *et al.* A pathway in quiescent cells that controls p27Kip1 stability, subcellular localization, and tumor suppression. *Genes Dev* **20**, 47-64, doi:20/1/47 [pii]10.1101/gad.1384406 (2006).

10   Malek, N. P. *et al.* A mouse knock-in model exposes sequential proteolytic pathways that regulate p27Kip1 in G1 and S phase. *Nature* **413**, 323-327, doi:10.1038/3509508335095083 [pii] (2001).

11   Coats, S., Flanagan, W. M., Nourse, J. & Roberts, J. M. Requirement of p27Kip1 for restriction point control of the fibroblast cell cycle. *Science* **272**, 877-880 (1996).

12   Georgia, S. & Bhushan, A. p27 Regulates the transition of beta-cells from quiescence to proliferation. *Diabetes* **55**, 2950-2956, doi:10.2337/db06-0249 (2006).

13   Kossatz, U. *et al.* Skp2-dependent degradation of p27kip1 is essential for cell cycle progression. *Genes Dev* **18**, 2602-2607, doi:10.1101/gad.321004 (2004).

14   Sutterluty, H. *et al.* p45SKP2 promotes p27Kip1 degradation and induces S phase in quiescent cells. *Nat Cell Biol* **1**, 207-214, doi:10.1038/12027 (1999).

15   Viatour, P. *et al.* Hematopoietic stem cell quiescence is maintained by compound contributions of the retinoblastoma gene family. *Cell Stem Cell* **3**, 416-428, doi:10.1016/j.stem.2008.07.009 (2008).

16   Mason-Richie, N. A., Mistry, M. J., Gettler, C. A., Elayyadi, A. & Wikenheiser-Brokamp, K. A. Retinoblastoma function is essential for establishing lung epithelial quiescence after injury. *Cancer Res* **68**, 4068-4076, doi:10.1158/0008-5472.CAN-07-5667 (2008).

17   Mayhew, C. N. *et al.* Liver-specific pRB loss results in ectopic cell cycle entry and aberrant ploidy. *Cancer Res* **65**, 4568-4577 (2005).

18   Dyson, N. The regulation of E2F by pRB-family proteins. *Genes Dev* **12**, 2245-2262 (1998).

19   Qin, X. Q., Chittenden, T., Livingston, D. M. & Kaelin, W. G., Jr. Identification of a growth suppression domain within the retinoblastoma gene product. *Genes Dev* **6**, 953-964 (1992).

20   Hiebert, S. W., Chellappan, S. P., Horowitz, J. M. & Nevins, J. R. - The interaction of RB with E2F coincides with an inhibition of the transcriptional activity of E2F. - *Genes Dev* **- 6**, - 177-185 (1992).

21   Qin, X.-Q. *et al.* The transcription factor E2F-1 is a downstream target of RB action. *Molec. and Cellular Biology* **15**, 742-755 (1995).

22   Otterson, G. A., Chen, W., Coxon, A. B., Khleif, S. N. & Kaye, F. J. Incomplete penetrance of familial retinoblastoma linked to germ-line mutations that result in partial loss of RB function. *Proc Natl Acad Sci U S A* **94**, 12036-12040 (1997).

23   Sellers, W. R. *et al.* Stable binding to E2F is not required for the retinoblastoma protein to activate transcription, promote differentiation, and suppress tumor cell growth. *Genes Dev* **12**, 95-106 (1998).

24   Whitaker, L. L., Su, H., Baskaran, R., Knudsen, E. S. & Wang, J. Y. Growth suppression by an E2F-binding-defective retinoblastoma protein (RB): contribution from the RB C pocket. *Mol Cell Biol* **18**, 4032-4042 (1998).

25   Binne, U. K. *et al.* Retinoblastoma protein and anaphase-promoting complex physically interact and functionally cooperate during cell-cycle exit. *Nat Cell Biol* **9**, 225-232 (2007).

26   Ji, P. *et al.* An Rb-Skp2-p27 pathway mediates acute cell cycle inhibition by Rb and is retained in a partial-penetrance Rb mutant. *Mol Cell* **16**, 47-58, doi:S1097276504005726 [pii]10.1016/j.molcel.2004.09.029 (2004).

27   Alexander, K. & Hinds, P. W. Requirement for p27(KIP1) in retinoblastoma protein-mediated senescence. *Mol Cell Biol* **21**, 3616-3631, doi:10.1128/MCB.21.11.3616-3631.2001 (2001).

28   Wang, H. *et al.* Skp2 is required for survival of aberrantly proliferating Rb1-deficient cells and for tumorigenesis in Rb1+/- mice. *Nat Genet* **42**, 83-88, doi:10.1038/ng.498 (2010).

29   Zhao, H. *et al.* Skp2 deletion unmasks a p27 safeguard that blocks tumorigenesis in the absence of pRb and p53 tumor suppressors. *Cancer Cell* **24**, 645-659, doi:10.1016/j.ccr.2013.09.021 (2013).

30   Cecchini, M. J. *et al.* A retinoblastoma allele that is mutated at its common E2F interaction site inhibits cell proliferation in gene targeted mice. *Molecular and cellular biology* **34**, 2029-2045, doi:10.1128/MCB.01589-13 (2014).

31   Cecchini, M. J., Amiri, M. & Dick, F. A. Analysis of cell cycle position in mammalian cells. *J Vis Exp* **59**, e3491, doi:10.3791/3491 (2012).

32   Thwaites, M. J., Cecchini, M. J. & Dick, F. A. Analyzing RB and E2F during the G1-S transition. *Methods Mol Biol* **1170**, 449-461, doi:10.1007/978-1-4939-0888-2_24 (2014).

33   Fero, M. L. *et al.* A syndrome of multiorgan hyperplasia with features of gigantism, tumorigenesis, and female sterility in p27(Kip1)-deficient mice. *Cell* **85**, 733-744, doi:S0092-8674(00)81239-8 [pii] (1996).

34   Ritchie, K., Watson, L. A., Davidson, B., Jiang, Y. & Berube, N. G. ATRX is required for maintenance of the neuroprogenitor cell pool in the embryonic mouse brain. *Biol Open* **3**, 1158-1163, doi:10.1242/bio.20148730 (2014).

35   Park, M. S. *et al.* p27 and Rb are on overlapping pathways suppressing tumorigenesis in mice. *Proc Natl Acad Sci U S A* **96**, 6382-6387 (1999).

36   Buttitta, L. A. & Edgar, B. A. Mechanisms controlling cell cycle exit upon terminal differentiation. *Curr Opin Cell Biol* **19**, 697-704, doi:10.1016/j.ceb.2007.10.004 (2007).

37   Busuttil, R. A., Rubio, M., Dolle, M. E., Campisi, J. & Vijg, J. Oxygen accelerates the accumulation of mutations during the senescence and immortalization of murine cells in culture. *Aging Cell* **2**, 287-294 (2003).

38   Williams, B. O. *et al.* Cooperative tumorigenic effects of germline mutations in Rb and p53. *Nat Genet* **7**, 480-484 (1994).

39   Harrison, D. J., Hooper, M. L., Armstrong, J. F. & Clarke, A. R. Effects of heterozygosity for the Rb-1t19neo allele in the mouse. *Oncogene* **10**, 1615-1620 (1995).

40 Bilodeau, S., Roussel-Gervais, A. & Drouin, J. Distinct developmental roles of cell cycle inhibitors p57Kip2 and p27Kip1 distinguish pituitary progenitor cell cycle exit from cell cycle reentry of differentiated cells. *Mol Cell Biol* **29**, 1895-1908, doi:10.1128/MCB.01885-08 (2009).

41 Cobrinik, D. Pocket proteins and cell cycle control. *Oncogene* **24**, 2796-2809 (2005).

42 Morris, E. J. & Dyson, N. J. Retinoblastoma protein partners. *Advances in Cancer Research* **82**, 1-54 (2001).

43 Finn, R. S. *et al.* PD 0332991, a selective cyclin D kinase 4/6 inhibitor, preferentially inhibits proliferation of luminal estrogen receptor-positive human breast cancer cell lines in vitro. *Breast Cancer Res* **11**, R77, doi:10.1186/bcr2419 (2009).

44 Rader, J. *et al.* Dual CDK4/CDK6 inhibition induces cell-cycle arrest and senescence in neuroblastoma. *Clin Cancer Res* **19**, 6173-6182, doi:10.1158/1078-0432.CCR-13-1675 (2013).

45 Gelbert, L. M. *et al.* Preclinical characterization of the CDK4/6 inhibitor LY2835219: in-vivo cell cycle-dependent/independent anti-tumor activities alone/in combination with gemcitabine. *Invest New Drugs* **32**, 825-837, doi:10.1007/s10637-014-0120-7 (2014).

46 Cadoo, K. A., Gucalp, A. & Traina, T. A. Palbociclib: an evidence-based review of its potential in the treatment of breast cancer. *Breast Cancer (Dove Med Press)* **6**, 123-133, doi:10.2147/BCTT.S46725 (2014).

Chapter 3

3 Multiple molecular interactions redundantly contribute to RB-mediated cell cycle control.

3.1 Abstract

The G1-S phase transition is critical to maintaining proliferative control and preventing carcinogenesis. The retinoblastoma tumor suppressor (pRB) is a key regulator of this step in the cell cycle. Here we use a structure-function approach to evaluate the contributions of multiple protein interaction surfaces on pRB towards cell cycle regulation. SAOS2 cell cycle arrest assays showed that disruption of three separate binding surfaces were necessary to inhibit pRB-mediated cell cycle control. Surprisingly, mutation of some interaction surfaces had no effect on their own. Rather, they only contributed to cell cycle arrest in the absence of other pRB dependent arrest functions. Specifically, our data shows that pRB-E2F interactions are competitive with pRB-CDH1 interactions, implying that interchangeable growth arrest functions underlie pRB's ability to block proliferation. Additionally, disruption of similar cell cycle control mechanisms in genetically modified mutant mice results in ectopic DNA synthesis in the liver. Our work demonstrates that pRB utilizes a network of mechanisms to prevent cell cycle entry. This has important implications for the use of new CDK4/6 inhibitors that aim to activate this proliferative control network.

3.2 Introduction

Uninhibited cellular division is a feature of cancer cells. As such, pathways that regulate proliferation are typically disrupted in human cancer [1]. At a molecular level, the

cell division cycle is frequently controlled by decisions made in the G1 phase [2]. Once through this phase, the cell is committed to DNA replication and ultimately completion of cell division. The retinoblastoma gene product (pRB) is a key regulator of the restriction point that is responsible for controlling S-phase entry [3]. The best known function of pRB is the repression of E2F transcription factor activity [4]. RB performs this function by directly binding the transactivation domain of E2Fs, preventing the recruitment of transcriptional activators to influence gene transcription [4]. In addition, pRB can recruit chromatin regulating enzymes, such as histone deacetylases, to assist in transcriptional repression [5]. This blocks gene expression that is necessary for DNA synthesis and cell cycle entry [2]. In the presence of mitogens Cyclin dependent kinases phosphorylate pRB, changing its conformation and releasing E2Fs [6]. Free E2Fs are then able to stimulate transcription and S-phase progression. While this model describes cell cycle entry quite accurately, the role for the same molecular interactions between pRB and E2Fs in cell cycle exit is less clear as pRB dependent arrest can occur much faster than E2F repression [7].

The minimal interaction domain that mediates stable E2F binding to pRB is the large pocket, and this fragment is also the minimal growth suppressing domain [8,9]. The large pocket is composed of three regions called A, B, and C [3]. The A and B domains of pRB form the pocket in which the transactivation domain of E2Fs bind [10,11]. In addition, pRB interacts with a number of chromatin regulators, including HDAC containing complexes, through a well conserved interaction site on the B box of pRB known as the LxCxE binding cleft [5]. This binding site is well defined for its ability to contact the LxCxE motif in viral oncoproteins [12]. Simultaneous interactions between E2Fs, pRB, and chromatin

regulators through LxCxE interactions form the basis of active transcriptional repression through E2Fs. The C-terminus of pRB is largely unstructured and serves as a contact point for numerous protein interactions [3,13]. It is required for stable interaction with E2F-DP dimers [14], as well as a unique interaction with the marked box domain of E2F1 [15]. Analysis of the large pocket of pRB has contributed to our knowledge of E2Fs in cell cycle control. However, there is little to reconcile how multiple competing protein interactions through this domain contribute to pRB's overall influence on cell proliferation.

Genetic ablation of RB causes defects in cell proliferation control in tissues and in primary cell culture experiments [16,17]. However, early studies of pRB-mediated cell cycle regulation exploited the RB null SAOS2 osteosarcoma cell line [8,9,18]. RB expression in these cells leads to a robust accumulation of 2N DNA content, indicating a G1 arrest [19]. These studies looked at a variety of mutant versions of pRB in which strong cancer derived mutations were functionless, but low penetrance RB mutations retained the ability to at least partially restrict cell cycle entry [8,9,20,21]. Surprisingly, the low penetrance mutation R661W was defective for E2F binding, but retained the ability to inhibit cell cycle entry [20-22]. More recently, a number of studies have shown that the R661W mutant can regulate Cyclin dependent kinase activity through p27, independent of E2F transcriptional control [7,23]. Importantly, these studies established that the LxCxE binding cleft and C domains within the large pocket also mediate interactions with the anaphase promoting complex and Skp2 to stabilize p27 expression [7,24]. Surprisingly, a unified model of how E2F dependent and independent proliferative control mechanisms interact has yet to emerge.

To understand the importance of different protein interaction points in the RB large pocket, targeted mutations to disrupt the LxCxE binding cleft [25-28], the canonical E2F binding site [29,30], and pRB's unique interaction with E2F1 in the C-terminus [31,32], have been generated in mice. Analysis of proliferation in cells and tissues from these mutant animals suggests that individual protein interactions play context specific roles. For example, LxCxE binding cleft mutant mice (called *Rb1^L*, or *Rb1^NF*) are viable with hyper proliferation largely limited to mammary ductal epithelium, that is likely due to unresponsiveness to growth inhibitory signals from TGF-β [33]. Importantly, these mice are not spontaneously cancer prone [27,34], and they are capable of blocking E2F transcription under several physiological circumstances [35]. However, repression of E2F targets is diminished following DNA damage, and the ability of these cells to enter senescence is compromised [35,36]. Furthermore, mutagen treatment induces cancer in these mice under conditions where E2F repression fails [26]. Disruption of pRB's unique E2F1 interaction in mice (called *Rb1^S*) shows no detectable change in proliferative control in tissues or isolated cells [32]. Lastly, mutational disruption of pRB-E2F interactions in *Rb1^{G/G}* mice results in cells with accelerated entry into the cell cycle, but normal cell cycle exit [29,30]. Remarkably, this mutation does not predispose mice to cancer [29], however, disruption of this interaction in combination with p27 deficiency deregulates cell cycle arrest functions and these mice are highly cancer prone [30]. This result is also provocative because the cell cycle arrest defects in *Rb1^{G/G}*; p27 deficient compound mutants aren't found in either single mutant strain alone. These data suggest that pRB dependent cell cycle arrest may depend on a complex network of proliferative control signals such that loss of individual functions have limited effect on their own. This concept is underscored by the fact that no

targeted knock in strain recapitulates the complete proliferative control and cancer

susceptibility phenotypes of $Rb1^{-/-}$ mice. In this manuscript, we aimed to eliminate

individual binding surfaces in the pRB large pocket to determine the extent that each

contributes to cell cycle control alone and in combinations using SAOS2 arrest as a read

out. Here, we demonstrate that multiple individual binding surfaces in the large pocket

contribute to pRB-mediated cell cycle control in cell culture, and provide proof of

principle that this network functions endogenously to regulate DNA replication in the

liver.

3.3   Materials and Methods

3.3.1   GST pulldowns and western blotting

C33A cells were transfected with either HA-E2F1-3 (along with DP1), myc

tagged CDH1 or pRB expression plasmids under the control of CMV promoters using

standard calcium phosphate precipitation techniques. Forty hours after transfection cells

were washed and collected in GSE buffer (20mM Tris, pH 7.5, 420 mM NaCl, 1.5 mM

$MgCl_2$, 0.2mM EDTA, 25% glycerol, 5 µg/ml leupeptin, 5 µg/ml aprotinin, 0.1 mM

Na_3VO_4, 0.5 mM NaF, and 1 mM DTT) and frozen at -80°C. Cell extracts were

centrifuged and the supernatant was diluted 2-fold in low salt GSE (20mM Tris, pH 7.5,

1.5 mM $MgCl_2$, 0.2mM EDTA, 25 mM DTT, 0.1% NP-40) and combined with

glutathione beads and recombinant fusion proteins. GST-RB large pocket (amino acids

379-928) and GST-HPV-E7 recombinant proteins were expressed and purified as

previously described [29]. Beads were then washed twice with low salt GSE, boiled in SDS-

sample buffer, resolved by SDS-PAGE, and western blotted. HA-tagged proteins were

detected using anti-HA 3F10 (Roche), myc-tagged CDH1 was detected using monoclonal

antibody 9E11, and pRB was detected with G3-245 (BD Pharmagen). To test pRB stability, cells transfected with CMV expressed pRB were treated with 100µg/mL cycloheximide for 24 hours. Extracts were prepared in GSE buffer every three hours up to 15 hours. Extracts were spun down and western blotted for pRB.

3.3.2   SAOS2 cell cycle arrest assays

SAOS2 cells were transfected and harvested as previously described [37]. Briefly 10^6 cells were plated in 6cm dishes and transfected with 0.15µg of CMV-pRB, 1µg of CMV-CD20 and 3.85µg of CMV-β-gal, or 1µg of CMV-CD20 and 4µg of CMV-β-gal as a negative control, using X-tremeGENE transfection reagent (Roche). Cells were re-plated onto 10cm dishes 24 hours after transfection, and harvested 48 hours later. Cells were then stained with a fluorescein conjugated anti-CD20 antibody to mark successfully transfected cells, as well as with propidium iodide (PI) to determine their DNA content. Flow cytometry was then performed to identify the percentage of CD20 positive cells with 2N DNA content as a measure of G1. In experiments expressing cell cycle arrest as percent change in G1, arrest data was scaled using CMV-pRB and CMV-β-gal as standards for maximal increase and unchanged G1 content allowing comparisons between different batches of experiments.

3.3.3   Animal housing, dissection and histology

All animals were housed and handled as approved by the Canadian Council on Animal Care. Mice were sacrificed at 8 weeks of age, dissected, and livers were processed for downstream applications. For histology, livers were fixed in formalin for 72 hours followed by 72 hours in PBS before being stored in 70% ethanol. Livers were then embedded in paraffin and five micron sections were cut and stained with

Hematoxylin and Eosin. Images were captured on a Zeiss Axioskop 40 microscope and Spot Flex camera, and nuclear area in the livers was calculated using EyeImage software (Empix Imaging, Mississauga, Ontario, Canada).

3.3.4   Ploidy analysis of adult livers

A small piece of frozen liver was added to buffer A (25mM Tris pH 7.5, 50mM KCl, 2mM $MgCl_2$, 1mM EDTA, 1mM PMSF). Tissue was ground on ice with a mechanical tissue grinder. Tissue was then homogenized using a 1mL dounce homogenizer and tight pestle. Nuclei were centrifuged at 12000xg, then washed in buffer A and centrifuged. The pellet was then resuspended in Propidium Iodide solution (0.5mg/mL PI, 0.1% NP-40, 0.1% sodium citrate, 40µg/mL RNase A in PBS). Samples were then analyzed by flow cytometry using standard methods to quantitate DNA content.

3.3.5   RNA isolation and E2F target gene quantification.

RNA from livers was isolated using an RNeasy fibrous tissue kit (Invitrogen). Expression levels of the E2F target genes, *Pcna, Ccne1* (Cyclin E1)*, Ccna2* (Cyclin A2)*, Tyms* (thymidylate synthase)*, Mcm3*, and *Rbl1* (p107), were determined using the Quantigene Plex 2.0 reagent system from Affymetrix (Santa Clara, CA) and a BioPlex200 multiplex analysis system as previously reported [38]. Expression levels were normalized to the expression of β-actin.

3.3.6   BrdU staining of tissue sections.

To analyze DNA replication, mice were injected with 200µL of 16µg/mL BrdU (Sigma) in their peritoneal cavity 2 hours before sacrifice. Livers were then isolated,

fixed in formalin, embedded, and sectioned according as above. Sections were

deparaffinized and rehydrated using a series of xylene and ethanol washes. The sections

were brought to a boil in sodium citrate buffer and then maintained at 95°C for 10 min.

The cooled sections were rinsed in water three times for 5 minutes, and then rinsed in

PBS for 5 minutes. The sections were blocked in phosphate buffered saline (PBS)

supplemented with 2.5% horse serum and 0.3% Triton X-100 for 1 hour. The sections

were then incubated with anti-BrdU antibodies (BD-Biosciences) in blocking buffer

overnight at 4°C and rinsed in PBS three times for 5 minutes each time. The slides were

incubated with horse anti-mouse immunoglobulin G-fluorescein isothiocyanate (Vector)

for 1h and rinsed in PBS. The slides were then mounted with Vectashield plus DAPI

(Vector). Fluorescent images were captured on a Zeiss Axioskop40 microscope and Spot

Flex camera and colored using EyeImage software (Empix Imaging, Mississauga,

Ontario, Canada), or a similar system.

3.4   Results

3.4.1   A cell culture assay demonstrates molecular redundancy of RB functions in proliferative control.

Tumor suppression by the retinoblastoma protein has typically been associated

with its ability to block cell cycle progression and repress E2F transcription factors [4].

However, defective E2F binding by pRB has been shown to have modest effects on

proliferative control in SAOS2 cell culture experiments [15,20-22], and gene targeted mouse

models [29,30]. In an attempt to describe the molecular interactions necessary for pRB-

mediated cell cycle arrest we investigated forms of pRB that were individually mutated at

each of three distinct binding surfaces in the large pocket; the general E2F binding site
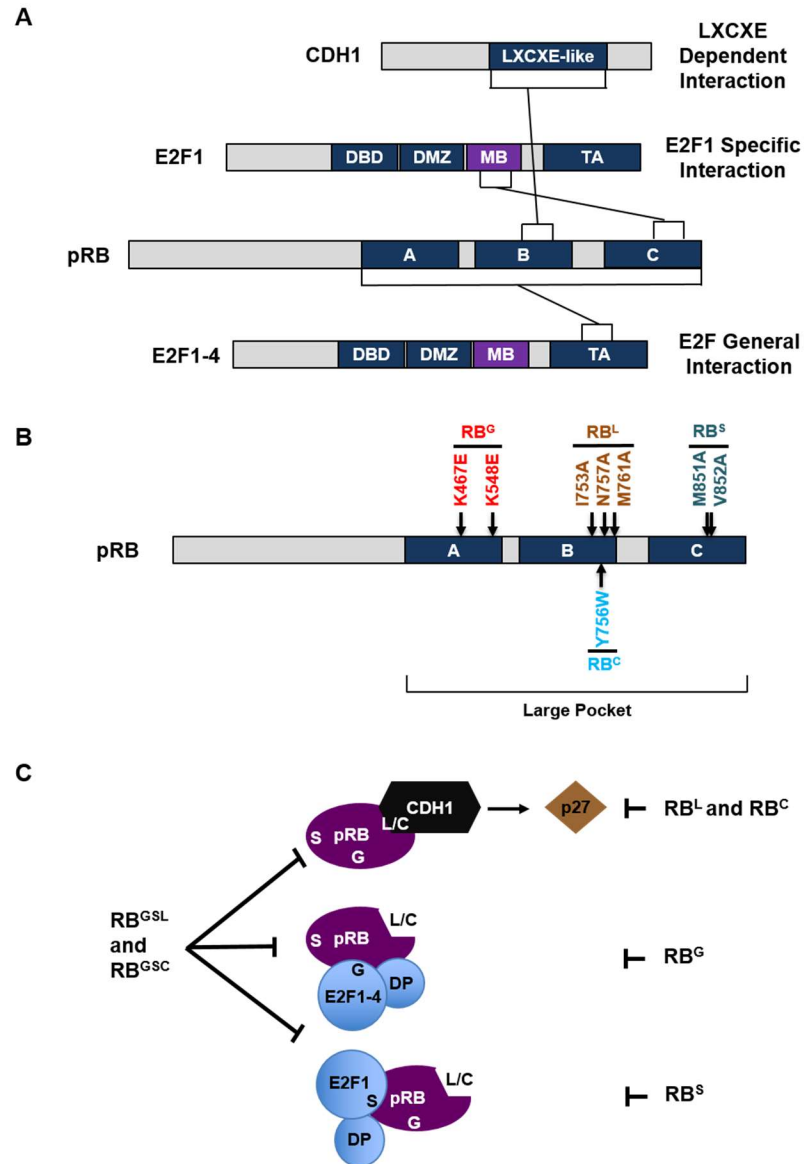
Figure 3.1: Interaction domains located in the large pocket of pRB and substitutions used in this study.

(A) Linear diagrams of open reading frames for the indicated proteins highlighting the regions that mediate interactions with pRB. Note pRB can bind E2F1-4 through the transactivation domain in the C-terminus of E2Fs known as the 'general' interaction. Alternatively, pRB can also bind the marked box domain of E2F1 through its C-terminal domain, termed the pRB-E2F1 'specific' interaction. **(B)** Locations of point mutations within the pRB open reading frame used in this study. RB^G refers to mutations that disrupt the E2F general interaction, RB^S is a mutation that disrupts the E2F1 specific interaction. RB^C and RB^L both disrupt interactions through the LxCxE binding cleft. All codon numbers correspond to the human sequence. The large pocket domain is amino acids 379-928. **(C)** Diagram depicting the cell cycle control mechanisms that can be influenced by the 3 pRB binding surface mutations used in this study.

(RB^G), the E2F1 specific site (RB^S), and the LxCxE binding cleft (using either the RB^L or RB^C mutations). **Figure 3.1A** diagrams pRB protein interactions and shows the relevant regions in each open reading frame that participate. Amino acid substitutions that are demonstrated to disrupt these contacts are shown in Figure 3.1b [24,37,39,40], along with single letter nomenclature for each allele (e.g. RB^G). Lastly, the types of interactions between pRB and E2Fs, or LxCxE motif proteins, are illustrated with the alleles that disrupt them individually shown on the right, and the intended effect of a combined mutant allele on the left (**Figure 3.1C**).

GST-tagged versions of the pRB large pocket (GST-RBLP, pRB amino acids 379-928) containing the 3 mutations described above, as well as the triple mutant, were produced in bacteria. GST pulldowns were performed to test interaction defects predicted to occur in these mutants (**Figure 3.2A**). RB deficient C33A lysates derived from transfections with the indicated E2Fs, or CDH1 were produced and used in pulldown experiments. As expected the RB^G mutation disrupts binding of the activator E2Fs, E2F2 and E2F3. RB^L disrupts the LxCxE binding cleft and is defective for binding the anaphase promoting complex targeting subunit CDH1. Finally, since E2F1 can associate with pRB through two qualitatively different interactions, the general site and the specific site, binding is only lost following mutation of both sites in the triple mutant RB^{GSL}. Full length pRB constructs containing these mutations were then transfected into SAOS2 cells to determine their effectiveness in causing a G1 cell cycle accumulation. As previously shown, expression of wild-type pRB in SAOS2 cells lead to a build up of cells in G1 as determined by propidium iodide staining and flow cytometry (**Figure 3.2B**)[19]. Expression of the mutant constructs of pRB had various levels of effectiveness for
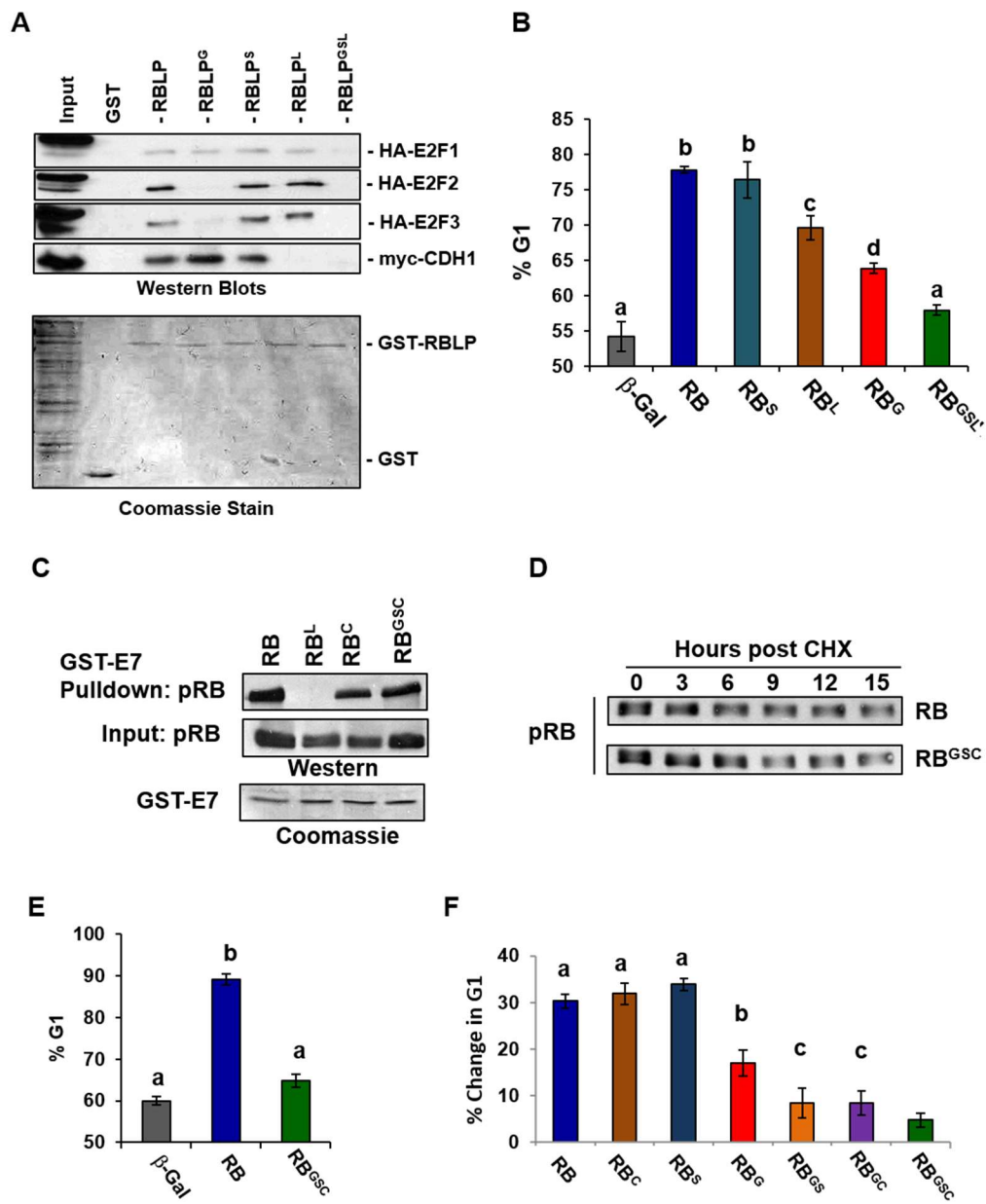
Figure 3.2: Multiple point mutations are needed to overcome RB-mediated cell cycle arrest.

Figure 3.2: Multiple point mutations are needed to overcome RB-mediated cell cycle arrest.

(A) GST-tagged RB large pocket proteins corresponding to the RB^G, RB^S, RB^L, and RB^{GSL} mutant versions of pRB were produced and purified. These GST-fusions were incubated with C33A extracts transfected with the indicated expression constructs. Bound proteins were isolated by precipitation and identified by western blotting. **(B)** Constructs containing full-length RB harboring the indicated mutations under the control of a CMV promoter were transfected into SAOS2 cells along with a CD20 reporter. Cells were then stained with propidium iodide and the percentage of cells in G1 were determined by DNA content of CD20 positive cells. Bars indicate the mean of three separate experiments, and error bars indicate one standard deviation from the mean. Letters indicate groups that are significantly different from one another (ANOVA, Tukey test, $p < 0.05$). **(C)** Full length CMV-RB constructs were transfected into C33A cells and extracts were incubated with recombinant HPV-E7. Bound proteins were isolated by precipitation and western blotted to detect pRB. **(D)** Full length RB^{WT} and RB^{GSC} were transfected into C33A cells prior to cycloheximide treatment (CHX). Extracts were prepared over a 15 hour time course and stability was monitored by Western blotting. **(E)** Constructs containing full-length RB harboring the various mutations, or combinations of mutations, under the control of a CMV promoter were transfected into SAOS2 cells along with a CD20 reporter. Cells were then stained with propidium iodide and the percentage of cells in G1 were determined by DNA content of CD20 positive cells. Bars indicate the mean of three separate experiments, and error bars indicate one standard deviation from the mean. **(F)** Transfections and cell cycle analysis were performed as in B and E, except the increase in G1 cells is shown as Change in % G1 (relative to β-Gal control). Letters indicate groups that are significantly different from one another (ANOVA, Tukey test, $p < 0.05$).

inducing a G1 cell cycle arrest (**Figure 3.2B**). Notably, the RB^S mutation showed a

similar ability to block proliferation as wild-type RB (**Figure 3.2B**). By contrast,

disruption of the general binding pocket in the RB^G mutant, or disruption of the LxCxE

binding cleft (RB^L) resulted in a significant, but partial decrease in the percentage of cells

in the G1 phase of the cell cycle (**Figure 3.2B**). Importantly, no individual mutation can

completely disrupt RB function. However, when all three mutations were combined into

one pRB molecule (RB^{GSL}), the ability of pRB^{GSL} to induce a G1 arrest was not

statistically different from that of the β-Gal negative control (**Figure 3.2B**). As disruption

of the various interactions lead to an inability of pRB to bind to any of its LxCxE or E2F

interactors, we next aimed to confirm that combination mutations led to disruption of

these binding surfaces, as opposed to simply disrupting pRB structure or stability. To

address this possibility, we used the RB^C mutation that retains the ability to associate

with HPV-E7, but has previously been shown to be defective for its interaction with

CDH1 [24,37,39,40]. Figure 3.2c demonstrates that both the RB^C, and an RB^{GSC} combination

could maintain RB-E7 interaction, suggesting this mutant combination retains it structure.

Furthermore, the stability of the RB^{GSC} mutation was determined by expressing both

RB^{WT} and RB^{GSC} in C33A cells. Cells were then treated with cycloheximide and protein

was isolated over a period of 15 hours. Western blots confirmed that RB^{WT} and RB^{GSC}

have equal stability, further suggesting that these substitutions do not result in the

misfolding and hence pleiotropic loss of pRB function (**Figure 3.2D**). Finally, SAOS2

cell cycle arrest assays were performed using the RB^C mutant alone or in double and

triple combinations (RB^{GC} or RB^{GSC}). As with the RB^{GSL} mutant, the triple mutant

combination RB^{GSC} was unable to increase the proportion of G1 cells beyond that of β-

Gal controls (**Figure 3.2E**). In addition, SAOS2 cell cycle arrest following transfection with the RB^{GC} and RB^{GS} double mutants diminished the ability to induce a G1 cell cycle arrest beyond any single mutant, but was less detrimental than the RB^{GSC} combination (**Figure 3.2F**). These results demonstrate that pRB's activity in this arrest assay can be defined through loss of individual protein interactions.

The combination of RB^{G} and RB^{L} mutations in RB^{GSL} is more severe than either alone (**Figure 3.2B**). It is difficult to envision LxCxE interaction defects enhancing loss of function of pRB-E2F binding defects through transcriptional control since the RB^{G} mutation already disrupts recruitment to E2F promoters [29,30]. For this reason, we investigated non-E2F dependent mechanisms that could be lost because of the RB^{L} mutation such as binding to CDH1. To investigate how E2F and CDH1 dependent arrest mechanisms may relate to one another, we tested pRB's ability to interact with each simultaneously. For this experiment, we mixed C33A extracts containing myc-tagged CDH1 with increasing amounts of HA-E2F3/DP1 extracts and tested their ability to bind to GST-RBLP in pulldown experiments (**Figure 3.3**). This experiment reveals that increasing quantities of HA-E2F3/DP1 prevent myc-CDH1 from binding to GST-RBLP (**Figure 3.3, left side**). Disruption of E2F3 binding to pRB using a GST-RBLP^{G} mutant prevents competition with myc-CDH1 for binding to pRB. This experiment suggests that pRB is unable to engage E2F3 and CDH1 dependent functions simultaneously, suggesting that these functions are interchangeable. This mirrors findings from recent *in vivo* approaches to pRB dependent cell cycle control [30], and this will be explored further in the discussion.
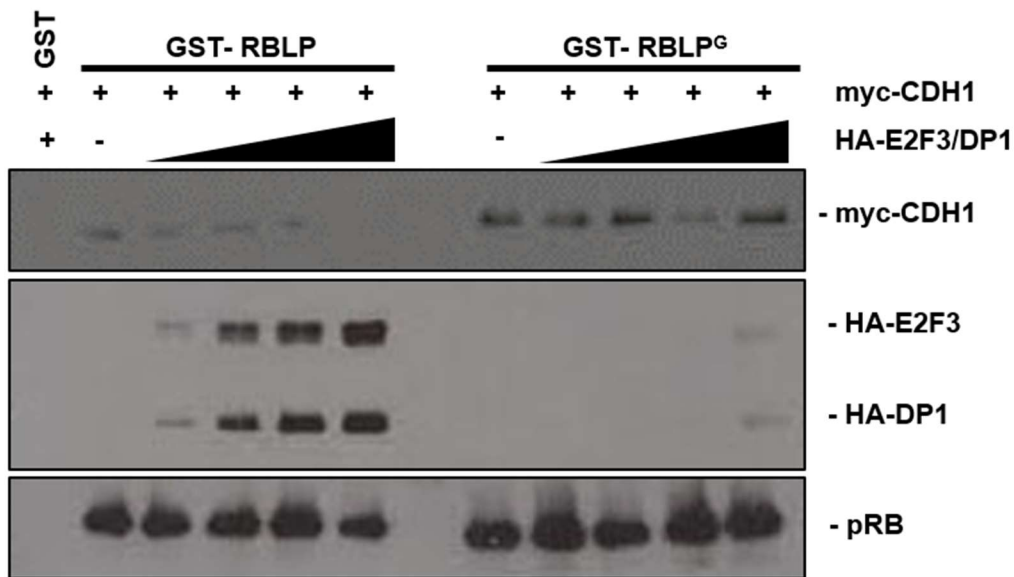
Figure 3.3: Competition between E2Fs and CDH1 for pRB binding.

Purified GST-RBLP or an -RBLP^G mutant was incubated with constant levels of myc-CDH1, and increasing quantities of HA-tagged E2F3/DP1 from transfected lysates. GST-pulldowns were performed and associated levels of myc-CDH1 and HA-E2F3/DP1 were determined by western blotting. Western blots using anti-pRB antibodies show the levels of GST-RBLP proteins precipitated in each experiment.

3.4.2 A compound mutant mouse model demonstrates molecular redundancy in RB control of DNA replication.

Mutation of all three binding surfaces in the RB large pocket was required to maximally impair RB-mediated cell cycle control (**Figure 3.2BE**). This finding, combined with the fact that individual mutations for each of these binding sites in gene targeted mice did not phenocopy the $Rb1^{-/-}$ proliferative control defects in primary cell culture, suggests that the function of pRB in cell cycle control may be composed of several distinct mechanisms [28,29,32]. To approximate the dysfunction of the RB^{GSL} mutation *in vivo* as diagrammed in **Figure 3.1C**, we combined our previously published $Rb1^{G/G}$ animals that disrupts pRB-E2F interactions with p27 null mice ($Cdkn1b^{-/-}$) to eliminate its influence on cell cycle control [30]. In addition, we crossed these mice into an E2F1 null background to eliminate any effect on cell cycle regulation by the pRB-E2F1 specific interaction. This combination of mutations $Rb1^{G/G}; Cdkn1b^{-/-}; E2f1^{-/-}$, represents one potential scenario of the effects of the RB^{GSL} mutation *in vivo* on cell cycle control. Interestingly, $Rb1^{G/G}; Cdkn1b^{-/-}; E2f1^{-/-}$ (triple mutant) animals are viable and occur at normal Mendelian ratios (**Table 3.1**).

Since triple mutant mice did not phenocopy the embryonic lethality seen in $Rb1^{-/-}$ animals we next sought to determine if any tissues display loss of cell cycle control [41]. Previously, Mayhew *et al.* showed that tissue specific knockout of pRB in the murine liver resulted in the up regulation of E2F target genes and ectopic DNA replication, endoreduplication, and accumulation of nuclei with elevated ploidy [42]. Since hepatocytes often endoreduplicate it is possible to detect the accumulation of misregulated DNA

Table 3.1: Frequency of compound mutant mice.

$E2f1^{-/-}; Rb1^{G/+}; Cdkn1b^{+/-}$ X $E2f1^{-/-}; Rb1^{G/+}; Cdkn1b^{+/-}$	
Genotype	**P14**
$E2f1^{-/-}; Rb1^{+/+}; Cdkn1b^{+/+}$	8 (13)
$E2f1^{-/-}; Rb1^{+/+}; Cdkn1b^{+/-}$	29 (26)
$E2f1^{-/-}; Rb1^{+/+}; Cdkn1b^{-/-}$	12 (13)
$E2f1^{-/-}; Rb1^{G/+}; Cdkn1b^{+/+}$	29 (26)
$E2f1^{-/-}; Rb1^{G/+}; Cdkn1b^{+/-}$	64 (52)
$E2f1^{-/-}; Rb1^{G/+}; Cdkn1b^{-/-}$	9* (26)
$E2f1^{-/-}; Rb1^{G/G}; Cdkn1b^{+/+}$	12 (13)
$E2f1^{-/-}; Rb1^{G/G}; Cdkn1b^{+/-}$	35 (26)
$E2f1^{-/-}; Rb1^{G/G}; Cdkn1b^{-/-}$	10 (13)
Total	208

The indicated genotypes of mice were crossed and all resulting progeny were genotyped. The number of live animals obtained at two weeks of age is indicated for each genotype and the expected number based on Mendelian inheritance is indicated in brackets. * Indicates significance as determined by chi-squared test.

replication over time [35]. We therefore, aimed to analyze aspects of cell cycle control in the livers of $Rb1^{G/G}$; $Cdkn1b^{-/-}$; $E2f1^{-/-}$ animals to determine if these mutations were capable of disrupting pRB control of DNA replication. H&E staining of livers revealed that hepatocyte triple mutant adult livers had enlarged nuclei that on average were three times larger that wild-type and $Rb1^{G/G}$; $Cdkn1b^{-/-}$ double mutant animals as well as twice as large as $Rb1^{G/G}$ and $Rb1^{G/G}$; $E2f1^{-/-}$ nuclei (**Figure 3.4AB**). We also quantitated the density of hepatocytes per microscopic field of view and did not see significant differences between genotypes (**Figure 3.4C**). Since nuclear area in liver histology correlates with DNA content [43], this suggested elevated levels of endoreduplication in $Rb1^{G/G}$; $Cdkn1b^{-/-}$; $E2f1^{-/-}$ triple mutant livers. To test whether our triple mutant had elevated ploidy in their hepatocytes, nuclei were extracted from livers of $Rb1^{+/+}$, $Rb1^{G/G}$, and $Rb1^{G/G}$; $Cdkn1b^{-/-}$; $E2f1^{-/-}$ mice, stained with propidium iodine, and analyzed by flow cytometry for DNA content. Consistent with previous results we found that $Rb1^{+/+}$ livers at 8 weeks of age display very low levels of 8N DNA content, however triple mutant livers displayed a significant increase in the level of 8N DNA at this time point (**Figure 3.4C**), that is similar to what is reported when $Rb1$ is conditionally deleted in this organ [42]. This increase in nuclear size and subsequent DNA content indicates that triple mutant livers undergo endoreduplication. While this is a normal phenotype for liver cells over time, this suggests that the loss of these three regulatory elements controlled by pRB results in earlier endoreduplication, potentially due to a loss of cell cycle control.

We next wanted to determine the effect of our combined mutations on the regulation of pRB functions related to cell cycle control. To accomplish this, RNA was isolated from adult livers to analyze the expression of E2F target gene transcription.
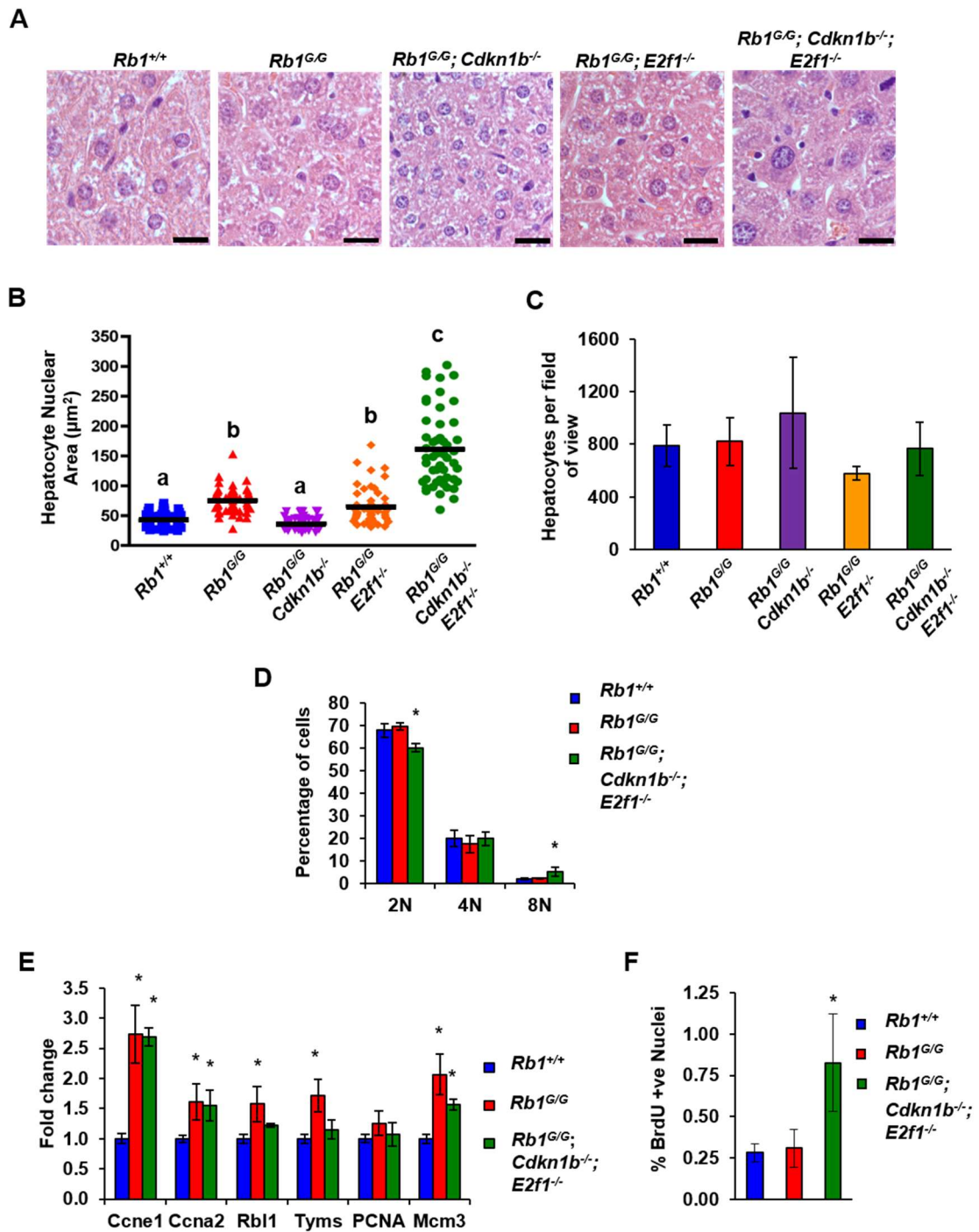
Figure 3.4: Ectopic DNA-replication in *Rb1^{G/G}; Cdkn1b^{-/-}; E2f1^{-/-}* compound mutant mice.

Figure 3.4: Ectopic DNA-replication in *Rb1$^{G/G}$; Cdkn1b$^{-/-}$; E2f1$^{-/-}$* compound mutant mice.

(A) H&E staining of liver sections from eight-week old wild type, *Rb1$^{G/G}$*, double mutant *Rb1$^{G/G}$; Cdkn1b$^{-/-}$*, and *Rb1$^{G/G}$; E2f1$^{-/-}$* mice, as well as *Rb1$^{G/G}$; Cdkn1b$^{-/-}$; E2f1$^{-/-}$* triple mutant animals. The scale bars represent 20 μm. **(B)** Nuclear size from the images in A was determined and the mean size is indicated. Measurements were made from at least 50 nuclei, a, b, c represents statistically different groups as determined by ANOVA followed by Tukey's test ($p < 0.05$). **(C)** Total number of hepatocytes per 20X field of view was averaged from the indicated genotypes. No statistical differences were observed by AVONA followed by Tukey's test ($p < 0.05$) **(D)** Nuclei were extracted from livers, stained with propidium iodide, and analyzed for DNA content by flow cytometry. **(E)** The relative expression level of six E2F cell cycle target genes from wild type, *Rb1$^{G/G}$*, and *Rb1$^{G/G}$; Cdkn1b$^{-/-}$; E2f1$^{-/-}$* was determined from RNA extracted from 8-week-old livers. **(F)** Eight-week-old mice were pulse labeled with BrdU two hours prior to sacrifice and livers were sectioned and stained for BrdU. The percentage of BrdU positive nuclei was determined. At least 500 nuclei were counted per mouse. All bar graphs represent at least 3 individual experiments, and error bars indicate one standard deviation from the mean. An asterisk represents a statistically significant difference from the wild type control (*t*-test, $P < 0.05$).

Consistent with our previous findings, E2F target gene expression in $Rb1^{G/G}$ animals is higher than wild-type levels [29]. Interestingly, triple mutant livers show high expression of some of these target genes (**Figure 3.4E**). However, in some cases, E2F target gene expression is unchanged from wild type and this will be discussed later. To directly measure proliferation in livers, 8-week-old animals were injected with BrdU to label nuclei with actively replicating DNA. Livers were dissected, sectioned and stained for BrdU incorporation. This analysis showed that while both $Rb1^{G/G}$ and $Rb1^{G/G}$; $Cdkn1b^{-/-}$; $E2f1^{-/-}$ livers display increases in the expression of E2F target genes only triple mutant livers displayed increased BrdU incorporation (**Figure 3.4EF**). Taken together with the increased nuclear area and 8N DNA content in triple mutant livers, these results suggest that by mutating the general binding site of pRB, and eliminating both p27 and E2F1, we have recapitulated the DNA replication defects associated with conditional deletion of *Rb1* in adult livers. These *in vivo* results also mirror the effects seen in the SAOS2 arrest assays that suggest that no individual protein interaction with pRB accounts for its activity in cell cycle control. Instead, these data indicate that pRB likely sits in the center of a network of regulators that control DNA replication and cell division.

3.5   Discussion

In this manuscript, we aimed to further the understanding of pRB-mediated cell cycle control by disrupting pRB-binding interactions in the large pocket to quantitatively account for its arrest mechanisms. This structure-function analysis demonstrated that to disrupt the vast majority of pRB's cell cycle arrest activity, three different binding surfaces needed to be altered. Surprisingly, no single interaction site was indispensable and disruption of some interaction sites had little effect on their own. We used a genetic

cross to cripple these three aspects of pRB function endogenously and the combination caused ectopic DNA replication in the liver. This suggests that pRB may interchangeably use different protein interactions to influence cell cycle advancement. Insights and caveats of our study are discussed below.

It is difficult to predict the proliferative control defects of an *Rb1* deficient mouse beyond neonatal lethality due to muscle atrophy [44]. Interestingly, chimeric mice composed of a mixture of wild type and *Rb1*^{-/-} cells are viable and demonstrate normal tissue cellularity, even in organs where *Rb1*^{-/-} cells contribute extensively [17]. This study reveals that livers containing *Rb1*^{-/-} hepatocytes display random, large nuclei, similar to our findings in triple mutant livers [17]. In addition, conditional ablation of *Rb1* in the livers of adult mice is reported to cause unscheduled DNA replication [42]. The increase in DNA copy number and BrdU incorporation was indicative of a loss of regulation of DNA synthesis [42]. In an effort to model the effects of the RB[GSL] mutant *in vivo*, we combined *Rb1*[G/G] animals with p27 and E2F1 deficiency to produce triple mutant animals (*Rb1*[G/G]; *Cdkn1b*^{-/-}; *E2f1*^{-/-}). This combination of mutations lead to a very similar DNA replication phenotype in the liver as complete *Rb1* deletion. While this is a similar phenotype as conditional deletion of *Rb1*, by no means does our study elucidate all that pRB or E2Fs do to block the cell cycle in this or other tissues. We anticipate that viability of triple mutant mice suggests additional pRB dependent cell cycle arrest mechanisms likely remain functional in these animals. Another important consideration in our efforts to model the RB[GSL] mutant *in vivo* is that deleting *Cdkn1b* and *E2f1* is not the equivalent to disrupting the binding sites on pRB that regulate them, as these interaction sites may have additional regulatory effects beyond the downstream targets we have chosen. In addition,

loss of E2F1 could diminish cell proliferation even when entry into S-phase is deregulated and this could further complicate the interpretation of our analysis of triple mutant livers. Importantly, others have demonstrated that the choice between proliferation and endoreduplication in hepatocytes is determined by opposing effects of activator E2Fs (such as E2F1) and the E2F7 and E2F8 repressors [45,46]. It is difficult to predict how the triple mutant combination used here would affect the regulation of this network of genes to cause a switch to endoreduplication. Future experiments using *Rb1* gene targeted mice carrying a combination of G, S, or L mutations in a single allele will help resolve some of these complexities.

We observed that some individual mutations contributed modestly to proliferative control alone, and more strongly when in combination with other substitutions. We suggest that this may be due in part to the competition between different cell cycle control mechanisms for access to pRB. For example, we demonstrate that E2F3 and CDH1 can compete for the opportunity to interact with pRB, and this is consistent with previous reports of E2F1 and CDH1 competing for pRB [47]. We suggest that CDH1 interactions with pRB are fundamentally different than other pRB interactors that contact the LXCXE binding site simultaneously with E2Fs [3]. Another way to consider redundancy of function through endogenous pRB is a gene targeted mouse model bearing an R654W mutation (the murine equivalent of the low penetrance human mutation R661W). This mutation not only disrupts E2F binding, it also compromised interactions at the LXCXE cleft [20], potentially illustrating the effects of multiple mutations in a single pRB molecule akin to RB[GC] in our studies. Fibroblast cells from these mice possess many features of deregulated proliferation seen in *Rb1*^{-/-} cells and this mutation is lethal during

embryogenesis [48]. However, some aspects of pRB's role in differentiation and its ability to respond to senescence inducing stimuli and resistance to tumor formation are retained [48,49], suggesting that simultaneous deficiency by pRB for multiple interactions can reveal a more dramatic phenotype than loss of single interactions. This conclusion is further supported by deregulated cell cycle control and cancer incidence in $Rb1^{G/G}$; $Cdkn1b^{-/-}$ mice[50], suggesting loss of multiple pRB dependent proliferative control pathways can be dramatically different than loss of a single pathway.

Consistent with multiple interactions needing to be compromised to abrogate cell cycle arrest by pRB, we also note that some mutations tested in this study, such as the M851A, V852A changes (RB^S), have no effect on proliferative control in the SAOS2 assay on their own. We suggest that it may represent a latent proliferative control mechanism used by pRB, and there may be others. A long standing puzzle in the RB field has been the existence of proliferative control mechanisms that are mediated by the N-terminus of pRB, outside of the original growth suppressing large pocket domain [51-53]. Recent work has suggested that the N-terminus also plays a role in regulating DNA replication [53]. This may explain the phenotypic difference in proliferative control between $Rb1^{-/-}$ animals and that of triple mutant $Rb1^{G/G}$; $Cdkn1b^{-/-}$; $E2f1^{-/-}$ animals as the N-terminus is unaffected by our three mutations. There may also be redundancy between N-terminal and large pocket growth arrest mechanisms. Provocatively, there are also low penetrance mutations in human $RB1$ that target this region of pRB; further suggesting the N-terminus contributes to pRB's proliferative control and tumor suppressor functions [54]. We think that interchangeability of different pRB functions in proliferative control best

explains our data and also encompasses additional work in the field that has previously been difficult to reconcile.

RB dependent proliferative control is functionally inactivated in the vast majority of cancers. This study furthers our understanding of the importance of the various interaction surfaces of pRB and their roles in cell cycle control. In addition, CDK4/6 inhibitors have recently been developed to reactivate the RB-pathway in cancer [55-57]. Understanding the molecular interactions made by pRB and how they influence cell cycle control and tumor suppression is crucial to the proper implementation of these drugs. We expect that the mutational status of both pRB, as well as its regulation of p27 and E2Fs, will play a critical role in the effectiveness of these drugs. We suggest that patients whose tumor cells have pRB activatable p27 will benefit most from CDK4/6 inhibitors.

3.6   References

1   Hanahan, D. & Weinberg, R. A. Hallmarks of cancer: the next generation. *Cell* **144**, 646-674, doi:10.1016/j.cell.2011.02.013 (2011).

2   Coller, H. A. What's taking so long? S-phase entry from quiescence versus proliferation. *Nat Rev Mol Cell Biol* **8**, 667-670, doi:10.1038/nrm2223 (2007).

3   Dick, F. A. & Rubin, S. M. Molecular mechanisms underlying RB protein function. *Nat Rev Mol Cell Biol* **14**, 297-306, doi:10.1038/nrm3567 (2013).

4   Bertoli, C., Skotheim, J. M. & de Bruin, R. A. Control of cell cycle transcription during G1 and S phases. *Nat Rev Mol Cell Biol* **14**, 518-528, doi:10.1038/nrm3629 (2013).

5   Classon, M. & Harlow, E. The retinoblastoma tumour suppressor in development and cancer. *Nat. Rev. Cancer* **2**, 910-917 (2002).

6   Burke, J. R., Deshong, A. J., Pelton, J. G. & Rubin, S. M. Phosphorylation-induced conformational changes in the retinoblastoma protein inhibit E2F transactivation domain binding. *J Biol Chem* **285**, 16286-16293, doi:M110.108167 [pii]10.1074/jbc.M110.108167 (2010).

7   Ji, P. *et al.* An Rb-Skp2-p27 pathway mediates acute cell cycle inhibition by Rb and is retained in a partial-penetrance Rb mutant. *Mol Cell* **16**, 47-58, doi:S1097276504005726 [pii]10.1016/j.molcel.2004.09.029 (2004).

8   Hiebert, S. W. Regions of the retinoblastoma gene product required for its interaction with the E2F transcription factor are necessary for E2 promoter repression and pRb-mediated growth suppression. *Molecular and cellular biology* **13**, 3384-3391 (1993).

9   Qin, X. Q., Chittenden, T., Livingston, D. M. & Kaelin, W. G., Jr. Identification of a growth suppression domain within the retinoblastoma gene product. *Genes Dev* **6**, 953-964 (1992).

10 Lee, C., Chang, J. H., Lee, H. S. & Cho, Y. Structural basis for the recognition of the E2F transactivation domain by the retinoblastoma tumor suppressor. *Genes Dev* **16**, 3199-3212 (2002).

11 Xiao, B. *et al.* Crystal structure of the retinoblastoma tumor suppressor protein bound to E2F and the molecular basis of its regulation. *Proc Natl Acad Sci U S A* **100**, 2363-2368 (2003).

12 Lee, J. O., Russo, A. A. & Pavletich, N. P. Structure of the retinoblastoma tumour-suppressor pocket domain bound to a peptide from HPV E7. *Nature* **391**, 859-865 (1998).

13 Morris, E. J. & Dyson, N. J. Retinoblastoma protein partners. *Advances in Cancer Research* **82**, 1-54 (2001).

14 Helin, K. *et al.* Heterodimerization of the transcription factors E2F-1 and DP-1 leads to cooperative trans-activation. *Genes Dev* **7**, 1850-1861 (1993).

15 Dick, F. A. & Dyson, N. pRB contains an E2F1-specific binding domain that allows E2F1-induced apoptosis to be regulated separately from other E2F activities. *Mol Cell* **12**, 639-649 (2003).

16 Herrera, R. E. *et al.* Altered cell cycle kinetics, gene expression, and G1 restriction point regulation in Rb-deficient fibroblasts. *Mol. Cell. Biol.* **16**, 2402-2407 (1996).

17 Williams, B. O. *et al.* Extensive contribution of Rb-deficient cells to adult chimeric mice with limited histopathological consequences. *EMBO J.* **13**, 4251-4259 (1994).

18 Hinds, P. W. *et al.* Regulation of retinoblastoma protein functions by ectopic expression of human cyclins. *Cell* **70**, 993-1006 (1992).

19 Zhu, L. *et al.* Inhibition of cell proliferation by p107, a relative of the retinoblastoma protein. *Genes Dev* **7**, 1111-1125 (1993).

20 Otterson, G. A., Chen, W., Coxon, A. B., Khleif, S. N. & Kaye, F. J. Incomplete penetrance of familial retinoblastoma linked to germ-line mutations that result in partial loss of RB function. *Proc Natl Acad Sci U S A* **94**, 12036-12040 (1997).

21   Sellers, W. R. *et al.* Stable binding to E2F is not required for the retinoblastoma protein to activate transcription, promote differentiation, and suppress tumor cell growth. *Genes Dev* **12**, 95-106 (1998).

22   Whitaker, L. L., Su, H., Baskaran, R., Knudsen, E. S. & Wang, J. Y. Growth suppression by an E2F-binding-defective retinoblastoma protein (RB): contribution from the RB C pocket. *Mol Cell Biol* **18**, 4032-4042 (1998).

23   Alexander, K. & Hinds, P. W. Requirement for p27(KIP1) in retinoblastoma protein-mediated senescence. *Mol Cell Biol* **21**, 3616-3631, doi:10.1128/MCB.21.11.3616-3631.2001 (2001).

24   Binne, U. K. *et al.* Retinoblastoma protein and anaphase-promoting complex physically interact and functionally cooperate during cell-cycle exit. *Nat Cell Biol* **9**, 225-232 (2007).

25   Markey, M. P. *et al.* Loss of the retinoblastoma tumor suppressor: differential action on transcriptional programs related to cell cycle control and immune function. *Oncogene* **26**, 6307-6318, doi:10.1038/sj.onc.1210450 (2007).

26   Bourgo, R. J. *et al.* RB restricts DNA damage-initiated tumorigenesis through an LXCXE-dependent mechanism of transcriptional control. *Molecular cell* **43**, 663-672, doi:10.1016/j.molcel.2011.06.029 (2011).

27   Vormer, T. L. *et al.* RB family tumor suppressor activity may not relate to active silencing of E2F target genes. *Cancer Res* **74**, 5266-5276, doi:10.1158/0008-5472.CAN-13-3706 (2014).

28   Isaac, C. E. *et al.* The retinoblastoma protein regulates pericentric heterochromatin. *Mol Cell Biol* **26**, 3659-3671 (2006).

29   Cecchini, M. J. *et al.* A retinoblastoma allele that is mutated at its common E2F interaction site inhibits cell proliferation in gene targeted mice. *Molecular and cellular biology* **34**, 2029-2045, doi:10.1128/MCB.01589-13 (2014).

30   Thwaites, M. J., Cecchini, M. J., Passos, D. T., Welch, I. & Dick, F. A. Interchangeable roles for E2F transcriptional repression by the retinoblastoma protein and p27KIP1-CDK regulation in cell cycle control and tumor suppression. *Mol Cell Biol*, doi:10.1128/MCB.00561-16 (2016).

31   Coschi, C. *et al.* Haploinsufficiency of an RB-E2F1-Condensin II complex leads to aberrant replication and aneuploidy. *Cancer Discov* **4**, 840-853 (2014).

32   Ishak, C. A. *et al.* An RB-EZH2 Complex Mediates Silencing of Repetitive DNA Sequences. *Mol Cell* **64**, 1074-1087, doi:10.1016/j.molcel.2016.10.021 (2016).

33   Francis, S. M. *et al.* A functional connection between pRB and transforming growth factor beta in growth inhibition and mammary gland development. *Mol Cell Biol* **29**, 4455-4466 (2009).

34   Coschi, C. H. *et al.* Mitotic chromosome condensation mediated by the
        retinoblastoma protein is tumor-suppressive. *Genes Dev* **24**, 1351-1363,
        doi:gad.1917610 [pii]10.1101/gad.1917610 (2010).

35   Talluri, S. *et al.* A G1 checkpoint mediated by the retinoblastoma protein that is
        dispensable in terminal differentiation but essential for senescence. *Mol Cell Biol*
        30, 948-960, doi:10.1128/MCB.01168-09 (2010).

36   Talluri, S. & Dick, F. A. The retinoblastoma protein and PML collaborate to
        organize heterochromatin and silence E2F-responsive genes during senescence.
        Cell Cycle **13**, 641-651 (2013).

37   Dick, F. A., Sailhamer, E. & Dyson, N. J. Mutagenesis of the pRB pocket reveals
        that cell cycle arrest functions are separable from binding to viral oncoproteins.
        Mol Cell Biol **20**, 3715-3727 (2000).

38   Thwaites, M. J., Cecchini, M. J. & Dick, F. A. Analyzing RB and E2F during the
        G1-S transition. *Methods Mol Biol* **1170**, 449-461, doi:10.1007/978-1-4939-0888-
        2_24 (2014).

39   Cecchini, M. J. & Dick, F. A. The biochemical basis of CDK phosphorylation-
        independent regulation of E2F1 by the retinoblastoma protein. *Biochem J* **434**,
        297-308, doi:BJ20101210 [pii]10.1042/BJ20101210 (2011).

40   Julian, L. M., Palander, O., Seifried, L. A., Foster, J. E. & Dick, F. A.
        Characterization of an E2F1-specific binding domain in pRB and its implications
        for apoptotic regulation. *Oncogene* **27**, 1572-1579 (2008).

41   Jacks, T. *et al.* Effects of an Rb mutation in the mouse. *Nature* **359**, 295-300,
        doi:10.1038/359295a0 (1992).

42   Mayhew, C. N. *et al.* Liver-specific pRB loss results in ectopic cell cycle entry
        and aberrant ploidy. *Cancer Res* **65**, 4568-4577 (2005).

43   Watanabe, T. & Tanaka, Y. Age-related alterations in the size of human
        hepatocytes. A study of mononuclear and binucleate cells. *Virchows Arch B Cell
        Pathol Incl Mol Pathol* **39**, 9-20 (1982).

44   Wu, L. *et al.* Extra-embryonic function of Rb is essential for embryonic
        development and viability. *Nature* **421**, 942-947 (2003).

45   Pandit, S. K. *et al.* E2F8 is essential for polyploidization in mammalian cells. *Nat
        Cell Biol* **14**, 1181-1191, doi:10.1038/ncb2585 (2012).

46   Chen, H. Z. *et al.* Canonical and atypical E2Fs regulate the mammalian
        endocycle. *Nat Cell Biol* **14**, 1192-1202, doi:10.1038/ncb2595 (2012).

47   Gao, D. *et al.* Cdh1 regulates cell cycle through modulating the claspin/Chk1 and
        the Rb/E2F1 pathways. *Mol Biol Cell* **20**, 3305-3316, doi:10.1091/mbc.E09-01-
        0092 (2009).

48   Sun, H. *et al.* An E2F binding-deficient Rb1 protein partially rescues developmental defects associated with Rb1 nullizygosity. *Mol Cell Biol* **26**, 1527-1537 (2006).

49   Sun, H. *et al.* E2f binding-deficient Rb1 protein suppresses prostate tumor progression in vivo. *Proc Natl Acad Sci U S A* **108**, 704-709, doi:<u>1015027108</u> <u>[pii]10.1073/pnas.1015027108</u> (2011).

50   Thwaites, M. J., Cecchini, M. J., Passos, D. T., Welch, I. & Dick, F. A. Interchangeable Roles for E2F Transcriptional Repression by the Retinoblastoma Protein and p27KIP1-Cyclin-Dependent Kinase Regulation in Cell Cycle Control and Tumor Suppression. *Mol Cell Biol* **37**, doi:10.1128/MCB.00561-16 (2017).

51   Goodrich, D. W. How the other half lives, the amino-terminal domain of the retinoblastoma tumor suppressor protein. *J Cell Physiol* **197**, 169-180, doi:10.1002/jcp.10358 (2003).

52   Mukherjee, P., Winter, S. L. & Alexandrow, M. G. Cell cycle arrest by transforming growth factor beta1 near G1/S is mediated by acute abrogation of prereplication complex activation involving an Rb-MCM interaction. *Mol Cell Biol* **30**, 845-856, doi:10.1128/MCB.01152-09 (2010).

53   Borysov, S. I., Nepon-Sixt, B. S. & Alexandrow, M. G. The N Terminus of the Retinoblastoma Protein Inhibits DNA Replication via a Bipartite Mechanism Disrupted in Partially Penetrant Retinoblastomas. *Mol Cell Biol* **36**, 832-845, doi:10.1128/MCB.00636-15 (2015).

54   Hassler, M. *et al.* Crystal structure of the retinoblastoma protein N domain provides insight into tumor suppression, ligand interaction, and holoprotein architecture. *Mol Cell* **28**, 371-385 (2007).

55   Finn, R. S. *et al.* PD 0332991, a selective cyclin D kinase 4/6 inhibitor, preferentially inhibits proliferation of luminal estrogen receptor-positive human breast cancer cell lines in vitro. *Breast Cancer Res* **11**, R77, doi:10.1186/bcr2419 (2009).

56   Rader, J. *et al.* Dual CDK4/CDK6 inhibition induces cell-cycle arrest and senescence in neuroblastoma. *Clin Cancer Res* **19**, 6173-6182, doi:10.1158/1078-0432.CCR-13-1675 (2013).

57   Gelbert, L. M. *et al.* Preclinical characterization of the CDK4/6 inhibitor LY2835219: in-vivo cell cycle-dependent/independent anti-tumor activities alone/in combination with gemcitabine. *Invest New Drugs* **32**, 825-837, doi:10.1007/s10637-014-0120-7 (2014).

Chapter 4

4 Tumor-suppressive functions of pRB independent of E2F repression

4.1 Introduction

The maintenance of cell cycle control is crucial to the prevention of tumorigenesis[1].

Cell cycle progression is regulated through a number of checkpoints that ensure proper

signalling is present instructing the cell to grow and divide[1]. Cancer develops when these

mechanisms are perturbed resulting in cells that continue to cycle regardless of the

presence or absence of growth stimuli[1]. To ensure that cells only replicate their genome

once per cell cycle the primary regulation of cellular division occurs prior to the onset of

DNA synthesis[2]. The transition from Gap 1 (G1) phase to that of synthesis (S) phase is

therefore also known as the restriction point[2]. Several intra- and extracellular signals

contribute to cell cycle decisions. These signals influence two main complexes which

control the restriction point and ultimately cell cycle entry, pRB and Cyclin E/CDK2[3,4].

These two proteins work in opposition to one another with pRB restricting cell cycle

entry and Cyclin E/CDK2 promoting division[4].

Overall, cell cycle entry is determined by the total amount of Cyclin E/CDK2 activity

which is responsible for phosphorylating a vast network of transcription factors and is

critical in the firing of replication origins initiating the process of DNA replication[5]. Both

Cyclin E/CDK2 and pRB can also influence the activity of each other ensuring that the

cell doesn't undergo division prematurely or indecisively[5,6]. This interplay is primarily

due to the ability of Cyclin E/CDK2 to hyperphosphorylate pRB resulting in a

conformational change and subsequent release of the E2F transcription factors[4]. The lack

of pRB binding to E2Fs leads to the upregulation of the E2F transcriptional program which contains several genes involved in S-phase progression, one of which is *CCNE1* encoding Cyclin E[6]. This then increases the overall level of Cyclin E/CDK2 complexes resulting in further phosphorylation of pRB[4,5]. This feed forward loop ensures that once the cell is appropriately stimulated to divide the cell is committed to completing the cell cycle[5,7]. In addition to regulating E2F-mediated transcription, we and others have characterized an additional axis of pRB-mediated cell cycle control through the stabilization of p27[8-10].

The two main functions which help to regulate cell cycle progression, E2F repression and p27 stabilization are mediated through two independent binding surfaces[4,8]. The first and most well known is through the direct repression of E2F transcription factor activity, facilitated through the pocket domain on pRB[4]. This interaction prevents the transcription of genes required for DNA synthesis and cell cycle progression[4]. The second method of pRB-mediated cell cycle control, p27 stabilization, is dependent on Cdh1 binding to pRB through the LxCxE binding cleft (**Chapter 3**)[9]. This interaction enhances the ability of APC[Cdh1] to degrade its target Skp2 resulting in the stabilization of p27[9,10]. Stabilization of p27 leads to the inhibition of Cyclin/CDK (Cyclin dependent kinase) complexes preventing S-phase entry and DNA synthesis[5]

Given the importance of pRB in regulating both E2F target gene expression and CDK activity, pRB plays a critical role in maintaining the G1 restriction point[4,9,10]. As disruption of the restriction point is a necessary step in carcinogenesis, it is unsurprising that the pRB pathway is often the target of mutations in human cancers[11]. Significantly, the vast majority of mutations that disrupt pRB function are often upstream of pRB

through the deletion of p16 or the amplification of Cyclin D leading to the hyperphosphorylation of pRB[11]. The hyperphosphorylation of pRB simulates active growth signalling resulting in E2F target gene expression and cell cycle entry.

However, recent studies have suggested that this is not the whole story[10,12,13]. In particular, the *Rb1*[G/G] mouse model developed by *Cecchini et al*., in which pRb was mutated to disrupt pRb-E2F binding, shows no overt phenotypes[12]. This finding demonstrates that the ability of pRB to repress E2Fs is dispensable for cell cycle control and tumor-suppression[12]. In support of this hypothesis we have also shown that at least 3 different binding surfaces play a role in regulating cell cycle control (**Chapter 3**).

Two critical proteins which influence pRB and the cell cycle are Kras and p53[14,15]. These pathways are also typically mutated in human cancers[3,16]. These two proteins work in opposition to one another with Kras being activated through growth factor stimulation, resulting in increased Cyclin/CDK activity and inactivation of pRB[14,15]. By contrast p53, which is stimulated by DNA damage, increases the transcription of the Cyclin dependent kinase inhibitor p21[15]. The increased level of p21 inhibits the function of Cyclin/CDKs thereby allowing pRB to remain hypophosphorylated and active, restricting cell cycle progression[15]. The collective input from these signals along with others determines the phosphorylation status of pRB, its subsequent activity, and overall cell cycle progression[4,14,15].

As we have previously shown, loss of E2F repression by pRB leads to tumorigenesis in the absence of p27 (**Chapter 2**)[8]. To determine the importance of E2F repression by pRB in tumorigenesis, we performed a series of genetic experiments where our *Rb1*[G/G]

mice were combined with oncogenic Kras[G12D] as well as inactivation of the p53 pathway through deletion of either p53 or p21. These crosses demonstrated that pRB-E2F interactions are inconsequential in the face of constitutive proliferative signalling through oncogenic Kras activation. However, regulation of E2Fs by pRB does influence tumor-free survival in conjugation with *Trp53* deletion. Finally, we found that deletion of p21 in the *Rb1*[G/G] background did not result in tumor formation despite having a defective DNA damage response. This is of particular interest as an ineffective DNA damage response is likely partially responsible for the pituitary tumor formation we observed in *Rb1*[G/G]*;Cdkn1b*^{-/-} animals in chapter 2[8].

4.2   Materials and Methods

4.2.1   Phenotypic analysis of animals.

LSL-Kras[G12D] mice (B6.129S4-Kras[tm4Tyj]/J) mice and *UBC-Cre-ERT2* (B6.Cg-Tg(UBC-cre/ERT2)1Ejb/2J) were combined with our *Rb1*[G/G] mouse model to produce both control *Kras*[G12D]*; Cre-ERT2* animals and experimental *Rb1*[G/G]*; Kras*[G12D]*; Cre-ERT2* animals[12,17,18]. Animals were then injected with 75mg/kg tamoxifen at 8 weeks of age resulting in sporadic *Kras*[G12D] expression throughout the body. Animals were then monitored for tumor formation and sacrificed at animal protocol endpoints. Survival data were subjected to Kaplan-Meier analysis, and significant differences were compared using a log rank test.

Trp53^{-/-} mice (129-Trp53[tm1Tyj]/J), and *Cdkn1a*^{-/-} mice (B6.129S6(Cg)-Cdkn1a[tm1Led]/J) have been described previously and were obtained from Jackson Laboratory[19,20]. These two strains were combined with our previously described *Rb1*[G/G]

mouse model and were genotyped as previously described[12,19,20]. Mice were monitored

for tumor development and sacrificed at animal protocol endpoints. Survival data were

subjected to Kaplan-Meier analysis, and significant differences were compared using a

log rank test. All animals were housed and handled as approved by the Canadian Council

on Animal Care.

4.2.2   Histological analysis of tumors

Following euthanasia, mice were subject to necropsy where tissues of interest

were fixed in formaldehyde for 72 hours. Tissues were then washed twice in PBS before

storage in 70% ethanol. Tissues were then embedded in paraffin, 5μm sections were cut

and stained with hematoxylin and eosin (H&E). Images were obtained using a Zeiss

Axioskop 40 microscope and Spot Flex camera and software (Mississauga, Ontario,

Canada).

4.2.3   Proliferation analysis

Mouse embryonic fibroblasts (MEFs) were derived from E13.5 embryos of the

indicated genotypes. Cells were cultured using standard methods in Dulbecco's modified

Eagle's medium containing 10% fetal bovine serum (FBS) 2mM glutamine, 50U/ml

penicillin and 50μg/ml streptomycin. Cells were treated with 15 Gy of ionizing radiation

as previously described[8]. 48 hours after treatment cells were labeled with BrdU for 2

hours. Cell cycle analysis was then carried out as previously discribed[21].

4.2.4   Expression analysis of pluripotency factors

MEFs of the indicated genotypes were cultured in Dulbecco's modified Eagle's

medium containing 10% fetal bovine serum (FBS) 2mM glutamine, 50U/ml penicillin

and 50µg/ml streptomycin and RNA was isolated using Trizol reagent according to manufactures instructions and previously published protocols[12]. Expression levels of Sox2, Klf4, Oct4, and Nanog were analyzed by qRT-PCR and normalized to GAPDH using iQ Sybr-green Super mix (Bio-Rad) and the following primer sets: Sox2 Fwd (5`ACAGATGCAACCGATGCACC 3`), Sox2 Rev (5`TGGAGTTGTACTGCAGGGCG 3`), Oct4 Fwd (5`ACATCGCCAATCAGCTTGG 3`), Oct4 Rev (5`AGAACCATACTCGAACCACATCC 3`), Klf4 Fwd (5`GCACACCTGCGAACTCACAC 3`), Klf4 Rev (5`CCGTCCCAGTCACAGTGGTAA 3`), Nanog Fwd (5`CCTCCAGCAGATGCAAGAACTC 3`), Nanog Rev (5`CTTCAACCACTGGTTTTTCTGCC 3`). GAPDH Fwd (5` GCACAGTCAAGGCCGAGAAT 3`), GAPDH Fwd. (5` GCCTTCTCCATGGTGGTGAA 3`).

4.3   Results

4.3.1   Oncogenic Kras[G12D]-mediated development of squamous papillomas is unaffected by loss of pRB-E2F interactions

Maintenance of the G1 to S-phase restriction point is critical at preventing aberrant growth. The involvement of pRB in the G1 to S transition is well established however, as demonstrated by *Cecchini et al.,* and others pRB-E2F interactions are dispensable for cell cycle arrest[10,12,13]. As derepression of E2F target genes in the *Rb1[G/G]* mice was unable to lead to tumorigeneses we attempted to stimulate aberrant growth signalling *in vivo* by combining the *Rb1[G]* mutation with oncogenic *Kras[G12D]* expression[12,17]. The Kras[G12D]
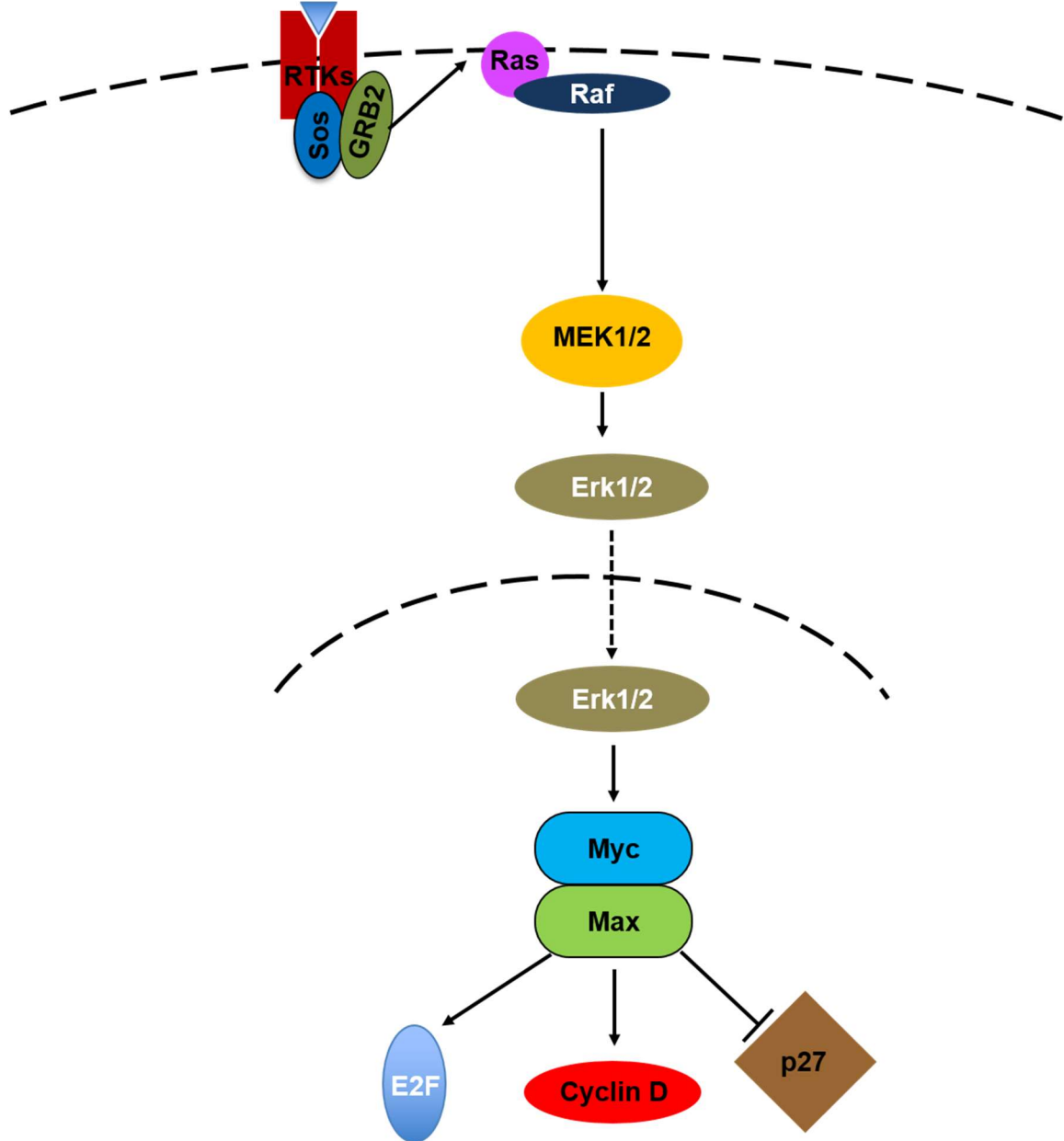
Figure 4.1: Schematic representation of Ras signaling.

Following binding of growth stimulatory ligands receptor tyrosine kinases (RTKs). This signals the activation of son of sevenless (SOS) and GRB2 which activate Ras. Following activation, Raf is recruited to the membrane and phosphorylated by Ras. This signaling cascade results in the activation of MEK1/2 and ERK1/2 by phosphorylation. Erk1/2 then translocates to the nucleus and activates the transcription factor Myc/Max which results in inhibition of transcription of cell cycle repressors such as p27. Additionally, Myc/Max increases the expression of cell cycle promoting factors such as Cyclin D as well as E2F target genes.

mutation results in constitutive Kras signalling in the absence of normal growth signalling[17]. Signalling through Kras results in a cascade that leads to an active Myc/Max transcription factor which can regulate gene transcription driving the cell cycle (**Figure 4.1**). In particular, a decrease in the expression of *Cdkn1b* (p27) as well as an increase in Cyclin D results in increased hyperphosphorylation of pRB and increased E2F activity[3]. Additionally, the Myc/Max transcription factor can also induce the transcription of E2F target genes further driving the cell into S-phase[22]. The inability of $Rb1^G$ to associate with E2F suggests that in the face of increased E2F expression, the tumor-suppressive ability of pRB would be compromised by this mutation. To induce expression of oncogenic $Kras^{G12D}$ in adult tissues we used a Lox-Stop-Lox system which can activate oncogenic $Kras^{G12D}$ expression following Cre recombinase activity[17]. This knock-in strain was introduced into the $Rb1^{G/G}$ mouse line along with a transgene encoding Cre recombinase fused to ERT2 hormonal response element[12,17,18].

Both control *LSL-Kras^{G12D}; Ert2-Cre$^+$* mice and experimental *Rb1$^{G/G}$; LSL-Kras^{G12D}; Ert2-Cre$^+$* mice were produced at normal Mendelian ratios (**Table 4.1**). Typically, to activate *Ert2-Cre* via tamoxifen injection, 75mg/kg is delivered intraperitoneally once per day for a period of 5 days. However, following this protocol both control and experimental mice reached endpoints within one week of the final injection without tumor development. To induce more sporadic activation of *Kras^{G12D}* expression and thereby prevent the rapid decline of treated animals, we used an altered dosing regiment. Eight-week-old *Rb1$^{G/G}$; LSL-Kras^{G12D}; Ert2-Cre$^+$* and *LSL-Kras^{G12D}; Ert2-Cre$^+$* control animals were injected with one dose of 75mg/kg tamoxifen. Tamoxifen then binds the ERT2 element and shuttles Cre recombinase into the nucleus, removing the stop

Table 4.1: Frequency of generation of $Rb1^{G/G}$; $Kras^{G12D}$; $Ert2$-Cre^+ compound mutant mice.

	$Rb1^{G/+}$; $Kras^{G12D}$ x $Rb1^{G/+}$; $Ert2$-Cre^+	
	Observed	Expected
$Rb1^{+/+}$	12	8
$Rb1^{+/+}$; $Kras^{G12D}$	7	8
$Rb1^{+/+}$; $Ert2$-Cre^+	9	8
$Rb1^{+/+}$; $Kras^{G12D}$; $Ert2$-Cre^+	9	8
$Rb1^{G/+}$	15	17
$Rb1^{G/+}$; $Kras^{G12D}$	10	17
$Rb1^{G/+}$; $Ert2$-Cre^+	20	17
$Rb1^{G/+}$; $Kras^{G12D}$ $Ert2$-Cre^+	15	17
$Rb1^{G/G}$;	18*	8
$Rb1^{G/G}$; $Kras^{G12D}$	6	8
$Rb1^{G/G}$; $Ert2$-Cre^+	6	8
$Rb1^{G/G}$; $Kras^{G12D}$ $Ert2$-Cre^+	8	8
Total	135	

The indicated genotypes of mice were crossed and all resulting progeny were genotyped. The number of live animals obtained at two weeks of age is indicated for each genotype and the expected number based on Mendelian inheritance is indicated. * denotes significance as determined by chi-squared test.

cassette in front of the oncogenic $Kras^{G12D}$ allele allowing for expression (**Figure 4.2A**).

These mice were then monitored for tumor formation. Both $Rb1^{G/G}$; $LSL\text{-}Kras^{G12D}$; $Ert2\text{-}$

Cre and control $LSL\text{-}Kras^{G12D}$; $Ert2\text{-}Cre$ mice developed masses very early after

tamoxifen injection with an average survival of 56.5 days and 65 days post injection

respectively (**Figure 4.2B**). Necropsy also identified masses forming in the interior of the

mouth as well as on the stomach in both genotypes (**Figure 4.2C**). H&E staining of

sections of the masses removed from these animals identified them as squamous cell

papillomas (**Figure 4.2C**). Further, these masses appear to arise out of esophageal tissue

and have similar structures in both the mouth and stomach tumors (**Figure 4.2C**).

Importantly, the same tumor development as well as lifespan was seen both control

$Kras^{G12D}$ animals as well as experimental $Rb1^{G/G}$ $Kras^{G12D}$ cohorts (**Figure 4.2BC**).

Taken together this cross demonstrates that tumor development caused by oncogenic

$Kras^{G12D}$ expression is unaffected by the $Rb1^G$ mutation in the context of the squamous

papillomas which were produced. Conclusions about the interaction between oncogenic

Kras and the $Rb1^G$ mutations in other tumor types would require a tissue specific

approach.

4.3.2 Loss of E2F repression by pRB exacerbates the tumor phenotype of $Trp53^{-/-}$ animals

In chapter 2 we have shown that the combination of $Rb1^G$ mutation and the deletion

of p27 lead to an ineffective DNA damage response and ultimately tumor formation[8].

This ineffective response to DNA damage seen in $Rb1^{G/G}$; $Cdkn1b^{-/-}$ cells and animals

seems to suggest that Rb1^G, which is incapable of inhibiting E2Fs, is still involved in the
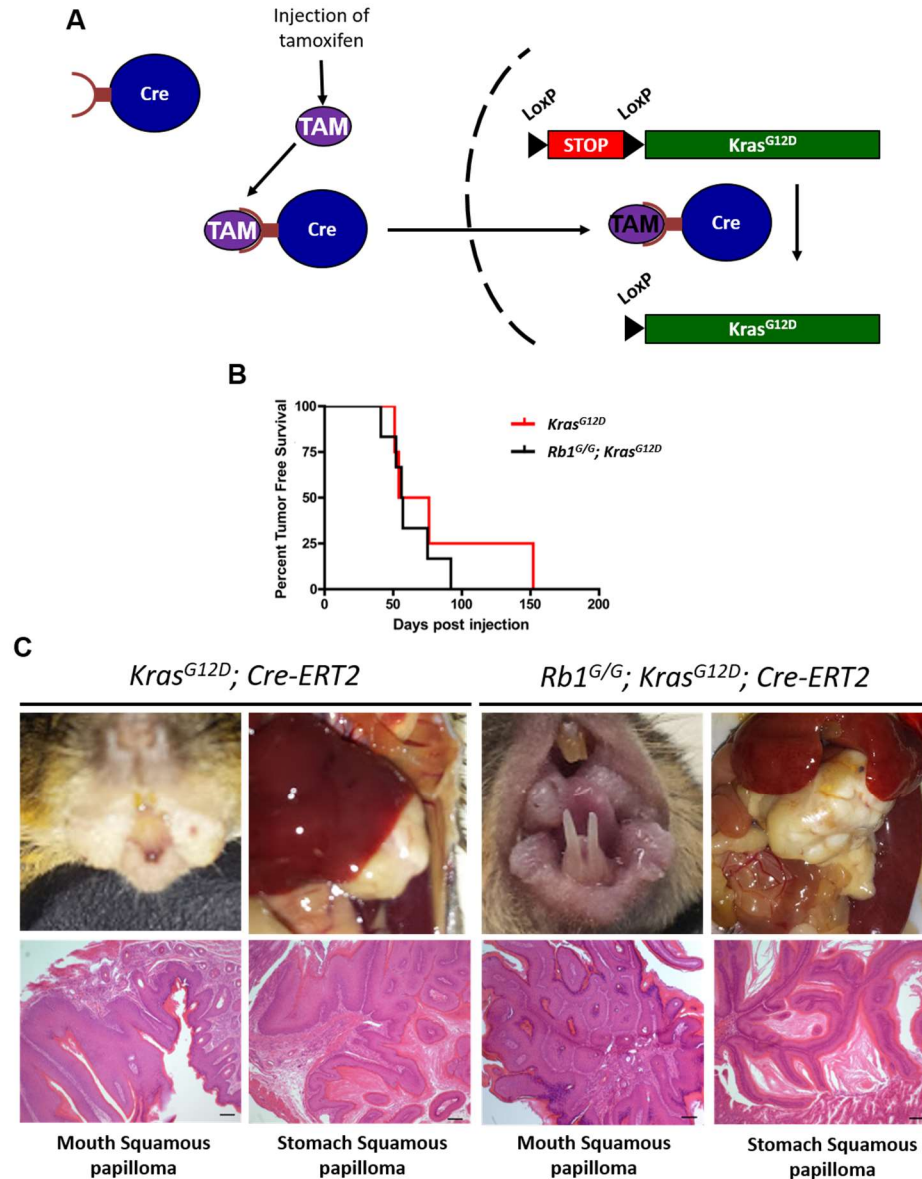
Figure 4.2: Expression of oncogenic *Kras^{G12D}* leads to rapid tumor development independent of E2F regulation.

(A) Schematic representation of tamoxifen induced expression of Kras^{G12D}. Following injection, tamoxifen binds to the ERT-Cre fusion protein leading to nuclear translocation. Cre is then able to excise the stop cassette ahead of Kras^{G12D} resulting in expression. **(B)** Kaplan Meier analysis of tumor-free survival of indicated genotypes. Mice were monitored until natural endpoint, those having tumors are shown. *Rb1$^{G/G}$; Kras^{G12D}* (56.5 days post injection) (n=6) and *Kras^{G12D}* mice (65 days post injection) (n=4) are not statistically different from one another using the log rank test (p=0.475). **(C)** Whole mount and H&E analysis of squamous papillomas that develop in *Kras^{G12D}* mice. Squamous papillomas developed out of the mouth as well as stomach of both control *Kras^{G12D}* and *Rb1$^{G/G}$; Kras^{G12D}* animals. Scale bars are equal to 100µm.

DNA damage response[8]. To determine if insensitivity to DNA damage is the critical factor resulting in tumor development in $Rb1^{G/G}$; $Cdkn1b^{-/-}$ animals, $Rb1^{G/G}$ mice were crossed into the $Trp53^{-/-}$ background which are known to have elevated levels of DNA damage[8,20]. Under normal circumstances, following DNA damage ATM phosphorylates and activates p53[23]. Active p53 then stimulates transcriptional programs leading to the expression of genes that result in cell cycle arrest and apoptotic signalling[23]. Importantly, p53 activation triggers the expression of $Cdkn1a$ which encodes for p21 a CKI capable of inhibiting the function of Cyclin/CDK complexes[24]. This in turn leads to the hypophophorylation of pRB and subsequent cell cycle arrest (**Figure 4.3**).

Once again both $Trp53^{-/-}$, and $Rb1^{G/G}$; $Trp53^{-/-}$ mice were produced at appropriate Mendelian frequencies (**Table 4.2**). The tumors inherent to the p53 knockout model typically present as lymphomas and occasional sarcomas beginning around 6 months of age for homozygous deletion (**Figure 4.4B**)[20]. The introduction of the $Rb1^{G}$ mutation into the p53 null mouse line resulted in a decrease of both overall survival as well as tumor free survival in the $Rb1^{G/G}$; $Trp53^{-/-}$ animals (150 days) relative to $Trp53^{-/-}$ controls (194.5 days) (**Figure 4.4AB**).

Consistent with previous studies $Trp53^{-/-}$ animals presented with thymic lymphomas (77%) and sarcomas (33%) (**Figure 4.4C**)[20]. Interestingly, while most of the $Rb1^{G/G}$; $Trp53^{-/-}$ animals developed thymic lymphomas (62.5%), 38.5% of animals spontaneously died very young (average of 125 days) with no discernible tumor phenotype (**Figure 4.4A**). Whole mount and H&E stained sections of these tumors confirmed that those masses that did develop in $Rb1^{G/G}$; $Trp53^{-/-}$ animals were thymic lymphomas
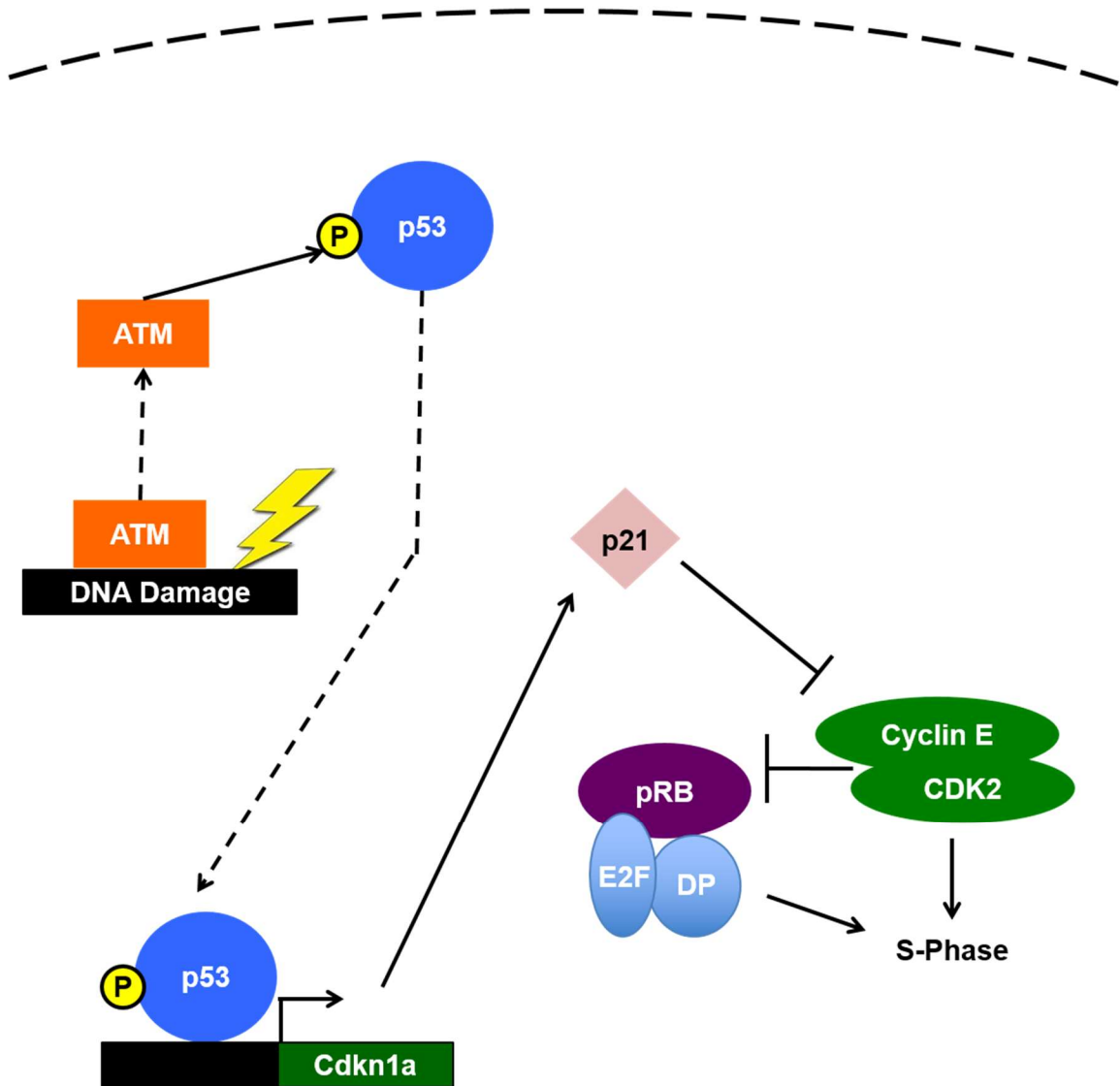
Figure 4.3: Schematic representation of p53 cell cycle arrest signaling.

Following genetic insults in the form of DNA damage, p53 is activated though ATM-mediated phosphorylation. Following activation p53 can induce the transcription of a variety of genes that are critical to the activation of apoptotic and cell cycle arrest mechanisms. In particular, the expression of *Cdkn1a*, is primarily responsible for initiating a p53 dependent cell cycle arrest. Following expression, p21 is then capable of inhibiting Cyclin/CDK complexes which results in the hypophosphorylation of pRB and subsequent cell cycle arrest.

Table 4.2 Frequency of generation of *Rb1$^{G/G}$; Trp53$^{-/-}$* compound mutant mice.

	Rb1$^{G/+}$; Trp53$^{+/-}$ x *Rb1$^{G/+}$; Trp53$^{+/-}$*	
	Observed	Expected
Rb1$^{+/+}$; Trp53$^{+/+}$	33*	19
Rb1$^{+/+}$; Trp53$^{+/-}$	44	38
Rb1$^{+/+}$; Trp53$^{-/-}$	13	19
Rb1$^{G/+}$; Trp53$^{+/+}$	45	38
Rb1$^{G/+}$; Trp53$^{+/-}$	80	76
Rb1$^{G/+}$; Trp53$^{-/-}$	19*	38
Rb1$^{G/G}$; Trp53$^{+/+}$	20	19
Rb1$^{G/G}$; Trp53$^{+/-}$	39	38
Rb1$^{G/G}$; Trp53$^{-/-}$	12	19
Total	305	

The indicated genotypes of mice were crossed and all resulting progeny were genotyped. The number of live animals obtained at two weeks of age is indicated for each genotype and the expected number based on Mendelian inheritance is indicated. * denotes significance as determined by chi-squared test.
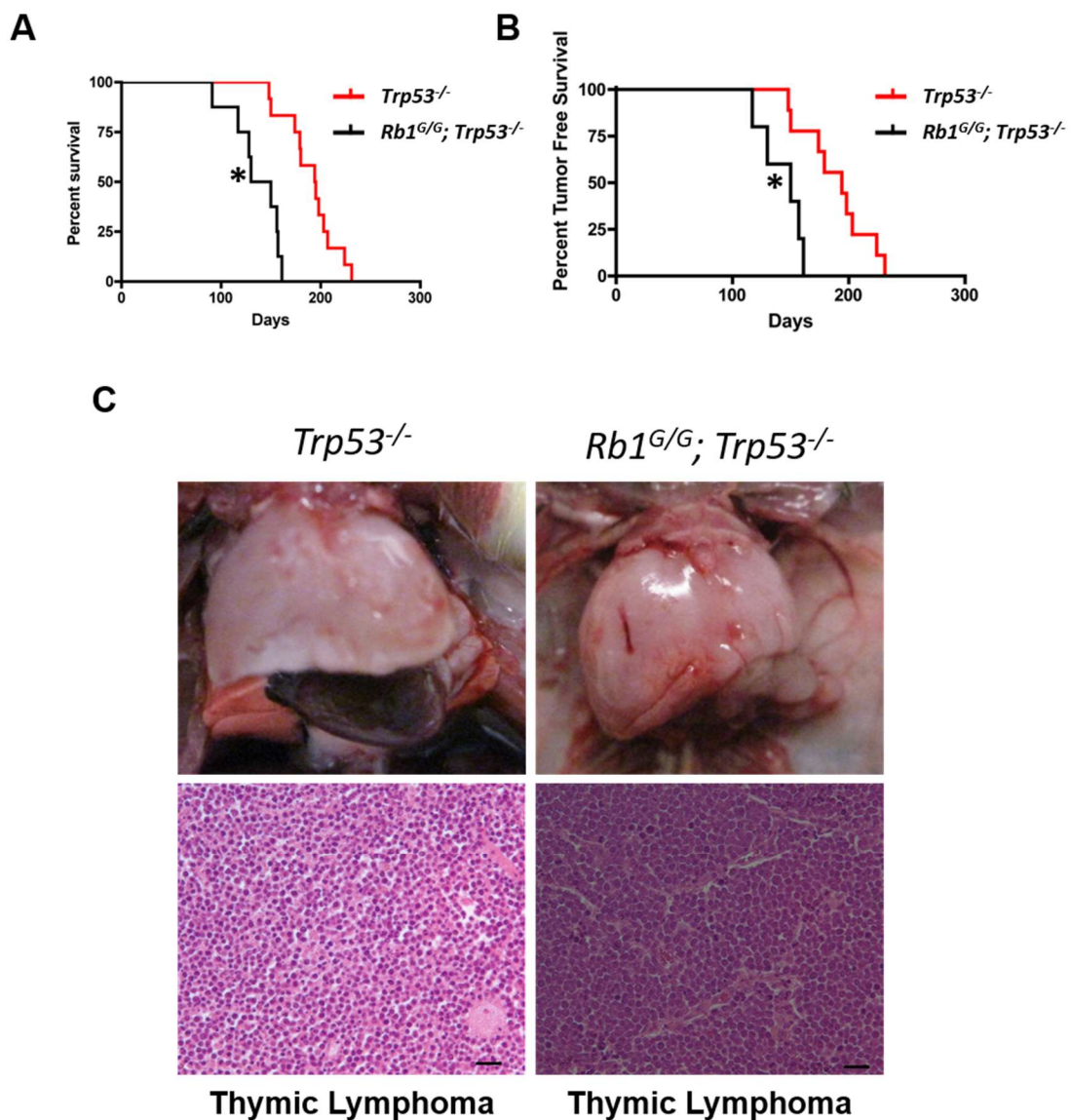
Figure 4.4: Loss of E2F regulation by pRb exacerbates *Trp53$^{-/-}$* tumor development.

(A) Kaplan Meier analysis of overall survival of indicated genotypes. Mice were monitored until natural endpoint. *Rb1$^{G/G}$; Trp53$^{-/-}$* (140 days) (n=8), *Trp53$^{-/-}$* (194.5 days) (n=12) are statically significant from one another using the log-rank test (p<0.0001). **(B)** Kaplan Meier analysis of tumor-free survival of indicated genotypes. Mice were monitored until natural endpoint, those having tumors are shown. *Rb1$^{G/G}$; Trp53$^{-/-}$* (150 days) (n=5), *Trp53$^{-/-}$* (194 days) (n=9) are statically significant from one another using the log-rank test (p=0.0046). **(C)** Whole mount and H&E analysis of thymic lymphomas found in both *Rb1$^{G/G}$; Trp53$^{-/-}$* and *Trp53$^{-/-}$* mice. Scale bars are equal to 50μm.

(**Figure 4.4C**). Given the propensity of double mutant $Rb1^{G/G}$; $Trp53^{-/-}$ mice to phenocopy $Trp53^{-/-}$ animals it suggests that the $Rb1^G$ mutation exacerbates the $Trp53^{-/-}$ phenotype by removing an additional cell cycle checkpoint allowing for unchecked E2F target gene expression.

The correlation between defective DNA damage signalling and tumor formation in $Rb1^{G/G}$; $Cdkn1b^{-/-}$ mice suggests that loss of appropriate DNA damage signaling in $Rb1^{G/G}$ mice would result in pituitary tumor formation (**Chapter 2**)[8]. However, this was not the case even though $Trp53^{-/-}$ MEFs display the same defective DNA damage response found in $Rb1^{G/G}$; $Cdkn1b^{-/-}$ MEFs[25,26]. One possible explanation for this finding, is that due to the rapid morbidity of the p53 knockout mouse strain, it is difficult to determine if the $Rb1^G$ mutation would lead to the development of pituitary tumors over a longer period of time (**Figure 4.4AB**). Therefore, we wanted to determine the effect of the $Rb1^G$ mutation in a mouse model which had the same cell cycle arrest problems in response to DNA damage without rapid tumor development displayed by p53 knockout stains. To address this question we chose to use the $Cdkn1a^{-/-}$ knockout model lacking p21, which exhibits a defective cell cycle response to DNA damage without rapid morbidity[19].

4.3.3   *Cdkn1a* (p21) deletion is incapable of inducing tumorigenesis in the *Rb1*$^{G/G}$ background

Following DNA damage, p53 activates a cell cycle arrest mechanism through the transcriptional stimulation of $Cdkn1a$[24]. The $Cdkn1a$ gene encodes for p21 which then elicits a cell cycle arrest prior to DNA repair[24]. p21 is member of the CIP/KIP family of

Cyclin dependent kinase inhibitors[5]. As such p21 can induce a cell cycle arrest through the inhibition of a broad range of Cyclin/CDKs[5]. Importantly, previous publications have shown that cells lacking p21 have a defective DNA damage response similar to that exhibited in *Rb1*$^{G/G}$*; Cdkn1b*$^{-/-}$ MEFs (**Figure 4.5A**)[8,27]. This included the inability to arrest in response to ionizing radiation (**Figure 4.5A**) as well as rapid immortalization in 3T3 assays[27,28]. Despite these deficiencies tumor development in *Cdkn1a*$^{-/-}$ (p21 null) mice is rare and inconsistent in the literature depending on strain background[27,29]. Given the rarity of cancers in *Cdkn1a*$^{-/-}$ mice and the lack of DNA damage response we chose to combine p21 null mice with our *Rb1*$^{G/G}$ animals. By doing so we were able to determine if the tumor development that we found in our *Rb1*$^{G/G}$*; Cdkn1b*$^{-/-}$ double mutant mice was dependent on a lack of an effective DNA damage response[8]. Additionally, this cross was used to determine whether the tumor phenotype displayed in *Rb1*$^{G/G}$*; Cdkn1b*$^{-/-}$ mice is specific to p27 loss or if loss of p21 could result in the same effect[8].

Firstly, we confirmed the overall sensitivity of *Cdkn1a*$^{-/-}$ and *Rb1*$^{G/G}$*; Cdkn1a*$^{-/-}$ MEFs to DNA damage treatment (**Figure 4.5A**). As predicted by previous studies, p21 null MEFs display a defective arrest in response to ionizing radiation (IR) with or without the inclusion of the *Rb1*^{G} mutation (**Figure 4.5A**). Importantly, the defective arrest in response to IR in p21 null and *Rb1*$^{G/G}$*; Cdkn1a*$^{-/-}$ MEFs is similar to that of *Rb1*$^{G/G}$*; Cdkn1b*$^{-/-}$ MEFs (**Figure 4.5A**). Therefore, if the defective DNA damage response in *Rb1*$^{G/G}$*; Cdkn1b*$^{-/-}$ is responsible for tumor formation, *Rb1*$^{G/G}$*; Cdkn1a*$^{-/-}$ would be predicted to develop similar malignancies. Both *Cdkn1a*$^{-/-}$ and *Rb1*$^{G/G}$*; Cdkn1a*$^{-/-}$ mice were produced at appropriate Mendelian ratios (**Table 4.3**).
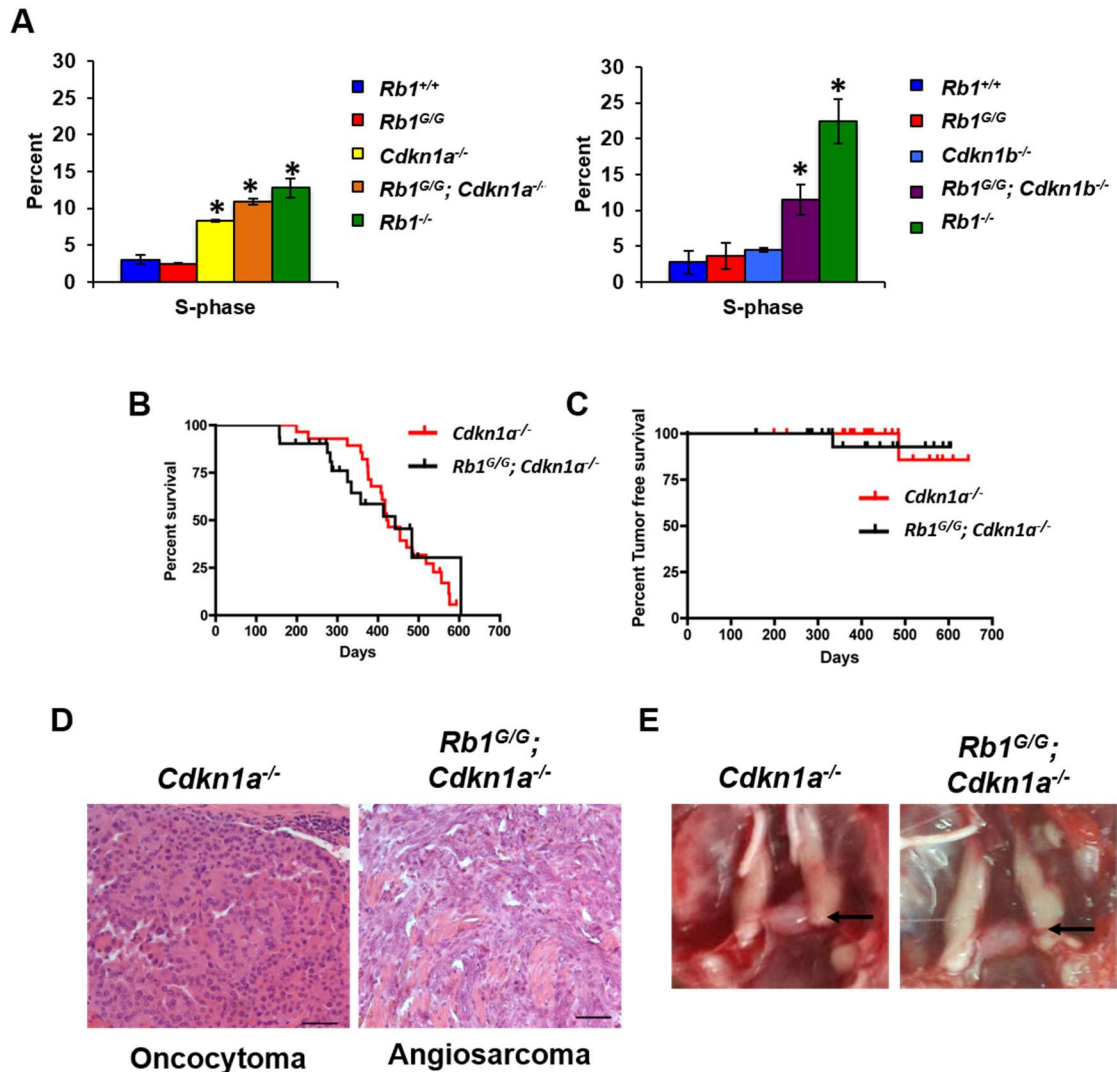
Figure 4.5: Combination of the *Rb1^G* mutation and loss of p21 (*Cdkn1a^-/-*) does not lead to tumor formation despite defective DNA damage response.

(A) Cell cycle analysis of MEFs following treatment with 15Gy of ionizing radiation. S-phase was determined by BrdU incorporation and Flow Cytometry. Average of 3 replicates are shown, error bars indicate standard deviation. * indicates $p<0.05$. **(B)** Kaplan Meier analysis of overall survival of indicated genotypes. Mice were monitored until natural endpoint. *Rb1^{G/G}; Cdkn1a^-/-* (419 days) (n=25), *Cdkn1a^-/-* (442 days) (n=24) are not statically significant from one another using the log-rank test (p=0.9059). **(C)** Kaplan Meier analysis of tumor-free survival of indicated genotypes. Mice were monitored until natural endpoint, those having tumors are shown as events. *Rb1^{G/G}; Cdkn1a^-/-* and *Trp53^-/-* are not statically significant from one another using the log-rank test (p=0.7919). **(D)** H&E analysis of the two tumors found in *Rb1^{G/G}; Cdkn1a^-/-* and *Cdkn1a^-/-* mice. Scale bars are equal to 50μm. **(E)** whole mount images of pituitaries of aged *Cdkn1a^-/-* and *Rb1^{G/G}; Cdkn1a^-/-* animals demonstrate no hyperplasia. Pituitaries are denoted by black arrows.

Table 4.3: Frequency of generation of *Rb1$^{G/G}$; Cdkn1a$^{-/-}$* compound mutant mice.

	Rb1$^{G/+}$; Cdkn1a$^{+/-}$ x *Rb1$^{G/+}$; Cdkn1a$^{+/-}$*	
	Observed	Expected
Rb1$^{+/+}$; Cdkn1a$^{+/+}$	17	21
Rb1$^{+/+}$; Cdkn1a$^{+/-}$	64*	43
Rb1$^{+/+}$; Cdkn1a$^{-/-}$	26	21
Rb1$^{G/+}$; Cdkn1a$^{+/+}$	29*	43
Rb1$^{G/+}$; Cdkn1a$^{+/-}$	82	86
Rb1$^{G/+}$; Cdkn1a$^{-/-}$	39	43
Rb1$^{G/G}$; Cdkn1a$^{+/+}$	19	21
Rb1$^{G/G}$; Cdkn1a$^{+/-}$	37	43
Rb1$^{G/G}$; Cdkn1a$^{-/-}$	29	21
Total	342	

The indicated genotypes of mice were crossed and all resulting progeny were genotyped. The number of live animals obtained at two weeks of age is indicated for each genotype and the expected number based on Mendelian inheritance is indicated. * denotes significance as determined by chi-squared test.

Surprisingly however, despite the homology between p21 and p27, $Rb1^{G/G}$; $Cdkn1a^{-/-}$ mice showed no change in overall survival as compared to $Cdkn1a^{-/-}$ controls (**Figure 4.5B**). Furthermore, at endpoint the vast majority of these mice displayed no observable masses (**Figure 4.5C**). Out of the 25 $Rb1^{G/G}$; $Cdkn1a^{-/-}$ mice 1 had a mass in the lower abdomen which has been identified as an angiosarcoma (**Figure 4.3CD**). Additionally, one $Cdkn1a^{-/-}$ mouse had an oncocytoma which arose out of the kidney (**Figure 4.3CD**). Importantly, these animals were far older, 334 and 485 days respectively, than $Rb1^{G/G}$; $Cdkn1b^{-/-}$ mice succumbing to pituitary tumors, which had an average tumor free survival of 214 days (**Chapter 2**)[8]. Furthermore, the pituitaries of these mice showed no overt aberrant growth, whereas tumor formation in $Rb1^{G/G}$; $Cdkn1b^{-/-}$ mice ubiquitously occurred in the intermediate lobe of the pituitary (**Figure 4.5E**)[8].

Given the homology between p21 and p27 and the similar inability to respond properly to DNA damage, it is surprising that p21 loss does not synergize with loss of E2F repression as p27 does[5,8]. This suggests that p27 is playing a unique tumor-suppressive role which can not be compensated for by p21 (**Figure 4.3A**)[28]. As mentioned in the introduction $Rb1^{+/-}$ animals develop normally into adulthood, however following loss of heterozygosity, $Rb1^{-/-}$ cells result in pituitary tumor formation[30,31]. Additionally Cre-mediated deletion of pRB in the pituitary of mice have resulted in the same malignancy[32]. Several studies have attempted to modulate this phenotype through the deletion of various genes (**Table 4.4, 4.5**). Co-deletion of p21, p27 or p53 in the $Rb1^{+/-}$ background lead to a decreased tumor-free survival with the loss of additional tumor suppressors (**Table 4.4**)[33-35]. By contrast co-deletion of *Skp2* or *E2f1* in the $Rb1^{+/-}$

Table 4.4: Effect of codeletion of various genes on pituitary tumor development in *Rb1*^{+/-} mice.

Gene	Survival of *Rb1*^{+/-}	Survival of compound mice	Change	Pathology	Citation
Id2^{-/-}	276 days	334 days	+58 days	Pituitary tumors	[36]
Skp2^{-/-}	~380 days	No tumorigenesis	No tumors	Pituitary tumors	[37]
Cdkn1b^{-/-}	337 days	178 days	-159 days	Pituitary tumors	[34]
Cdkn1a^{-/-}	340 days	261 days	-79 days	Pituitary tumors	[33]
Trp53^{-/-}	357 days	105 days	-252 days	Lymphoma (40%), Pituitary (33%), Sarcoma (14%), Other (13%)	[35]
E2f1^{-/-}	340 days	521 days	43	Pituitary tumors (62%)	[38]

Table 4.5: Effect of codeletion of *Sox2* on pituitary tumor development in conditional *Rb1*^{-/-} mice.

Control Genotype	Experimental Genotype	Survival of mice	Phenotype of control	Experimental Phenotype	Citation
Rb1^{f/f}	*Rb1*^{f/f}; *POMC*^{Cre}	125 days	No tumors (14 months)	Pituitary tumors	[32]
Rb1^{f/f}; *Rosa26*^{CreER}	*Rb1*^{f/f}; *Sox2*^{f/f}; *Rosa26*^{CreER}	Sacrificed at 9 weeks post injection	Pituitary tumors	No tumors	[39]

background resulted in the rescue of pituitary tumorigeneses (**Table 4.4**)[37,38]. As both E2F1 and Skp2 promote cell cycle entry and are both inhibited by pRB activity, the deletion of these genes not surprisingly significantly reduced tumorigenesis (**Table 4.4**).

In addition to the deletion of these tumor-suppressors and oncogenes, two studies have shown that the pituitary tumor phenotype is also rescued by the deletion of the pluripotency factors *Id2* and *Sox2* (**Table 4.4, 4.5**)[36,39]. Sox2 is of particular interest as it is a marker of pluripotency in the intermediate lobe of the pituitary[40]. This suggests that the ability to maintain pluripotency is necessary to develop pituitary tumors in this background[39]. These stem-like cells could be far easier to be transformed resulting in tumor formation. Additionally, previous work has shown that both $Rb1^{-/-}$ cells and our $Rb1^{G/G}$ cells reprogram into stem cells more efficiently than wildtype controls following expression of reprogramming factors (Oct4, Klf4, cMyc, Sox2)[39]. This raises the possibility that E2F repression plays a role in maintaining a differentiated state.

Interestingly, while p21 and p27 play similar roles in their ability to regulate the cell cycle through the inhibition of Cyclin/CDK complexes, $Cdkn1b^{-/-}$ cells show differential reprogramming efficacy when compared to $Cdkn1a^{-/-}$ cells[5,41]. When only 2 reprogramming factors (Oct4, Klf4) were expressed in p21 and p27 null cells, p27 null cells reprogrammed into stem cells at 4 times the rate of p21 null cells[41]. Additionally, the expression of the pluripotency factor Sox2, which is necessary for tumor development in $Rb1^{-/-}$ pituitaries, is regulated by p27[41]. Chromatin immunoprecipitation has shown that both pRB and p27 are capable of binding to the upstream enhancer SRR2 influencing Sox2 expression[39,41].

To determine if there is an increased level of pluripotency factors inherent to the $Rb1^{G/G}$; $Cdkn1b^{-/-}$ MEFs we isolated RNA and performed qRT-PCR expression analysis of 4 keys stem cell factors (Sox2, Oct4, Klf4, and Nanog). Overall, we found no significant difference between the various genotypes tested, likely due to the huge amount of variability present across samples (**Figure 4.6**). However, as stem cell factors are expressed at very low levels in non-stem cells it is not surprising from one population to the next the expression of these factors may vary wildly. In summary, the lack of a tumor phenotype in $Rb1^{G/G}$; $Cdkn1a^{-/-}$ animals lacking 21 as compared to the pituitary tumors formed in $Rb1^{G/G}$; $Cdkn1b^{-/-}$ mice missing p27, suggests that p27 is playing a unique tumor suppressive role in addition to cell cycle arrest mechanisms following DNA damage in the context of the $Rb1^{G}$ mutation (**Figure 4.5BC**)[8]. This role may include prevention of stem cell like reprogramming, however more studies are required to fully address these questions.

4.4   Discussion

In this chapter, we aimed to investigate the tumor-suppressive abilities of pRB independent of E2F transcription factor repression. We show that, while the $Rb1^{G}$ mutation does exacerbate the tumor development of $Trp53^{-/-}$ mice, there is no effect on tumor-free survival in the presence of oncogenic $Kras^{G12D}$ expression, nor following loss of p21 ($Cdkn1a^{-/-}$). In conjugation with the results presented in chapter 2 demonstrating that $Rb1^{G/G}$; $Cdkn1b^{-/-}$ animals, lacking p27, form pituitary tumors, these genetic crosses provide an interesting picture of how pRB-E2F interactions influence tumor-suppression in the face of various cancer causing mutations[8].
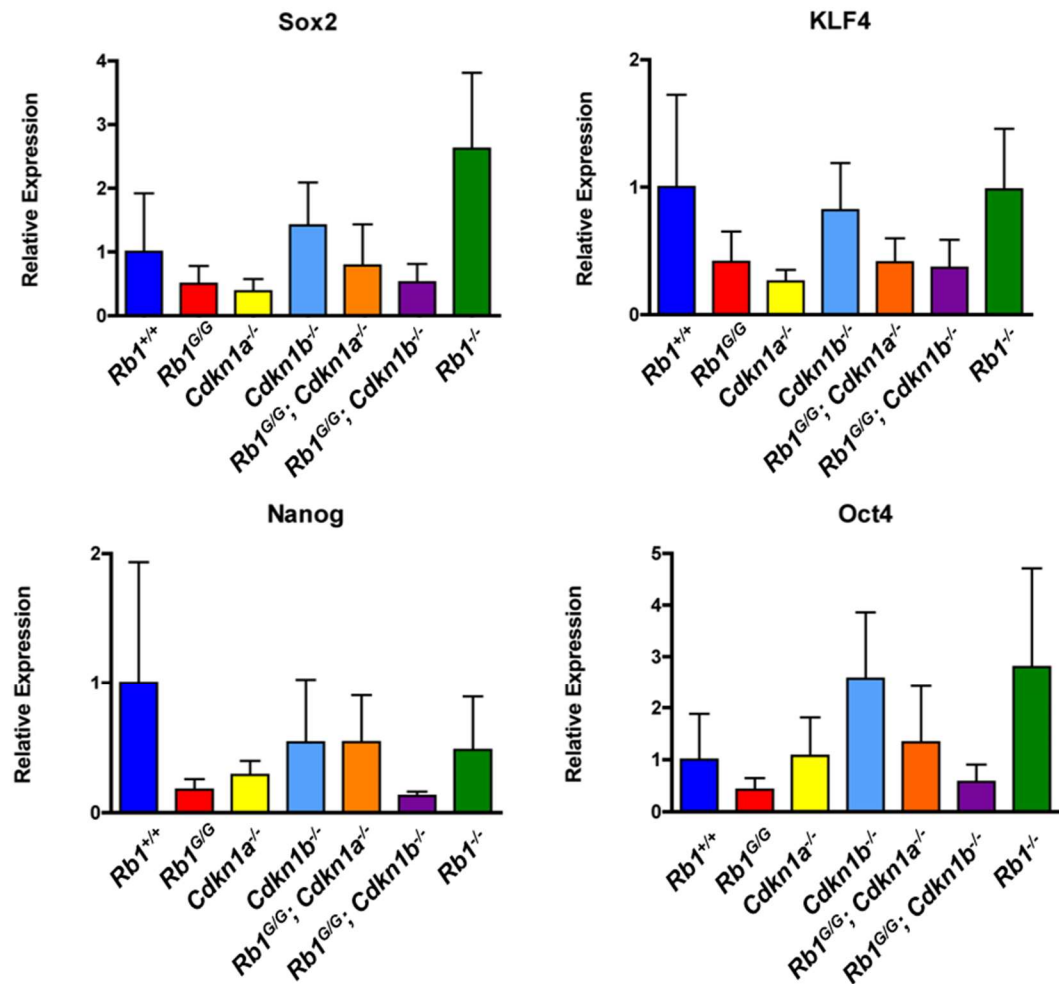
Figure 4.6: Expression of pluripotency factors *Sox2, Klf4, Oct4*, and *Nanog*, in *Rb1^{G/G}; Cdkn1b^{-/-}* MEFs.

Expression of genes was determined by qRT-PCR, normalized to GAPDH. Average of 3 replicates is shown, error bars indicate standard error. No statistically significant differences were found among any genotypes as determined by one-way ANOVA and Tukey's test ($p > 0.05$).

The expression of the $Rb1^G$ mutation in the presence of oncogenic Kras^{G12D} had no effect on tumor free survival (**Figure 4.2B**). One compelling explanation for this finding is uncovered through analysis of the method by which oncogenic Kras leads to tumor formation. Overall, oncogenic Kras^{G12D} causes a signalling cascade which results in both the expression of E2Fs, an increase in Cyclin/CDK complexes and the suppression of p27 activity[14,15]. Importantly, although Kras^{G12D} activation results in increased activity of E2Fs, which can not be sequestered by pRB^G, the increased Cyclin/CDK activity results in the hyperphosphorylation of pRB[3]. This in turn leads to the compaction of the pRB protein and the complete disruption of both the pRB pocket domain and the LxCxE binding cleft which eliminates the E2F regulatory and p27 stabilization functions of pRB-mediated cell cycle control respectively[4]. As such, the expression of oncogenic $Kras^{G12D}$ results in the hyperphophorylation of pRB and any effect that pRB^G could have been masked by the complete disruption of pRB-mediated cell cycle control. Alternatively, the extremely fast rate at which expression of $Kras^{G12D}$ induces tumor development it is possible that the $Rb1^G$ mutation could not cooperate to achieve any change in tumor latency. Potentially future studies using tissue specific Cre driver lines may cause slower growing tumors and the $Rb1^G$ mutation may alter the kinetics.

Our findings in chapter 2 demonstrated that the combined loss of pRB-E2F repression and p27 results in a defective DNA damage response and eventual pituitary tumor formation (**Chapter 2**)[8]. Furthermore, this defective arrest was also seen in embryonic pituitaries of combined mutant mice ($Rb1^{G/G}$; $Cdkn1b^{-/-}$)[8]. As these findings suggest a defective DNA damage response is involved in the tumorigenesis observed, we aimed to better understand the involvement of pRB-E2F interaction in this paradigm. By

introducing our *Rb1*[G] mutation into the *Trp53*^{-/-} background we determined the tumor-suppressive capabilities of *Rb1*[G] in the presence of elevated DNA damage inherent to *Trp53*^{-/-} mice[20]. The fact that *Rb1*[G/G]; *Trp53*^{-/-} mice develop similar tumors with faster kinetics to that of *Trp53*^{-/-} controls indicates that pRB-E2F interactions are important for regulating cellular responses to DNA damage, but not the tumor tropism (**Figure 4.4AB**)[20].

Interestingly, this function must lie outside of canonical understanding of pRB activation following DNA damage. Under wild-type conditions, DNA damage would be identified and ATM/ATR kinases would stabilize and activate p53 through phosphorylation[15]. This in turn would upregulate a number of genes, one of which is p21 encoded by the *CDKN1A* gene[15]. Once expressed, p21 is then able to bind to and inhibit the activity of Cyclin/CDK complexes maintaining pRB in a hypophosphorylated state[4,5]. The fact that *Rb1*[G/G]; *Trp53*^{-/-} show decreased tumor-free survival as compared to controls suggests that pRB is still playing a role in tumor-suppression in the presence of DNA damage despite the inability of signaling to propagate via p53 and p21 to pRB[24]. One possible explanation for this is that, *Rb1*[G/G]; *Trp53*^{-/-} mice have reduced survival simply due to cells harboring an additional mutation in a critical binding pocket of an important tumor suppressor, the general E2F interacting site. This line of thinking would indicate that the pRB and p53 pathways in this context are functioning independently and the loss of p53 as well as E2F transcriptional repression simply makes a cell more amenable to tumorigenesis.

Lastly, to test the effect of the *Rb1*[G] mutation in a mouse model harboring a defective DNA damage response, we combined our *Rb1*[G/G] mutant mouse with the *Cdkn1a*^{-/-}

background which have a deletion of p21. Given the high degree of homology between p21 and p27 it is surprising that *Rb1*[G/G]*; Cdkn1a*^{-/-} mice do not show any tumor incidence in contrast to *Rb1*[G/G]*; Cdkn1b*^{-/-} animals, which ubiquitously develop pituitary tumors (**Figure 4.5BC**)[8]. p21 and p27 are both members of the CIP/KIP family of CKIs which influence cell cycle control through the inhibition of Cyclin/CDK activity[5]. When combined with the *Rb1*[G] mutation, p27 deletion prevents cells from responding appropriately to DNA damage, potentially leading to the development of the pituitary tumors observed[8]. Importantly, the defective cell cycle arrest in response to DNA damage exhibited in the *Rb1*[G/G]*; Cdkn1b*^{-/-} cells is also present in cells null for p21 (**Figure 4.5A**)[27,28]. Together this indicates that p27 must be playing a specific role in preventing tumor formation when pRB-E2F interactions are disrupted that can't be compensated for by p21, and is therefore is beyond influencing DNA damage induced cellular arrest.

One role of p27 that is unique among CIP/KIP family members is the ability to regulate the expression of the *Sox2* gene through the regulation of the SRR2 enhancer[41]. Sox2 is a pluripotency factor that is critical to the development of the pituitary[40]. Additionally, Sox2 is required to allow for tumor formation in *Rb1*^{-/-} pituitaries[39]. This expression of a pluripotency factor could lead to a more stem-like phenotype in *Rb1*[G/G]*; Cdkn1b*^{-/-} pituitaries resulting in transformation and subsequent tumor formation. However, when analyzed by qRT-PCR we found no differences in the overall level of these factors in any of the genotype tested (**Figure 4.6**). Importantly, in this experiment we found a huge degree of variability in the expression of these genes likely due to their overall low abundance in non-stem cells. Additionally, stem-cell reprogramming occurs at a cell to cell basis. Even when cells are reprogrammed through the expression of the

canonical reprogramming factors (Oct4, Klf4, cMyc and Sox2) this is a rare event[39].

Therefore, the lack of any meaningful change in the expression of the stem cell markers

(Sox2, Klf4, Oct4 and Nanog) in MEF population is perhaps unsurprising as any

alteration can be drowned out by population effects (**Figure 4.6**). While we have not

discerned a direct link between our *Rb1*$^{G/G}$*; Cdkn1b*$^{-/-}$ MEFs and increased amenability to

stem cell reprogramming this remains a formal possibility which requires further

investigation.

Overall, we show that our *Rb1*^{G} mutation can enhance the ability of cells to form

tumors in *Trp53*$^{-/-}$ mice (**Figure 4.4B**). However, in the presence of the oncogenic driver

mutation *Kras*^{G12D}, the inability of pRB to regulate E2F target transcription did not affect

tumor-free survival (**Figure 4.2B**). Finally, the surprising finding that p21 and p27

deletion have very different phenotypic effects in our *Rb1*$^{G/G}$ mutant animals indicates

that p27 has a unique tumor-suppressive role in the absence of pRB-E2F interactions

(**Figure 4.5C**)[8].

The findings of these genetic crosses may have important implications in the practical

use of a novel family of cancer therapeutics, CDK4/6 inhibitors by providing diagnostic

markers for effective treatment administration. Specifically, re-activation of pRB-

mediated cell cycle control would be most effective in tumors which retain p53 activity

and would likely not be effected p21 deletion. Finally, as oncogenic Kras^{G12D} typically

influences tumorigenesis through the hyperphosphorylation of pRB, use of CDK4/6

inhibitors in these tumors would likely be an effective strategy to combat tumor growth.

Provided, of course, that adequate inhibition of CDK4/6 can be achieved in the presence

of oncogenic Kras. Further studies analyzing CDK4/6 inhibitors in cells harboring these

mutations will provide additional information towards more effective administration of

these novel compounds.

4.5　References

1　Hanahan, D. & Weinberg, R. A. Hallmarks of cancer: the next generation. *Cell* **144**, 646-674, doi:10.1016/j.cell.2011.02.013 (2011).

2　Coller, H. A. What's taking so long? S-phase entry from quiescence versus proliferation. *Nat Rev Mol Cell Biol* **8**, 667-670, doi:10.1038/nrm2223 (2007).

3　Coleman, M. L., Marshall, C. J. & Olson, M. F. RAS and RHO GTPases in G1-phase cell-cycle regulation. *Nat Rev Mol Cell Biol* **5**, 355-366, doi:10.1038/nrm1365 (2004).

4　Dick, F. A. & Rubin, S. M. Molecular mechanisms underlying RB protein function. *Nat Rev Mol Cell Biol* **14**, 297-306, doi:10.1038/nrm3567 (2013).

5　Hydbring, P., Malumbres, M. & Sicinski, P. Non-canonical functions of cell cycle cyclins and cyclin-dependent kinases. *Nat Rev Mol Cell Biol* **17**, 280-292, doi:10.1038/nrm.2016.27 (2016).

6　Geng, Y. *et al.* Regulation of cyclin E transcription by E2Fs and retinoblastoma protein. *Oncogene* **12**, 1173-1180 (1996).

7　Yao, G., Lee, T. J., Mori, S., Nevins, J. R. & You, L. A bistable Rb-E2F switch underlies the restriction point. *Nat Cell Biol* **10**, 476-482, doi:10.1038/ncb1711 (2008).

8　Thwaites, M. J., Cecchini, M. J., Passos, D. T., Welch, I. & Dick, F. A. Interchangeable Roles for E2F Transcriptional Repression by the Retinoblastoma Protein and p27KIP1-Cyclin-Dependent Kinase Regulation in Cell Cycle Control and Tumor Suppression. *Mol Cell Biol* **37**, doi:10.1128/MCB.00561-16 (2017).

9　Binne, U. K. *et al.* Retinoblastoma protein and anaphase-promoting complex physically interact and functionally cooperate during cell-cycle exit. *Nat Cell Biol* **9**, 225-232 (2007).

10　Ji, P. *et al.* An Rb-Skp2-p27 pathway mediates acute cell cycle inhibition by Rb and is retained in a partial-penetrance Rb mutant. *Mol Cell* **16**, 47-58, doi:S1097276504005726 [pii]10.1016/j.molcel.2004.09.029 (2004).

11　Burkhart, D. L. & Sage, J. Cellular mechanisms of tumour suppression by the retinoblastoma gene. *Nat Rev Cancer* **8**, 671-682, doi:nrc2399 [pii]10.1038/nrc2399 (2008).

12　Cecchini, M. J. *et al.* A retinoblastoma allele that is mutated at its common E2F interaction site inhibits cell proliferation in gene-targeted mice. *Mol Cell Biol* **34**, 2029-2045, doi:10.1128/MCB.01589-13 (2014).

13   Sellers, W. R. *et al.* Stable binding to E2F is not required for the retinoblastoma protein to activate transcription, promote differentiation, and suppress tumor cell growth. *Genes Dev* **12**, 95-106 (1998).

14   Downward, J. Cell cycle: Routine role for ras. *Current Biology* **7**, R258-R260 (1997).

15   Sherr, C. J. & McCormick, F. The RB and p53 pathways in cancer. *Cancer Cell* **2**, 103-112 (2002).

16   Muller, P. A. & Vousden, K. H. p53 mutations in cancer. *Nat Cell Biol* **15**, 2-8, doi:10.1038/ncb2641 (2013).

17   Jackson, E. L. *et al.* Analysis of lung tumor initiation and progression using conditional expression of oncogenic K-ras. *Genes Dev* **15**, 3243-3248, doi:10.1101/gad.943001 (2001).

18   Ruzankina, Y. *et al.* Deletion of the developmentally essential gene ATR in adult mice leads to age-related phenotypes and stem cell loss. *Cell Stem Cell* **1**, 113-126, doi:10.1016/j.stem.2007.03.002 (2007).

19   Deng, C., Zhang, P., Harper, J. W., Elledge, S. J. & Leder, P. Mice lacking p21CIP1/WAF1 undergo normal development, but are defective in G1 checkpoint control. *Cell* **82**, 675-684 (1995).

20   Jacks, T. *et al.* Tumor spectrum analysis in p53-mutant mice. *Curr Biol* **4**, 1-7 (1994).

21   Cecchini, M. J., Amiri, M. & Dick, F. A. Analysis of cell cycle position in mammalian cells. *J Vis Exp*, doi:10.3791/3491 (2012).

22   Leone, G., DeGregori, J., Sears, R., Jakoi, L. & Nevins, J. R. Myc and Ras collaborate in inducing accumulation of active cyclin E/Cdk2 and E2F. *Nature* **387**, 422-426, doi:10.1038/387422a0 (1997).

23   Vogelstein, B., Lane, D. & Levine, A. J. Surfing the p53 network. *Nature* **408**, 307-310, doi:10.1038/35042675 (2000).

24   Roos, W. P. & Kaina, B. DNA damage-induced cell death by apoptosis. *Trends Mol Med* **12**, 440-450 (2006).

25   Harvey, M. *et al.* In vitro growth characteristics of embryo fibroblasts isolated from p53-deficient mice. *Oncogene* **8**, 2457-2467 (1993).

26   Coles, A. H. *et al.* Deletion of p37Ing1 in mice reveals a p53-independent role for Ing1 in the suppression of cell proliferation, apoptosis, and tumorigenesis. *Cancer Res* **67**, 2054-2061, doi:10.1158/0008-5472.CAN-06-3558 (2007).

27   Brugarolas, J. *et al.* Radiation-induced cell cycle arrest compromised by p21 deficiency. *Nature* **377**, 552-557 (1995).

28   Pantoja, C. & Serrano, M. Murine fibroblasts lacking p21 undergo senescence and are resistant to transformation by oncogenic Ras. *Oncogene* **18**, 4974-4982, doi:10.1038/sj.onc.1202880 (1999).

29   Martin-Caballero, J., Flores, J. M., Garcia-Palencia, P. & Serrano, M. Tumor susceptibility of p21(Waf1/Cip1)-deficient mice. *Cancer Res* **61**, 6234-6238 (2001).

30   Hu, N. *et al.* Heterozygous Rb-1 delta 20/+mice are predisposed to tumors of the pituitary gland with a nearly complete penetrance. *Oncogene* **9**, 1021-1027 (1994).

31   Harrison, D. J., Hooper, M. L., Armstrong, J. F. & Clarke, A. R. Effects of heterozygosity for the Rb-1t19neo allele in the mouse. *Oncogene* **10**, 1615-1620 (1995).

32   Vooijs, M., van der Valk, M., te Riele, H. & Berns, A. Flp-mediated tissue-specific inactivation of the retinoblastoma tumor suppressor gene in the mouse. *Oncogene* **17**, 1-12 (1998).

33   Brugarolas, J., Bronson, R. T. & Jacks, T. p21 is a critical CDK2 regulator essential for proliferation control in Rb-deficient cells. *J Cell Biol* **141**, 503-514 (1998).

34   Park, M. S. *et al.* p27 and Rb are on overlapping pathways suppressing tumorigenesis in mice. *Proc Natl Acad Sci U S A* **96**, 6382-6387 (1999).

35   Harvey, M., Vogel, H., Lee, E. Y., Bradley, A. & Donehower, L. A. - Mice deficient in both p53 and Rb develop tumors primarily of endocrine origin. - *Cancer Res* - **55**, - 1146-1151 (1995).

36   Lasorella, A., Rothschild, G., Yokota, Y., Russell, R. G. & Iavarone, A. Id2 mediates tumor initiation, proliferation, and angiogenesis in Rb mutant mice. *Mol Cell Biol* **25**, 3563-3574, doi:10.1128/MCB.25.9.3563-3574.2005 (2005).

37   Wang, H. *et al.* Skp2 is required for survival of aberrantly proliferating Rb1-deficient cells and for tumorigenesis in Rb1+/- mice. *Nat Genet* **42**, 83-88, doi:10.1038/ng.498 (2010).

38   Yamasaki, L. *et al.* Loss of E2F-1 reduces tumorigenesis and extends the lifespan of Rb1(+/-)mice. *Nat Genet* **18**, 360-364 (1998).

39   Kareta, M. S. *et al.* Inhibition of pluripotency networks by the Rb tumor suppressor restricts reprogramming and tumorigenesis. *Cell Stem Cell* **16**, 39-50, doi:10.1016/j.stem.2014.10.019 (2015).

40   Adachi, K., Suemori, H., Yasuda, S. Y., Nakatsuji, N. & Kawase, E. Role of SOX2 in maintaining pluripotency of human embryonic stem cells. *Genes Cells* **15**, 455-470, doi:10.1111/j.1365-2443.2010.01400.x (2010).

41   Li, H. *et al.* p27(Kip1) directly represses Sox2 during embryonic stem cell differentiation. *Cell Stem Cell* **11**, 845-852, doi:10.1016/j.stem.2012.09.014 (2012).

Chapter 5

5   Discussion

5.1   Summary of findings

The retinoblastoma tumor-suppressor protein (pRB) has been the subject of a significant volume of research that aims to understand the mechanism through which pRB can prevent tumorigenesis. Originally predicted through the genetic analysis of children developing retinoblastoma, pRB is now often described as the main gate-keeper of the G1 to S-phase transition of the cell cycle and whose activity is perturbed in a majority of human tumors[1-3]. pRB-mediated cell cycle control is maintained through the repression of the E2F family of transcription factors which influence the transcription of genes required for S-phase entry[4,5]. However, the function of pRB resists simplicity as a growing body of literature has been suggesting new roles in cell cycle control and tumor suppression independent of E2F transcriptional repression[6-10]. Building on this, Cecchini *et al.,* through the development of the *Rb1*[G/G] mouse model, demonstrated that the loss of pRB-E2F interactions is largely dispensable for cell cycle control and tumor-suppression[11]. In this thesis, by exploiting the *Rb1*[G/G] mouse model, I continued to explore the tumor-suppressive ability of pRB outside of pRB-E2F interactions, using a variety of *in vitro* and *in vivo* approaches to further characterize these interactions.

My findings in this thesis demonstrate that cell cycle control and tumor-suppression by pRB is multifaceted and extends beyond simple repression of E2F transcription factors. In chapter 2, through analysis of the *Rb1*[G/G] mouse model in combination with loss of p27 we present *in vivo* evidence of an E2F independent

mechanism of pRB-mediated cell cycle control through the stabilization of p27 in response to DNA damage[12]. As pRB-E2F interactions are dispensable for this function, in chapter 3, we next explored the various contributions to cell cycle control of 3 specific binding surfaces in the pRB large pocket. These experiments confirmed that the RB pocket domain, LxCxE binding cleft, and the E2F1 specific site all contribute to cell cycle control as determined by Saos-2 cell cycle arrest assays as well as *in vivo* analysis of murine livers. Finally, through a series of genetic experiments we were able garner further information about pRB-mediated tumor-suppression outside of E2F target gene repression (**Chapter 4**). Together the experiments presented in this thesis outline the importance of the entire pRB large pocket, the regulation of cell cycle, and tumor suppression. These findings are consistent with the prevalence of cancer derived mutations that result in the complete inactivation of pRB typically through hyperphosphorylation[3].

5.2 Evidence for pRB as a multifaceted regulator of cell cycle control

The work presented in this thesis highlights and addresses the disparity between the linear model of pRB-mediated tumor suppression (**Figure 5.1A**) and a growing body of literature which points towards pRB-mediated tumor suppression as a function of the regulation of multiple pathways controlled through the various pRB interacting domains, the network model (**Figure 5.1B**). This idea that pRB-mediated tumor-suppression is dependent on several interactors, provides compelling explanations for several unusual findings which would be odd in the context of the linear model of cell cycle control by pRB through E2F repression. Firstly, even though the pRB large pocket
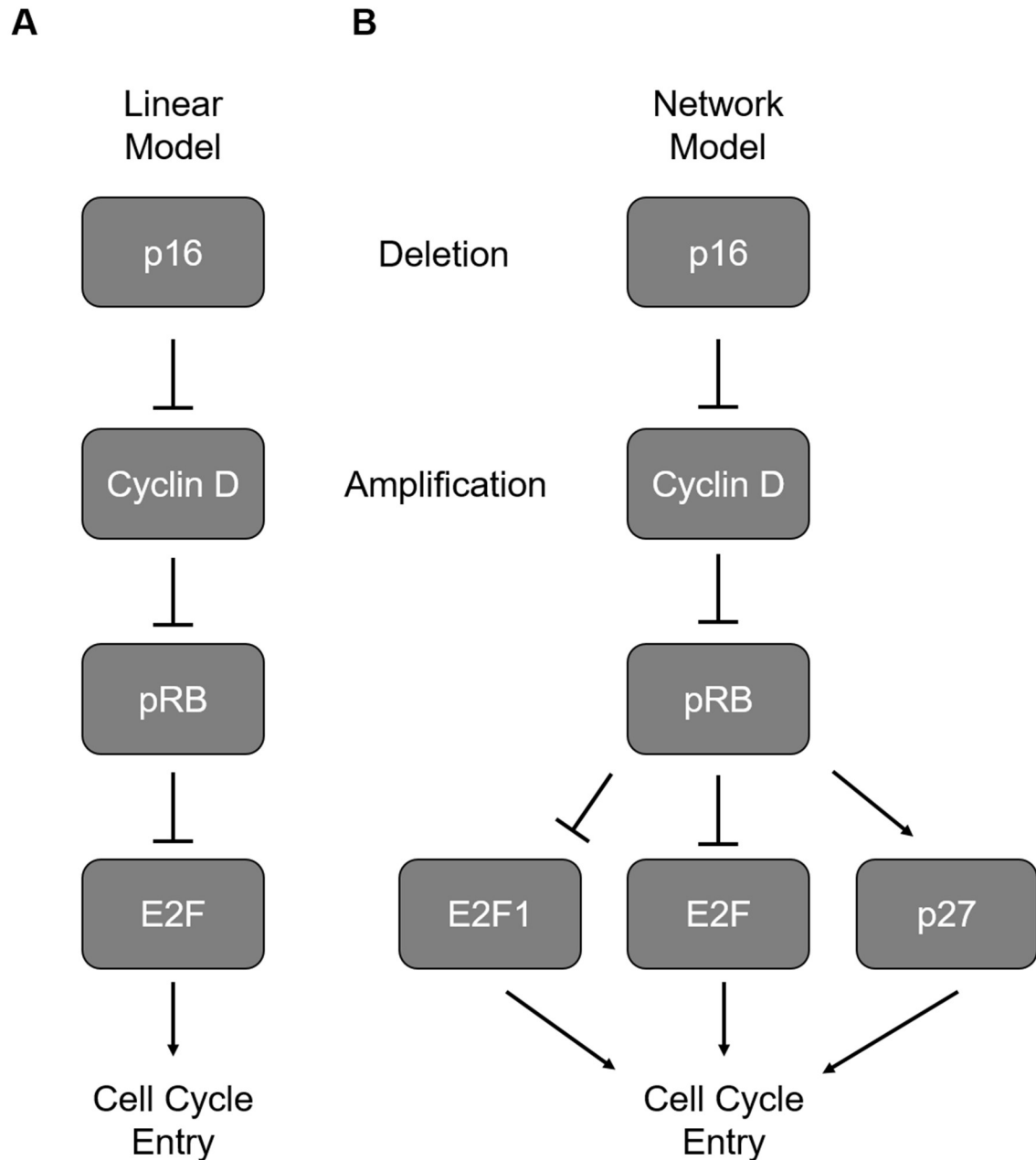
Figure 5.1: pRB utilizes multiple mechanisms to ensure cell cycle control and tumor-suppression.

Human tumors often contain deletion mutants of p16 or amplifications of Cyclin D resulting in the hyperphosphorylation of pRB. **(A)** Linear model of pRB-mediated tumor suppression. Following inactivation of pRB by phosphorylation, E2F is released and is responsible for driving cell entry leading to tumorigenesis. **(B)** Network model of pRB-mediated tumor suppression. pRB sits at the center of a network controlling at least three methods of cell cycle control and tumor suppression: E2F repression, p27 stabilization and regulation of E2F1 via the pRB-E2F1 specific interaction.

is the minimal domain necessary both for E2F interactions and to initiate a cell cycle arrest in Soas-2 cells, this region also contains the LxCxE and specific site binding surfaces (**Figure 1.2B**)[13,14]. Importantly however, later studies exploiting pRB variants which specifically disrupt pRB-E2F interactions demonstrated that pRB could still retain some level of cell cycle control despite the inability of pRB to regulate E2F target gene expression[10,15]. Additionally, investigation of viral oncoproteins capable of inactivation of pRB, in particular E1A, required the elimination of both pRB-E2F interactions as well as LxCxE interactors through the stable binding of E1A's CR1 and CR2 domains to pRB[16]. This notion that the ability of pRB to regulate the cell cycle is mediated both by the pocket domain and the LxCxE binding cleft is further evidenced by the conformational changes that occur to pRB following hyperphosphorylation[6]. Hyperphosphorylation results in the compaction of the pRB protein and the blocking of both the pRB pocket domain as well as the LxCxE binding cleft[6]. Taken together these findings provide a solid foundation which suggests that the role of pRB in regulating the cell cycle extends well beyond the repression of E2F transcription factors. Finally, our lab has produced three strains of mice which target the three binding surfaces discussed in this thesis: the pocket domain ($Rb1^{G/G}$), the LxCxE binding cleft ($Rb1^{L/L}$) and the pRB-E2F1 specific interaction ($Rb1^{S/S}$)[8,11,17]. These animals are viable and develop normally, which is in direct contrast to $Rb1^{-/-}$ mice which are embryonic lethal further supporting the notion that pRB regulates cell cycle control and tumor suppression through a multifaceted approach[11,18].

5.3 Prevalence of perturbations to pRB function in cancer

Given that pRB acts as a critical gate-keeper to cellular division it is perhaps unsurprising that the pRB pathway is perturbed in a large majority of human cancers[3]. Interestingly however, mutations in pRB itself is relatively rare outside of small cell lung cancer, retinoblastoma and osteosarcoma (**Figure 5.2A**)[3]. Typically, mutations in the pRB pathway occur upstream of pRB (**Figure 5.2B**)[3]. These mutations typically include amplifications of Cyclins, or their catalytic partner CDK, as well as deletions of Cyclin dependent kinase inhibitors (CKIs) (**Figure 5.2B**). The functional consequence of these alterations would be the hyperphosphorylation of pRB and subsequent loss of binding to both the pRB pocket domain and the LxCxE binding cleft[3,6]. Furthermore, the majority of those mutations that do occur within the coding sequence of pRB typically result in the formation of novel stop codons (**Figure 5.2C**). This in turn creates a non-functional truncated protein. Finally, the small subset of mutations in the pRB coding sequence that do result in missense changes are equally spread across the coding region (**Figure 5.2D**). Using a binomial distribution test with a Bonferroni correction we determined if any of the missense changes occurred at a frequency higher than expected (**Figure 5.2D**). While some amino acid changes did appear more often than expected, all of them are buried in the interior of the pocket domain of pRB based on previous analysis and are not likely to influence interactions[19]. However, these changes substitute small amino acids for large ones, which could significantly disrupt the overall structure of pRB leading to a dysfunctional protein.
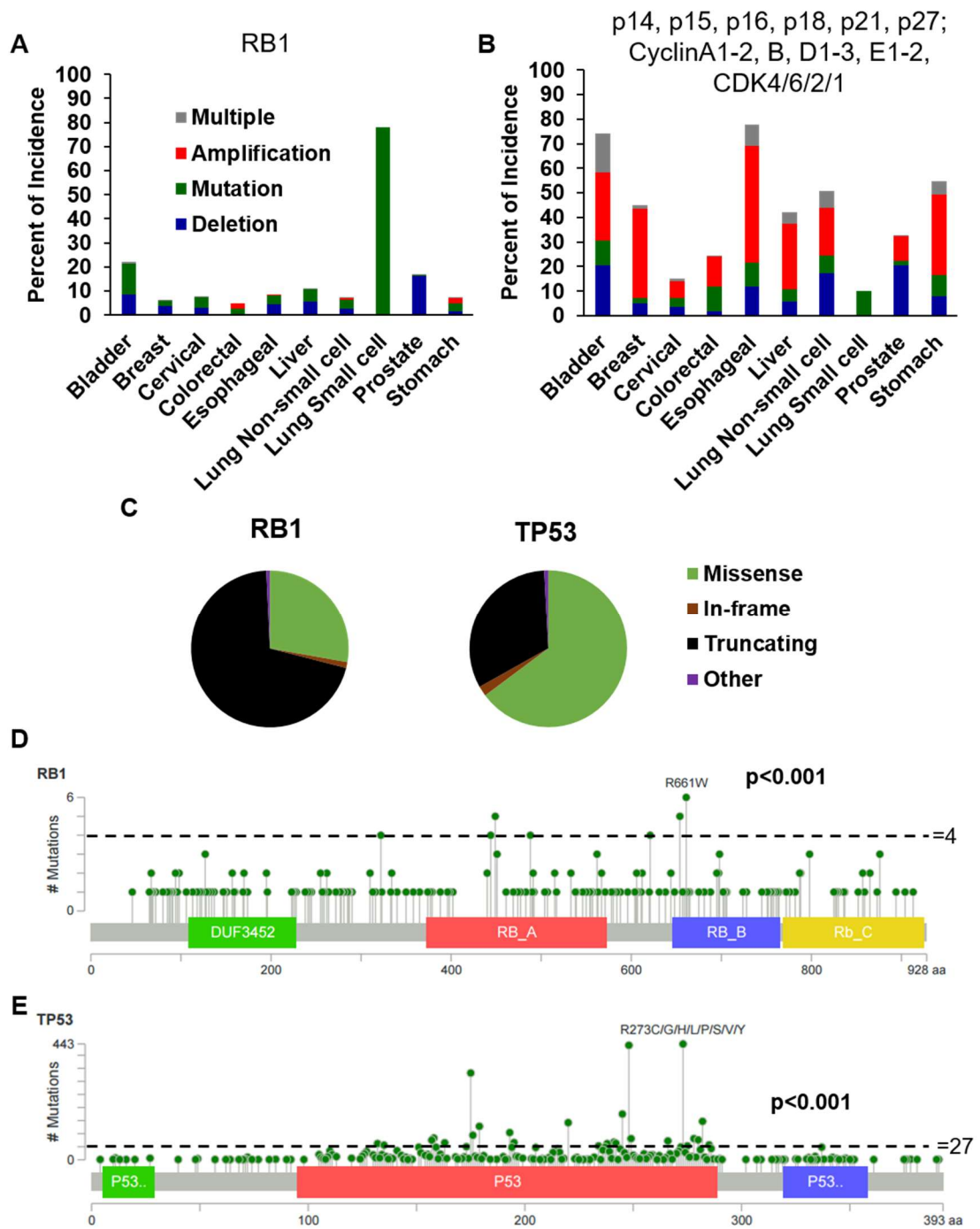
Figure 5.2: Direct pRB mutation is relatively rare in human cancers and mutations that do exist result in null alleles.

Figure 5.2: Direct pRB mutation is relatively rare in human cancers and mutations that do exist result in null alleles.

(A) Incidence of *RB1* mutation, deletion or amplification in the ten most common human malignancies. Data obtained from C-bio portal (2017). **(B)** Incidence of p14, p15, p16, p18, p21, p27, CyclinA1-2, B, D1-3, E1-2, CDK1/2/4/6 mutation, deletion or amplification in the ten most common human malignancies. Data obtained from C-bio portal (2017). **(C)** Breakdown of coding sequence mutations in *RB1* and *TP53* Data obtained from C-bio portal (2017). **(D)** Alignment of cancer derived mutations occurring in the *RB1* coding region, as curated by C-bio portal (2017). **(E)** Alignment of cancer derived mutation occurring in the *TP53* coding region, as curated by C-bio portal (2017). Dashed lines indicate threshold for significance of p<0.001 of mutational frequency (*RB1*=4 and *TP53*=27) as determined by binomial distribution with a Bonferroni correction.

The lack of hotspot mutations in critical interaction domains of *RB1* is peculiar given the importance prescribed to pRB-E2F interactions in pRB-mediated tumor suppression. By comparison, other tumor suppressors such as *TP53* and *PTEN* are dominated by missense mutations that disrupt well defined hotspots which occur within critical structures of the protein such as the DNA binding domain of p53 and the phosphatase domain of PTEN (**Figure 5.2E**)[20,21]. The fact that pRB is inactivated in the majority of human cancers through hyperphosphorylation or nonsense substitutions suggests that pRB is a crucial tumor-suppressor that must be overcome to allow for cancer development and progression[3]. Secondly, the lack of missense mutations in the *RB1* gene demonstrates that the tumor suppressive function of pRB is likely not limited to a single interaction as is the case for p53 through its DNA binding domain (**Figure 5.2C-E**)[21]. Instead these findings imply that multiple functions of pRB contribute to its tumor-suppressive functions and as such, disruption of the whole protein through deletion, truncation, or hyperphosphorylation is more prevalent in human tumors (**Figure 5.2B-D**)[3]. Moreover, this hypothesis is supported by our data which suggested that at least 3 different binding surfaces contribute to the cell cycle control as mediated by pRB (**Chapter 3**). Finally, the requirement for additional tumor-suppressive pathway disruptions in the *Rb1^{G/G}* background is consistent with the complete disruption of pRB function through hyperphosphorylation or truncation seen in human tumors. (**Figure 5.2B-D**) (**Chapter 2, 4**)[11,12].

5.4   Non-canonical functions of p27

One of the most striking findings presented in this thesis is the stark phenotypic difference between *Rb1^{G/G}; Cdkn1a^{-/-}* mice, lacking p21 and *Rb1^{G/G}; Cdkn1b^{-/-}* mice

which have a deletion of p27. As discussed in the results chapters, *Rb1*[G/G]; *Cdkn1a*^{-/-} mice, deficient for p21, showed relatively limited overt phenotypes, with the development of only 1 malignancy out of 25 animals (**Figure 4.5C**). Importantly there was no difference in terms of overall or tumor free survival when compared to *Cdkn1a*^{-/-} controls (**Chapter 4**). By comparison, *Rb1*[G/G]; *Cdkn1b*^{-/-} mice, lacking p27, ubiquitously developed pituitary tumors with a tumor free survival of 214 days, while control *Rb1*[G/G] and *Cdkn1b*^{-/-} animals showed no tumor development (**Chapter 2**)[12]. Taken together, these results indicate that p27 is playing a unique role in regulating pRB-mediated tumor suppression. This is surprising considering there is a high degree of homology between p21 and p27 and the fact that both contribute to the regulation of the cell cycle through the inhibition of a broad range of CDKs[22]. As deletion of p21 in the *Rb1*[G/G] background did not result in tumor formation we can conclude that p27 is influencing pRB in a manner that is independent of cell cycle control in the presence of DNA damage as this is also defective in *Cdkn1a*^{-/-} and *Rb1*[G/G]; *Cdkn1a*^{-/-} MEFs lacking p21.

In addition to the ability of p27 to influence the cell cycle, through the inhibition of CDKs, non-canonical roles in tumor suppression for p27 have been described[23]. Interestingly, some of these alternative functions of p27 are tumor-suppressive whereas others are oncogenic[23]. As discussed in chapter 4, p27 has been implicated in the maintenance of stemness of cells, a characteristic of tumor cells, and in particular cancer stem cells (CSCs) which can give rise to metastasis[23,24]. Overall p27 levels are relatively low in undifferentiated cells and differentiation coincides with an increase in p27[25,26]. Moreover, p27 has been shown to be a transcriptional repressor of SOX2 in different cell lines[27]. Furthermore, *Cdkn1b*^{-/-} animals lacking p27, display increased expression of *Sox2*

in a variety of tissues[27]. Finally, Li *et al*. also demonstrated that the gigantism phenotype displayed in some strains of *Cdkn1b*^{-/-} animals can be rescued with the co-deletion of *Sox2*, implying that *Sox2* overexpression in the absence of p27 can result in aberrant growth[27]. This result together with the finding that both *Rb1*[G/G] and *Cdkn1b*^{-/-} MEFs reprogram more efficiently than wildtype controls, suggests a potential mechanism of tumorigenesis in *Rb1*[G/G]; *Cdkn1b*^{-/-} animals[27,28]. The role for p27 in transcriptional repression also extends beyond the regulation of *Sox2*, through the formation of transcriptional repressor complexes with p130 and E2F4[29]. This complex is then capable of recruiting co-repressors such as HDACs which can compact the DNA around various target genes including those involved in RNA processing and the cell cycle[29]. Importantly while this repression is lost following p27 deletion, a mutant version of p27, which is incapable of inhibiting CDKs (p27[CK]) is as efficient as wildtype in repressing transcription[29].

Critical to the function of p27 is its subcellular localization, cytoplasmic or nuclear. While the ability of p27 to inhibit Cyclin/CDKs and transcriptionally repress genes involved in cell cycle, RNA processing and pluripotency occurs in the nucleus, additional roles for p27 in the cytoplasm have also been described[30,31]. Following phosphorylation of p27 on S10, p27 is exported from the nucleus[32]. However, the ramifications of cytoplasmic p27 are unclear as p27 appears to have both tumor-suppressive and oncogenic functions[23,30,32,33]. Cytoplasmic p27 can inhibit cell cycle progression through the disruption of the Ras signalling cascade[30]. Through interaction with GRB2, p27 can attenuate Ras signalling by disrupting GRB2-SOS interactions[30]. This in turn prevents the activation of the Ras signalling cascade[30]. Consistent with this finding, in the absence of

p27, Ras signalling remains activated at a higher level than controls resulting in Erk1/2 phosphorylation, MAPK target gene expression, and faster cell cycle entry[33].

5.5 Cytoplasmic p27 regulates cellular migration and invasion

In opposition to the tumor suppressive functions described above, cytoplasmic p27 has also been shown to be tumorigenic through the regulation of actomyosin[31]. Indeed, cytoplasmic p27 is a marker of poor prognosis in melanoma[34]. Additionally, mouse models harboring a mutation disrupting the S10 site required for cytoplasmic localization of p27 (p27^{S10A}), are resistant to tumor development in response to urethane treatment[32]. Following cytoplasmic localization, p27 associates with RhoA, inhibiting RhoA from becoming activated by GTP[31]. This inhibition of the RhoA-ROCK pathway results in the loss of actomyosin stability and leads to increased migration and invasion[31]. However, this promotion of migration by p27 is not universal and in several cell types p27 has been shown to inhibit migration[35-38].

Overall, several non-canonical functions of p27 have been described, which may help to understand why $Rb1^{G/G}$; $Cdkn1b^{-/-}$ animals developed pituitary tumors where as $Rb1^{G/G}$; $Cdkn1a^{-/-}$ animals, deficient for p21, generally showed no tumor phenotype (**Chapter 2,4**)[12]. It is possible that the loss of p27 results in a combination of factors which maintain a stem cell like state and promote proliferation through the upregulation of cell cycle target genes and increased Ras signalling, however further studies are necessary to fully elucidate this mechanism[27,29,30].

5.6 Perspectives and therapeutic implications

The work presented in the thesis has enhanced our understanding of pRB-mediated cell cycle control and tumor-suppression. Using a variety of techniques, we have shown that the linear model of pRB repression of E2F target genes is incomplete (**Figure 5.1A**). Instead, pRB sits in the center of a network of regulation activating multiple downstream pathways which together maintain cell cycle control and prevent tumorigenesis (**Figure 5.1B**). This multifaceted approach to cell cycle regulation by pRB provides a number of redundant mechanisms, through which the cell can prevent tumorigenesis. This finding is also supported by the relative rarity of missense mutation in the *Rb1* coding sequence (**Figure 5.2D**). Instead, cancers typically harbor mutations in upstream pathway members, which result in the hyperphosphorylation of pRB and subsequent functional inactivation (**Figure 5.2AB**). This method of pRB inactivation through phosphorylation allows the possibility of therapeutic intervention through the inhibition of the upstream kinases responsible for pRB phosphorylation.

Currently there are three drugs which aim to restore pRB activity through the inhibition of pRB phosphorylation in cancer cells: Palbociclib (Pfizer), Ribociclib (Novartis) and Abemaciclib (Eli Lilly). These compounds work by inhibiting upstream kinases of pRB, CDK4 and CDK6. Following inhibition of CDK4/6, pRB becomes hypophosphorylated and can re-activate its various cell cycle functions including those highlighted in this thesis. Currently, Palbociclib is approved for use in ER+ breast cancers in combination with letrozole. In addition, Ribociclib and Abemaciclib are in phase three clinical trials. To insure effectiveness of treatment by these drugs, only patients with wildtype pRB are given these inhibitors. However, pRB-mediated cell cycle

control and tumor-suppression is a product of a network of pathways which may influence the effectiveness of these inhibitors. Through our various genetic crosses in the absence of pRB-E2F interactions we have shown that loss of p27 or p53 result in enhanced tumorigenesis. Therefore, we would predict that the presence of both wildtype p27 and p53 would likely enhance the effectiveness of these CDK4/6 inhibitors in patients. Importantly, in addition to disrupting DNA damage response signalling, p27 appears to play a unique, non-CKI role in regulating tumor-suppression in the absence of pRB-E2F interactions[12]. While this function is currently unknown, several non-canonical functions of p27 have been previously identified and largely depend on the subcellular localization of p27[23]. Therefore, in addition to the expression level and mutational profile of p27, subcellular localization may be a critical determinant for the effectiveness of this new class of CDK4/6 inhibitors.

In the several years following the discovery of pRB, the field has been dominated by the linear model through which pRB is tumor-suppressive by way of regulating E2F transcription factors (**Figure 5.1A**). However, in recent years, several non-canonical functions of pRB have been described. Through the development and use of the *Rb1*[G/G] mouse model we had the unique opportunity to look at these pRB-mediated, non-E2F methods of cell cycle control *in vivo*[11]. Moreover, as the *Rb1*[G/G] animals avoid the embryonic lethality of *Rb1*^{-/-} mice, using this model we can specifically study pRB functions in tumorigenesis as opposed to development. The fact that pRB-E2F interactions are dispensable for cell cycle control and tumorigenesis, indicates that other pathways must play significant roles in regulating cell cycle control and tumor-suppression[11]. Through a variety of *in vitro*, cell culture and *in vivo* approaches we have

identified at least three interacting domains in the large pocket of pRB which play a role in modulating cell cycle control (**Chapter 3**). Furthermore, the loss of pRB-E2F regulation interacted synergistically with *Cdkn1b* deletion resulting in an ineffective DNA damage response and eventual tumor formation (**Chapter 2**)[12]. Finally, the *Rb1^G* mutation dramatically shortened the lifespan of p53 null animals while not effecting the outcome of mice expressing oncogenic *Kras^{G12D}* nor those lacking p21 (**Chapter 4**). Critically, the lack of phenotype of *Rb1$^{G/G}$; Cdkn1a$^{-/-}$* mice lacking p21 as compared to *Rb1$^{G/G}$; Cdkn1b$^{-/-}$* lacking p27, suggests that p27, is playing a unique role in modulating the tumor-suppressive function of pRB. However, the inhibition of CDKs in response to DNA damage cannot be ruled out as a contributing factor to the tumor development in *Rb1$^{G/G}$; Cdkn1b$^{-/-}$* animals. To definitively determine if the tumorigenesis observed in *Rb1$^{G/G}$* lacking p27 is dependent on the ability of p27 to inhibit CDKs, *Rb1$^{G/G}$* mice would have to be combined with the p27^{CK} mutation. Overall this thesis presents several lines of evidence which suggest that pRB is a hub protein at the center of a network of functions which together result in cell cycle control and tumor-suppression.

5.7   References

1   Hanahan, D. & Weinberg, R. A. Hallmarks of cancer: the next generation. *Cell* **144**, 646-674, doi:10.1016/j.cell.2011.02.013 (2011).

2   Knudson, A. G., Jr. Mutation and cancer: statistical study of retinoblastoma. *Proc Natl Acad Sci U S A* **68**, 820-823 (1971).

3   Burkhart, D. L. & Sage, J. Cellular mechanisms of tumour suppression by the retinoblastoma gene. *Nat Rev Cancer* **8**, 671-682, doi:nrc2399 [pii]10.1038/nrc2399 (2008).

4   Dyson, N. The regulation of E2F by pRB-family proteins. *Genes Dev* **12**, 2245-2262 (1998).

5   Giacinti, C. & Giordano, A. RB and cell cycle progression. *Oncogene* **25**, 5220-5227 (2006).

6   Dick, F. A. & Rubin, S. M. Molecular mechanisms underlying RB protein function. *Nat Rev Mol Cell Biol* **14**, 297-306, doi:10.1038/nrm3567 (2013).

7   Coschi, C. H. *et al.* Haploinsufficiency of an RB-E2F1-Condensin II complex leads to aberrant replication and aneuploidy. *Cancer discovery* **4**, 840-853, doi:10.1158/2159-8290.CD-14-0215 (2014).

8   Ishak, C., Marshall, AE., Passos, DT., White, CR., Kim, SJ., Cecchini, MJ., Ferwati, S., MacDonald, WA., Howlett, CJ., Welch, ID., Rubin, SM., Mann, MRW., and Dick, FA. An RB-EZH2 Complex Mediates Silencing of Repetitive DNA Sequences. *Molecular Cell*, doi:http://dx.doi.org/10.1016/j.molcel.2016.10.021 (2016).

9   Binne, U. K. *et al.* Retinoblastoma protein and anaphase-promoting complex physically interact and functionally cooperate during cell-cycle exit. *Nat Cell Biol* **9**, 225-232 (2007).

10   Ji, P. *et al.* An Rb-Skp2-p27 pathway mediates acute cell cycle inhibition by Rb and is retained in a partial-penetrance Rb mutant. *Mol Cell* **16**, 47-58, doi:S1097276504005726 [pii]10.1016/j.molcel.2004.09.029 (2004).

11   Cecchini, M. J. *et al.* A retinoblastoma allele that is mutated at its common E2F interaction site inhibits cell proliferation in gene-targeted mice. *Mol Cell Biol* **34**, 2029-2045, doi:10.1128/MCB.01589-13 (2014).

12   Thwaites, M. J., Cecchini, M. J., Passos, D. T., Welch, I. & Dick, F. A. Interchangeable Roles for E2F Transcriptional Repression by the Retinoblastoma Protein and p27KIP1-Cyclin-Dependent Kinase Regulation in Cell Cycle Control and Tumor Suppression. *Mol Cell Biol* **37**, doi:10.1128/MCB.00561-16 (2017).

13   Hiebert, S. W. - Regions of the retinoblastoma gene product required for its interaction with the E2F transcription factor are necessary for E2 promoter repression and pRb-mediated growth suppression. - *Mol Cell Biol* **- 13**, - 3384-3391 (1993).

14   Qin, X. Q., Chittenden, T., Livingston, D. M. & Kaelin, W. G., Jr. Identification of a growth suppression domain within the retinoblastoma gene product. *Genes Dev* **6**, 953-964 (1992).

15   Sellers, W. R. *et al.* Stable binding to E2F is not required for the retinoblastoma protein to activate transcription, promote differentiation, and suppress tumor cell growth. *Genes Dev* **12**, 95-106 (1998).

16   Pelka, P., Ablack, J. N., Fonseca, G. J., Yousef, A. F. & Mymryk, J. S. Intrinsic structural disorder in adenovirus E1A: a viral molecular hub linking multiple diverse processes. *J Virol* **82**, 7252-7263, doi:10.1128/JVI.00104-08 (2008).

17   Isaac, C. E. *et al.* The retinoblastoma protein regulates pericentric heterochromatin. *Mol Cell Biol* **26**, 3659-3671 (2006).

18   Jacks, T. *et al.* Effects of an Rb mutation in the mouse. *Nature* **359**, 295-300 (1992).

19   Lee, J. O., Russo, A. A. & Pavletich, N. P. Structure of the retinoblastoma tumour-suppressor pocket domain bound to a peptide from HPV E7. *Nature* **391**, 859-865 (1998).

20   Narayan, S., Bader, G. D. & Reimand, J. Frequent mutations in acetylation and ubiquitination sites suggest novel driver mechanisms of cancer. *Genome Med* **8**, 55, doi:10.1186/s13073-016-0311-2 (2016).

21   Greenblatt, M. S., Bennett, W. P., Hollstein, M. & Harris, C. C. Mutations in the p53 tumor suppressor gene: clues to cancer etiology and molecular pathogenesis. *Cancer Res* **54**, 4855-4878 (1994).

22   Hydbring, P., Malumbres, M. & Sicinski, P. Non-canonical functions of cell cycle cyclins and cyclin-dependent kinases. *Nat Rev Mol Cell Biol* **17**, 280-292, doi:10.1038/nrm.2016.27 (2016).

23   Sharma, S. S. & Pledger, W. J. The non-canonical functions of p27(Kip1) in normal and tumor biology. *Cell Cycle* **15**, 1189-1201, doi:10.1080/15384101.2016.1157238 (2016).

24   Croker, A. K. & Allan, A. L. Cancer stem cells: implications for the progression and treatment of metastatic disease. *J Cell Mol Med* **12**, 374-390, doi:10.1111/j.1582-4934.2007.00211.x (2008).

25   Menchon, C., Edel, M. J. & Izpisua Belmonte, J. C. The cell cycle inhibitor p27Kip(1) controls self-renewal and pluripotency of human embryonic stem cells by regulating the cell cycle, Brachyury and Twist. *Cell Cycle* **10**, 1435-1447, doi:10.4161/cc.10.9.15421 (2011).

26   Egozi, D. *et al.* Regulation of the cell cycle inhibitor p27 and its ubiquitin ligase Skp2 in differentiation of human embryonic stem cells. *FASEB J* **21**, 2807-2817, doi:10.1096/fj.06-7758com (2007).

27   Li, H. *et al.* p27(Kip1) directly represses Sox2 during embryonic stem cell differentiation. *Cell Stem Cell* **11**, 845-852, doi:10.1016/j.stem.2012.09.014 (2012).

28   Kareta, M. S. *et al.* Inhibition of pluripotency networks by the Rb tumor suppressor restricts reprogramming and tumorigenesis. *Cell Stem Cell* **16**, 39-50, doi:10.1016/j.stem.2014.10.019 (2015).

29   Pippa, R. *et al.* p27Kip1 represses transcription by direct interaction with p130/E2F4 at the promoters of target genes. *Oncogene* **31**, 4207-4220, doi:10.1038/onc.2011.582 (2012).

30   Moeller, S. J., Head, E. D. & Sheaff, R. J. p27Kip1 inhibition of GRB2-SOS formation can regulate Ras activation. *Mol Cell Biol* **23**, 3735-3752 (2003).

31   Besson, A., Gurian-West, M., Schmidt, A., Hall, A. & Roberts, J. M. p27Kip1 modulates cell migration through the regulation of RhoA activation. *Genes Dev* **18**, 862-876, doi:10.1101/gad.11855041185504 [pii] (2004).

32   Besson, A. *et al.* A pathway in quiescent cells that controls p27Kip1 stability, subcellular localization, and tumor suppression. *Genes Dev* **20**, 47-64, doi:20/1/47 [pii]10.1101/gad.1384406 (2006).

33   Fabris, L. *et al.* p27kip1 controls H-Ras/MAPK activation and cell cycle entry via modulation of MT stability. *Proc Natl Acad Sci U S A* **112**, 13916-13921, doi:10.1073/pnas.1508514112 (2015).

34   Chen, G., Cheng, Y., Zhang, Z., Martinka, M. & Li, G. Prognostic significance of cytoplasmic p27 expression in human melanoma. *Cancer Epidemiol Biomarkers Prev* **20**, 2212-2221, doi:10.1158/1055-9965.EPI-11-0472 (2011).

35   Goukassian, D. *et al.* Overexpression of p27(Kip1) by doxycycline-regulated adenoviral vectors inhibits endothelial cell proliferation and migration and impairs angiogenesis. *FASEB J* **15**, 1877-1885, doi:10.1096/fj.01-0065com (2001).

36   Sun, J. *et al.* Role for p27(Kip1) in Vascular Smooth Muscle Cell Migration. *Circulation* **103**, 2967-2972 (2001).

37   Baldassarre, G. *et al.* p27(Kip1)-stathmin interaction influences sarcoma cell migration and invasion. *Cancer Cell* **7**, 51-63, doi:10.1016/j.ccr.2004.11.025 (2005).

38   Schiappacassi, M. *et al.* p27Kip1 expression inhibits glioblastoma growth, invasion, and tumor-induced neoangiogenesis. *Mol Cancer Ther* **7**, 1164-1175, doi:10.1158/1535-7163.MCT-07-2154 (2008).

Appendix A: A retinoblastoma allele that is mutated at its common E2F interaction site inhibits cell proliferation in gene-targeted mice

A Retinoblastoma Allele That Is Mutated at Its Common E2F Interaction Site Inhibits Cell Proliferation in Gene-Targeted Mice

Matthew J. Cecchini,[a,c] Michael J. Thwaites,[a,c] Srikanth Talluri,[a,c] James I. MacDonald,[a,c] Daniel T. Passos,[a,c] Jean-Leon Chong,[e] Paul Cantalupo,[f] Paul M. Stafford,[a,c] M. Teresa Sáenz-Robles,[f] Sarah M. Francis,[a,c] James M. Pipas,[f] Gustavo Leone,[e] Ian Welch,[d] Frederick A. Dick[a,b,c]

London Regional Cancer Program,[a] Children's Health Research Institute,[b] Department of Biochemistry,[c] and Veterinary Services,[d] Western University, London, Ontario, Canada; Department of Human Genetics and Cancer Center, Ohio State University, Columbus, Ohio, USA[e]; Department of Biology, University of Pittsburgh, Pittsburgh, Pennsylvania, USA[f]

The retinoblastoma protein (pRB) is best known for regulating cell proliferation through E2F transcription factors. In this report, we investigate the properties of a targeted mutation that disrupts pRB interactions with the transactivation domain of E2Fs. Mice that carry this mutation endogenously ($Rb1^{\Delta G}$) are defective for pRB-dependent repression of E2F target genes. Except for an accelerated entry into S phase in response to serum stimulation, cell cycle regulation in $Rb1^{\Delta G/\Delta G}$ mouse embryonic fibroblasts (MEFs) strongly resembles that of the wild type. In a serum deprivation-induced cell cycle exit, $Rb1^{\Delta G/\Delta G}$ MEFs display a magnitude of E2F target gene derepression similar to that of $Rb1^{-/-}$ cells, even though $Rb1^{\Delta G/\Delta G}$ cells exit the cell cycle normally. Interestingly, cell cycle arrest in $Rb1^{\Delta G/\Delta G}$ MEFs is responsive to p16 expression and gamma irradiation, indicating that alternate mechanisms can be activated in G_1 to arrest proliferation. Some $Rb1^{\Delta G/\Delta G}$ mice die neonatally with a muscle degeneration phenotype, while the others live a normal life span with no evidence of spontaneous tumor formation. Most tissues appear histologically normal while being accompanied by derepression of pRB-regulated E2F targets. This suggests that non-E2F-, pRB-dependent pathways may have a more relevant role in proliferative control than previously identified.

The retinoblastoma tumor suppressor protein (pRB) has a central role in the regulation of the G_1-to-S-phase transition. Inactivation of its control over cell cycle progression is one of the most common events in cancer (1). The RB protein is thought to regulate entry into S phase through its ability to repress E2F-dependent transcription (2). In the G_1 phase of the cell cycle, a direct interaction between the large pocket domain of pRB (RBLP) and the transactivation domain of E2Fs blocks transcription and recruits chromatin regulators that maintain the cell in G_1 (3). Activation of cyclin-dependent kinases (CDKs) results in the phosphorylation of pRB and the release of E2F transcription factors (4). Free E2Fs then activate a transcriptional program that drives the cell into S phase (3). This model of pRB regulation of E2F dominates our understanding of G_1-to-S-phase control. Much of our knowledge of this model was derived from studies using viral oncoproteins encoded by small DNA tumor viruses (5, 6). Of particular note, the human papillomavirus E7 protein has been shown to compete for pRB-E2F interactions to deregulate proliferation (7, 8). However, E7 must also target pRB for degradation in order to induce proliferation (8). Thus, the experimental system that gave rise to the pRB-E2F regulatory axis in cell cycle control also suggests that pRB may engage other growth-suppressing activities beyond E2F regulation. By comparison with the pRB-E2F pathway, we know very little about pRB's non-E2F-dependent growth control mechanisms and their relative contribution to cell cycle regulation and tumor suppressor activities.

The minimal growth-suppressive region of pRB has been mapped to the A, B, and C regions of its open reading frame, a domain called the "large pocket" that includes amino acids 379 to 928 (3). This is also the minimal domain needed for stable interaction with E2Fs and to repress their transcription (9–12). E2Fs are a family of transcription factors, and each of E2F1, E2F2, E2F3, and E2F4 is capable of binding to pRB at endogenous levels

through its transactivation domain; this is termed the "general" interaction (13, 14). E2F1 is unique among E2Fs in that it has roles outside transcriptional activation of cell cycle genes, including the regulation of apoptotic targets (15, 16) and DNA replication (17–19). E2F1 is also capable of making a protein interaction with pRB qualitatively different from that of the other E2Fs (13, 20), and this interaction is mediated by separate protein-protein contacts (13, 20–22). This E2F1 "specific" interaction has been suggested to allow it to regulate apoptotic target genes independently of E2F transcriptional control during the cell cycle (13, 15, 20, 23). One reason that the specific interaction with pRB is distinct from the general interaction is because E2F1 bound to pRB through this site is unable to efficiently bind the consensus E2F promoter element (13) but contributes to regulation of apoptotic target genes such as TA-p73 (15, 23). Furthermore, the regulation of this interaction is distinct, as the specific pRB-E2F1 interaction is resistant to disruption by CDK phosphorylation (21, 24). Thus, recent structural and functional insights into pRB-E2F interactions indicate that pRB's relationship with E2F transcription factors may be more complex than simply silencing their activity during cell cycle arrest. This background highlights the difficulty in understanding how individual biochemical aspects of pRB function contribute to its complete role as a cell cycle regulator and tumor suppressor.

In order to investigate pRB-dependent functions in cell cycle

Cecchini et al.

control that are independent of canonical E2F transcriptional control, we generated a gene-targeted mouse allele whose encoded protein is selectively deficient for the general interaction. We call this allele $Rb1^{\Delta G}$ because it disrupts the interaction between the transactivation domain of E2Fs and pRB. Our analysis indicates that this mutant protein is defective for pRB-E2F interactions at cell cycle promoters and is unable to regulate E2F transcriptional activity in reporter assays. Primary fibroblast cultures and tissues from $Rb1^{\Delta G/\Delta G}$ mice exhibit derepression of direct pRB-E2F transcriptional targets and yet maintain the ability to control proliferation in response to serum deprivation, p16 expression, and gamma irradiation. Furthermore, $Rb1^{\Delta G/\Delta G}$ mice are relatively normal in development and remain cancer free throughout their lives. This study suggests that pRB functions that are independent of E2F transcriptional control can contribute to its tumor suppressor activity in a meaningful way.

MATERIALS AND METHODS

Protein interaction analysis and Western blotting. To generate extracts for glutathione S-transferase (GST) pulldowns and gel shifts, cells were washed twice with phosphate-buffered saline (PBS) and collected in 1 ml of gel shift extract (GSE) buffer (20 mM Tris, pH 7.5, 420 mM NaCl, 1.5 mM MgCl$_2$, 0.2 mM EDTA, 25% glycerol, 5 μg/ml leupeptin, 5 μg/ml aprotinin, 0.1 mM Na$_3$VO$_4$, 0.5 mM NaF, and 1 mM dithiothreitol [DTT]) per 15-cm dish of cells. Cells were frozen at −80°C and thawed rapidly to lyse them; cellular debris was removed by centrifugation at 14,000 rpm. For GST pulldowns, extracts were diluted approximately 2-fold in wash buffer without NaCl (20 mM Tris, pH 7.5, 1.5 mM MgCl$_2$, 0.2 mM EDTA, 25 mM DTT, and 0.1% NP-40) to approximately physiological salt concentrations. Beads and fusion proteins were added and incubated with rocking for 1 h at 4°C. The protein G-Sepharose beads and associated proteins were washed twice with immunoprecipitation (IP) wash buffer and then resuspended in 1× SDS-PAGE sample buffer and boiled at 95°C for 5 min to elute the bound proteins. The eluted material was resolved by SDS-PAGE and transferred to a nitrocellulose membrane by standard techniques.

Nuclear extracts were prepared from mouse embryonic fibroblasts (MEFs) as previously described (25). A sheep anti-pRB antibody was generated using the C terminus of murine pRB, and antibodies were purified using a peptide corresponding to amino acids 867 to 881 of murine pRB coupled to agarose using the Sulfolink immobilization kit (Pierce). Five micrograms of antibody, which had previously been covalently coupled to protein G Dynabeads using bis(sulfosuccinimidyl suberate) (BS3; Pierce), was used to immunoprecipitate pRB from 1 mg of nuclear extract. Precipitated proteins were detected in Western blot assays using the following antibodies: pRB was detected using G3-245 (BD Pharmingen), E2F1 with C-20 (Santa Cruz), E2F2 with TFE-25 (Santa Cruz), E2F3 with PG37 (Upstate) or C-18 (Santa Cruz), and E2F4 with C-20 (Santa Cruz). Other antibodies used for Western blotting included PCNA F2 (Santa Cruz), p107 C-18 (Santa Cruz), Mcm3 4012S (Cell Signaling), cyclin E M20 (Santa Cruz), and cyclin A H432 (Santa Cruz). Rabbit anti-SP1 H225 (Santa Cruz) was used as a loading control.

EMSAs. Electrophoretic mobility shift assays (EMSAs) were performed using DNA probes described in the work of Seifried et al. (26). These probes were labeled with 50 μCi of [α-^{32}P]dCTP with Klenow fragment for 15 min at room temperature. The labeled probes were purified on a G25 spin column. Extracts were prepared from confluent MEFs in GSE buffer as described above. Five micrograms of nuclear extract was diluted into EMSA buffer (20 mM Tris, pH 7.5, 4% Ficoll 400-DL [Sigma], 2.5 mM MgCl$_2$, 40 mM KCl, 0.1 mM EGTA, 2 mM spermine, 0.5 mM DTT, 0.25 μg salmon sperm DNA, 10 μg bovine serum albumin) in a 20-μl total volume. Samples with cold competitors were first incubated with 40 ng of wild-type or mutant unlabeled oligonucleotides for 10 min on ice. Four hundred picograms of labeled probe was then added to each

reaction mixture and incubated on ice for 10 min. For antibody supershifts, antibodies were added and the samples were incubated on ice for a further 25 min. For supershifts, 1 μg of anti-pRB 21C9 (a kind gift from Sibylle Mittnacht, London, United Kingdom) and anti-CDK2 (Upstate) was used. Samples were loaded onto a 4% polyacrylamide gel (containing 0.25× Tris-borate-EDTA and 2.5% glycerol) and electrophoresed at 4°C for 4 h at 180 V. Gels were dried, and protein-DNA complexes were detected by autoradiography. Gel shifts for determining differences of affinity were carried out essentially as described above, except that C33A nuclear extracts containing overexpressed hemagglutinin (HA)-tagged E2F1, E2F2, E2F3, and E2F4 with HA-DP1 proteins were used. Anti-HA antibodies (12CA5 hybridoma supernatant) were used to shift HA-E2F/DP1 complexes, and the indicated amounts of GST or GST-RBLP proteins were added.

Gene targeting and phenotypic analysis of animals. Embryonic stem (ES) cell culture, transfection, and selection were performed using standard methods. Correctly targeted ES cells were identified by Southern blotting. Genomic DNA was digested with KpnI, and the indicated probes outside the 5′ and 3′ arms of homology were used to detect homologous recombinants. MscI digestion was also performed to cut DNA within the neomycin resistance gene and outside the 5′ arm of homology. A probe specific to the neomycin resistance gene was used to probe this Southern blot to ensure that the targeted clones contained only a single site of integration of the targeting vector. Correctly targeted ES clones were grown and injected into blastocysts to generate chimeric mice. Male chimeras were mated with B6.FVB *EIIa-cre* transgenic mice to remove the PGK-Neo selectable marker that was flanked by LoxP sites. Progeny were then intercrossed to generate mice that had excised the selectable marker and did not contain *EIIa-cre*. $Rb1^{\Delta G}$ mice were genotyped by amplification of a genomic sequence that surrounds the remaining LoxP site. Using L-F (5′ CTGCAATCTGCGCATTTTTA 3′) and L-R (5′ CGATGCTGCA GGCCTATAAT 3′) primers, a 250- or a 330-bp fragment that corresponds to the wild-type or mutant allele, respectively, is produced.

$E2f1^{-/-}$ mice (B6; 129S4-$E2f1^{tm1Meg}$/J) (27) were obtained from the Jackson Laboratory and genotyped as recommended by the distributor. All animals were housed and handled as approved by the Canadian Council on Animal Care. Mice were monitored throughout their lives, and animals were euthanized after the development of signs of tumor burden or at defined ages as indicated in the figure legends. Survival data were subjected to Kaplan-Meier analysis, and significant differences were compared using a log rank test.

Euthanized animals were subjected to a necropsy where tissues of interest and tumors were fixed in formalin. Tumors and tissues were fixed in formalin for at least 72 h, washed in phosphate-buffered saline (PBS), and then transferred to 70% ethanol. The tissues were embedded in paraffin, and 5-μm sections were cut from superficial and deep sections of the tissue blocks. Sections were subsequently stained with hematoxylin and eosin (H&E), and images were captured on a Zeiss Axioskop 40 microscope and Spot Flex camera using EyeImage software (Empix Imaging, Mississauga, Ontario, Canada) or similar system.

Luciferase reporter assays. Luciferase reporter assays were performed as described previously (28). Saos-2 cells were plated at 5×10^5 per well of a 6-well dish. Transfection mixtures contained 100 ng of a luciferase reporter and 200 ng of cytomegalovirus (CMV)–β-galactosidase (β-Gal). CMV-RB expression plasmids were included up to a total of 100 ng, and where indicated, 15 ng of CMV-HA-E2F and 15 ng of CMV-HA-DP1 were included. Total CMV plasmid DNA was normalized with the addition of CMV-CD20. Cells were lysed 36 h after transfection in reporter lysis buffer (Promega). Luciferase activity was determined using the luciferase assay system (Promega) and normalized to β-Gal activity. Each data point is the average of three independent transfections, and the error bars indicate 1 standard deviation from the mean.

Mouse embryonic fibroblasts (MEFs), retroviral infections, and myogenic differentiation. Wild-type, $Rb1^{\Delta G/\Delta G}$, and $Rb1^{-/-}$ fibroblasts were derived from E13.5 embryos, and experiments were carried out us-

ing passage 3 to 5 MEFs. Asynchronous cell populations were cultured according to standard methods. Cell culture was carried out in Dulbecco's modified Eagle's medium containing 10% fetal bovine serum (FBS), 2 mM L-glutamine, penicillin (50 U/ml), and streptomycin (50 μg/ml). Growth curves were generated by plating MEFs at low density followed by trypsinization and counting for 5 consecutive days. Cells deprived of serum were cultured for 60 h in medium as described above except with 0.1% FBS. For serum restimulation assays, 10% FBS was added following 60 h of serum deprivation. Gamma irradiation was performed by exposing cells to a cobalt-60 radiation source until a dose of 15 Gy was received.

Retroviral infections of MEFs were undertaken with pBabe-p16 and pBabe-MyoD constructs at passage 3. Infections were performed as described in the work of Pear et al. (29). BOSC or Phoenix-Eco packaging cells were plated at a density of 10 million cells per 15-cm plate on the day before the transfections. On the following day, the cells were transfected with 60 μg of pBabe plasmid or pBabe containing p16 using calcium phosphate, and on the next morning, the medium was replaced. The medium was removed 48 h later, filtered through a 0.45-μm filter, and supplemented with 4 μg/ml of Polybrene. The filtered viral supernatant was placed directly on MEFs that had been plated the previous day at 8×10^5 cells in a 10-cm dish. Fresh medium was added to the transfected packaging cells for another 12 h. After 12 h, the medium from the MEFs was removed and a second round of infection was performed by once again adding the filtered viral supernatant with Polybrene to the MEFs. The viral supernatant was incubated on the MEFs for a further 8 to 12 h and then replaced with medium containing 5 μg/ml of puromycin for 4 days. The infected MEFs were then replated in puromycin-containing medium for subsequent analysis. Myogenic differentiation was carried out using MEFs infected with a pBABE-MyoD-expressing retrovirus and by following the cell culture methods of Novitch et al. (30). Once differentiated, cells were restimulated with 15% serum and labeled with bromodeoxyuridine (BrdU) for 24 h. Cells were fixed and stained for BrdU, myosin heavy chain (MHC), and DNA with 4′,6-diamidino-2-phenylindole (DAPI) and analyzed by fluorescence microscopy. BrdU incorporation in MHC-positive and -negative cells was quantitated as previously reported (31).

Chromatin immunoprecipitation (ChIP) experiments. Asynchronously growing $Rb1^{+/+}$, $Rb1^{\Delta G/\Delta G}$, and $Rb1^{-/-}$ MEFs were washed twice with PBS followed by incubation with 2 mM ethylene glycol bissuccinimidylsuccinate (EGS) diluted in PBS for 1 h with shaking at room temperature (RT). Formaldehyde was then added to a final concentration of 1% and incubated at RT for 15 min. Glycine was then added to a final concentration of 0.125 M to quench the reaction. Cells were washed twice and then collected in PBS. Cell pellets were resuspended in buffer 1 (10 mM HEPES, pH 6.5, 10 mM EDTA, 0.5, EGTA, 0.25% Triton X-100), incubated on ice for 5 min, and pelleted at $600 \times g$ at 4°C. Pellets were then resuspended twice in buffer 2 (10 mM HEPES, pH 6.5, 1 mM EDTA, 0.5, EGTA, 200 mM NaCl), incubated on ice for 5 min, and pelleted at $600 \times g$ at 4°C between each wash. Cells were then suspended in SDS-lysis buffer (1% SDS, 1 mM EDTA, 50 mM Tris-HCl, pH 8.0, and protease inhibitors) and incubated for 15 min on ice followed by 35 min of sonication in a Bioruptor (Diagenode). Seventy-five micrograms of chromatin was diluted 10-fold in dilution buffer (0.01% SDS, 0.4% Triton X-100, 1 mM EDTA, 20 mM Tris, pH 8, 200 mM NaCl, and protease inhibitors) and precleared for 1.5 h with IgG prebound to Dynabeads. IPs were performed at 4°C for 16 h using 5 μg each of the following antibodies mixed together and prebound to Dynabeads: M-153 and C-15 (both from Santa Cruz), Rb 4.1 (Developmental Studies Hybridoma Bank), an affinity-purified sheep antibody raised against amino acids 867 to 881 of mouse pRB, and an affinity-purified rabbit antibody raised against amino acids 847 to 859 of mouse pRB. Beads were then serially washed for 5 min with rotation at 4°C for the following washes: twice in low-salt buffer (0.1% SDS, 1% Triton X-100, 2 mM EDTA, 20 mM Tris-HCl, pH 8, 150 mM NaCl), once in high-salt buffer (0.1% SDS 1% Triton X-100, 2 mM EDTA, 20 mM Tris-HCl, pH 8, 500 mM NaCl), and twice in TE (10 mM Tris-HCl, pH 8, 1 mM EDTA). Protein was eluted with 2 serial

incubations with 150 μl of elution buffer (1% SDS, 0.1 M NaHCO₃) at 65°C for 10 min each. Cross-links were reversed by adding NaCl to a final concentration of 200 mM and incubating the mixture at 65°C for 4 h. RNase was added and incubated at 37°C for 30 min followed by addition of 50 μg/ml protease K and 10 mM EDTA and incubation at 45°C for 1 h. DNA was then isolated using a PCR purification kit (Invitrogen).

Real-time PCR analysis of ChIP. DNA isolated from ChIPs was analyzed using iQ Sybr green Super Mix (Bio-Rad). Primer sets used for analysis were as indicated below, and their locations were chosen based on human pRB ChIP sequencing data previously published by Chicas et al. (32) visualized on the UCSC genome browser. Primers included *Rbl1* TSS Fwd (5′ CTT CGG GGT TTT CTT TTC CCT C 3′), *Rbl1* TSS Rev (5′ TAG AGT CCG AGG TCC ATC TTC TTA T 3′), *Rbl1* Neg Fwd (5′ AGT CGT TTC AGG AAT AGA GAT GGT C 3′), *Rbl1* Neg Rev (5′ TAC CTG GTG CAT CTG AAT GCT ATT A 3′), *Mcm3* TSS Fwd (5′ ATC CAG GAA GTC CAA GTA GTC TCT C 3′), *Mcm3* TSS Rev (5′ TTG AAG TGG TTA GCC AAT CAT AAC G 3′), *PCNA* TSS Fwd (5′ CAG AGT AAG CTG TAC CAA GGA GAC 3′), *PCNA* TSS Rev (5′ CGT TCC TCT TAG AGT AGC TCT CAT C 3′), *PCNA* Neg Fwd (5′ CAT CAG TGA ATA CGT CTC TGT TCC A 3′), *PCNA* Neg Rev (5′ CTG CTT CTC AGT TGT TTT AGG AAG G 3′), glyceraldehyde-3-phosphate dehydrogenase (*GAPDH*) Fwd (5′ GAG CCA GGG ACT CTC CTT TT 3′), and *GAPDH* Rev (5′ CTG CAC CTG CTA CAG TGC TC 3′). Percent inputs were calculated as follows: $2^{-(\text{antibody } C_T - \text{input } C_T)} \times \%$ input used, where C_T is threshold cycle. Values were then normalized to percent input of *GAPDH*.

Cell cycle analysis. Cell cycle analysis of MEFs was performed by pulse-labeling cells with bromodeoxyuridine (BrdU; Amersham Biosciences) for 1.5 h before harvesting cells. The cells were fixed in ethanol and immunostained with anti-BrdU antibodies (BD Biosciences), along with propidium iodide (PI) as reported in the work of Cecchini et al. (25). Cell populations were analyzed by flow cytometry on a Beckman-Coulter Epics XL-MCL instrument, and the relative abundance of each phase was determined. Gates were used to quantitate the proportion of cells with 8N DNA content, and the average forward scatter was determined on G₁-phase cells where indicated.

mRNA quantitation. Total RNA was extracted from cells or minced tissues using TRIzol reagent according to the manufacturer's instructions (Invitrogen). RNA from tissues was isolated using an RNeasy fibrous tissue kit (Invitrogen). Expression levels of the E2F target genes, *Pcna*, *Ccne1* (cyclin E1), *Ccna2* (cyclin A2), *Tyms* (thymidylate synthase), *Mcm3*, and *Rbl1* (p107), were determined using the Quantigene Plex 2.0 reagent system from Affymetrix (Santa Clara, CA) and a BioPlex200 multiplex analysis system. Expression levels were normalized to the expression of actin.

Microarray analysis. Total RNA was extracted from MEFs following serum starvation using TRIzol reagent. RNA was quality controlled using an Agilent 2100 Bioanalyzer before labeling and hybridization onto an Affymetrix mouse 1.0 ST gene array in the London Regional Genomics Centre. Affymetrix.cel files were normalized with robust multiarray averaging (33–35) using BRB-Array Tools (http://linus.nci.nih.gov /BRB-ArrayTools.html). Log ratios of $Rb1^{\Delta G/\Delta G}$ RNA compared with wild type were determined by subtracting the average wild-type log signal value from each replicate of $Rb1^{\Delta G/\Delta G}$. The three log ratios were subjected to hierarchical clustering using Euclidian distance and average linkage using MeV (http://www.tm4.org/mev.html). In the figures, positive log ratios are colored red, and negative ratios are colored green.

Isolation of intestinal villi. Isolation of villi was carried out essentially as described previously (36). Mice were sacrificed by cervical dislocation, and the small intestine was immediately removed, measured, and cut into thirds. The middle section, corresponding roughly to the jejunum, was opened using blunt-end scissors washed 3 times in PBS and placed in 25 ml of PBS supplemented with 1 mM DTT and 5 mM EDTA for 30 min. The intestine was then transferred to a 15-ml tube with 10 ml of Release buffer (PBS, 1 mM DTT) and shaken gently to release intact villi from the intestine. Five sequential fractions were obtained with increasingly more vigorous shaking. To release the intestinal crypts, the intestine was placed

Cecchini et al.

in 25 ml of PBS supplemented with 1 mM DTT and 9 mM EDTA and incubated for 20 min at room temperature. The intestine was then placed once again in a 15-ml tube with 10 ml of release buffer and mixed to release the crypts from the intestines. This was repeated with 5 tubes to sequentially release the crypts from the intestine. During the fractionation process, the release of cells was monitored under a dissecting microscope to quantify the proportion of villi and crypts isolated. Fractions were further enriched for villi by allowing samples to settle and decanting the supernatant, which contains largely crypts. In contrast, crypts were enriched by filtering samples through 100-μm nylon cell strainers (Fisher Scientific). Only samples with significant enrichment were utilized for subsequent analysis.

BrdU staining of intestinal tissue sections. To analyze proliferation, mice were injected with 200 μl of 16-μg/ml BrdU (Sigma) 2 h before sacrifice. Intestines were then isolated, fixed in formalin, embedded in paraffin, and sectioned according to standard protocols. Paraffin was removed, and sections were rehydrated using a series of xylene extractions and ethanol washes. The sections were brought to a boil in sodium citrate buffer and then maintained at 95°C for 10 min. The cooled sections were rinsed in water three times for 5 min each time and then rinsed in PBS for 5 min. The sections were blocked in phosphate-buffered saline (PBS) supplemented with 2.5% horse serum and 0.3% Triton X-100 for 1 h. The sections were incubated with anti-BrdU antibodies (BD Biosciences) in blocking buffer overnight at 4°C and then rinsed in PBS three times for 5 min each time. The slides were incubated with horse anti-mouse immunoglobulin G-fluorescein isothiocyanate (Vector) for 1 h and then rinsed in PBS. The slides were mounted with Vectashield plus 4′,6-diamidino-2-phenylindole (DAPI) (Vector). Fluorescent images were captured on a Zeiss Axioskop 40 microscope and Spot Flex camera and colored using EyeImage software (Empix Imaging, Mississauga, Ontario, Canada) or a similar system.

BrdU staining of embryos. To analyze proliferation in the embryos, pregnant mice at embryonic day 18.5 (E18.5) were injected with 10 μg of BrdU/g of body weight, 2 h before sacrifice. Embryos were collected, fixed in formalin, embedded in paraffin, and sectioned according to standard protocols. Paraffin was removed, and sections were rehydrated using a series of xylene extractions and ethanol washes. The sections were incubated in 2 N HCl at 37°C for 60 min followed by neutralization in 0.1 M Na_2BO_4 two times for 5 min each. Sections were rinsed in PBS twice for 5 min. Endogenous peroxidases were blocked by incubating the sections in 3% H_2O_2 for 20 min followed by washing in PBS twice for 5 min. The sections were blocked in phosphate-buffered saline (PBS) supplemented with 5% horse serum for 1 h at room temperature. The sections were incubated with anti-BrdU antibodies (BD Biosciences) in blocking buffer for 1 h at room temperature and then rinsed in PBS three times for 5 min each. The slides were incubated with biotinylated anti-mouse immunoglobulin (Vector Laboratories) for 1 h and then rinsed in PBS three times for 5 min each. The slides were incubated with streptavidin-horseradish peroxidase (HRP) (Vector Laboratories) for 30 min and then rinsed in PBS before incubation with ImmPACT diaminobenzidine (DAB) substrate (Vector Laboratories). The slides were counterstained with hematoxylin, dehydrated in ethanol, and mounted with Vectamount (Vector Laboratories) for analysis. Microscopic examination and photography of slides were performed as described above.

RESULTS

Characterization of an *Rb1* mutant that is defective for E2F transactivation domain binding. To better understand pRB-dependent functions outside E2F transcriptional control, we sought to develop a gene-targeted mutant mouse line that is deficient for this function. The interaction between pRB and E2F transcription factors is complex (Fig. 1A), as pRB possesses a well-studied mechanism in which it interacts with the C-terminal transactivation domain of E2Fs, but it also forms an alternate interaction with E2F1 that has little effect on canonical E2F transcriptional regula-

tion (13, 21, 22). We set about designing an *Rb1* allele that disrupts only pRB's contact site with the transactivation domain of E2F1, E2F2, E2F3, and E2F4.

We focused on conserved acidic side chains used by E2F1, E2F2, E2F3, and E2F4 to interact with basic residues in the groove formed by the A and B domains of the pRB pocket (Fig. 1B and C). We generated a charge reversal mutant in which R467 and K548 on pRB were changed to glutamate to antagonize E2F binding (21). This mutant was titled ΔG because it disrupts the general interaction that pRB makes with the E2F transactivation domain (13, 21). To determine the severity of this mutation, we utilized electrophoretic mobility shift assays to quantitate the defect in pRB-E2F interactions. HA-tagged E2F1, E2F2, E2F3, and E2F4 were produced by transfection and mixed with a ^{32}P-labeled double-stranded oligonucleotide containing an E2F binding site. E2F binding was then tested by titrating increasing amounts of GST-RBLP proteins, a domain that contains both E2F binding sites. Figure 1D demonstrates analysis for HA-E2F2 and reveals the inability of the GST-ΔG-RBLP protein to form a complex with HA-E2F2 on DNA. The percentage of HA-E2F2 bound to wild-type or mutant GST-RBLP was determined for each lane of the gel and was plotted in Fig. 1E. From these data, we determined half-maximal binding quantities for GST-RBLP and the ΔG mutant for each of E2F1, E2F2, E2F3, and E2F4 (Fig. 1F). This indicates that the ΔG substitutions have a strong effect on E2F binding, as the interactions with E2F2, E2F3, and E2F4 are nearly undetectable. As stated above, E2F1 has the ability to form an alternate complex with pRB that is reported to have reduced binding to the E2F sequence element in this probe (13). For this reason, E2F1's apparent affinity for GST-RBLP is lower and is relatively unaffected by the ΔG mutations (Fig. 1F).

In order to assess the effects of ΔG-pRB on E2F transcriptional control, we transfected cells with CMV-RB expression vectors and a p107-luciferase reporter (Fig. 1G). This experiment demonstrates that ΔG-pRB is unable to repress transcription of this reporter when relying on endogenous E2Fs. In addition, we have also tested the ability of ΔG-pRB to block transcriptional activation of an E2F-responsive reporter when individual E2Fs are overexpressed. As shown in Fig. 2A, wild-type pRB is capable of repressing transcription by each of E2F1, E2F2, or E2F3. Conversely, ΔG-pRB has a similar defect in controlling each E2F, even though it is still capable of binding E2F1 in interaction assays. These results are consistent with previous reports that demonstrate that the pRB-E2F1 complex formed through their alternate interaction is a poor regulator of cell cycle E2F transcriptional targets (13, 21, 22). Importantly, regulation of a TA-p73 reporter, a uniquely E2F1-responsive proapoptotic target gene (16), is similar between wild type and ΔG-pRB (Fig. 2B). Taken together with the *in vitro* binding assays above, the ΔG substitutions dramatically reduce the affinity of pRB for the E2F transactivation domain and prevent transcriptional repression of canonical E2F-responsive genes, even when overexpressed.

Introduction of an E2F-binding-deficient allele of *Rb1* into the endogenous murine locus. Our next goal was to introduce the R467E and K548E substitutions (R461E and K542E in murine numbering) into the *Rb1* gene and create an endogenous *Rb1*^{ΔG} mutant. Figure 3A contains a diagram of the *Rb1* locus, the targeting vector used to introduce the ΔG mutations, along with relevant restriction enzyme cut sites that were used to map homologous recombination. Southern blotting assays were performed
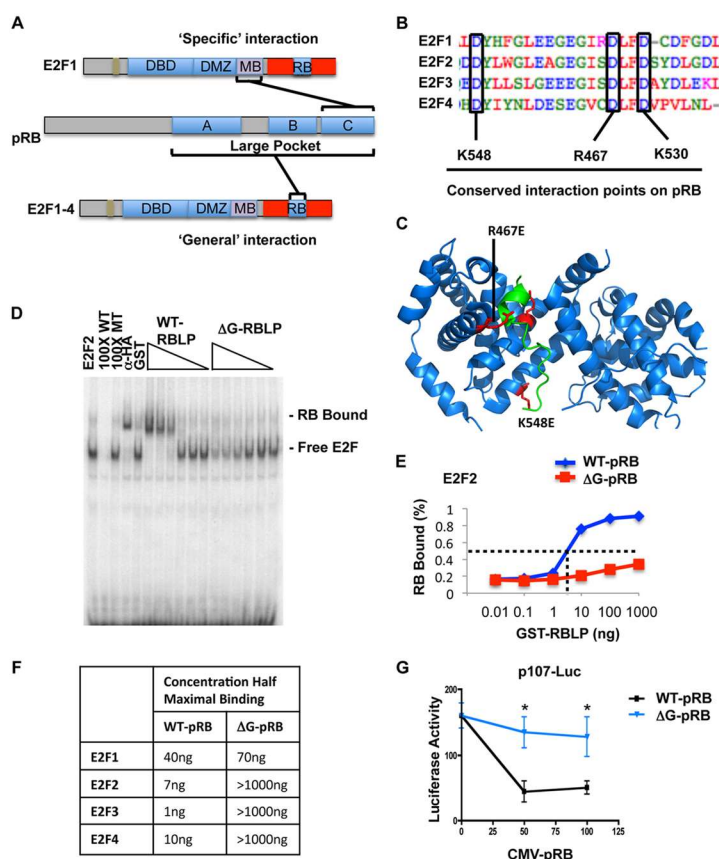
FIG 1 Characterization of an RB mutant that is defective for binding the E2F transactivation domain. (A) The domain structures of pRB and E2F proteins are depicted. Mapped interaction sites for the different classes of E2F interaction are shown. DBD, DNA binding domain; DMZ, dimerization (with DP) domain; MB, marked box domain. The E2F transactivation domain is shown in red, and the minimal RB interaction site within it is indicated. (B) Sequence alignment of the pRB binding region of E2F1, E2F2, E2F3, and E2F4 created using ClustalW. Three conserved aspartate residues in E2Fs make contacts with distinct basic amino acids on pRB. Codon positions use human numbering. (C) Locations of basic amino acids that were mutagenized to disrupt E2F binding are shown in red in a crystal structure of the small pocket of pRB (PDB entry 1O9K) (63). RB is shown in blue, and an E2F1-derived peptide is shown in green. (D) Electrophoretic mobility shift assays utilizing extracts expressing HA-E2F2 and HA-DP1 were combined with a radiolabeled probe containing a canonical E2F binding site. Migration positions for free E2F bound to the probe and E2Fs bound to GST-RBLP proteins are shown on the right of the gel. 100× WT and 100× MT denote samples with excess cold oligonucleotide. The α-HA lane denotes the addition of the 12CA5 antibody recognizing the HA epitope on the exogenous E2F/DP proteins. The GST lane contains 1 µg of GST as a negative control, and the remaining 12 lanes consist of a 10-fold dilution series of recombinant GST-WT-RBLP and ΔG-RBLP (R467E and K548E) from 1 µg to 10 pg. (E) To compare the affinities of WT and ΔG for each E2F, the proportion of RB bound relative to residual free E2F was determined for each quantity of GST-RBLP used. A graph of percent RB bound versus GST-RBLP quantity is shown for E2F2. (F) The table shows the half-maximal binding quantity for WT-RBLP and ΔG-RBLP in EMSAs for each of E2F1, E2F2, E2F3, and E2F4. (G) Increasing amounts of CMV-RB expression vector were cotransfected along with a constant level of a p107(promoter)-luciferase reporter construct in Saos-2 cells. Extracts were prepared to assess relative luciferase activity and determine transcriptional repression by the overexpressed ΔG-pRB mutant. Error bars indicate 1 standard deviation from the mean (n = 3). An asterisk indicates a statistically significant difference from E2F/DP1 transfection alone (t test, P < 0.05).

using 5′ and 3′ external probes, as well as the neomycin resistance gene, for two candidate clones (Fig. 3B). The smaller KpnI fragments found in both targeted clones are indicative of homologous recombination at both ends of the targeting vector. The single band in the MscI-digested, Neo^r gene-probed lane indicated that

the targeting vector was integrated only once. These clones were expanded and used to produce chimeric male mice that were bred to B6; FvB *EIIa-cre* transgenic animals to establish germ line transmission, excise the selectable marker, and create the gene structure shown at the bottom of Fig. 3A. Success in creating the *Rb1*^ΔG
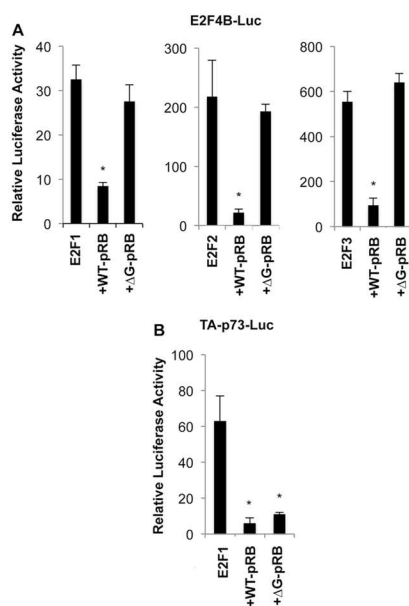
FIG 2 Regulation of E2F transcriptional activity by ΔG-pRB. (A) The E2F4B-luciferase construct containing four tandem E2F recognition sites was cotransfected with E2F1/DP1, E2F2/DP1, or E2F3/DP1. Where indicated, wild-type pRB or ΔG-pRB was transfected to assess the ability of each to regulate E2F. (B) A reporter construct containing the TA-p73 promoter was transfected with E2F1/DP1 and the indicated pRB expression vectors to assess regulation of E2F1. Error bars indicate 1 standard deviation from the mean ($n = 3$). An asterisk indicates a statistically significant difference from E2F/DP1 transfection alone (t test, $P < 0.05$).

allele was assessed by breeding to homozygosity and sequencing exons 15 and 17 (Fig. 3C), which demonstrated that the relevant codons were successfully changed to encode glutamate. Furthermore, GST-E7 and GST-E1A pulldowns from $Rb1^{+/+}$ and $Rb1^{\Delta G/\Delta G}$ fibroblasts were used to confirm that ΔG-pRB in these extracts was capable of binding to viral oncoproteins (Fig. 3D). Lastly, we examined ΔG-pRB expression by Western blotting in comparison with wild-type and knockout MEFs (Fig. 3E). This revealed a slight increase in ΔG-pRB expression relative to the wild-type control. Taken together, these experiments reveal that the $Rb1^{\Delta G}$ allele stably expresses pRB and that ΔG-pRB is capable of binding viral proteins through its pocket domain, suggesting that it is correctly folded.

The properties of ΔG-pRB were investigated further in $Rb1^{\Delta G/\Delta G}$ cells by immunoprecipitation and Western blotting (Fig. 4A). Anti-pRB precipitates were blotted for E2F1, E2F2, E2F3, and E2F4, and in this analysis, E2F2, E2F3, and E2F4 levels were greatly reduced but E2F1 levels were considerably increased (Fig. 4A). This suggests that E2F1's interaction with pRB at its alternative interaction site may be competitive with pRB interactions with E2Fs through the general interaction site that we disrupted by mutation. Because the specific pRB-E2F1 complex pre-

fers to bind to sequences such as those in the TA-p73 promoter and not the consensus E2F sites found in cell cycle genes, we used DNA binding specificity to identify the type of pRB-E2F1 complexes present in $Rb1^{\Delta G/\Delta G}$ extracts. To investigate the configuration of pRB-E2F1 complexes that form in $Rb1^{\Delta G/\Delta G}$ cells, we took advantage of the fact that the pRB-E2F1 specific interaction has low affinity for consensus E2F binding elements by EMSA (Fig. 4B). This analysis revealed that pRB-E2F complexes can readily be detected in wild-type extracts using an antibody supershift for pRB (Fig. 4B; compare lanes 3 and 4). However, the presence of other E2F-containing complexes that migrate to the same position obscures this complex, and they can be shifted by adding anti-Cdk2 antibodies (Fig. 4B; compare lanes 3 and 5). Gel shifts of $Rb1^{\Delta G/\Delta G}$ extracts demonstrate that pRB-E2F complexes are undetectable, even when anti-Cdk2 antibodies are used to shift other complexes away from this position in the gel (Fig. 4B; compare lanes 6 and 12). Based on this analysis, pRB-E2F complexes that are competent to repress cell cycle target genes appear to be absent in $Rb1^{\Delta G/\Delta G}$ cells.

Given the importance of disrupting endogenous pRB-E2F complexes in the interpretation of phenotypes in $Rb1^{\Delta G/\Delta G}$ mice, we also investigated this question by chromatin immunoprecipitation (ChIP). The presence of pRB-E2F complexes was quantitatively assessed by ChIP in which pRB was precipitated, and known E2F-responsive promoter regions were PCR amplified. ChIP sequence tracks for human pRB (32), at three E2F target genes that were used as a guide to design positive- and negative-control PCR amplicons to determine if ΔG-pRB can associate with these promoters (Fig. 4C, top). This experiment demonstrates that PCR amplification of sequences within the peak of pRB occupancy can readily detect wild-type pRB at these promoters, whereas it is reduced or missing at the negative-control location (Fig. 4C, bottom; compare black bars). PCR amplification of ΔG-pRB precipitates demonstrates that occupancies are similar between the peak and negative-control amplicons (Fig. 4C, bottom; compare gray bars), and these are generally equivalent to background levels defined by ChIP from $Rb1^{-/-}$ cells (Fig. 4C, bottom; compare white bars).

The characterization of pRB from $Rb1^{\Delta G/\Delta G}$ cells reveals that it has a specific defect in E2F interactions. Presumably because pRB can autoregulate itself through repression of E2F transcription factors (37), pRB is mildly increased in $Rb1^{\Delta G/\Delta G}$ cells. Despite its overexpression, and increased association with E2F1, pRB-E2F complexes that are capable of interaction with cell cycle E2F promoter elements are undetectable in $Rb1^{\Delta G/\Delta G}$ MEFs.

Normal cell cycle progression in asynchronous $Rb1^{\Delta G/\Delta G}$ MEFs. Given the biochemical defect in pRB-E2F interactions described above, we sought to understand the functional consequences of this defect in transcriptional and cell cycle control. Asynchronously proliferating MEFs were pulse-labeled with BrdU and processed for flow cytometry to examine cell cycle phases in $Rb1^{\Delta G/\Delta G}$ cells. As shown in Fig. 5A, $Rb1^{\Delta G/\Delta G}$ MEFs have a cell cycle phase distribution very similar to that of the wild type, and this is clearly different from $Rb1^{-/-}$ cells that are characterized by lower G_1, higher S-phase, and higher G_2/M levels (38). We also carried out growth curves to see if the proliferation rate of $Rb1^{\Delta G/\Delta G}$ cells differs from those of knockout or wild-type controls. As shown in Fig. 5B, the quantity of cells increased similarly between genotypes over a 5-day period, suggesting that proliferation rates were similar across all genotypes. It is known that
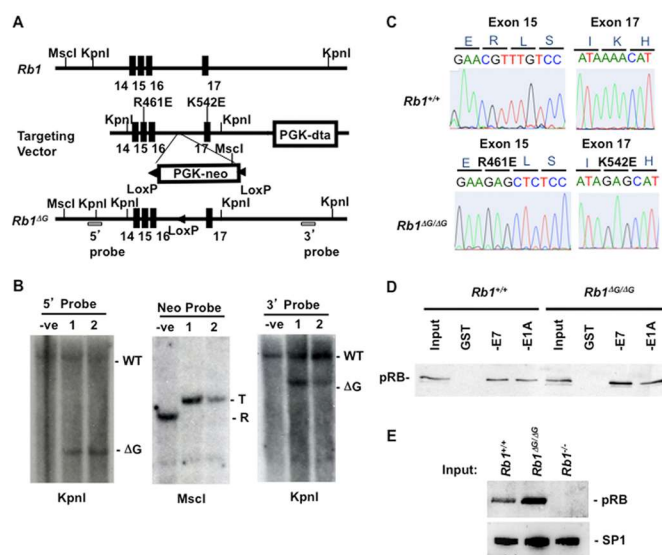
FIG 3 Gene targeting of the murine $Rb1^{\Delta G}$ allele. (A) The region of the $Rb1$ gene targeted in this study is shown on top. The locations of exons are indicated by black rectangles, and relevant KpnI locations are shown. The targeting vector is shown in the middle with the locations of selectable markers (and additional KpnI and MscI cut sites), as well as newly introduced restriction sites and the mutations in exons 15 and 17 (amino acid positions are described using murine numbering). The bottom diagram shows the $Rb1^{\Delta G}$ allele after homologous recombination and removal of the PGK-Neo cassette by breeding to $EIIa$-cre transgenic mice. The locations of 5′ and 3′ probes used in Southern blotting are shown. (B) Genomic DNA from two candidate clones was digested with the indicated restriction enzymes and analyzed by Southern blotting to demonstrate homologous recombination and single integration. T, targeted; R, random integration. (C) DNA was extracted from $Rb1^{\Delta G/\Delta G}$ embryos, and exons 15 and 17 were PCR amplified and sequenced. Electropherograms of the relevant regions are shown for wild type and $Rb1^{\Delta G/\Delta G}$ (using murine codon numbering). (D) Extracts were prepared from wild-type and $Rb1^{\Delta G/\Delta G}$ MEFs, and GST, GST-E7, or GST-E1A was added to precipitate pRB. The amount of precipitated pRB was determined by Western blotting. (E) Nuclear extracts from cells of the indicated genotypes were analyzed by SDS-PAGE and Western blotting for pRB and SP1.

$Rb1^{-/-}$ MEFs enter S phase prematurely under these growth conditions, and this is detectable by smaller cell size in G_1 (38). Figure 5C demonstrates that the average forward scatter size measurements are similar between wild-type and $Rb1^{\Delta G/\Delta G}$ cells but statistically different from that of $Rb1^{-/-}$ cells. Taken together with cell cycle phase proportions in Fig. 5A and similar proliferative rates in Fig. 5B, this suggests that cell cycle phase lengths, particularly G_1, are unchanged between wild-type and $Rb1^{\Delta G/\Delta G}$ MEFs. Lastly, we also quantitated 8N cells between these genotypes of MEFs as a surrogate marker for endoreduplication. Again, $Rb1^{\Delta G/\Delta G}$ fibroblasts are similar to those of the wild type, whereas $Rb1^{-/-}$ cells have elevated levels of 8N cells (Fig. 5D). Taken together, these analyses demonstrate the surprising finding that impairing E2F transcriptional repression by pRB has little effect on cell cycle progression.

Discrete defects in E2F transcriptional control in $Rb1^{\Delta G/\Delta G}$ fibroblasts in cell cycle arrest. The retinoblastoma protein is perhaps best known for its role in mediating negative growth signals and arresting the cell cycle (39). For this reason, we investigated a number of cell cycle exit scenarios to determine the effects of the $Rb1^{\Delta G/\Delta G}$ genotype on proliferative control. In response to serum deprivation for 60 h, we discovered that known E2F transcriptional targets of pRB fail to be repressed in $Rb1^{\Delta G/\Delta G}$ cells compared to wild-type levels (Fig. 6A). Similar levels of gene expres-

sion were found in $Rb1^{-/-}$ cells following the same treatment. In addition, we also utilized BrdU labeling and flow cytometry to investigate proliferative control at the same time point following serum withdrawal, and this revealed that $Rb1^{\Delta G/\Delta G}$ fibroblasts respond equivalently to the wild type in their ability to exit the cell cycle (Fig. 6B). Conversely, $Rb1^{-/-}$ cells are defective for cell cycle withdrawal under these conditions (Fig. 6B). Since this cell cycle exit scenario reveals an instance in which $Rb1^{\Delta G/\Delta G}$ cells resemble a wild-type cell cycle arrest, we further investigated E2F regulation under these conditions. Expression levels of known E2F target genes were compared between wild-type, $Rb1^{\Delta G/\Delta G}$, and $Rb1^{-/-}$ cells by microarray (Fig. 6C). Log$_2$ ratios were generated comparing $Rb1^{\Delta G/\Delta G}$ expression levels relative to that of the wild type, as well as ratios of $Rb1^{-/-}$ expression levels to that of the wild type. Gene expression changes are clustered based on similarity, and this reveals that $Rb1^{\Delta G/\Delta G}$ cells are mostly defective in repressing E2F targets that function in DNA replication (Fig. 6C). Interestingly, this class of E2F target genes is known to be direct regulatory targets of pRB in senescence (32). Not surprisingly, since $Rb1^{-/-}$ cells fail to arrest under these serum deprivation conditions, most E2F targets display increased expression relative to the wild type in this microarray experiment (Fig. 6C). The implication of these experiments is that ΔG-pRB may have the ability to arrest the cell cycle independently of E2F repression at cell cycle genes.

Cecchini et al.
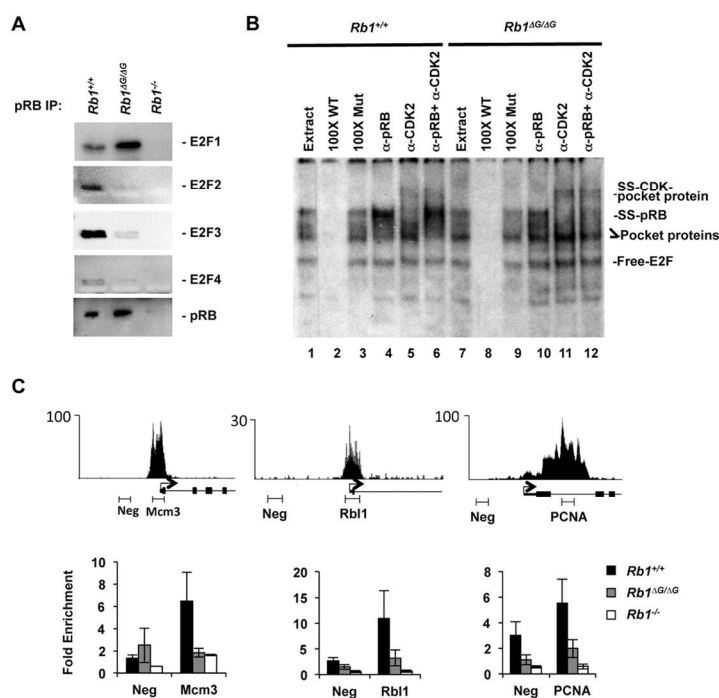
FIG 4 Loss of ΔG-pRB binding at E2F-responsive promoters. MEFs were induced to exit the cell cycle by serum withdrawal, and pRB's interaction with E2Fs was investigated. (A) Anti-pRB antibodies were used to precipitate pRB, and associated E2F transcription factors were detected by Western blotting. (B) EMSAs were performed to compare the abundance of all pRB-E2F-containing complexes in $Rb1^{+/+}$ and $Rb1^{\Delta G/\Delta G}$ nuclear extracts. The migration positions of free E2F, E2Fs bound to RB family proteins (labeled as pocket protein), antibody-supershifted pRB-E2F complexes (SS-pRB), and antibody-supershifted complexes containing p107/p130–E2F-cyclin-CDK (SS-CDK-pocket protein) are all indicated to the right. Cold competitor probes (100× WT and 100× Mut), as well as the antibodies used to shift complexes, are listed on top. (C) Sequence read peaks from ChIP sequence analysis of human pRB are shown for $Mcm3$, $Rbl1$, and $Pcna$ on top. The locations of negative-control and proximal promoter PCR amplicons used in this study are shown along with the transcriptional start site and exons. ChIP quantitative PCR analysis was undertaken for pRB at the indicated promoters. All ChIP enrichment values are scaled relative to a neutral genome location, the $GAPDH$ promoter. Error bars indicate the standard errors.

Much of our knowledge of pRB-E2F control of transcription and their response to cyclin/CDK regulation comes from serum starvation and restimulation experiments. Under these circumstances, $Rb1^{-/-}$ and $p107^{-/-}$; $p130^{-/-}$ double-knockout cells display accelerated progression through G_1 and premature expression of E2F target genes (38, 40). We subjected wild-type, $Rb1^{\Delta G/\Delta G}$, and $Rb1^{-/-}$ cells to serum stimulation and monitored their progress through G_1 and into S phase by BrdU labeling and flow cytometry analysis. This experiment revealed that $Rb1^{\Delta G/\Delta G}$ cells progress rapidly through G_1 in response to serum, and they reach peak BrdU incorporation at the same time as $Rb1^{-/-}$ cells. In this respect, $Rb1^{\Delta G/\Delta G}$ MEFs very much resemble knockout cells, and this suggests a context where pRB-dependent repression of E2F transcription is key to regulating cell cycle progression.

In addition to serum withdrawal, we also tested if ΔG-pRB could be activated through inhibition of cyclin D-associated kinases and gamma irradiation as a means to assess if it could arrest the cell cycle in response to these signals. Ectopic expression of p16Ink4a in proliferating wild-type, $Rb1^{\Delta G/\Delta G}$, and $Rb1^{-/-}$ cells was used to induce a G_1 arrest, and BrdU labeling and flow cytometry were used to measure DNA replication 3 days later (Fig. 7A). These data demonstrate that $Rb1^{\Delta G/\Delta G}$ cells exhibit a reduction in BrdU incorporation similar to that of the wild type, whereas $Rb1^{-/-}$ MEFs continue to proliferate. At the same time point that these cultures were analyzed for cell cycle progression, we also extracted RNA and measured relative expression levels of E2F target genes. These experiments reveal a modest but similar reduction in E2F target gene expression in $Rb1^{+/+}$ and $Rb1^{\Delta G/\Delta G}$ MEFs (Fig. 7B). Surprisingly, a similar reduction in expression was observed for $Ccne1$ and $Tyms$ in $Rb1^{-/-}$ cells (Fig. 7B). We also carried out PI-BrdU analysis and E2F gene expression profiling of $Rb1$ wild-type, mutant, and knockout MEFs in response to gamma irradiation (Fig. 7C and D). These experiments again revealed that $Rb1^{\Delta G/\Delta G}$ cells were fully capable of arresting proliferation in response to DNA breaks. Furthermore, investigation of
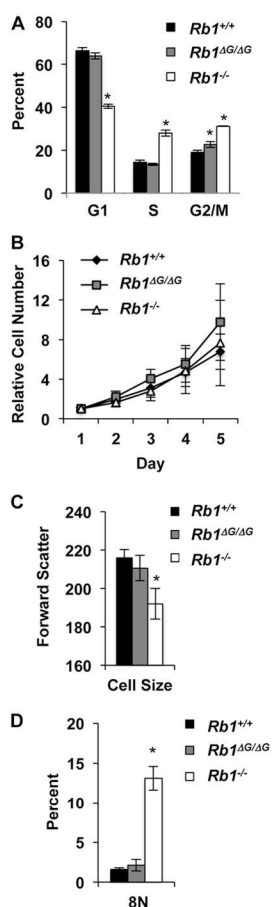
FIG 5 Normal cell cycle progression in asynchronous $Rb1^{\Delta G/\Delta G}$ MEFs. (A) Asynchronously proliferating cell cultures were pulse-labeled and stained for BrdU incorporation along with total DNA using propidium iodide. The proportion of cells in each respective cell cycle phase was determined by flow cytometry. (B) Growth curve for $Rb1^{+/+}$, $Rb1^{\Delta G/\Delta G}$, and $Rb1^{-/-}$ cells over a 5-day period of proliferation. (C and D) Mean forward scatter (C) and 8N DNA content (D) from cultures of asynchronously grown $Rb1^{+/+}$, $Rb1^{\Delta G/\Delta G}$, and $Rb1^{-/-}$ cells. Error bars indicate 1 standard deviation from the mean (n = 3). An asterisk represents a statistically significant difference from the wild-type control (t test, $P < 0.05$).

E2F target gene expression again revealed that expression in $Rb1^{\Delta G/\Delta G}$ cells was reduced as much as it was in the wild type, and $Rb1^{-/-}$ cells also reduced expression of E2F targets even though they did not arrest.

In summary, $Rb1^{\Delta G/\Delta G}$ MEFs undertake relatively normal progression through the cell cycle during asynchronous proliferation. In response to serum deprivation, ectopic p16 expression, and

gamma irradiation, $Rb1^{\Delta G/\Delta G}$ cells again display wild-type levels of cell cycle arrest activity. Importantly, $Rb1^{\Delta G/\Delta G}$ cells exhibit an acceleration through G_1 in response to serum stimulation that very much resembles the defect found in $Rb1^{-/-}$ cells. From this perspective, $Rb1^{\Delta G/\Delta G}$ MEFs have defects in cell cycle control that are consistent with restraining cell cycle entry rather than facilitating cell cycle exit. During some situations of cell cycle arrest, E2F target gene expression in wild-type, $Rb1^{\Delta G/\Delta G}$, and $Rb1^{-/-}$ cells was decreased. While this was surprising, it should be noted that p107 and p130 are also capable of repressing E2F target genes and that these pocket proteins would be expected to be dephosphorylated and active in cells that successfully arrest cell cycle progression. The implications of these experiments for linking E2F transcriptional control and cell cycle progression will be discussed later.

Cell cycle control in development and homeostasis of $Rb1^{\Delta G/\Delta G}$ mice. In addition to the cell cycle defects observed in $Rb1^{-/-}$ fibroblasts, $Rb1$ knockout mice also have defects in development that lead to embryonic lethality beginning at 13.5 days of gestation (E13.5) (41–43). We investigated $Rb1^{\Delta G/\Delta G}$ mutants to characterize the role of E2F transcriptional repression in these developmental contexts. Live $Rb1^{\Delta G/\Delta G}$ mice were obtained and are indistinguishable from wild-type littermates on a gross anatomical level (Fig. 8A and B). We also examined embryos at distinct developmental stages, and newborns, to characterize the viability of $Rb1^{\Delta G/\Delta G}$ mice. As shown in Table 1, $Rb1^{\Delta G/\Delta G}$ embryos were obtained at the expected Mendelian ratios up until birth. After birth, approximately half of the $Rb1^{\Delta G/\Delta G}$ animals die. Based on these observations, we focused our investigation at E18.5 to search for developmental defects. Figure 8C shows hematoxylin and eosin (H&E) staining as well as BrdU immunohistochemistry on sections from a number of major organs and tissues. We observed that approximately half of the $Rb1^{\Delta G/\Delta G}$ animals display an atrophy phenotype in their skeletal muscle without accompanying increases in proliferation (Fig. 8C and D). Most notably, we observed this phenotype in the diaphragm, which may explain newborns that were observed struggling to breathe. Analysis of dying and surviving newborns at postnatal day 0.5 (P0.5) revealed that defective skeletal muscle correlates with poor survival (Fig. 9A). This prompted us to investigate muscle development in $Rb1^{\Delta G/\Delta G}$ mice and cells. We isolated RNA from skeletal muscle and analyzed E2F target gene expression. As shown in Fig. 9B, there were few differences between wild-type muscle, histologically normal muscle from $Rb1^{\Delta G/\Delta G}$ mice, and atrophied muscle from $Rb1^{\Delta G/\Delta G}$ animals. This further suggests that the muscle defects observed in some $Rb1^{\Delta G/\Delta G}$ mice were not caused by aberrant proliferation or loss of transcription of these E2F cell cycle target genes. However, to investigate the question of cell cycle exit in $Rb1^{\Delta G/\Delta G}$ muscle development in a separate context where we can better detect proliferation, we generated myotubes in culture. Interestingly, differentiation of wild-type, $Rb1^{\Delta G/\Delta G}$, or $Rb1^{-/-}$ MEFs into myotubes, followed by restimulation with serum, indicated that only the $Rb1^{-/-}$ controls can be induced to incorporate BrdU (Fig. 9C and D). This suggests that muscle defects in $Rb1^{\Delta G/\Delta G}$ cells are very unlikely to be caused by cell cycle arrest deficiency, and our gene expression profiling suggests that E2F target gene expression levels do not correlate with this phenotype.

In addition to the developmental stage where some $Rb1^{\Delta G/\Delta G}$ animals fail to survive, we also searched for examples of defective proliferative control and E2F gene derepression in adult mice.

Cecchini et al.
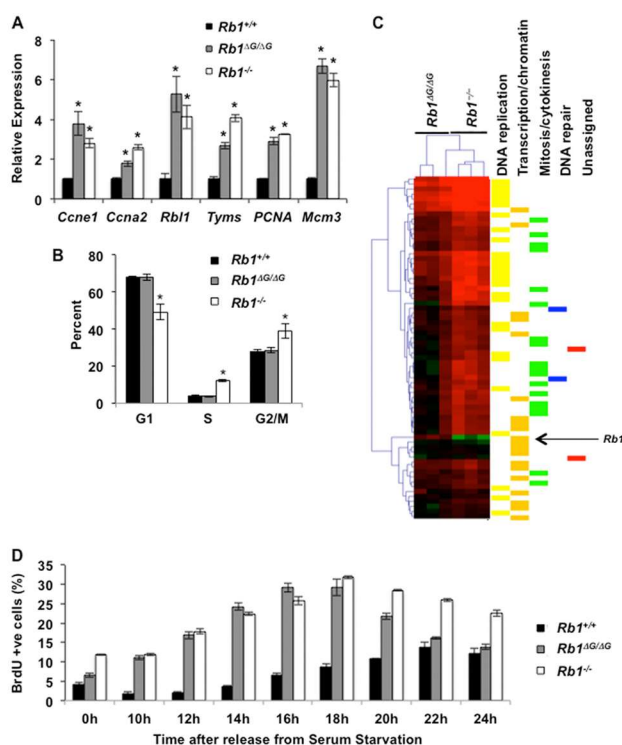
FIG 6 Discrete defects in E2F transcriptional control in $Rb1^{\Delta G/\Delta G}$ MEFs. (A) The relative expression levels of six pRB-regulated E2F cell cycle target genes are shown. Each transcript was quantified from serum-starved $Rb1^{+/+}$, $Rb1^{\Delta G/\Delta G}$, and $Rb1^{-/-}$ fibroblasts with the relative level of message present in wild type scaled to 1. (B) Serum-starved cell cultures were pulse-labeled and stained for BrdU incorporation along with total DNA using propidium iodide. The proportion of cells in each respective cell cycle phase was determined by flow cytometry. (C) Microarray analysis was performed on serum-starved $Rb1^{+/+}$, $Rb1^{\Delta G/\Delta G}$, and $Rb1^{-/-}$ cells, and E2F target gene expression is shown. Log ratios of expression of $Rb1^{\Delta G/\Delta G}$ or $Rb1^{-/-}$ relative to that of wild-type control are shown as a heat map, and genes were clustered based on similarity of expression. The genotypes of each lane are shown above. Categories of E2F target genes are shown to the right. (D) Serum-starved cells of the indicated genotypes were stimulated to reenter the cell cycle with 10% FBS. $Rb1^{+/+}$, $Rb1^{\Delta G/\Delta G}$, and $Rb1^{-/-}$ cells were pulse-labeled with BrdU and harvested at the indicated time points. All graphs represent at least 3 individual experiments, and error bars indicate 1 standard deviation from the mean. An asterisk represents a statistically significant difference from the wild-type control (t test, $P < 0.05$).

Previously, we have demonstrated that transforming factor β (TGF-β)-induced arrest of mammary epithelium requires E2F repression (44). Accordingly, we investigated the histology of mammary ductal epithelium and determined its state in 6- to 8-week-old females (Fig. 10A and B). Mutant ducts were hyperplastic, as characterized by additional layers of epithelium, and these were more frequent in $Rb1^{\Delta G/\Delta G}$ females than in controls (Fig. 10B). From this perspective, loss of E2F repression by ΔG-pRB leads to excessive proliferation but does not compromise the ability of $Rb1^{\Delta G/\Delta G}$ females to nurse their pups. Interestingly, numerous other tissues display normal histology with little evidence of hyperplasia. Figures 10C, E, and G show normal histology of $Rb1^{\Delta G/\Delta G}$ lungs, cardiac muscle, and brain, respectively. We have also examined skeletal muscle, kidney, liver, and intestines with similar results (Fig. 10I and data not shown). Measurement of pRB-E2F target transcript levels revealed that upregulation of at

least some of these genes is detectable in these tissues (Fig. 10D, F, and H). We also investigated cell cycle arrest and E2F target gene expression in columnar epithelial cells from the surface of intestinal villi, as they are known to require pRB function for cell cycle arrest. Unlike most other tissue isolates that are a mix of cell types, they can be isolated to allow gene expression to be assessed specifically within this cell type (45). $Rb1^{\Delta G/\Delta G}$ intestinal epithelium retained normal tissue structure, characterized by a single layer of polarized epithelial cells (Fig. 10I), despite derepression of E2F transcriptional targets in these cells (Fig. 10J). BrdU labeling and staining of intestines further revealed that DNA synthesis was absent in epithelial cells of $Rb1^{\Delta G/\Delta G}$ and wild-type villi, but conditional deletion of $Rb1$ resulted in BrdU labeling of more than 10% of epithelial cells (Fig. 10K and L).

Taken together, results of histological analysis of developing $Rb1^{\Delta G/\Delta G}$ mice demonstrate that loss of E2F repression by ΔG-
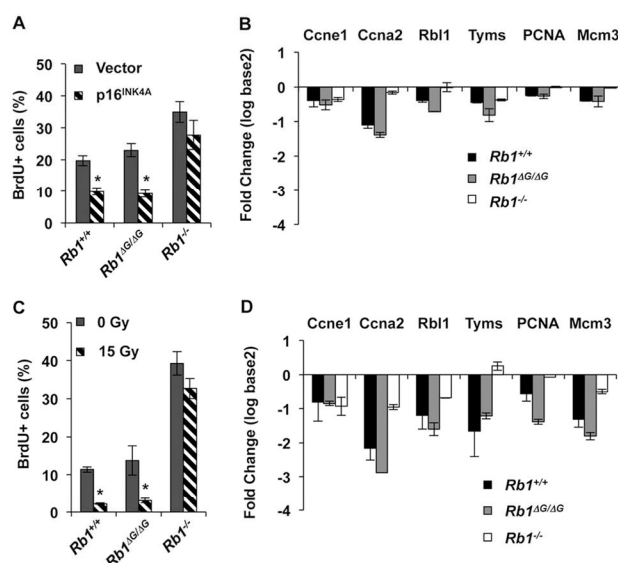
FIG 7 $Rb1^{\Delta G/\Delta G}$ MEFs are able to exit the cell cycle in response to p16 expression or DNA damage. (A) Fibroblast cells of the indicated genotypes were transduced with control or p16^{INK4A}-expressing retroviruses. Following drug selection, cells were pulse-labeled with BrdU and the percentage of positive cells was determined by flow cytometry. All graphs represent at least 3 individual experiments, and error bars indicate 1 standard deviation from the mean. An asterisk represents a statistically significant difference from the wild-type control (t test, $P < 0.05$). (B) Expression of E2F target genes was measured at the same time point as was BrdU labeling in panel A. Fold repression of six pRB-dependent E2F cell cycle target genes is shown for $Rb1^{+/+}$, $Rb1^{\Delta G/\Delta G}$, and $Rb1^{-/-}$ cells. Measurements are expressed as a log$_2$ ratio of p16-expressing cells over empty vector for each respective gene target and genotype of cells. All graphs represent at least 3 individual experiments, and error bars indicate 1 standard deviation from the mean. (C) Fibroblast cells of the indicated genotypes were treated with 15 Gy of radiation or allowed to grow asynchronously. Forty-eight hours following exposure, cells were pulse-labeled with BrdU and the percentage of positive cells was determined by flow cytometry. Statistical analysis is as reported for panel A. (D) Following irradiation, the expression of E2F target genes was measured in $Rb1^{+/+}$, $Rb1^{\Delta G/\Delta G}$, and $Rb1^{-/-}$ cells. Gene expression measurements were made as in panel B.

pRB is largely tolerated during developmental proliferative control events. Most tissues tested demonstrate derepression of some E2F targets with few examples of hyperplasia, and the strongest developmental phenotype, partially penetrant muscle atrophy, appears not to be proliferation related.

$Rb1^{\Delta G/\Delta G}$ mice do not develop spontaneous tumors. Possession of one null allele of $Rb1$ predisposes mice to develop pituitary tumors within the first year of life (46, 47). Chimeric mice containing $Rb1^{-/-}$ cells, or conditionally deleted for $Rb1$ in the pituitary, succumb to pituitary tumors in the first 4 months of life (48, 49). Consequently, we followed a cohort of wild-type and $Rb1^{\Delta G/\Delta G}$ mice to investigate the incidence of spontaneous tumor formation in these animals (Fig. 11A). Wild-type and $Rb1^{\Delta G/\Delta G}$ animals were tumor free beyond 1.5 years of life; in contrast, $Rb1^{+/-}$ control mice developed pituitary tumors with a mean survival of 400 days. This suggests that loss of E2F repression by pRB alone is not sufficient to predispose these mice to cancer.

While $Rb1^{\Delta G/\Delta G}$ mutants did not succumb to pituitary or other cancers, we searched for evidence of neoplastic lesions in these mice (Fig. 11B). Pituitary adenocarcinomas are known to be slowly progressing tumors, so we searched for evidence of hyperplasia in 8- to 11-month-old animals, as well as in aged $Rb1^{\Delta G/\Delta G}$ mice. However, gross morphology of $Rb1^{\Delta G/\Delta G}$ pituitaries was indistinguishable from

that of wild-type controls (Fig. 11B). Furthermore, H&E staining of pituitaries failed to reveal aberrant proliferation even in aged $Rb1^{\Delta G/\Delta G}$ mutants (Fig. 11C). Lastly, it has been demonstrated that pituitary tumorigenesis can be suppressed in $Rb1^{+/-}$ mice if the intermediate lobe fails to properly develop (50). We note that the intermediate lobe is present in $Rb1^{\Delta G/\Delta G}$ animals and shows normal histology (Fig. 11C, marked by "I").

Throughout this report, we have provided evidence that pRB's specific interaction with E2F1 represents a separate biochemical function that is not related to the control of cell cycle E2F target genes. However, we decided to challenge this interpretation by crossing $Rb1^{\Delta G/\Delta G}$ mutants with $E2f1^{-/-}$ mice to see if compound mutant mice or cells have more severe phenotypes that do $Rb1^{\Delta G/\Delta G}$ mice alone. We found that compound mutant mice displayed a reduction in survival similar to that of $Rb1^{\Delta G/\Delta G}$ mutants based on the genotype of P14 pups (Fig. 12A and Table 1). In addition, preparation of compound mutant fibroblasts and subjection of them to serum withdrawal growth arrest failed to reveal a defect in this cell cycle exit paradigm (Fig. 12B). Lastly, we followed small cohorts of $E2f1^{-/-}$ and $Rb1^{\Delta G/\Delta G}$; $E2f1^{-/-}$ mice over a 450-day period and failed to observe spontaneous tumor formation in compound mutant mice (Fig. 12C). Based on these further analyses of pRB-E2F1 function, we conclude that the specific pRB-
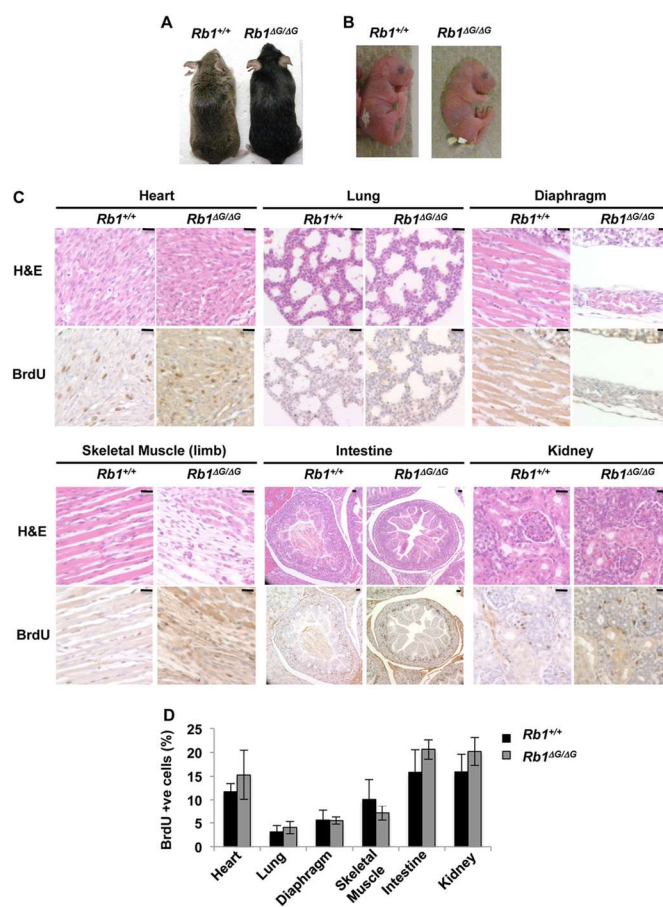
FIG 8 Viability of $Rb1^{\Delta G/\Delta G}$ mutant mice and proliferative control during early development. (A) Photographs of 1-year-old wild-type and $Rb1^{\Delta G/\Delta G}$ mice. (B) Photographs of newborn pups at P0.5. The wild-type animal and the $Rb1^{\Delta G/\Delta G}$ mutant were both viable. (C) Embryos were isolated at E18.5 and fixed in formalin, and serial sections were cut and stained with either hematoxylin and eosin or BrdU to assess tissue architecture and proliferation. Representative images of major organs, including heart, lung, diaphragm, skeletal muscle, intestine, and kidney, from $Rb1^{+/+}$ and $Rb1^{\Delta G/\Delta G}$ mice are included. In total, 9 embryos from each genotype were examined and stained for BrdU incorporation. (D) Quantification of BrdU-positive cells in the indicated tissue types. Error bars indicate 1 standard deviation from the mean ($n = 4$). Bars, 20 μm.

TABLE 1 Early development of $Rb1^{\Delta G/\Delta G}$ mice[a]

Genotype	No. of offspring at time point:			
	E13.5	E18.5	P0.5	P14
$Rb1^{+/+}$	11 (16)	24 (23)	15 (15)	163 (127)
$Rb1^{\Delta G/+}$	34 (32)	46 (46)	29 (31)	291 (254)
$Rb1^{\Delta G/\Delta G}$	19 (16)	22 (23)	9 live; 9 dead (15)	54 (127)
Total	64	92	62	508

[a] Intercrosses between $Rb1^{\Delta G/+}$ mice were used to determine the frequency of wild-type, heterozygous, and $Rb1^{\Delta G/\Delta G}$ animals. Numbers in parentheses represent the expected values based on Mendelian predictions.

E2F1 interaction is unlikely to replace general E2F interactions to control cell cycle E2F target genes.

Collectively, our analysis of cancer incidence in $Rb1^{\Delta G/\Delta G}$ mice suggests that loss of E2F transcriptional repression is insufficient to cause tumor formation and has limited effects on cell cycle control. Our data suggest that tumor suppression by pRB is likely to be a more complex process than this individual biochemical function.

DISCUSSION

The strongest phenotype observed in $Rb1^{\Delta G/\Delta G}$ mice is partially penetrant muscle degeneration. Previous work has suggested that
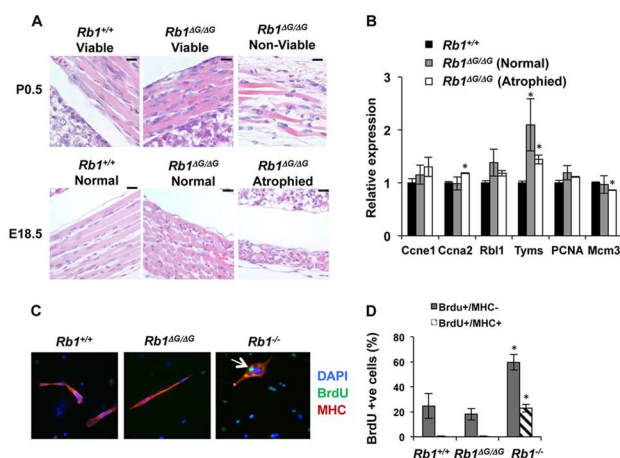
FIG 9 Muscle degeneration in $Rb1^{\Delta G/\Delta G}$ embryos. (A) H&E staining of tissue sections from newborn diaphragms of the indicated genotypes. The leftmost $Rb1^{\Delta G/\Delta G}$ sample is from a viable newborn, and the rightmost $Rb1^{\Delta G/\Delta G}$ sample is from a newborn that was found struggling to breathe and died shortly after birth. Analogous sections from embryos isolated at E18.5 with either normal or atrophied diaphragm (and other skeletal muscle) are presented. (B) The relative expression levels of six pRB-dependent E2F cell cycle target genes are shown. Each transcript was quantified from RNA isolated from dissected quadriceps muscle from E18.5 mice. The relative level of message present in the wild type was scaled to 1, and the $Rb1^{\Delta G/\Delta G}$ embryos were stratified into normal and atrophied based upon H&E staining of skeletal muscle. Error bars indicate 1 standard deviation from the mean ($n = 3$). Statistically significant differences are indicated by an asterisk (t test, $P > 0.05$). (C) Wild-type, $Rb1^{\Delta G/\Delta G}$, and $Rb1^{-/-}$ MEFs were infected with a MyoD-expressing retrovirus and induced to differentiate into myotubes. Upon differentiation, cells were stimulated with 15% FBS and labeled with BrdU for 24 h. Cells were fixed and stained for myosin heavy chain (MHC), BrdU incorporation, and DNA as shown. The arrow indicates an MHC- and BrdU-positive cell. (D) The frequency of double-positive BrdU- and MHC-stained cells, as well as single-positive cells that stained only for BrdU, was determined. Graphs indicate the averages, error bars represent 1 standard deviation, and an asterisk indicates a statistically significant difference from the wild-type control (t test, $P < 0.05$). Bars, 20 µm.

pRB plays a crucial role in regulating autophagy and that in its absence muscle cells catabolize themselves, leading to an apoptosis-independent death (51). Importantly, inhibition of autophagy rescues this phenotype even in the absence of pRB function (51). Intriguingly, Araki et al. have recently demonstrated that loss of nuclear localization by pRB interferes with sarcomere structure in skeletal muscle, leading to a nonapoptotic cell death (52). This may offer a nontranscriptional explanation of our phenotype, as loss of E2F binding likely reduces pRB anchorage in the nucleus. It is not clear if both of these mechanisms or others are contributing to the observed defect in $Rb1^{\Delta G/\Delta G}$ mice, but our results further strengthen the role for pRB in muscle development. We expect that the partial penetrance of this muscle phenotype is due to genetic modifiers. Crossing homozygous mutants leads to full viability of offspring (data not shown), indicating that this trait could be bred out of our colony. We note that there are other examples of genetic background effects on pRB- and E2F-related phenotypes such as the role of E2F3 in proliferation (53), the impact of E2F1 on tumorigenesis (54), and the effects of p107 and p130 on proliferative control in development (55, 56).

Interactions between pRB and E2Fs are commonly considered to be the mechanism that regulates the transition between the G_1 and S phases of the cell cycle (1). Our data demonstrate that the $Rb1^{\Delta G}$ mutation disrupts this regulatory interaction, but mice carrying this allele tolerate its effects and display few defects in cell cycle control. The strongest defect in proliferative control that we observed in $Rb1^{\Delta G/\Delta G}$ mutants was in restraining cell cycle entry

following serum stimulation. This is intriguing because a number of key cell cycle regulators, D- and E-type cyclins, are dispensable for asynchronous proliferation and knockout embryos develop almost to term (57, 58). Strikingly, knockout MEFs deficient for all D- or E-type cyclins are impaired for cell cycle reentry following serum starvation. This suggests that the cellular response to serum stimulation may be fundamentally different from cell cycle exit paradigms as cyclin-CDK and now pRB-E2F functions are essential in coordinating cell cycle reentry in response to growth factor signaling.

We suggest that the data in this report should be considered carefully. While our biochemical measurements of pRB-E2F interaction and regulation indicate a strong loss of function in the ΔG-pRB protein, it is important to separate its effects in isolation from the broader role of E2F transcriptional control in cell proliferation. For example, p16 expression and gamma irradiation experiments indicate that $Rb1^{\Delta G/\Delta G}$ cells can arrest; however, E2F transcript levels drop even at E2F target genes, where we show that pRB no longer localizes. In these arrest assays, p16 and gamma irradiation inhibit cyclin-CDK activity and the other pocket proteins become active and can block E2F transcription. Importantly, it is known that p107/p130 and E2F4/E2F5 are required to arrest in response to p16 (59, 60). For this reason, we think that our data do not indicate that the E2F transcriptional regulatory network is unnecessary for proliferative control but rather that it retains some function independent of pRB. This is reinforced by the reduction in E2F gene expression that takes place in $Rb1^{-/-}$ cells

Cecchini et al.
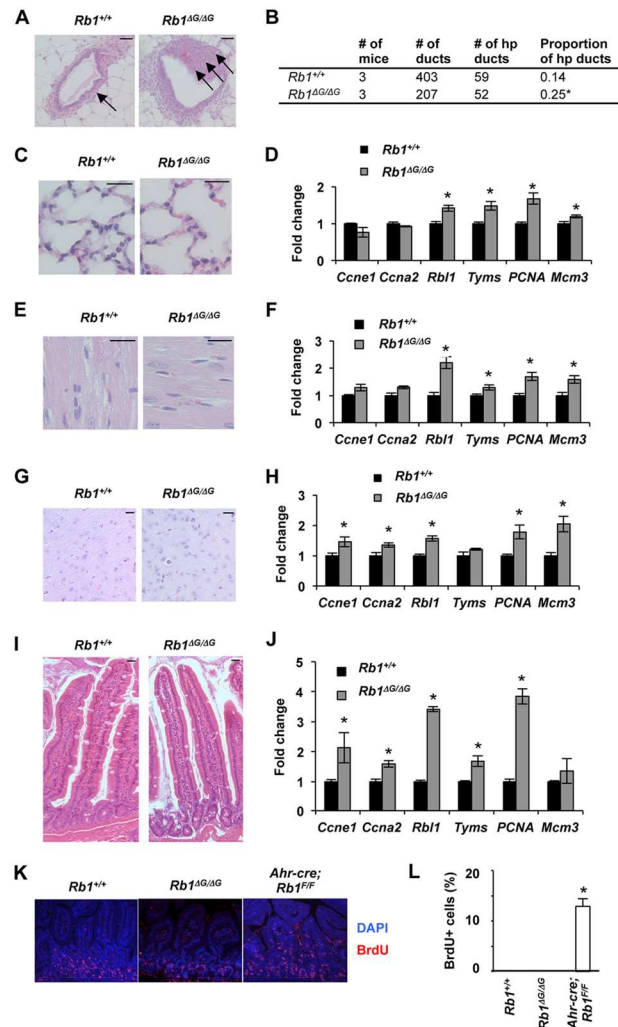
FIG 10 Limited hyperplasia in tissues of $Rb1^{\Delta G/\Delta G}$ mice. (A) Sections of mammary ducts from 8-week-old wild-type and $Rb1^{\Delta G/\Delta G}$ mice stained with H&E. Arrows indicate cell layers in the lumen of the duct. (B) Quantification of the proportions of hyperplastic (hp) ducts found in wild-type and $Rb1^{\Delta G/\Delta G}$ mammary glands. Ducts three or more cells thick were scored as hyperplastic. Proportions were compared by χ^2 test (*, significant difference, $P < 0.05$). (C) H&E staining of lung tissue from 8-week-old mice. (D) Relative mRNA levels for cyclin E1 (*Ccne1*), cyclin A2 (*Ccna2*), p107 (*Rbl1*), thymidylate synthase (*Tyms*), Pcna, and Mcm3 were also determined in wild-type and $Rb1^{\Delta G/\Delta G}$ lung tissue from 8-week-old mice. Wild-type expression levels are scaled to 1. (E and F) H&E staining of cardiac muscle from 6- to 8-week-old mice is shown along with expression analysis of E2F transcriptional targets. (G and H) H&E staining of brain tissue from 8-week-old mice. Accompanying analysis of E2F transcriptional targets from this tissue is shown to the right. (I) H&E staining of crypts and villi from the small intestines of 8-week-old mice. (J) The relative expression level of six E2F cell cycle target genes in mRNA prepared from isolated villi is shown. (K) Eight-week-old mice of the indicated genotypes were injected with BrdU 2 h prior to sacrifice. Tissue sections from intestines were stained for BrdU incorporation (red) and DNA (blue). (L) The frequency of BrdU-positive nuclei in columnar epithelial cells of villi is shown. Each graph represents at least 3 individual experiments, and error bars indicate 1 standard deviation from the mean. An asterisk represents a statistically significant difference from the wild-type control (*t* test, $P < 0.05$). Bars, 20 μm (5 μm in panel C).
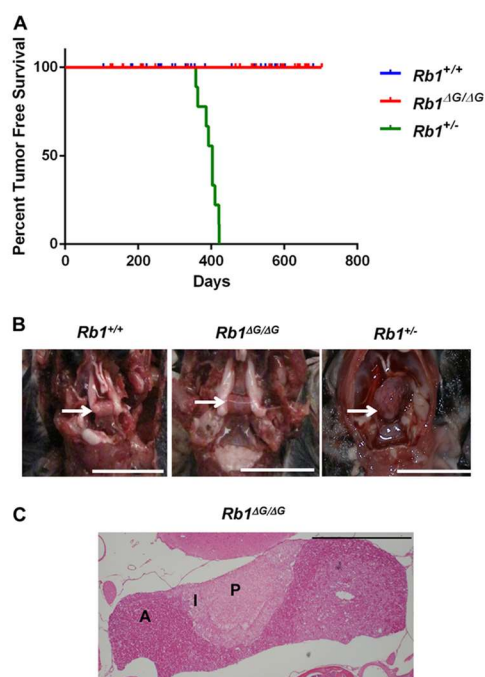
FIG 11 *Rb1^(ΔG/ΔG)* mutant mice have normal life expectancy. (A) Mice of the indicated genotypes were allowed to age to determine their life span and natural demise. Kaplan-Meier plots depict tumor-free survival of the indicated genotypes. Tick marks indicate the ages at which individual mice were analyzed anatomically and histologically for abnormalities. Wild-type (*n* = 40) and *Rb1^(ΔG/ΔG)* (*n* = 42) mice are significantly different from *Rb1^(+/−)* (*n* = 9) mice (log rank test, *P* < 0.05). (B) Photographs of pituitary glands from wild type, *Rb1^(ΔG/ΔG)*, and *Rb1^(+/−)* mice are representative of findings for animals between 8 and 12 months of age. Arrows identify the locations of pituitary glands. Bars, 1 cm. (C) H&E staining of a tissue section from the pituitary gland of a 2-year-old *Rb1^(ΔG/ΔG)* mutant. The different lobes of the pituitary are labeled: A, anterior lobe; I, intermediate lobe; P, posterior lobe. Bar, 1 mm.

FIG 12 E2F1 loss does not affect cell cycle control, viability, or cancer susceptibility in *Rb1^(ΔG/ΔG)* mice. (A) Genotypes of offspring at P14 from a cross of compound heterozygote *Rb1^(ΔG/+)*; *E2f1^(+/−)* mice. The expected number of mice based on Mendelian ratios is presented in parentheses. (B) Serum-starved cell cultures from compound mutant fibroblasts of the indicated genotypes were pulse-labeled and stained for BrdU incorporation along with total DNA using propidium iodide. The proportion of cells in each respective cell cycle phase was determined by flow cytometry. (C) Mice of the indicated genotypes were allowed to age to determine their life span and natural demise. Kaplan-Meier plots depict tumor-free survival of the indicated genotypes. Tick marks indicate individual mice that were analyzed anatomically and histologically for abnormalities.

even though they do not arrest proliferation in response to p16 or gamma irradiation. Lastly, in 1998 Dyson (61) described the lack of E2F regulation data in cell cycle exit paradigms such as these as a "quirk" of the pRB-E2F literature, and we suggest that our study adds valuable new information in this area.

E2F gene expression levels in *Rb1^(ΔG/ΔG)* embryonic and adult tissues are upregulated at a modest level, and there is no evidence of increased proliferation in these tissues. Conversely, conditional deletion of *Rb1* in intestinal epithelia as reported by Chong et al. displays approximately 20- to 40-fold-increased expression of E2F target genes (45). In considering these *Rb1* knockout data, it is important to remember that loss of *Rb1* in these cells is accompanied by proliferation. In quiescent cells, p130 is dephosphorylated and active for repression of E2F target genes (40, 62). Furthermore, when cells are stimulated to proliferate, E2Fs and Myc transcribe E2F genes, further leading to amplification of E2F tran-

scription levels (61). For this reason, it is difficult to examine the expression data in proliferating knockout cells and quiescent *Rb1^(ΔG/ΔG)* mutant cells and determine the level of expression that is necessary to advance the cell cycle. As with our cell cycle exit experiments, these measurements also reinforce the idea that loss of pRB-E2F transcriptional control does not necessarily stimulate advancement of the cell cycle or fully activate the E2F transcriptional program.

Based on data from this study, we propose the models in Fig. 13. Figure 13A shows the RB pathway in cell cycle regulatory con-

Cecchini et al.
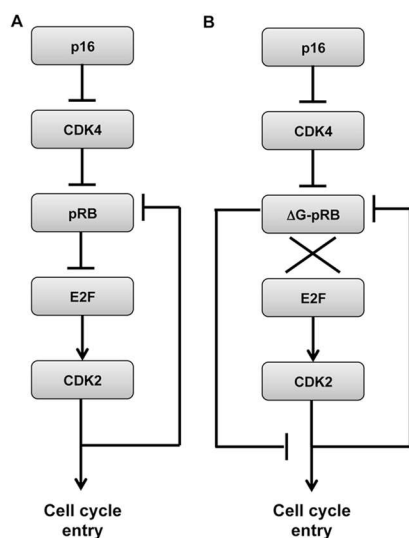
FIG 13 Model for cell cycle control in $Rb1^{\Delta G/\Delta G}$ mutant cells. (A) Cell cycle regulation by the RB pathway in normal cells. pRB restricts E2F transcription to prevent Cdk2 activation, negative feedback to pRB, and cell cycle advancement. (B) ΔG-pRB is responsive to p16 activation and, in the absence of regulation of E2F transcription factors, retains the ability to prevent cell cycle entry.

trol as it is widely accepted, in which pRB control of E2F transcription is central to the regulation of entry into S phase. Figure 13B depicts cell cycle regulation in the absence of pRB repression of E2Fs in which alternate pathways allow control of S-phase entry even in the absence of physical control of E2Fs by pRB (14). Mechanisms in which pRB function influences cell cycle control outside E2F transcription, but before the commitment to DNA replication, may prove to be important means to influence cell cycle progression.

REFERENCES

1. **Hanahan D, Weinberg RA.** 2000. The hallmarks of cancer. Cell **100:**57–70. http://dx.doi.org/10.1016/S0092-8674(00)81683-9.
2. **Massague J.** 2004. G1 cell-cycle control and cancer. Nature **432:**298–306. http://dx.doi.org/10.1038/nature03094.
3. **Classon M, Harlow E.** 2002. The retinoblastoma tumour suppressor in development and cancer. Nat. Rev. Cancer **2:**910–917. http://dx.doi.org/10.1038/nrc950.
4. **Sherr CJ, McCormick F.** 2002. The RB and p53 pathways in cancer. Cancer Cell **2:**103–112. http://dx.doi.org/10.1016/S1535-6108(02)00102-2.
5. **DeCaprio JA.** 2009. How the Rb tumor suppressor structure and function was revealed by the study of adenovirus and SV40. Virology **384:**274–284. http://dx.doi.org/10.1016/j.virol.2008.12.010.
6. **zur Hausen H.** 2002. Papillomaviruses and cancer: from basic studies to clinical application. Nat. Rev. Cancer **2:**342–350. http://dx.doi.org/10.1038/nrc798.
7. **Chellappan S, Kraus KB, Kroger B, Munger K, Howley PM, Phelps WC, Nevins JR.** 1992. Adenovirus E1A, simian virus 40 tumor antigen, and the human papillomavirus E7 protein share the capacity to disrupt the interaction between transcription factor E2F and the retinoblastoma gene product. Proc. Natl. Acad. Sci. U. S. A. **89:**4549–4553. http://dx.doi.org/10.1073/pnas.89.10.4549.
8. **Gonzalez SL, Stremlau M, He X, Basile JR, Munger K.** 2001. Degradation of the retinoblastoma tumor suppressor by the human papillomavirus type 16 oncoprotein is important for functional inactivation and is separable from proteasomal degradation of E7. J. Virol. **75:**7583–7591. http://dx.doi.org/10.1128/JVI.75.16.7583-7591.2001.
9. **Hiebert SW.** 1993. Regions of the retinoblastoma gene product required for its interaction with the E2F transcription factor are necessary for E2 promoter repression and pRb-mediated growth suppression. Mol. Cell. Biol. **13:**3384–3391.
10. **Hiebert SW, Chellappan SP, Horowitz JM, Nevins JR.** 1992. The interaction of RB with E2F coincides with an inhibition of the transcriptional activity of E2F. Genes Dev. **6:**177–185. http://dx.doi.org/10.1101/gad.6.2.177.
11. **Qin X-Q, Livingston DM, Ewen M, Sellers WR, Arany Z, Kaelin WG.** 1995. The transcription factor E2F-1 is a downstream target of RB action. Mol. Cell. Biol. **15:**742–755.
12. **Qin XQ, Chittenden T, Livingston DM, Kaelin WG, Jr.** 1992. Identification of a growth suppression domain within the retinoblastoma gene product. Genes Dev. **6:**953–964. http://dx.doi.org/10.1101/gad.6.6.953.
13. **Dick FA, Dyson N.** 2003. pRB contains an E2F1-specific binding domain that allows E2F1-induced apoptosis to be regulated separately from other E2F activities. Mol. Cell **12:**639–649. http://dx.doi.org/10.1016/S1097-2765(03)00344-7.
14. **Dick FA, Rubin SM.** 2013. Molecular mechanisms underlying RB protein function. Nat. Rev. Mol. Cell Biol. **14:**297–306. http://dx.doi.org/10.1038/nrm3567.
15. **Ianari A, Natale T, Calo E, Ferretti E, Alesse E, Screpanti I, Haigis K, Gulino A, Lees JA.** 2009. Proapoptotic function of the retinoblastoma tumor suppressor protein. Cancer Cell **15:**184–194. http://dx.doi.org/10.1016/j.ccr.2009.01.026.
16. **Pediconi N, Ianari A, Costanzo A, Belloni L, Gallo R, Cimino L, Porcellini A, Screpanti A, Screpanti I, Balsano C, Alesse E, Gulino A, Levrero M.** 2003. Differential regulation of E2F1 apoptotic target genes in response to DNA damage. Nat. Cell Biol. **5:**552–558. http://dx.doi.org/10.1038/ncb998.
17. **Avni D, Yang Martelli HF, Hofmann F, ElShamy WM, Ganesan S, Scully R, Livingston DM.** 2003. Active localization of the retinoblastoma protein in chromatin and its response to S phase DNA damage. Mol. Cell **12:**735–746. http://dx.doi.org/10.1016/S1097-2765(03)00355-1.
18. **Mendoza-Maldonado R, Paolinelli R, Galbiati L, Giadrossi S, Giacca M.** 2010. Interaction of the retinoblastoma protein with Orc1 and its recruitment to human origins of DNA replication. PLoS One **5:**e13720. http://dx.doi.org/10.1371/journal.pone.0013720.
19. **Wells J, Yan PS, Cechvala M, Huang T, Farnham PJ.** 2003. Identification of novel pRb binding sites using CpG microarrays suggests that E2F recruits pRb to specific genomic sites during S phase. Oncogene **22:**1445–1460. http://dx.doi.org/10.1038/sj.onc.1206264.
20. **Chau BN, Pan CW, Wang JY.** 2006. Separation of anti-proliferation and anti-apoptotic functions of retinoblastoma protein through targeted mutations of its A/B domain. PLoS One **1:**e82. http://dx.doi.org/10.1371/journal.pone.0000082.
21. **Cecchini MJ, Dick FA.** 2011. The biochemical basis of CDK phosphorylation-independent regulation of E2F1 by the retinoblastoma protein. Biochem. J. **434:**297–308. http://dx.doi.org/10.1042/BJ20101210.
22. **Julian LM, Palander O, Seifried LA, Foster JE, Dick FA.** 2008. Characterization of an E2F1-specific binding domain in pRB and its implications for apoptotic regulation. Oncogene **27:**1572–1579. http://dx.doi.org/10.1038/sj.onc.1210803.
23. **Carnevale J, Palander O, Seifried LA, Dick FA.** 2012. DNA damage signals through differentially modified E2F1 molecules to induce apoptosis. Mol. Cell. Biol. **32:**900–912. http://dx.doi.org/10.1128/MCB.06286-11.
24. **Calbo J, Parreno M, Sotillo E, Yong T, Mazo A, Garriga J, Grana X.**

2002. G1 cyclin/cyclin-dependent kinase-coordinated phosphorylation of endogenous pocket proteins differentially regulates their interactions with E2F4 and E2F1 and gene expression. J. Biol. Chem. **277:**50263–50274. http://dx.doi.org/10.1074/jbc.M209181200.

25. **Cecchini MJ, Amiri M, Dick FA.** 2012. Analysis of cell cycle position in mammalian cells. J. Vis. Exp. **2012**(59):3491. http://dx.doi.org/10.3791/3491.

26. **Seifried LA, Talluri S, Cecchini M, Julian LM, Mymryk JS, Dick FA.** 2008. pRB-E2F1 complexes are resistant to adenovirus E1A-mediated disruption. J. Virol. **82:**4511–4520. http://dx.doi.org/10.1128/JVI.02713-07.

27. **Field SJ, Tsai F-Y, Kuo F, Zubiaga AM, Kaelin JWG, Livingston DM, Orkin SH, Greenberg ME.** 1996. E2F-1 functions in mice to promote apoptosis and suppress proliferation. Cell **85:**549–561. http://dx.doi.org/10.1016/S0092-8674(00)81255-6.

28. **Dick FA, Sailhamer E, Dyson NJ.** 2000. Mutagenesis of the pRB pocket reveals that cell cycle arrest functions are separable from binding to viral oncoproteins. Mol. Cell. Biol. **20:**3715–3727. http://dx.doi.org/10.1128/MCB.20.10.3715-3727.2000.

29. **Pear WS, Nolan GP, Scott ML, Baltimore D.** 1993. Production of high-titer helper-free retroviruses by transient transfection. Proc. Natl. Acad. Sci. U. S. A. **90:**8392–8396. http://dx.doi.org/10.1073/pnas.90.18.8392.

30. **Novitch BG, Mulligan GJ, Jacks T, Lassar AB.** 1996. Skeletal muscle cells lacking the retinoblastoma protein display defects in muscle gene expression and accumulate in S and G_2 phases of the cell cycle. J. Cell Biol. **135:**441–456. http://dx.doi.org/10.1083/jcb.135.2.441.

31. **Talluri S, Isaac CE, Ahmad M, Henley SA, Francis SM, Martens AL, Bremner R, Dick FA.** 2010. A G1 checkpoint mediated by the retinoblastoma protein that is dispensable in terminal differentiation but essential for senescence. Mol. Cell. Biol. **30:**948–960. http://dx.doi.org/10.1128/MCB.01168-09.

32. **Chicas A, Wang X, Zhang C, McCurrach M, Zhao Z, Mert O, Dickins RA, Narita M, Zhang M, Lowe SW.** 2010. Dissecting the unique role of the retinoblastoma tumor suppressor during cellular senescence. Cancer Cell **17:**376–387. http://dx.doi.org/10.1016/j.ccr.2010.01.023.

33. **Bolstad BM, Irizarry RA, Astrand M, Speed TP.** 2003. A comparison of normalization methods for high density oligonucleotide array data based on variance and bias. Bioinformatics **19:**185–193. http://dx.doi.org/10.1093/bioinformatics/19.2.185.

34. **Irizarry RA, Bolstad BM, Collin F, Cope LM, Hobbs B, Speed TP.** 2003. Summaries of Affymetrix GeneChip probe level data. Nucleic Acids Res. **31:**e15. http://dx.doi.org/10.1093/nar/gng015.

35. **Irizarry RA, Hobbs B, Collin F, Beazer-Barclay YD, Antonellis KJ, Scherf U, Speed TP.** 2003. Exploration, normalization, and summaries of high density oligonucleotide array probe level data. Biostatistics **4:**249–264. http://dx.doi.org/10.1093/biostatistics/4.2.249.

36. **Markovics JA, Carroll PA, Robles MT, Pope H, Coopersmith CM, Pipas JM.** 2005. Intestinal dysplasia induced by simian virus 40 T antigen is independent of p53. J. Virol. **79:**7492–7502. http://dx.doi.org/10.1128/JVI.79.12.7492-7502.2005.

37. **Shan B, Chang CY, Jones D, Lee WH.** 1994. The transcription factor E2F-1 mediates the autoregulation of RB gene expression. Mol. Cell. Biol. **14:**299–309.

38. **Herrera RE, Sah VP, Williams BO, Makela TP, Weinberg RA, Jacks T.** 1996. Altered cell cycle kinetics, gene expression, and G1 restriction point regulation in Rb-deficient fibroblasts. Mol. Cell. Biol. **16:**2402–2407.

39. **Hanahan D, Weinberg RA.** 2011. Hallmarks of cancer: the next generation. Cell **144:**646–674. http://dx.doi.org/10.1016/j.cell.2011.02.013.

40. **Hurford RK, Jr, Cobrinik D, Lee MH, Dyson N.** 1997. pRB and p107/p130 are required for the regulated expression of different sets of E2F responsive genes. Genes Dev. **11:**1447–1463. http://dx.doi.org/10.1101/gad.11.11.1447.

41. **Clarke AR, Maandag ER, van Roon M, van der Lugt NM, van der Valk M, Hooper ML, Berns A, te Riele H.** 1992. Requirement for a functional Rb-1 gene in murine development. Nature **359:**328–330. http://dx.doi.org/10.1038/359328a0.

42. **Jacks T, Fazeli A, Schmitt EM, Bronson RT, Goodell MA, Weinberg RA.** 1992. Effects of an Rb mutation in the mouse. Nature **359:**295–300. http://dx.doi.org/10.1038/359295a0.

43. **Lee EY, Chang CY, Hu N, Wang YC, Lai CC, Herrup K, Lee WH, Bradley A.** 1992. Mice deficient for Rb are nonviable and show defects in neurogenesis and haematopoiesis. Nature **359:**288–294. http://dx.doi.org/10.1038/359288a0.

44. **Francis SM, Bergsied J, Isaac CE, Coschi CH, Martens AL, Hojilla CV,**

Chakrabarti S, Dimattia GE, Khoka R, Wang JY, Dick FA.** 2009. A functional connection between pRB and transforming growth factor beta in growth inhibition and mammary gland development. Mol. Cell. Biol. **29:**4455–4466. http://dx.doi.org/10.1128/MCB.00473-09.

45. **Chong JL, Wenzel PL, Saenz-Robles MT, Nair V, Ferrey A, Hagan JP, Gomez YM, Sharma N, Chen HZ, Ouseph M, Wang SH, Trikha P, Culp B, Mezache L, Winton DJ, Sansom OJ, Chen D, Bremner R, Cantalupo PG, Robinson ML, Pipas JM, Leone G.** 2009. E2f1–3 switch from activators in progenitor cells to repressors in differentiating cells. Nature **462:**930–934. http://dx.doi.org/10.1038/nature08677.

46. **Harrison DJ, Hooper ML, Armstrong JF, Clarke AR.** 1995. Effects of heterozygosity for the Rb-1t19neo allele in the mouse. Oncogene **10:**1615–1620.

47. **Hu N, Gutsmann A, Herbert DC, Bradley A, Lee W-H, Lee EY.** 1994. Heterozygous Rb-1 delta 20/+ mice are predisposed to tumors of the pituitary gland with a nearly complete penetrance. Oncogene **9:**1021–1027.

48. **Vooijs M, van der Valk M, te Riele H, Berns A.** 1998. Flp-mediated tissue-specific inactivation of the retinoblastoma tumor suppressor gene in the mouse. Oncogene **17:**1–12. http://dx.doi.org/10.1038/sj.onc.1202169.

49. **Williams BO, Schmitt EM, Remington L, Bronson RT, Albert DM, Weinbert RA, Jacks T.** 1994. Extensive contribution of Rb-deficient cells to adult chimeric mice with limited histopathological consequences. EMBO J. **13:**4251–4259.

50. **Wang H, Bauzon F, Ji P, Xu X, Sun D, Locker J, Sellers RS, Nakayama K, Nakayama KI, Cobrinik D, Zhu L.** 2010. Skp2 is required for survival of aberrantly proliferating Rb1-deficient cells and for tumorigenesis in Rb1+/− mice. Nat. Genet. **42:**83–88. http://dx.doi.org/10.1038/ng.498.

51. **Ciavarra G, Zacksenhaus E.** 2010. Rescue of myogenic defects in Rb-deficient cells by inhibition of autophagy or by hypoxia-induced glycolytic shift. J. Cell Biol. **191:**291–301. http://dx.doi.org/10.1083/jcb.201005067.

52. **Araki K, Kawauchi K, Hirata H, Yamamoto M, Taya Y.** 2013. Cytoplasmic translocation of the retinoblastoma protein disrupts sarcomeric organization. eLife **2:**e01228. http://dx.doi.org/10.7554/eLife.01228.

53. **Humbert PO, Verona R, Trimarchi JM, Rogers C, Dandapani S, Lees JA.** 2000. E2f3 is critical for normal cellular proliferation. Genes Dev. **14:**690–703.

54. **Yamasaki L, Bronson R, Williams BO, Dyson NJ, Harlow E, Jacks T.** 1998. Loss of E2F-1 reduces tumorigenesis and extends the lifespan of Rb1(+/−) mice. Nat. Genet. **18:**360–364. http://dx.doi.org/10.1038/ng0498-360.

55. **LeCouter JE.** 1998. Strain-dependent embryonic lethality in mice lacking the retinoblastoma-related p130 gene. Development **125:**4669–4679.

56. **LeCouter JE, Kablar B, Hardy WR, Ying C, Megeney LA, May LL, Rudnicki MA.** 1998. Strain-dependent myeloid hyperplasia, growth deficiency, and accelerated cell cycle in mice lacking the Rb-related p107 gene. Mol. Cell. Biol. **18:**7455–7465.

57. **Geng Y, Yu Q, Sicinska E, Das M, Schneider JE, Bhattacharya S, Rideout WM, Bronson RT, Gardner H, Sicinski P.** 2003. Cyclin E ablation in the mouse. Cell **114:**431–443. http://dx.doi.org/10.1016/S0092-8674(03)00645-7.

58. **Kozar K, Ciemerych MA, Rebel VI, Shigematsu H, Zagozdzon A, Sicinska E, Geng Y, Yu Q, Bhattacharya S, Bronson RT, Akashi K, Sicinski P.** 2004. Mouse development and cell proliferation in the absence of D-cyclins. Cell **118:**477–491. http://dx.doi.org/10.1016/j.cell.2004.07.025.

59. **Bruce JL, Hurford RKJ, Classon M, Koh J, Dyson N.** 2000. Requirements for cell cycle arrest by p16INK4a. Mol. Cell **6:**737–742. http://dx.doi.org/10.1016/S1097-2765(00)00072-1.

60. **Gaubatz S, Lindeman GJ, Jakoi L, Nevins JR, Livingston DM, Rempel RE.** 2000. E2F4 and E2F5 play an essential role in pocket protein-mediated G1 control. Mol. Cell **6:**729–735. http://dx.doi.org/10.1016/S1097-2765(00)00071-X.

61. **Dyson N.** 1998. The regulation of E2F by pRB-family proteins. Genes Dev. **12:**2245–2262. http://dx.doi.org/10.1101/gad.12.15.2245.

62. **Moberg K, Starz MA, Lees JA.** 1996. E2F-4 switches from p130 to p107 and pRB in response to cell cycle reentry. Mol. Cell. Biol. **16:**1436–1449.

63. **Xiao B, Spencer J, Clements A, Ali-Khan N, Mittnacht S, Broceno C, Burghammer M, Perrakis A, Marmorstein R, Gamblin SJ.** 2003. Crystal structure of the retinoblastoma tumor suppressor protein bound to E2F and the molecular basis of its regulation. Proc. Natl. Acad. Sci. U. S. A. **100:**2363–2368. http://dx.doi.org/10.1073/pnas.0436813100.

Appendix B: List of plasmids

Name	Genes Encoded	Mutations	Obtained/ Constructed	Resistance	Stock Number
pScodon-GST-RBLP	GST, RBLP	N/A	F. Dick	AMP	0519
pMJC15	GST, RBLP	Y756W	M. Cecchini	AMP	0661
pMJC02	GST, RBLP	R467E, K548E	M. Cecchini	AMP	0561
pscodon-GST-RB delta L	GST, RBLP	I753A, N757A, M761A	S. Talluri	AMP	0668
pscodon1-GST-RBdS	GST, RBLP	M851A, V852A	O. Palander	AMP	0528
pMJC17	GST, RBLP	R467E, K548E, Y756W	M. Cecchini	AMP	0613
pMJC09	GST, RBLP	R467E, K548E, M851A, V852A	M. Cecchini	AMP	0568
pMJC22	GST, RBLP	R467E, K548E, Y756W, M851A, V852A	M. Cecchini	AMP	0618
pScodon-GST-RBLP^{GSL}	GST, RBLP	R467E, K548E, I753A, N757A, M761A, M851A, V852A	M. Thwaites	AMP	0735
pCMV-β-Gal	β-Gal	N/A	S. Salama	AMP	0042
pCMV-HA-DP1	DP1	N/A	M. Classon	AMP	0094
CMV-HA-E2F1	E2F1	N/A	F. Dick	AMP	0399
pCMV-HA-E2F2	E2F2	N/A	J. Lees	AMP	0319

pCMV-HA-E2F3	E2F3	N/A	J. Lees	AMP	0320
CMV-myc-Cdh1	Cdh1	N/A	N. Dyson	AMP	0520
pFAD102	RB	N/A	F. Dick	AMP	0039
pFAD200	RB	Y756W	M. Cecchini	AMP	0196
pMJC03	RB	R467E, K548E	M. Cecchini	AMP	0562
pFAD139	RB	I753A, N757A, M761A	F. Dick	AMP	0059
pFAD292	RB	M851A, V852A	F. Dick	AMP	0412
pMJC20	RB	R467E, K548E, Y756W	M. Cecchini	AMP	0616
pMJC21	RB	R467E, K548E, M851A, V852A	M. Cecchini	AMP	0617
pMJC22	RB	R467E, K548E, Y756W, M851A, V852A	M. Cecchini	AMP	0618
CMV-RB^{GSL}	RB	R467E, K548E, I753A, N757A, M761A, M851A, V852A	M. Thwaites	AMP	0736
Efla 4F puro	cMyc, Sox2, Oct4, KLF4	N/A	J. Sage	AMP	0737
Tet O 4F	cMyc, Sox2, Oct4, KLF4	N/A	J. Sage	AMP	0738
Tet O Sox2	Sox2	N/A	J. Sage	AMP	0739
Tet O Oct4	Oct4	N/A	J. Sage	AMP	0740
Tet O cMyc	cMyc	N/A	J. Sage	AMP	0741

Tet O KLF4	KLF4	N/A	J. Sage	AMP	0742
Gag/pol	Gag/pol	N/A	J. Sage	AMP	0743
Tat	Tat	N/A	J. Sage	AMP	0744
Rev	Rev	N/A	J. Sage	AMP	0745
VSVG	VSVG	N/A	J. Sage	AMP	0746
CMV p107 6x	p107	T480R, V490K, N556E, E560H, G786T, H797R	S. Rubin	AMP	0747
CMV HA-Skp2	Skp2	N/A	S. Meloche	AMP	0748
CMV HA-Skp2 S64A	Skp2	S64A	S. Meloche	AMP	0749
CMV HA-Skp2 AA	Skp2	S64A, S72A	S. Meloche	AMP	0750
CMV HA-Skp2 DD	Skp2	S64D, S72D	S. Meloche	AMP	0751
CMV RB^{GL}	RB Large Pocket	R467E, K548E, I753A, N757A, M761A	M. Thwaites	AMP	0752
CMV RB^{LS}	RB Large Pocket	I753A, N757A, M761A, M851A, V852A	M. Thwaites	AMP	0753
pScodon GST-RB^C	RB Large Pocket	Y756W	M. Thwaites	AMP	0754
pScodon GST-RB^{GSC}	RB Large Pocket	R467E, K548E, M851A, V852A, Y756W	M. Thwaites	AMP	0755
pScodon GST-p107 6x	p107	T480R, V490K, N556E, E560H, G786T, H797R	S. Rubin	AMP	0756
pScodon GST-RBC	RB C-terminus	N/A	M. Thwaites	AMP	0757

	mouse				
pet30a His-RBC	RB C-terminus mouse	N/A		M. Thwaites	KAN	0758

Appendix C: List of antibodies

Antibody	Protein recognized	Species	Supplier	CAT. #	Application
p27 (C-19)	p27	Rabbit	Santa Cruz Biotechnology	SC-528	WB (1:500)
Histone H3	Histone H3	Rabbit	abcam	ab70550	WB (1:1000)
E2F-3 (PG37)	E2F-3	Mouse	Santa Cruz Biotechnology	SC-69684	WB (1:500)
β-Actin (AC-74)	Actin	Mouse	Sigma	A2228	WB (1:1000)
BrdU (B44)	BrdU	Mouse	BD biosciences	347580	FC (1:200), IF (1:50)
CDK2	CDK2	Rabbit	Millipore	07-631	IP (4µg)
HA (3F10)	HA-Tag	Rat	Sigma	12158167001	WB (1:1000)
cMyc 9E11	Myc -Tag	Mouse	abcam	ab56	WB (1:10)
pRB G3-245	pRB	Mouse	BD biosciences	554136	WB (1:1000)
CD-20	CD-20	Mouse	BD biosciences	347673	FC (1:200)

Appendix D: PCR conditions

PCR Conditions *Rb1*

Master Mix per reaction
- 1.25 µL MgCl$_2$ (50mM)
- 2 µL dNTPs (2mM)
- 2 µL 10X PCR Buffer (200mM Tris pH8, 500mM KCl)
- 1µL 20µM P1-F
- 1µL 20µM P2-R
- 1µL 20µM P3
- 9 µL Water
- 0.75µL Taq (5units/µL)
Total   18µL
     + 2µL DNA sample

Reaction Conditions
Program - RB1 370bp ST
    1. 94°C   3:00
    2. 94°C   0:30
    3. 60°C   1:00
    4. 72°C   1:00
    5. Go to Step #2, 34 times
    6. 72°C   7:00
    7. 12°C   hold

Expected Results:

Mutant (**Null**) = ~470 bp
Heterozygote = 410 bp and ~470 bp
Wild type = 410 bp

Primers
P1: AAT TGC GGC CGC ATC TGC ATC TTT ATC GC
P2: CCC ATG TTC GGT CCC TAG
P3: GAA GAA CGA CAT CAG CAG

PCR Conditions *Cdkn1b (p27)*

Master Mix per reaction
- 0.5 µL MgCl$_2$ (50mM)
- 2 µL dNTPs (2mM)
- 2 µL 10X PCR Buffer (200mM Tris pH8, 500mM KCl)
- 1µL 20µM N1
- 1µL 20µM K3
- 1µL 20µM K5
- 10 µL Water
- 0.5µL Taq (5units/µL)
Total   18µL
     + 2µL DNA sample

Reaction Conditions
Program - P27LCM
    1. 94°C   2:00
    2. 94°C   0:45
    3. 57°C   0:45
    4. 72°C   0:45
    5. Go to Step #2, 34 times
    6. 72°C   7:00
    7. 12°C   hold

Expected Results:

Mutant (**Null**) = 129 bp
Heterozygote = 199 bp and 129 bp
Wild type = 199 bp

Primers
K3: TGGAACCCTGTGCCATCTCTAT
K5-199: AGATTGACTATTCATATGCTCTAA
N1-129: TTGCCAAGTTCTAATTCCATCA

PCR Conditions *Rb1-ΔG*

Master Mix per reaction
- 0.5 µL MgCl$_2$ (50mM)
- 2 µL dNTPs (2mM)
- 2 µL 10X PCR Buffer (200mM Tris pH8, 500mM KCl)
- 1µL 20µM LoxP-N-F-MC
- 1µL 20µM LoxP-N-R-MC
- 11 µL Water
- 0.5µL Taq (5units/µL)
Total   18µL
       + 2µL DNA sample

Reaction Conditions
Program - NEWRBPRIMERS
1. 94°C   2:00
2. 94°C   0:45
3. 55°C   0:45
4. 72°C   0:45
5. Go to Step #2, 39 times
6. 72°C   5:00
7. 12°C   hold

Expected Results:

Mutant = 280 bp
Heterozygote = 280 bp and 200 bp
Wild type = 200 bp

Primers
LOXP-N-F-MC:
CAAATTCTCTTCCATTTCCC
LOXP-N-R-MC:
GAATTACAAGTTCAAGACCTAG

PCR Conditions *UBC Cre ERT2*

Master Mix per reaction
- 0.5 µL MgCl$_2$ (50mM)
- 2 µL dNTPs (2mM)
- 2 µL 10X PCR Buffer (200mM Tris pH8, 500mM KCl)
- 0.25µL 20µM Fwd
- 0.25µL 20µM Rev
- 0.25µL 20µM Internal Fwd
- 0.25µL 20µM Internal Rev
- 12 µL Water
- 0.5µL Taq (5units/µL)
Total   18µL
       + 2µL DNA sample

Reaction Conditions
Program – SL01
1. 94°C   2:30
2. 94°C   0:20
3. 60°C   0:20
4. 70°C   2:00
5. Go to Step #2, 29 times
6. 72°C   10:00
7. 12°C   hold

Expected Results:

Positive = 100 bp
Internal Control = 324 bp

Primers
Fwd: GCG GTC TGG CAG TAA AAA CTA TC
Rev: GTG AAA CAG CAT TGC TGT CAC TT
Internal Fwd: CTA GGC CAC AGA ATT GAA AGA TCT
Internal Rev:
GTA GGT GGA AAT TCT AGC ATC ATC C

PCR Conditions *p53*

Master Mix per reaction
- 1 µL MgCl$_2$ (50mM)
- 2.5 µL dNTPs (2mM)
- 2.5 µL 10X PCR Buffer (200mM Tris pH8, 500mM KCl)
- 0.62µL 20µM AM3 primer
- 0.62µL 20µM AM4 primer
- 0.27µL 20µM neo-sense primer
- 0.27µL 20µM neo-antisense primer
- 11 µL Water
- 0.5µL Taq (5units/µL)
Total   18µL
        + 2µL DNA sample

Reaction Conditions
Program – P53 New
   1. 94°C   2:30
   2. 94°C   0:30
   3. 58°C   0:30
   4. 72°C   1:10
   5. Go to Step #2, 29 times
   6. 72°C   10:00
   7. 12°C   hold

Expected Results:

Mutant (**Null**) = 424 bp
Heterozygote = 424 bp and 548 bp
Wild type = 548 bp

Primers
AM3: ATAGGTCGGCGGTTCAT
AM4: CCCGAGTATCTGGAAGACAG
Neo-sense:
GGAAGGGACTGGCTGCTATTG
Neo-antisense:
CAATATCACGGGTAGCCAACG

PCR Conditions *Cdkn1a (p21)*

Master Mix per reaction
- 0.5 µL MgCl$_2$ (50mM)
- 2 µL dNTPs (2mM)
- 2 µL 10X PCR Buffer (200mM Tris pH8, 500mM KCl)
- 1µL 20µM N1
- 1µL 20µM K3
- 1µL 20µM K5
- 10 µL Water
- 0.5µL Taq (5units/µL)
Total   18µL
        + 2µL DNA sample

Reaction Conditions
Program - P21
   1. 94°C   2:00
   2. 94°C   0:45
   3. 57°C   0:45
   4. 72°C   0:45
   5. Go to Step #2, 34 times
   6. 72°C   7:00
   7. 12°C   hold

Expected Results:

Mutant (**Null**) = 700 bp
Heterozygote = 872 bp and 700 bp
Wild type = 872 bp

Primers
Wild-type: TGA CGA AGT CAA AGT TCC ACC
Common: AAG CCT TGA TTC TGA TGT GGG C
Mutant: GCT ATC AGG ACA TAG CGT TGG C

PCR Conditions *KrasG12D*
Master Mix per reaction
- 0.6 μL MgCl$_2$ (50mM)
- 2 μL dNTPs (2mM)
- 2 μL 10X PCR Buffer (200mM Tris pH8, 500mM KCl)
- 0.5μL 20μM Primer K1
- 0.5μL 20μM Primer K2
- 0.5μL 20μM Primer K3
- 11.4 μL Water
- 0.5μL Taq (5units/μL)
Total   18μL
        + 2μL DNA sample

Reaction Conditions
Program - P21
1. 95°C   2:00
2. 95°C   0:30
3. 61°C   0:30
4. 72°C   0:45
5. Go to Step #2, 34 times
6. 72°C   10:00
7. 4°C hold

Expected Results:

Wild type = 622 bp
LSL cassette = 500 bp
1 Lox (Recombined after Cre = 650 bp

Primers
Wild-type: TGA CGA AGT CAA AGT TCC ACC
Common: AAG CCT TGA TTC TGA TGT GGG C
Mutant: GCT ATC AGG ACA TAG CGT TGG C

Appendix E: Permission for publication by Molecular and Cellular Biology

Data presented in chapter 2 is published in the journal of Molecular and Cellular Biology

Thwaites, M. J., Cecchini, M. J., Passos, D. T., Welch, I. & Dick, F. A. Interchangeable Roles for E2F Transcriptional Repression by the Retinoblastoma Protein and p27KIP1-Cyclin-Dependent Kinase Regulation in Cell Cycle Control and Tumor Suppression. *Mol Cell Biol* **37**, doi:10.1128/MCB.00561-16 (2017).

Data presented in appendix is published in the journal of Molecular and Cellular Biology

Cecchini, M.J., Thwaites, M.J., Talluri, S., MacDonald, J.I., Passos, D.T., Chong, J.L., Cantalupo, P., Stafford, P.M., Saenz-Robles, M.T., Francis, S.M., et al. A retinoblastoma allele that is mutated at its common E2F interaction site inhibits cell proliferation in gene-targeted mice. *Mol Cell Biol* **34**, 2029-2045, doi:10.1128/MCB.01589-13 (2014).

See following page for the permission from Molecular and Cellular Biology

February 27, 2017

Dear Michael Thwaites,

Authors in ASM journals retain the right to republish discrete portions of his/her article in any other publication (including print, CD-ROM, and other electronic formats) of which he or she is author or editor, provided that proper credit is given to the original ASM publication. **ASM authors also retain the right to reuse the full article in his/her dissertation or thesis.** For more information, please see the Instructions for Authors section on copyright http://aac.asm.org/site/misc/journal-ita_edi.xhtml#06.

You are therefore free to reuse the articles you are an author on for your thesis:

Interchangeable Roles for E2F Transcriptional Repression by the Retinoblastoma Protein and p27KIP1–Cyclin-Dependent Kinase Regulation in Cell Cycle Control and Tumor Suppression
Michael J. Thwaites, Matthew J. Cecchini, Daniel T. Passos, Ian Welch, and Frederick A. Dick
Mol. Cell. Biol. January 2017 37:e00561-16; Accepted manuscript posted online 7 November 2016 , doi:10.1128/MCB.00561-16

And

A Retinoblastoma Allele That Is Mutated at Its Common E2F Interaction Site Inhibits Cell Proliferation in Gene-Targeted Mice
Matthew J. Cecchini, Michael J. Thwaites, Srikanth Talluri, James I. MacDonald, Daniel T. Passos, Jean-Leon Chong, Paul Cantalupo, Paul M. Stafford, M. Teresa Sáenz-Robles, Sarah M. Francis, James M. Pipas, Gustavo Leone, Ian Welch, and Frederick A. Dick
Mol. Cell. Biol. June 2014 34:2029-2045; Accepted manuscript posted online 24 March 2014 , doi:10.1128/MCB.01589-13

Provided you follow the guidelines listed above.

Please contact us if you have any questions.

Thank you
ASM Journals
journals@asmusa.org

Curriculum Vitae

Michael Thwaites

Education

2011-Present	PhD Candidate – Biochemistry
	Supervisor: Dr. Fred Dick
	University of Western Ontario
2007-2011	BSc – Honors Specialization in Genetics
	Supervisor: Dr. Kathleen Hill
	University of Western Ontario
2003-2007	High school– Honors
	Sir Winston Churchill Secondary School

Awards

2015-2016	Ontario Graduate Scholarship ($15000)
2015-2016	CIHR Strategic Training Program in Cancer Research and Technology Transfer (CaRTT) ($17000)
2014-2015	Ontario Graduate Scholarship ($15000)
2013-2015	CIHR Strategic Training Program in Cancer Research and Technology Transfer (CaRTT) ($38000)
2011-2016	Western Graduate Research Scholarship (Tuition ~$35000)
2008-2011	Dean's List, University of Western Ontario
2010	Biochemistry Undergraduate Summer Research Program (BUSRP) ($6000)
2005	Duke of Edinburgh Bronze Award

Publications

1. **Thwaites, M. J.,** Cecchini, M. J., Talluri, S., Passos, D. T., Carnevale, J., & Dick, F. A. Multiple molecular interactions redundantly contribute to RB-mediated cell cycle control. *Cell Div* **12**, 3, doi:10.1186/s13008-017-0029-6 (2017).
2. **Thwaites, M. J.,** Cecchini, M. J., Passos, D. T., Welch, I. & Dick, F. A. Interchangeable Roles for E2F Transcriptional Repression by the Retinoblastoma Protein and p27KIP1-Cyclin-Dependent Kinase Regulation in Cell Cycle Control and Tumor Suppression. *Mol Cell Biol* **37**, doi:10.1128/MCB.00561-16 (2017).
3. **Thwaites, M. J.,** Coschi, C. H., Isaac, C. E. & Dick, F. A. Cell Synchronization of Mouse Embryonic Fibroblasts. *Methods Mol Biol* **1342**, 91-99, doi:10.1007/978-1-4939-2957-3_5 (2016).

4. Liban, T. J., **Thwaites, M. J.,** Dick, F. A. & Rubin, S. M. Structural Conservation and E2F Binding Specificity within the Retinoblastoma Pocket Protein Family. *J Mol Biol* **428**, 3960-3971, doi:10.1016/j.jmb.2016.08.017 (2016).
5. **Thwaites, M. J.,** Cecchini, M. J. & Dick, F. A. Analyzing RB and E2F during the G1-S transition. *Methods Mol Biol* **1170**, 449-461, doi:10.1007/978-1-4939-0888-2_24 (2014).
6. Cecchini, M.J., **Thwaites, M.J.,** Talluri, S., MacDonald, J.I., Passos, D.T., Chong, J.L., Cantalupo, P., Stafford, P.M., Saenz-Robles, M.T., Francis, S.M., et al. A retinoblastoma allele that is mutated at its common E2F interaction site inhibits cell proliferation in gene-targeted mice. *Mol Cell Biol* **34**, 2029-2045, doi:10.1128/MCB.01589-13 (2014).
7. Forristal, C., Henley, S.A., MacDonald, J.I., Bush, J.R., Ort, C., Passos, D.T., Talluri, S., Ishak, C.A., **Thwaites, M.J.,** Norley, C.J., et al. Loss of the mammalian DREAM complex deregulates chondrocyte proliferation. *Mol Cell Biol* **34**, 2221-2234, doi:10.1128/MCB.01523-13 (2014).

<u>Abstracts</u> **(Presenting author is underlined)**

1. **<u>Thwaites, MJ.</u>**, Cecchini, M.J., Passos, D.T., Dick, F.A. (2016). A novel model to understand the interplay between RB and CDKs in tumor suppression identifies a cooperative role in DNA damage induced cell cycle arrest. Cell Cycle, Cold Spring Harbor, NY, May 2016. (Abstract selected for oral presentation)
2. **<u>Thwaites, MJ.</u>**, Cecchini, M.J., Passos, D.T., Talluri, S., Chong, J.-L., Cantalupo, P., Saenz- Robles, M.T., Francis, S.M., Stafford, P., Carnevale, J., Pipas, J.M., Leone, G., Welch, I., and Dick, F.A. (2013) pRB mediates cell cycle control and tumor-suppression through both E2F repression and CDK regulation in a redundant manner. Third International Retinoblastoma Meeting, Monterey, California, October 2013.
3. Cecchini, M.J., Passos, D.T., **Thwaites, MJ.**, Talluri, S., Chong, J.-L., Cantalupo, P., Saenz- Robles, M.T., Francis, S.M., Stafford, P., Carnevale, J., Pipas, J.M., Leone, G., Welch, I., and <u>Dick, F.A.</u> (2013) The retinoblastoma pathway utilizes a syncretic mechanism to suppress tumorigenesis through both E2F repression and CDK regulation. Cancer Genetics and Epigenetics, Lucca, Italy, April 2013.
4. <u>Cecchini, M.J.</u>, Passos, D.T., **Thwaites, MJ.**, Talluri, S., Welch, I., and Dick, F.A. (2012) Tumor suppression by the retinoblastoma protein in the absence of E2F transcriptional regulation. Mechanisms and Models of Cancer, Cold Spring Harbor, NY, August 2012.
5. Cecchini, M.J., Passos, D.T., **Thwaites, MJ.**, Talluri, S., Welch, I., and <u>Dick, F.A.</u> (2012) Tumor suppression by the retinoblastoma protein in the absence of E2F transcriptional regulation. Cell Cycle, Cold Spring Harbor, NY, May 2012. (Abstract selected for oral presentation)